Population Pharmacokinetic and Pharmacodynamic Modelling of NS2330 and its Major Metabolite in Alzheimer's Disease

Dissertation

zur Erlangung des akademischen Grades
doctor rerum naturalium (Dr.rer.nat.)

Vorgelegt der
Mathematisch-Naturwissenschaftlich-Technischen Fakultät
der Martin-Luther-Universität Halle-Wittenberg

von Thorsten Lehr
geb. am 05.02.1977 in Hanau

Gutachter:

1. Prof. Dr. Charlotte Kloft
2. Prof. Dr. Reinhardt Neubert
3. Prof. Dr. Inaki Troconiz

Halle (Saale), 19. Juli 2006

Meiner Mutter
in Liebe und Dankbarkeit
gewidmet.

Abstract

This thesis aims to contribute to a comprehensive characterisation of the pharmacokinetics (PK) and pharmacodynamics (PD) of NS2330, a new compound under clinical development for Alzheimer's disease (AD), and its major metabolite M1 using the population PK/PD modelling approach. Several PK and PD development questions were investigated in six different modelling projects. The population PK properties of NS2330 and its metabolite were explored in healthy volunteers and AD patients within projects I and II. The PK between healthy volunteers and AD patients were comparable. Low clearances and large volumes of distributions resulted in long terminal half-lives of more than 200 h for both compounds. Sex and creatinine clearance were identified as important covariates influencing the steady-state plasma concentrations of both compounds. Project III investigated whether an enterohepatic circulation (EHC) serves as an explanation for the long half-life and a multiple peak phenomenon of NS2330. Using a mechanistic modelling approach a generic EHC model was developed capable of describing the multiple peak phenomenon as well as the long half-life. It was demonstrated that an EHC might be a plausible mechanism to account for both observations. Simulations suggested that the interruption of the EHC might be an appropriate detoxification method for NS2330. Project IV applied a mechanistic modelling approach investigating the maximum impact of the inhibition of the CYP3A4 enzyme system by itraconazole on the elimination of NS2330. This project revealed a significant reduction of the NS2330 clearance by itraconazole, which might guide recommendations for the co-administration of CYP3A4 inhibiting drugs. The *in vivo* potency of the metabolite M1 in mice was explored within project V using a PK/PD modelling approach. M1 showed a 4.1 - 5.0-fold lower *in vivo* potency in mice in comparison to NS2330. This finding together with the approximately 60% lower steady-state plasma concentrations of M1 in humans compared to NS2330 suggested that the contribution of the metabolite M1 to the overall efficacy was probably low. Project VI, finally, investigated the concentration-response relationship of NS2330 and M1 in mild AD patients. Age and the baseline value of the efficacy parameter ADAS-COG were identified as important patient characteristics influencing the maximum achievable effect of both compounds in mild AD patients. By application of the population PK/PD modelling approach a significant contribution to the understanding of the PK and PD of NS2330 and M1 was achieved. The models developed underline the necessity for population PK/PD modelling in clinical development in order to understand dose-concentration-response relationships. The models and results can be used to scientifically interpret clinical results and to improve the planning of further clinical studies for an optimized therapeutic use.

Zusammenfassung

NS2330 ist ein neuer Arzneistoff in der klinischen Entwicklung zur Behandlung von Morbus Alzheimer. Ziel dieser Arbeit war, Beiträge zur umfassenden pharmakokinetischen (PK) und pharmakodynamischen (PD) Charakterisierung von NS2330 und seinem Hauptmetaboliten M1 zu leisten. In sechs verschiedenen Projekten wurden PK- und PD-Fragestellungen mittels des Populations-PK/PD-Modellierungsansatzes untersucht. Die PK von NS2330 und M1 wurde in den Projekten I und II in gesunden Probanden und in Alzheimer-Patienten untersucht. Die PK in beiden Gruppen war vergleichbar. Geringe Clearancewerte und große Verteilungsvolumina für Muttersubstanz und Metabolit resultierten in langen terminalen Halbwertszeiten von über 200 h. Geschlecht und Kreatininclearance wurden als wichtige Parameter identifiziert, die die Steady-State Plasmakonzentrationen von NS2330 und M1 beeinflussen. In Projekt III wurde untersucht, ob ein enterohepatischer Kreislauf (EHC) die lange Halbwertszeit und die multiplen Maxima in den Plasmakonzentrations-Zeitprofilen von NS2330 erklären könnte. Die erfolgreiche Entwicklung und Anwendung eines neuen EHC Modells, das diese Phänomene beschreiben konnte, unterstützte die EHC-Hypothese. Mit Simulationen konnte weiterhin gezeigt werden, dass die Unterbrechung des EHC möglicherweise eine adäquate Detoxifikationsmethode darstellt. In Projekt IV wurde ein mechanistischer Modellierungsansatz angewendet, um den maximalen Einfluss einer CYP3A4-Hemmung durch Itraconazol auf die Elimination von NS2330 zu untersuchen. Die CYP3A4-Hemmung zeigte einen deutlichen Einfluss. Dies sollte beachtet werden, wenn Komedikationsrichtlinien für die gleichzeitige Gabe von CYP3A4 Hemmstoffen erstellt werden. Innerhalb des Projekts V wurde die In-vivo-Wirkstärke des Metaboliten M1 in Mäusen mittels eines PK/PD Modellierungsansatzes untersucht. M1 zeigte eine 4.1- bis 5-fach geringere In-vivo-Wirkstärke im Vergleich zu NS2330. Diese Ergebnisse und die 60 % geringeren Steady-State Plasmakonzentrationen von M1 im Menschen lassen vermuten, dass der Beitrag des aktiven Metaboliten M1 zur Gesamtwirkung gering ist. Abschließend wurde in Projekt VI die Konzentrations-Wirkungs-Beziehung von NS2330 und M1 in Patienten mit einer milden Alzheimer-Demenz untersucht. Das Alter der Patienten und die ADAS-COG-Basalwerte konnten als wichtige Patientencharakteristika identifiziert werden, die den maximalen Effekt der Muttersubstanz und M1 beeinflussten. Durch Entwicklung und Anwendung von Populations-PK/PD-Modellen konnte ein bedeutender Beitrag zum Verständnis der PK und PD von NS2330 und M1 erreicht werden. Die entwickelten Modelle zeigen deutlich die Notwendigkeit für Populations-PK/PD-Modellierungsansätze in der klinischen Entwicklung, um die Dosis-Konzentrations-Wirkungsbeziehung zu verstehen. Diese Modelle und Erkenntnisse können verwendet werden, um die Interpretation von klinischen Ergebnissen zu unterstützen, um die weitere Planung von klinischen Studien wissenschaftlich zu verbessern und um die therapeutische Anwendung zu optimieren.

Contents

Abbreviations

Abbreviation		Definition
$A\beta$	=	Amyloid-β-protein
ACh	=	Acetylcholine
AChE	=	Acetylcholinesterase
AChEI	=	Acetylcholinesterase inhibitors
AD	=	Alzheimer's disease
ADAS	=	Alzheimer's Disease Assessment Scale
ADAS-COG	=	Part of Alzheimer's Disease Assessment Scale measuring cognitive features
ADAS-NONCOG	=	Part of Alzheimer's Disease Assessment Scale measuring non-cognitive features
AIC	=	Akaike information criteria
ALT	=	Alanine transferase
AP	=	Alkaline phosphatase
APE	=	Absolute prediction error
APP	=	Amyloid precursor protein
AST	=	Aspartate transferase
AUC	=	Area under the curve
AUC_{x-y}	=	Area under the curve from time point x to y
BI	=	Boehringer Ingelheim
BIL	=	Bilirubin
BMI	=	Body mass index
BSA	=	Body surface area
C_{enz}	=	Concentrations within the enzyme compartment (project IV)
CL	=	Clearance
CLCR	=	Creatinine clearance
Cl_{met}	=	Metabolic clearance of NS2330 (i.e. formation of M1 out of NS2330)

continued...

Abbreviation		Definition
$Cl_{non-met}$	=	Non-metabolic clearance of NS2330 (i.e. any elimination pathway except the building of M1 out of NS2330)
C_{max}	=	Maximum plasma concentration
CNS	=	Central nervous system
CRF	=	Case report forms
CV%	=	Coefficient of variation
DA	=	Dopamine
df	=	Degree(s) of freedom
DV	=	Dependent variable (observed data analysed by NONMEM)
EC_{50}	=	Value of the concentration that produces 50% of the maximal effect
EHC	=	Enterohepatic circulation
E_{max}	=	maximal effect achievable
EMEA	=	European Medicines Agency
Excel	=	Spreadsheet analysis software
F	=	Fraction of dose absorbed
FDA	=	US Food and Drug Administration
FO	=	First-Order estimation method
FOCE	=	First-Order Conditional Estimation method
FX	=	Gall bladder emptying function
GAM	=	Generalised additive modelling
hDAT	=	Dopamine transporter of human
HGT	=	Height
HIS	=	Hachinski Ischemic Scale
HPLC-MS/MS	=	High performance liquid chromatography coupled to tandem mass spectrometry
HT	=	Serotonin
IC_{50}	=	Value of the concentration that produces 50% of the maximal inhibition
IIV	=	Interindividual variability
IOV	=	Interoccasion variability
ip	=	Intraperitoneal
iv	=	Intravenous
ITZ	=	Itraconazole

continued...

Abbreviation		Definition
KA	=	First order absorption rate constant
KEO	=	First order rate constant
KM	=	Michaelis-Menten constants
K_{xy}	=	Rate constant from compartment x to y
LLOQ	=	Lower limit of quantification
MAPE	=	Median absolute prediction error
md	=	Multiple dose
mDAT	=	Dopamine transporter of mouse
MM	=	Michaelis-Menten
MMSE	=	Mini-Mental-State-Examination
MPE	=	Median prediction error
MX	=	Metabolite X of NS2330
NA	=	Noradrenalin
NCA	=	Non-compartmental analysis
NLME	=	Non-linear mixed effect(s)
NMDA	=	N-Methyl-D-Aspartate
NMRI	=	Naval Medical Research Institute
NONMEM	=	Non-linear mixed effect modelling program
Oels	=	Extended least square Objective function
OFV	=	Objective function value
Omega	=	Period of the sine function
PD	=	Pharmacodynamic(s)
PE	=	Prediction error
PGP	=	P-glycoprotein
PK	=	Pharmacokinetic(s)
PK/PD	=	Pharmacokinetic(s)/pharmacodynamic(s)
po	=	Per os
PoC	=	Proof of concept
Q	=	Intercompartmental clearance
qd	=	Quaque die, i.e. every day
R	=	Range
RSE	=	Relative standard error
s^2	=	Variance

continued...

Abbreviation		Definition
SAS	=	Statistical analysis software
SCR	=	Serum creatinine
sd	=	Single dose
SD	=	Standard deviation
SE	=	Standard error
SigmaPlot	=	Graphic software
SPE	=	Solid phase extraction
S-Plus	=	Statistical analysis software
STS	=	Standard two-stage method
$t_{1/2}$	=	Terminal half-life
TDEL	=	Shift of the sine function to the origin
tmax	=	Time of Cmax
Vx	=	Volume of distribution of the compartment x
VM	=	Maximum rates achievable (Michaelis-Menten parameter)
WT	=	Weight
WinNonlin	=	Pharmacokinetic analysis software
$\tilde{x}$	=	Median
$\overline{x}$	=	Arithmetic mean
xd	=	Mode
Xpose	=	Graphic library for S-Plus

end

1 Introduction

1.1 NS2330

NS2330 is a new central nervous system (CNS) active drug under clinical development for Alzheimer's disease and Parkinson's disease[1].

1.1.1 Pharmacodynamic Properties

In vitro and *in vivo* investigations revealed that NS2330 inhibited the presynaptic uptake of the neurotransmitters noradrenalin (NA), dopamine (DA) and serotonin (5-HT)[1]. Additionally, in microdialysis experiments in rats it was observed that the cholinergic system was indirectly stimulated[1]. This acetylcholine release was presumably caused by a feedback mechanism due to the increased dopamine concentrations in the striatum[2;3]. Moreover, *in vivo* investigations revealed a significant reduction of amyloid-β concentration in mouse brain under NS2330 treatment[4].

The *in vitro* activity of NS2330 and five of its metabolites on the uptake of [^{3}H]-DA, [^{3}H]-5-HT and [^{3}H]-NA was explored in synaptosomes prepared from rat brain[5]. IC_{50} values (Table 1.1) revealed a higher *in vitro* activity of the metabolite M1 compared to the parent compound, the remaining metabolites (M2-M5) showed predominantely a minor *in vitro* activity.

Table 1.1 *In vitro* inhibition (IC_{50}, nM) of neurotransmitter uptake in rat brain synaptosomes of NS2330 and its metabolites

Neurotransmitter	NS2330	M1	M2	M3	M4	M5
$[^3H]$-DA	6.5	3.0	46	25	170	3200
$[^3H]$-5-HT	11	2.0	49	12	44	460
$[^3H]$-NA	1.7	0.6	17	3.0	19	850

1.1.2 Pharmacokinetic Properties

Various preclinical and clinical studies have been conducted in recourse of the development of NS2330[5]. A brief summary of the already explored pharmacokinetic (PK) properties of NS2330 is given in the following.

1.1.2.1 Preclinical Pharmacokinetics

Rat, cynomolgus monkey and minipig were investigated during preclinical investigations to explore the pharmacokinetics of NS2330 in animals[5]. In addition, mouse, rabbit and dog were used to investigate the metabolism and excretion of NS2330[5]. An overview of the PK parameters gained by non-compartmental analysis can be found in Table 1.2.

Table 1.2 Selected mean pharmacokinetic parameters for NS2330 in different species

Species	Route	Dose	C_{max}	t_{max}	V	$t_{1/2}$	CL	F	Absorpt.
		(mg/kg)	(ng/mL)	(h)	(L/kg)	(h)	(mL/min/kg)	(%)	(% of dose[γ])
Rat	iv (bolus)	2	251	—	18	2.1	102	—	—
	po	4	72.3	2	—	3.0	—	63	95-100
Minipig	iv (bolus)	0.5	—	—	8-14	4	25-43	—	—
	po	1	10.7	6-9	—	11	—	20-30	87
Monkey	iv (30 min)	1	129	—	9.2	3.5	30	—	—
	po	4	149	2	—	6.8	—	37	87
Human	iv (6 h)	0.3-1.2[α]	0.5-1.6	—	9.6	220	0.5	—	—
	po	2[α]	2.8	4	9.3	191	0.5-0.67	>90[β]	—

[α] dose in mg, [β] estimated by historical comparison, [γ] ^{14}C-labelled NS2330

NS2330 was rapidly absorbed after oral administration in rats and monkeys and more slowly in minipigs. The systemic clearance (CL) after iv administration was high (30 to 102 mL/kg/min). Volume of distribution (V) was large and exceeded the total body volume of all species, indicating an extensive distribution of NS2330 into tissues. Terminal half-lives between 2.1 and 4 h after intravenous administration were determined. The oral bioavailability was observed to range between 20 and 63%. Studies with ^{14}C-labelled NS2330 showed almost complete absorption of NS2330 after oral administration. This indicates a mild to moderate first-pass effect of NS2330 in animals after oral administration.

Protein binding of NS2330 in rat, monkey and minipig was in the range of 86% to 92%. The mean binding of the major metabolite M1 was comparable to that of NS2330 (86% to 95%).

Binding of M1 to animal plasma proteins was non-saturable up to 1000 ng/mL M1.

In vitro metabolism of NS2330 was studied using S9 liver preparations from mouse, rat, rabbit, dog, monkey and man. The rate of metabolism of NS2330 was highest using rabbit liver and only slightly lower using monkey and rat liver preparations. The rate of metabolism was still lower using dog and mouse liver and lowest using human liver preparations. In all species except the dog, M1 was the major metabolite. A study using cDNA-expressed human CYP450 enzymes indicated that CYP3A4 was involved in the metabolism of NS2330. *In vivo* metabolism investigations of NS2330 revealed the formation of different metabolites (M1-M6). In rat, monkey and minipig M1 was found as an important metabolism product. Urinary excretion was found to be the predominant pathway of elimination of NS2330 metabolites in monkeys, dogs and minipigs. In rats a significant excretion of NS2330 with faeces was found, indicating biliary excretion.

1.1.2.2 Clinical Pharmacokinetics

Several studies were performed to investigate the absorption, distribution, metabolism and elimination of NS2330 in humans[5]. An overview of the PK parameters of NS2330, normalised to body weight, is shown in Table 1.2.

Dose-proportionality was demonstrated after single dose (sd) as well as after multiple dose (md) administration in the dose range tested (sd: 1 - 10 mg; md: 0.25 - 0.5 mg qd). The maximum plasma concentration (C_{max}) was reached after 6 - 8 h (t_{max}). NS2330 showed a high volume of distribution of about 600 L. In addition, NS2330 showed a low oral clearance of 30 - 40 mL/min. The high volume of distribution and low clearance resulted in a long half-life of NS2330 of about 200 h.

A food effect study revealed no clinically relevant difference in the pharmacokinetics of NS2330 administered with or without food. The absolute bioavailability of NS2330 was estimated to be >90% by a comparison of results of a separate iv and po study with NS2330. This indicates a negligible first-pass effect of NS2330 after oral administration. Plasma concentration-time profiles of NS2330 showed a multiple peak phenomenon over a long period of time after oral as well as after intravenous administration (Figure 7.23, Page 154). Reasons for this phenomenon are still unknown.

In human urine seven different metabolites (M1-M7) were found after oral administration of NS2330. The metabolic pattern was comparable with that seen in animals. M1 was the only metabolite found in human plasma and showed a longer half-life than the parent compound of about 300 - 400 h. The trough concentrations of M1 in humans after oral administration of NS2330 at steady-state are about one third of the trough steady-state concentrations of the

parent compound. Mass balance study showed that 7% of M1 were found in urine after oral administration of NS2330.

The metabolite M1 showed the same *in vitro* pharmacological profile as the parent compound with higher *in vitro* potency compared to NS2330 (Table 1.1). However, no *in vivo* investigations of the metabolite in any species had been conducted so far. Hence, the *in vivo* activity and the pharmacokinetic properties of the metabolite were still unknown.

A mass balance study in humans showed that the contribution of the renal clearance to the overall clearance of NS2330 was about 15 - 20%[5]. This study also revealed a significant faecal excretion of overall radioactivity, presumably indicating a biliary elimination of NS2330 and/or its metabolites.

Protein binding of NS2330 in human plasma was 91% and constant over the range of 5 - 100 ng/mL. The mean binding of the major metabolite M1 was comparable to that of NS2330 and non-saturable up to 100 ng/mL M1 in human plasma.

1.1.3 Safety

Preclinical toxicity studies indicated that NS2330 was free of any genotoxic potential, was not teratogenic and showed a low toxicity in a wide range of doses over time with a sufficient safety margin.

Overall, NS2330 was well tolerated and showed a sufficient safety margin when administered to humans. The dose of 6.75 mg NS2330 was considered to be the maximum tolerated single dose. Multiple daily doses up to 1.0 mg and loading doses up to 2.0 mg were considered to be well tolerated. No clinically significant changes in vital signs, electrocardiogram or laboratory parameters were observed, and no serious adverse events occurred up to this thesis.

In multiple dose studies the most prominent adverse events with decreasing incidence respective to placebo were dry mouth, dyspepsia, dizziness and insomnia. These adverse events were observed in at least 10% more subjects during treatment with NS2330 compared to subjects treated with placebo.

1.2 Alzheimer's Disease

Alzheimer's disease (AD) is a neurodegenerative disorder and the most common cause of dementia. It is clinically characterised by progressive intellectual deterioration together with reduced activities of daily living and neuropsychiatric symptoms or behavioural changes.

1.2.1 Epidemiology

Alzheimer's disease accounts for 60% to 70% of cases of progressive cognitive impairment in elderly patients[6]. The prevalence of AD doubles every 5 years after the age of 60 increasing from a prevalence of $\approx$1% among those 60- to 64-years-old up to $\approx$40% of those aged 85 years and older[7]. In the year 2000 approximately 0.65 million patients suffered in Germany from Alzheimer's disease[8], in the United States the total prevalence is estimated at 2.3 million[9]. The population of patients with AD will nearly quadruple in the next 50 years if the current trend continues[9].

1.2.2 Clinical Features

The classical clinical features of Alzheimer's disease are an amnesic type of memory impairment[10;11], deterioration of language[12], visuospatial deficits[13;14]. Motor and sensory abnormalities, gait disturbances and seizures are uncommon until the late phase of disease[15].

Characteristics of the Alzheimer's disease are functional and behavioural disturbances. In the early stage of AD higher-level activities of daily living, such as public transportation, are disturbed. When the disease enters advanced phases abnormalities of basic activities of daily living, such as eating, grooming and using the toilet, occur[16]. Alterations in mood and apathy develop early and persist for the duration of disease. In the middle and later phases of the disease psychosis and agitation are typical[17]. Patients with AD usually survive 7-10 years after onset of symptoms[18] and typically die from bronchitis or pneumonia[19].

1.2.3 Pathology

1.2.3.1 Histopathology

The current criteria for the post-mortem pathologic diagnosis of AD requires the presence of two occurrences: neuritic plaques and neurofibrillary tangles[20]. Both have to be present in excess of the abundance anticipated for age-matched healthy controls.

Neuritic plaques are microscopic foci of extracellular amyloid deposition and associated axonal and dendritic injury[21]. Those plaques are generally found in large numbers in the limbic and associated cortices. They contain extracellular deposits of amyloid-β-protein (Aβ) that principally occur in a filamentous form.

Many neurons in the brain regions typically affected in Alzheimer's disease contain large, non-membrane-bound bundles of abnormal fibres that occupy much of the perinuclear cytoplasm[21]. Those neurofibrillary tangles are the second major histopathological feature of AD.

They are composed of microtubule-associated abnormally phosphorylated tau protein. Up to now it has not become clear whether one or more kinases are responsible for initiating the hyperphosphorylation of tau *in vivo* that leads to its apparent dissociation from microtubulus and aggregation into insoluble paired filaments. There is a growing evidence, that the formation of tangles represents one of several cytological responses by neurons to the gradual accumulation of Aβ and Aβ-associated molecules[21].

AD is also characterised by reductions in synaptic density, loss of neurons and granulo-vascuolar degeneration in hippocampal neurons[22]. Neuronal loss or atrophy in the nucleus basalis, locus ceruleus and raphe nuclei of the brainstem lead to deficits in cholinergic, noradrenergic and serotonergic transmitters, respectively[22].

1.2.3.2 Pathogenesis

The pathogenesis is not completely elucidated. There are several hypotheses created since AD was discovered. Recently, there is an increasing consensus that the production and accumulation of Aβ is central to the pathogenesis of Alzheimer's disease[23]. The formation of neurofibrillary tangles, oxidation and lipid peroxidation, glutamatergic excitotoxicity, inflammation and activation of the cascade of apoptotic cell death are considered to be secondary consequences of the generation and deposition of Aβ[23]. Figure 1.1 schematically shows the current hypothesis and understanding of the pathogenesis of Alzheimer's disease. There were several findings supporting this hypothesis, some of them are listed in the following:

- Mutations in the amyloid precursor lead to early-onset Alzheimer's disease[24]. All currently known mutations associated with AD increase the production of Aβ[25–28].

- Genetic information for the Amyloid precursor protein (APP) is located on gene 21[29–32]. In consequence patients with down syndrome (trisomy 21) have three copies of this gene and they develop neuropathological characteristics of AD by midlife[33].

- Aβ is neurotoxic *in vitro* and leads to cell death[24].

- Overexpression of human APP in transgenic mouse models of AD results in neuritic plaques similar to those seen in humans with AD and those mice have evidence of learning and memory deficits[24].

- Apolipoprotein E ϵ4 genotype, a major risk factor for AD, leads to accelerated deposition of amyloid[34].
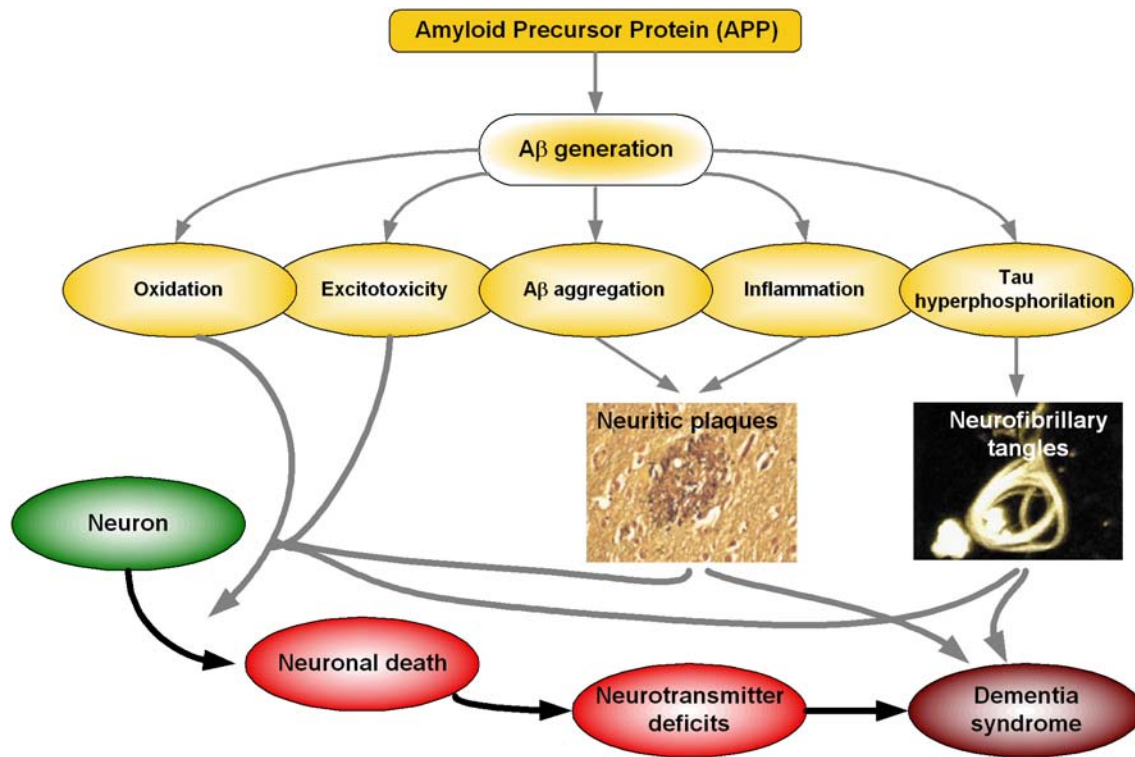
Figure 1.1 Pathogenesis of Alzheimer's Disease. Modified from Cummings [24].

Alternate hypotheses regarding the pathogenesis of AD place greater emphasis on the role of tau protein abnormalities, heavy metals or viral infections, but none of those hypotheses could be strongly supported by recent findings in the literature.

Overall, the pathogenesis of Alzheimer's disease still shows some important gaps in the understanding of the disease. Further research is highly imputed to enhance the understanding of the disease to reveal new and better therapeutic approaches.

1.2.4 Diagnosis

At present, no neuroimaging or laboratory markers exist for reliable presymptomatic diagnosis of Alzheimer's disease [35]. A definite diagnosis of AD can currently be made only by histopathologic examination of brain tissue after the patient's death [36]. Nevertheless, there are several diagnostic tools available after the patient became symptomatic. Usually standardised and easy-to-use scales to assess the cognitive function and activity of daily living in older adults are used to make early, accurate diagnosis. The most renown and widely used are the Mini-Mental-State-Examination (MMSE) and the Alzheimer's Disease Assessment Scale

(ADAS).

1.2.4.1 Mini-Mental-State-Examination

The MMSE[37] is a widely used method for assessing cognitive mental status[38]. The MMSE measures no aspects of mood, abnormal mental experiences or disordered forms of thinking. The MMSE test has a maximum score of 30 points, where the following grades can be distinguished: 0 - 11 severe dementia, 12 - 18 moderate dementia, 19 - 23 mild dementia, 24 - 26 cognitive impairment, 27 - 30 unimpaired cognitive function. Performance of the MMSE takes approximately 10 minutes. Reliability and construct validity of the test were judged to be satisfactory[38]. The MMSE has been suggested as being helpful in the early diagnosis of Alzheimer's disease with the addition of verbal fluency test[39]. Within clinical trials the MMSE is often used for screening procedure[40].

1.2.4.2 Alzheimer's Disease Assessment Scale

The ADAS is a widely used method for assessing cognitive function and non-cognitive function in Alzheimer's disease patients[41]. The assessment of the primary cognitive function (ADAS-COG) included components of memory, language and praxis, while the non-cognitive features (ADAS-NONCOG) include mood state and behavioural changes. The ADAS-COG is a widely used measurement to assess the change in cognitive function in clinical trials[40]. The ADAS-COG and ADAS-NONCOG scales have maximum scores of 70 and 50 points, respectively, where impaired functions are described by higher scores. The performance of the whole ADAS test takes approximately 40 minutes and requires adequately trained staff to achieve reliable and reproducible results.

1.2.5 Treatment

Currently, there is no cure for Alzheimer's disease. Drugs approved for the treatment of AD are palliative. They temporarily reduce neurotransmitter degradation and alleviate some of the symptoms of the disease. Nevertheless, patients significantly benefit from palliative treatment and can postpone disease progression for 6 month up to 2 years[42]. Currently there are only five drugs approved by the US Food and Drug Administration (FDA) and the European Medicines Agency (EMEA) and only a few promising candidates are in the late clinical phase[43].

1.2.5.1 Acetylcholinesterase Inhibitors

Within AD the homeostasis of acetylcholine (ACh) is disturbed due to the loss of cholinergic cells[44]. One therapeutic approach is to increase the ACh concentration by inhibiting the cleaving enzyme acetylcholinesterase (AChE).

Tacrine, donepezil, rivastigmine and galantamine are the four acetylcholinesterase inhibitors (AChEI) currently approved by the FDA and EMEA for the symptomatic treatment of patients with mild to moderate AD, although tacrine is rarely used because of its hepatotoxicity.

These agents have been shown to produce improvements in global function and cognition[45]. Secondary benefits may include reduction in behavioural disturbances, stabilisation of activities of daily living, delay of nursing home placement and reduced demands on caregiver time[46].

1.2.5.2 Memantine

Pathological activation of the N-Methyl-D-Aspartate (NMDA) receptors by glutamate has been identified as a potential cause of chronic neurodegeneration in a variety of dementias, including Alzheimer's disease[47].

Memantine is an NMDA antagonist[48] and the most recent drug approved by the FDA for the treatment of AD. It is the only drug released for the treatment of moderate-to-severe Alzheimer's disease. A double-blind, placebo controlled trial of memantine in patients with moderate-to-severe AD showed the superiority of memantine over placebo as indicated by both Activity of Daily Living Investigatory and the Severe Impairment Battery but not for the Global Deterioration Scale[48].

1.2.5.3 NS2330

NS2330 is a new drug under clinical development for the indication of Alzheimer's disease. Further details are mentioned in section 1.1.

The pharmacological properties of NS2330 show some differences compared to the drugs already approved for the treatment of AD. First, NS2330 impacts several neurotransmitter systems, compared to AChEI which only increase the acetylcholine concentration. NS2330 enhances also neurotransmitters noradrenalin and serotonin, both disturbed by the AD pathology. Secondly, NS2330 shows a reduction of the Aβ production. As Aβ is discussed being a gatekeeper protein in the pathogenesis of AD, the reduction of the Aβ production might result in a neuroprotective manner and a reduced disease progression. In consequence, patients

might initially benefit from the increase of the different neurotransmitter levels and on the long-term from the reduced disease progression under NS2330 treatment.

Several preclinical studies showed the enhancement of the cognitive function, the short and long-term memory and the attention in the animals tested. In an initial phase IIa trial performed in mild AD patients NS2330 showed a significant improvement in the cognitive function[1]. The efficacy in a larger population will be further evaluated in the upcoming clinical trials over a longer period of treatment. Overall, NS2330 is a promising new drug for the treatment of AD.

1.3 Population Pharmacokinetic/Pharmacodynamic Modelling

1.3.1 Overview

Population pharmacokinetic or pharmacodynamic modelling is a tool to study the variability in drug concentration or pharmacological effect between individuals when standard dosage regimens are administered[49]. The population approach can be utilised to support decisions in drug therapy and to make predictions and dosage recommendations, and thereby contributes to the efficiency of the drug development process and in daily use.

Since the first application of the non-linear mixed effects modelling (NLME) technique to the pharmacokinetic and pharmacodynamic (PD) data analysis by Sheiner et al.[50] and with the increase of computational power during the last decade the population approaches have received considerable attention. In the meantime the FDA recommends the use of the population approach[51] for a better understanding and safety of the drug, which should be reflected in the labelling. Also, the Common Technical Document, which is a standard format for submissions to the authorities and agencies responsible for regulation of pharmaceutical products in the Europe, USA and Japan, contains an entire subsection dedicated to the results of population analysis.

1.3.2 History

Analysis of variability in PK or PD is nothing new. Indeed, it has been the purpose of most PK and PD studies to estimate the variability in PK and PD parameters (e.g. clearance, volume of distribution, etc.) and explain these variability by physiological, genetic or environmental factors. Those studies are usually performed in a small number of individuals under well-controlled conditions. Calculation of the population parameter under these conditions can be performed using the standard two-stage method (STS)[52]. At the first stage, the estimates

from each individual will be obtained by analysing each individual separately. Subsequently, the actual population parameters are derived by calculating descriptive statistics, e.g. the mean and the standard deviation of the individual parameter estimates. Using STS for the population approach shows several drawbacks. First, it can only be used if the number of observations in each individual is sufficiently large to allow estimation of individual parameters. Second, the number of samples has to be balanced across the individuals to avoid bias in the calculation of the mean parameters.

By using the NLME technique an improved method for the calculation of population parameter became available to overcome the limitations of the STS approach. This method analyses the data of all individuals simultaneously, but takes the interindividual variability structure into account. This ensures that imbalance and confounding correlations are accounted for.

1.3.3 Non-Linear Mixed Effects Modelling

The NLME approach shows several advantages over the classical STS approach and provides more accurate estimates of the variability in the population [53].

The NLME approach can handle every kind of data situation (i.e. sparse, rich and unbalanced data). Handling of sparse data sampling allows to take samples at regular visits to the clinic. Hence, the PK and PD properties of the drug of interest can be more easily characterised in the patient population, to which the drug is intended to be given. Additionally, populations which are difficult to study from an ethical perspective, such as children, elderly or severely ill patients, can now be easily investigated. Further, the possibility to analyse unbalanced data allows for pooling different kinds of studies. This enables the investigation of a large number of individuals using the population approach.

One of the main benefits of the population approach is the possibility to describe the relation between covariates (i.e. individual-specific variables like age, weight) and model parameters (e.g. volume of distribution, clearance). This parameter-covariate relation can explain the variability in PK or PD model parameters to a certain extent. As a result sub-groups in the patient population that are e.g. at risk of receiving toxic or ineffective concentrations can be identified and benefits of dose adjustment can be assessed. In addition, covariate models can be used to decide whether and how dose adjustment should be achieved [54;55].

1.3.4 Software

Meanwhile there are several software packages available for estimating population parameters[56] based on non-linear mixed effects modelling. NONMEM[57] was the first software package available for population analysis. In the later years several other software packages became available (e.g. NLME in S-Plus, NLMIX in SAS, WINNONMIX), implementing comparable estimation methods. Some of the new software packages showed improved graphical user interfaces and other small improvements. Nevertheless, NONMEM is still the most widely used[58] software package and was also used for this thesis.

1.4 Objectives

Prior to the work performed for this thesis the PK/PD properties of NS2330 and its major metabolite were not fully understood. The objective of this thesis was to contribute to a comprehensive characterisation of the pharmacokinetics and pharmacodynamics of NS2330 and its major metabolite M1 using the population PK/PD modelling approach. PK and PD development questions were addressed in six projects with the following objectives:

I, II The development of a population pharmacokinetic model for NS2330 and its major metabolite to assess the mean pharmacokinetic parameter, the variability of them and to identify covariates influencing the PK properties of NS2330 and/or its metabolite. The analysis was planned to be performed in two different populations. Project I investigated data from phase I and IIa studies and project II used data from a proof of concept study in Alzheimer's disease patients.

III The development of a mechanistic model to assess whether NS2330 undergoes enterohepatic circulation and to assess the impact of an enterohepatic circulation on the pharmacokinetics of NS2330 (project III).

IV The development of a mechanistic model to assess the impact of CYP3A4 metabolism on the elimination of NS2330 (project IV).

V The development of a mechanistic model to assess the potency of the active metabolite M1 in relation to the parent compound NS2330 (project V).

VI The development of a population PK/PD model to assess the concentration-response relationship of NS2330 and its metabolite in mild Alzheimer's disease patients. The analysis was to include a covariate analysis to identify covariates influencing the PK/PD properties of NS2330 and M1 (project VI).

2 Methods and Studies

2.1 Population PK/PD Modelling

In this thesis the non-linear mixed effects modelling (NLME) technique was applied to perform population pharmacokinetic/pharmacodynamic analyses using the software package NONMEM[57]. The following method section will focus on the background of NLME with respect to the use of NONMEM.

2.1.1 Non-Linear Mixed Effects Modelling

Non-linear mixed effects modelling allows the estimation of typical model parameters, so called fixed effect parameters or population parameters, based on appropriate compartmental models and variability parameters, so called random effect parameters. The mixture of fixed and random effects results in mixed effects, where the name of the method "non-linear mixed effects modelling" results from. The typical NLME model (= population model) can be divided into three sub-models:

1. the structural model

2. the pharmacostatistical model

3. the covariate model

Figure 2.1 (left panel) schematically illustrates the interaction between the three sub-models. Fixed effect parameters are estimated by the structural and the covariate model, the random effects are estimated by the pharmacostatistical model. These models are explained in detail in the following sections.

2.1.1.1 Structural Model

The structural model describes the typical time profile of the measured variable (e.g. plasma concentration for PK, ADAS-COG score for PD) as a function of the corresponding model
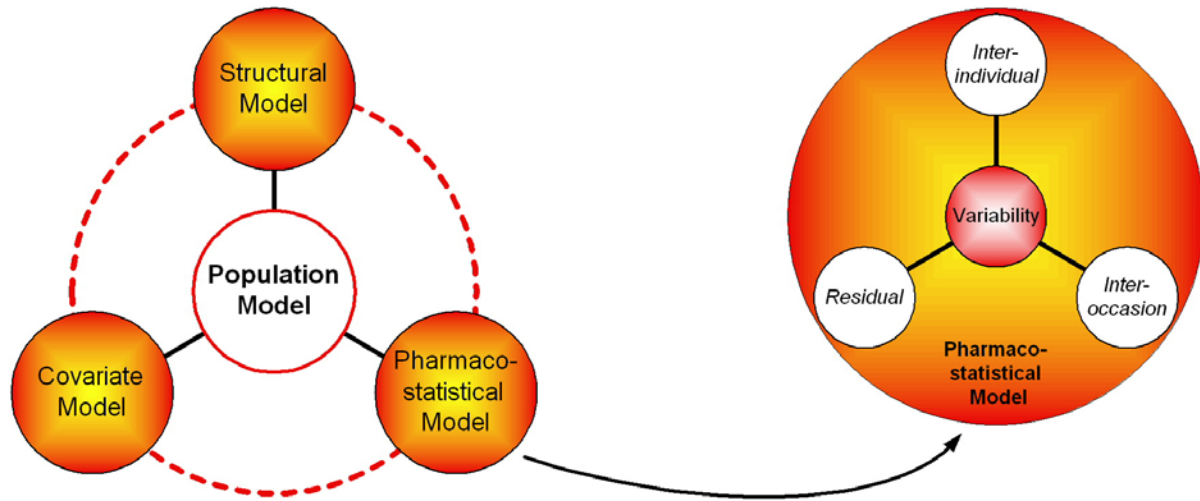
Figure 2.1 Schematic structure of the population model

parameters (e.g. typical clearance, typical Emax), the dosing schedule and the administered dose. The structural model can be described by the following function (Eq. 2.1):

$$f(\phi_i, X_{ij}) \tag{2.1}$$

where $f()$ is the function describing the structural model (PK or PD) that relates the independent variables, X_{ij} (e.g. time and dose at certain time point j), to the response given the i-th individual vector of the model parameters ϕ_i.

2.1.1.2 Pharmacostatistical Model

The pharmacostatistical model characterises the PK or PD variability of a drug and quantifies the influence of random effects, i.e. non-measurable and non-controllable factors. The random effects will cover e.g. uncertainty in measurements or discrepancies for recorded sampling time points. The overall variability of a population model is influenced by the following three components: the interindividual variability, the interoccasion variability and the residual variability (Figure 2.1, right panel).

Interindividual Variability The interindividual variability (IIV) covers the non-explainable difference of the model parameter between the individuals. This means that the individual parameter value varies from the typical population parameter value to a random extent (e.g. $CL_{individual}$ vs. $CL_{population}$). This difference can be investigated by different kinds of models.

An exponential model is exemplarily listed in the following (Eq. 2.2):

$$P_{ki} = \theta_k \cdot e^{\eta_{ki}} \tag{2.2}$$

where P_{ki} denotes the value of the parameter k of the individual i (= individual parameter), θ_k is the typical value of the population parameter k and η_{ki} is the difference between the natural logarithms of P_{ki} and θ_k, i.e. $\eta_{ki} = lnP_{ki} - ln\theta_k$.

It is assumed that all P_{ki} are log-normally distributed. In addition, all η_{ki} are assumed to be independently, multivariately symmetrically distributed with zero mean and the variance ω_k^2. The variance ω_k^2 is one of the random effects estimated by the NLME regression models. It is the diagonal element of the variance-covariance-matrix Ω. A correlation between two diagonal elements can be assessed by the estimation of the corresponding non-diagonal element of the Ω matrix $\omega_{k,k+1}$. The non-diagonal element describes the covariance between the diagonal elements.

The use of an exponential model has several attractive features. It ensures that all parameters are strictly positive avoiding the estimation of negative non-physiological individual values. Also ω_k^2 becomes dimensionless and expresses approximately the coefficient of variation in the model parameters[59].

Interoccasion Variability   The interoccasion variability (IOV) defines another level of random effects between the interindividual and the residual variability[60]. IOV arises when a parameter of the model, e.g. CL, varies within a subject between study occasions. The term "occasion" can be defined arbitrarily, usually logical frames for an occasion are chosen, e.g. each dosing interval in multiple dose studies or each treatment period of a cross-over study can be defined as an occasion. To assess the IOV of a specific parameter more than one measurement per individual has to be available per occasion.

The IOV can be implemented in the random variability model as described in the following (Eq. 2.3):

$$P_{ki} = \theta_k \cdot e^{\eta_{ki}+\kappa_{kiq}} \tag{2.3}$$

where P_{ki} denotes the i-th individual value of parameter P_k at the study occasion q. κ_{kiq} is a zero mean random variable with variance π^2, assumed to be multivariately symmetrically distributed.

Residual Variability   The residual variability describes the extent of deviation between the observed and the model predicted value, including IIV and IOV. Deviations might be caused by errors in the documentation of the dosing and blood sampling times, analytical errors,

misspecification in the models and other factors. The most renown error models describing the residual variability are presented in the following.

The simplest one is the additive error model (Eq 2.4):

$$y_{ij} = f(\phi_i, X_{ij}) + \epsilon_{ij} \tag{2.4}$$

where y_{ij} denotes the measured observation from the *i*-th individual at a certain time point *j*. By the function $f(\phi_i, X_{ij})$ the individual prediction is made using the structural model including the interindividual and the interoccasional variability. ϵ_{ij} denotes the random deviation between the individual prediction and the observed measurement for each individual *i* at a certain time point *j*. This model will be applied if a constant variance over the whole measurement range is probable.

Another common error model is the proportional error model (Eq. 2.5):

$$y_{ij} = f(\phi_i, X_{ij}) \cdot (1 + \epsilon_{ij}) \tag{2.5}$$

This error model will be applied if the absolute deviations from the individual predictions increase proportionally with higher observations.

The combined error model (Eq. 2.6) is another widespread error model in the population approach:

$$y_{ij} = f(\phi_i, X_{ij}) \cdot (1 + \epsilon_{1,ij}) + \epsilon_{2,ij} \tag{2.6}$$

This error model contains a proportional and an additive component. For small observation values this error model behaves like the additive error model, for higher observation values the proportional component is predominant.

For the determination of the residual variability model it is assumed that ϵ_{ij} is a zero mean random variable with variance σ^2, assumed to be multivariately symmetrically distributed. Variance σ^2 is estimated as a parameter of the population model and represents the diagonal element of the Σ matrix. The variance σ^2 reflects the extent of the residual variability.

2.1.1.3 Covariate Model

The covariate model describes the relation between covariates and model parameters. Covariates are individual-specific variables that describe the patients demographics (e.g. sex, age, weight), disease status (e.g. organ function indices like creatinine clearance) or environmental factors (e.g. concomitant medication, alcohol consumption). The parameter covariate relation should explain the variability in PK or PD model parameters to a certain extent.

For the identification and quantification of covariates influencing the PK or PD several methods are available, like the stepwise generalised additive modelling (GAM) analysis in Xpose and the direct analysis in an NLME analysis software program, e.g. NONMEM.

GAM Analysis   The GAM analysis is a procedure proposed by Mandema et al.[61] for identifying possible important covariates. In this procedure the individual parameter estimates P_{ki} are regressed on the individual covariates X_i according to the following equation (Eq. 2.7):

$$P_{ki} = \alpha_{k0} + \sum_{i=1}^{n} g_{kn}(X_{ni}) \tag{2.7}$$

where α_{k0} denotes the intercept, X_{ni} is the n-th covariate of the i-th individual, and the function $g_{kn}()$ represents the function describing the covariate influence on the P_k parameter. For each covariate a range of optional models is defined first. In Xpose the model scope contains the following three hierarchical possibilities of implementing each covariate: not included (i.e. no covariate effect), included in a linear relationship, included in a non-linear (spline) relationship. The model for the parameter was built using stepwise addition/deletion where the covariates were allowed to be incorporated in the model in any of the pre-defined relationships. In each step the single added (or deleted) term that decreased the Akaike information criteria[62] (AIC) to the greatest extent retained in the model. The search was stopped when no further decrease in AIC value is achievable.

Analysis in NONMEM   The analysis of covariates in NONMEM is taking place in the population model with respect to the significance of their influence on the pharmacokinetic or pharmacodynamic parameter. Several methods have been described on how covariate models have to be built (e.g.[61;63;64]), and many of them are still employed. Unfortunately, a consensus on how to best build covariate models does not exist. In general, the building of the covariate model follows the forward inclusion and backward elimination process. This approach was also chosen in this thesis and is described in more detail in section 2.1.3.

2.1.1.4 Population Model

The combination of all sub-models will result in a population model which can be described by the following equation (Eq. 2.8), where an additive error model was used exemplarily:

$$y_{ij} = f(g(\Theta, z_{ki}) + \eta_{ki} + \kappa_{iq}, x_{ij}) + \epsilon_{ij} \tag{2.8}$$

The equation describes each measured observation y (e.g. concentration or effect measurement) from the i-th individual at a certain time point j by the individual prediction of the

function $f()$ and the residual variability ϵ_{ij}. The function f characterises the relation between all investigated data and contains the documented and given independent variables x_{ij} (e.g. dose) and z_i (covariate, e.g. age), the vector Θ of all fixed effect parameters θ (PK and PD parameter and the covariate influence) and the vectors (or scalars if one dimensional) of the random effect parameters η_{ki}, κ_{iq} and ϵ_{ij}. The subfunction $g()$ describes the relation between z_{ki} (covariate, e.g. age) and the vector Θ.

2.1.2 Estimating the Population Parameters

Estimation of non-linear mixed effects models has been implemented in a number of software packages and includes different estimation methods [65]. As NONMEM was used for all work in this thesis, the technical description of the other methods will not be given here.

Aim of a modelling approach is an adaptation of the model function to the observations made to gain model parameters which describe the observed data best. In NONMEM this is done by the minimization of the extended least square objective (O_{ELS}) function, which provides maximum likelihood estimates under Gaussian conditions [66]. The equation calculating the O_{ELS} function is given in the following (Eq. 2.9):

$$O_{ELS} = \sum_{i=1}^{n} \left[\frac{(y_i - E(y_i))^2}{var(y_i)} + ln\,|var(y_i)| \right] \tag{2.9}$$

where $var(y_i)$ is the variance-covariance of y_i, i.e. the i-th individual vector of observations, and $E(y_i)$ is the expectation of y_i.

The objective function value is up to a constant, equal to minus twice the log-likelihood of the fit. Thus, a minimum objective function value reflects the maximum likelihood of the model parameters to describe the data best. The standard errors of the parameter estimates are also calculated by the maximum likelihood method.

In most PK/PD models it is not possible to obtain a closed form solution of $E(y_i)$ and $var(y_i)$. The simplest algorithm available in NONMEM, the first-order estimation method (FO), overcomes this by providing an approximate solution through a first-order Taylor series expansion with respect to the random variables η_i, κ_{iq} and ϵ_{ij} where it is assumed that these random effect parameters are independently multivariately normally distributed with mean zero. During an iterative process the fixed and random effects are estimated. The individual parameters (conditional estimates) are calculated *a posteriori* based on the fixed effects, the random effects and the individual observations using the maximum *a posteriori* Bayesian estimation method implemented as the "post hoc" option in NONMEM [67].

The FO method was the first algorithm available in NONMEM and has been evaluated by

simulation and used for PK and PD dynamic analysis[52]. Overall, the FO method showed a good performance in sparse data situations. However, there are situations where the FO method does not yield adequate results. For these situations improved approximation methods as the First-Order Conditional Estimation and the Laplacian method became available in NONMEM. The difference between both methods and the FO method lies in the way the linearization is done.

The First-Order Conditional Estimation method (FOCE) uses a first-order Taylor series expansion around the conditional estimates of the η's. This means that for each iteration step where population estimates are obtained the respective individual parameter estimates will be obtained by the FOCE estimation method. Thus, this method involves minimizations within each minimization step. The interaction option available in FOCE considers the dependency of the residual variability on the interindividual variability during the calculation of the objective function value. If the interaction method is not chosen, the residual variability will be estimated under consideration of the population estimates. The Laplacian estimation method is similar to the FOCE estimation method but uses a second-order Taylor series expansion around the conditional estimates of the η's. This method is especially useful when a high degree of non-linearity occurs in the model[67].

Due to the improved and complex mechanism both methods are more precise but also considerably slower than the FO method. For the PhD thesis all presented estimation methods were used, depending on the data situation available and the progress of the model development. The estimation method used for the estimation of the final model presented is reported in the respective result section of the projects.

2.1.3 Building Population Models

2.1.3.1 General Strategies

For model building purposes two different approaches are applicable, the top down and the bottom up approach. The top down approach starts with the most complex model allowed by the data and this full model will be reduced sequentially to include only the relevant features. This approach has the advantage that any change is evaluated in a model that includes as many true terms as possible, that means it is closer to the true model. Disadvantages are numerical instabilities of the full model. In addition, in most cases the top down approach is extremely time-consuming with respect to the computation times. The bottom up approach starts from the minimal model and expands this model until no more terms can be justified. As data situation seldom allows the application of the top down approach and the computation

times are so tremendous, the top down approach is not very common while the bottom up approach is widely used for the building of population models [57].

For all population models developed during this thesis the bottom up approach was applied. For each project an individual modelling strategy was developed, based on the data situation and the *a priori* information available. These strategies are described in detail in the respective sections (see sections 2.5.1.7, 2.5.2.7, 2.5.3.3, 2.5.4.7, 2.5.5.7 and 2.5.6.7). Creation of the sub-models was performed as described in the following sections. In general, the bottom up approach pursued the following workflow:

- Development of the structural and statistical model (i.e. base model)

- Development of the covariate model, if applicable (covariate analysis)

- Refinement of the model

2.1.3.2 Model Selection

To compare and evaluate different kinds of models created during the model development process graphical and statistical methods were applied. Both criteria had to be satisfied as described in the following.

Graphical Methods   Graphical analysis was used to explore model assumptions made and to assess the goodness of fit of the model. The graphical analysis was performed using the Xpose software [68] in S-Plus. The following basic goodness of fit plots were investigated:

- population or individual predictions versus the measured observations

- weighted residuals (= weighted difference between measured and population or individual predictions) versus population or individual predictions

- weighted residuals versus independent variable (e.g. time)

Figures spreading randomly and uniformly around the line of identity (predicted vs. observed) or around zero (for residual plots) are judged as optimal.

Statistical Methods   During the model building process improvements or deteriorations caused by modifications to a model can be judged on a statistical basis if the models are nested. Models are declared as nested if the more complicated model can be collapsed to the simple model by setting one or more of the parameters to a fixed value. The comparison is based on the difference in the objective function values (OFV), which is approximately χ^2-distributed.

This means that a difference of 3.84, 6.63, 7.88 and 10.83 points in the OFV is significant at a *p*-value level of 0.05, 0.01, 0.005 and 0.001, respectively (df=1). For the model building process the following *p*-values were defined: A *p*-value of 0.05 was applied for all model building activities except the backward elimination process during the covariate model building (section 2.1.3.5). In this case a *p*-value of 0.001 was applied. Another important aspect for the model building process was the precision of the parameter estimates, judged by the relative standard error (RSE). The RSE was calculated according the following equation (Eq. 2.10):

$$RSE, \% = \frac{\text{absolute standard error}}{\text{parameter estimate}} \cdot 100 \qquad (2.10)$$

For the population estimates the RSE should be equal or less then 50%, otherwise the 95% confidence interval would include zero.

2.1.3.3 Building the Structural Model

The aim of the development of the structural model was to describe the typical time profile of the measured variable as a function of the model parameters, the dosing and sampling schedules and the administered dose(s). Procedures for the building of the structural model of the several projects investigated are described in detail in the respective modelling strategy section. The discrimination between rival structural models was based on the difference in OFV (for nested models) and graphical analysis using goodness of fit graphics.

2.1.3.4 Building the Statistical Model

The aim of the development of the statistical model was the characterisation of variability within the PK and PD of the investigated compounds. Thus, the interindividual, the interoccasion and the residual variability were investigated. In general, for each model parameter it was investigated whether an interindividual variability could be included using an exponential error model (section 2.1.1.2). Correlation between individual random-effect parameters was first investigated by graphical analysis. If a correlation was observed, this correlation was accounted for by implementation of the respective covariance in NONMEM and the estimation of the correlation coefficient.

2.1.3.5 Building the Covariate Model

The aim of the development of the covariate analysis was to describe the relations between covariates and model parameters and to explain the variability in PK or PD model parameters to a certain extent. Based on the aim of the different projects a covariate model was built for

projects I, II and VI. A general approach for the building of the covariate model was applied with the following steps: candidate selection, univariate implementation into the model, forward inclusion and backward elimination. The procedure is described in the following section and presented schematically in the flowchart in figure 2.2.

Candidate selection   Different covariates that seemed to show a relation to model parameters were pre-selected. First, a GAM analysis was performed as described in section 2.1.1.3. Covariates identified were selected for the next step. In addition, physiologically plausible covariates were also selected manually to test their influence on parameters. For example the influence of creatinine clearance on the clearance of the renally eliminated drug was tested as a physiologically plausible covariate, independent from the result obtained in GAM.

Univariate Implementation into the Model   Covariates pre-selected as described before were incorporated univariately in the final base model. Covariates with a larger decrease than 3.84 points in the objective function value were used for the forward inclusion step. If highly correlated covariates were identified as significant, e.g. body weight and BMI, only the most significant covariate was used for further investigations.

Continuous covariates were implemented into the structural model using a linear relationship or a hockey stick function. The linear relationship was implemented according the following equation (Eq. 2.11):

$$\theta_{P-Cov} = \theta_P \cdot (1 + \theta_{Cov} \cdot (Cov - Cov_{median})) \tag{2.11}$$

where θ_{P-Cov} describes the typical population parameter value for an individual with a certain covariate Cov. θ_P denotes the typical population value for an individual with a median covariate. θ_{Cov} describes the influence of the covariate as a proportionate change from θ_P per change of one covariate unit from the median covariate value Cov_{median}.

If the covariate covers a large range of values the data may not be satisfactorily described by the above presented linear model. An alternative model for those situations is the hockey-stick or two-spline model described exemplarily in the following equation (Eq. 2.12):

$$\theta_{P-Cov} = \begin{cases} \theta_P \cdot (1 + \theta_{Cov} \cdot (Cov - Cov_{median})) & \text{if covariate} \leq \text{median} \\ \theta_P & \text{if covariate} > \text{median} \end{cases} \tag{2.12}$$

The hockey stick function assumes a linear relationship until a node point is reached, afterwards another relationship can be used. In the above equation the median was chosen as the node point and for all individuals having a larger covariate value than the median value no
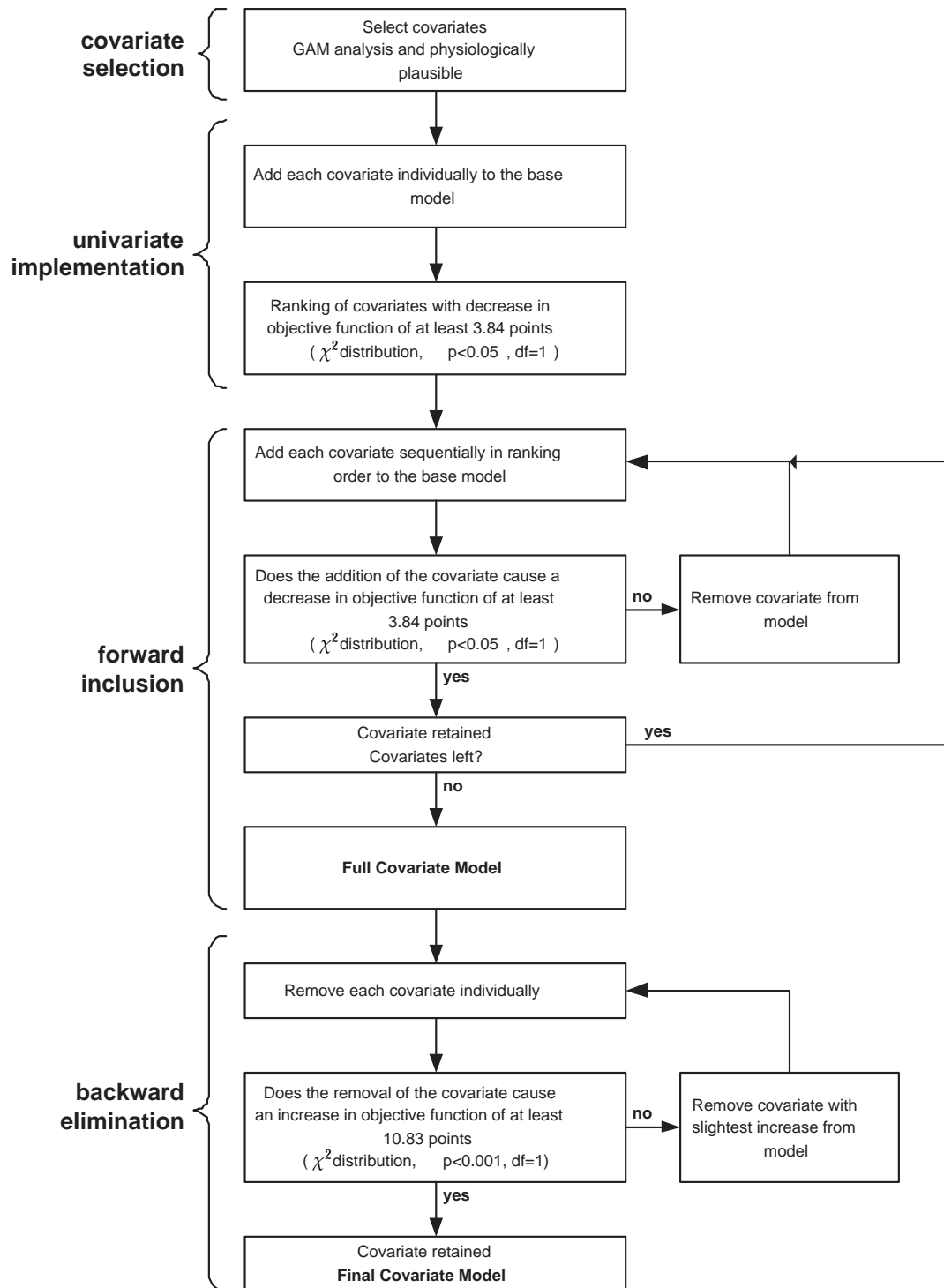
Figure 2.2 Flowchart of the covariate building process

influence of the covariate was assumed. Both methods (linear and hockey stick) were tested in parallel and the function resulting in the lower objective function value was selected for the further model development.

Categorical covariates were implemented as a step function, where an example for a sex difference is given in the following equation (Eq. 2.13):

$$\theta_{P-Cov} = \begin{cases} \theta_{P,\,male} & \text{if sex} = \text{male} \\ \theta_{P,\,female} & \text{if sex} = \text{female} \end{cases} \tag{2.13}$$

Forward inclusion   Covariates achieving a drop in the objective function value by less than 3.84 points (df=1) during the univariate implementation were not tested further during the forward inclusion. The covariate with the strongest influence obtained by the univariate implementation remained in the population model while the other covariates were incorporated into the model sequentially according to their ranking order of the significance level. If the additional covariate caused a significant drop of 3.84 points in the OFV the covariate remained in the model. If the drop was lower than 3.84 points the covariate was skipped and the next covariate in the ranking order was implemented. This forward inclusion procedure was continued until all covariates assessed as statistically significant during the univariate testing were tried to be incorporated in the model. A model developed so far was called the "full covariate model".

Backward Elimination   The full covariate model underwent the backward elimination procedure. For this process a stricter significance level of p=0.001 was applied. Within the backward elimination each covariate was removed separately from the model.

If the deletion of one or more covariates did not result in a significant increase of 10.83 points of the OFV then the covariate with the slightest non significant increase was removed from the model and the single removal of each covariate was started again from the new model. The backward elimination process was stopped when the removal of each remaining covariate resulted in a significant deterioration of the model, i.e. an increase of more than 10.83 points of the OFV (df=1). A such created model is called the "final covariate model". Contained the final covariate model a highly correlated covariate as described in the univariate covariate testing section, this covariate was exchanged by the correlated covariate to check the significance. The superior covariate was kept in the final model. Covariates were only be formally tested if they represented at least 10% of the patient population. Covariates which showed a clear trend during the graphical analysis but were present in less than 10% of the population were explored additionally in the final covariate model for mere informative purpose.

2.1.4 Model Evaluation

Aim of the model evaluation was to assess the quality and the predictive performance of the developed final model. A detailed description of the evaluation method applied for the project-specific final model is given in the respective sections (2.5.1.8, 2.5.2.8, 2.5.3.4, 2.5.4.8, 2.5.5.8 and 2.5.6.8).

2.2 Data Handling

2.2.1 Data Aquisition

2.2.1.1 Pharmacokinetic Measurement

NS2330 and M1 concentrations in plasma were determined by a fully validated high performance liquid chromatography coupled to tandem mass spectrometry (HPLC-MS/MS) method using deuterated internal standards[5]. The assay comprised sample clean-up by automated solid phase extraction (SPE) in the 96-well plate format. Chromatography was achieved on an analytical reversed-phase HLPC column with gradient elution. The substances were detected and quantified by HPLC-MS/MS using electrospray ionisation in the positive ion mode. Concentrations were determined in ng/mL and used for PK modelling.

Measurements of NS2330 or M1 concentrations were either performed at bioanalytical laboratories of Boehringer Ingelheim (BI), Biberach, Germany, or at Quintiles AB, Uppsala, Sweden. Lower limit of quantification (LLOQ) was 0.1 ng/mL for NS2330 and M1 for all studies, except the study PI.2 with 0.02 ng/mL and the study PV with 1 ng/mL. Measurement sites and further details about the measurements of the studies investigated can be found in the Appendix (Table 7.1, Page 115). Results from the bioanalytical measurements were managed and archived by the medical data service from Boehringer Ingelheim.

2.2.1.2 Pharmacodynamic Measurement

Pharmacodynamic measurements used for PD modelling were acquired for projects V and VI and are described in detail in the respective sections (2.5.5.6 and 2.5.6.6).

2.2.2 Dataset

2.2.2.1 Dataset Building

NONMEM data files included dependent variables (e.g. NS2330 concentrations), dosing information and subject-specific covariates describing the demographic, disease and other in-

dividual factors. The general structure of a dataset is predefined by the program[57]. For the building of each dataset for the respective project the raw data was provided by the medical data service. Data were combined manually to a complete dataset. Problems were discussed and resolved with the relevant parties to ensure a complete, consistent and accurate reporting database. Dataset for the analysis of project II was provided by data management. Each dataset was subject to intensive data checkout analysis.

2.2.2.2 Derived Covariates

For the covariate analysis several derived covariates were used and calculated as described below.

Calculation of Body Mass Index (BMI) was performed according to equation 2.14, where weight was given in kg and height in m.

$$\text{BMI}\,(\text{kg/m}^2) = \frac{\text{weight}}{\text{height}^2} \tag{2.14}$$

Calculation of Body Surface Area (BSA) was performed according to Du Bois and Du Bois[69] as described in equation 2.15, where weight was given in kg and height in cm.

$$\text{BSA}\,(\text{m}^2) = \text{weight}^{0.425} \cdot \text{height}^{0.725} \cdot 0.007184 \tag{2.15}$$

Calculation of Creatinine Clearance from Serum Creatinine Creatinine clearance (CLCR) was calculated according to Cockroft-Gault[70] as described in equation 2.16, where age was given in years, weight in kg and serum creatinine concentrations in mg/dL.

$$\text{CLCR}\,(\text{mL/min}) = \begin{cases} \frac{(140-\text{age})\cdot\text{weight}}{72\cdot\text{serum creatinine}} & \text{males} \\ \frac{(140-\text{age})\cdot\text{weight}}{72\cdot\text{serum creatinine}} \cdot 0.85 & \text{females} \end{cases} \tag{2.16}$$

2.2.2.3 Outlier

Outliers of the dependent variable, i.e. PK or PD observation used for modelling, were excluded if there was objective evidence of them being spurious, e.g. unexpected value due to non-compliance etc. Key models were evaluated with and without outliers, and the results obtained were judged to assess the influence of the outlier on the parameter estimates. All values excluded from the analysis were documented with reasons for their exclusion. Outliers were described in the results sections of the respective projects.

2.2.2.4 Missing Observations

Missing observations within the dependent variable were not included in the population analysis. If time for a particular observation was missing, protocol time for the particular observation was used. Individuals on placebo were excluded from pharmacokinetic analyses. Plasma concentrations below the LLOQ within the lag phase were initially set to zero to support the implementation of a lag phase. If implementation failed or zero values influenced the model development negatively, values below LLOQ within the lag phase were removed from the dataset. Values below LLOQ within the terminal elimination phase were removed *a priori* from the dataset. Missing observations were described in the results sections of the respective projects.

2.2.2.5 Missing Covariates

Within one subject completely missing covariates were replaced by the population median (continuous covariates) or the mode (categorical covariates). A missing covariate within a subject (across a time series) was carried forward from the last measurement until a new measurement was made. If any of the imputed covariates was found to be important in the population model, the impact of imputation was assessed by running the model with and without the patient(s) where imputed values were used. Missing covariates were described in the results sections of the respective projects.

2.3 Statistical Methods

Additional statistical analysis and evaluation were performed according to the standard statistical methods described in the following sections (2.3.1 and 2.3.2).

2.3.1 Descriptive Statistics

For the characterisation of the analysed data and the results obtained by the population analyses different localisation (Table 2.1) and dispersion (Table 2.2) parameters were used. Localisation parameters describe the location of a distribution or their central tendency. Dispersion parameter denote the variability of a distribution.

2.3.2 Analysis of Correlation

The correlation analysis investigates the strength of a linear relationship between two random variables. The correlation coefficient is a numeric measure of the strength of this linear

Table 2.1 Localisation Parameter

Arithmetic mean ($\overline{x}$)	sum of all the members of the set divided by the number of items in the set
Median ($\tilde{x}$)	value that separates the upper half of a sample, a population, or a probability distribution from the lower half
Mode (x_d)	value that has the largest number of observations
1st and 3rd Quartile	values cutting off the lowest or highest 25% of sorted data, respectively
5th and 95th Percentile	values cutting off the lowest or highest 5% of sorted data, respectively

Table 2.2 Dispersion Parameter

Range (R)	length of smallest interval which contains all data
Variance (s^2)	measure of the statistical dispersion of a variable, indicating how far from the expected value its values typically are
Standard deviation (SD)	measure of statistical dispersion
Coefficient of variation (CV%)	measure of dispersion of a distribution defined as the ratio of the standard deviation to the mean.

relationship between -1 and 1. If the variables are independent then the correlation is 0. The correlation coefficient is 1 in the case of an increasing linear relationship, -1 in the case of a decreasing linear relationship and some value in between in all other cases, indicating the degree of linear dependence between the variables. The closer the coefficient is to either -1 or 1, the stronger the correlation between the variables.

2.4 Software

All model fitting analyses were carried out using NONMEM (GloboMax, Version V). S-Plus (Mathsoft Incorporation, Version 5, 1999) in connection with Xpose (Version 3.104) was used for graphical analysis. Simulations were carried out using NONMEM, the Clinical Trial Simulator (Pharsight Corporation, Version 2.1.1, 2001) or Berkeley Madonna (Version 8.0.1, 2000). Figures were generated using SigmaPlot (SPSS, Version 8.0, 2002). Non-compartmental anal-

yses were performed using WinNonlin (Pharsight Corporation, Version 4.0, 2002).

NONMEM datasets were created and modified using Microsoft Excel (Microsoft Corporation, Version 2002 SP3, 2002) or SAS (SAS Institute Inc., Version 8.02C). Derived covariates (Section 2.2.2.2) were calculated by NONMEM, SAS or Excel. Calculation of statistics was performed using Excel or S-Plus.

2.5 Study Characteristics

2.5.1 Project I

2.5.1.1 Project Objectives

The aim of this analysis was to develop a population pharmacokinetic model that simultaneously described the plasma concentration-time profiles of NS2330 and M1 and to determine the interindividual variability in PK parameters. In addition, a covariate analysis should be performed to explore covariates that might influence the PK characteristics of NS2330 and/or M1.

2.5.1.2 Studies

Four phase I and two phase IIa studies were investigated within this combined analysis. Table 2.3 gives an overview of the studies. Selection criteria of the studies were: availability of parent and metabolite data, comparable bioanalytical methods and an agreement from BI to use data for analysis. All studies were performed at different study centres across Europe and the US between February 1999 and July 2003. All studies were performed in a randomised, double-blind, placebo controlled, parallel study design.

The objective of all six studies was to determine the safety, tolerability and pharmacokinetics of NS2330 after oral or intravenous administration. For the studies PI.5 and PI.6 an additional objective was to determine the preliminary efficacy in mild Alzheimer's disease patients.

2.5.1.3 Project Population

The population of the combined analysis contained healthy and renally impaired subjects as well as subjects from the patient population with mild Alzheimer's disease. The studies PI.1 and PI.3 were performed in males only, the remaining studies PI.2, PI.4, PI.5 and PI.6 were performed in females and males. The age range was dependent on the study objective. Study

Table 2.3 Overview of studies used within project I

Study	Phase	Route	Dosing	Population Characteristics
PI.1	I	iv	sd	healthy, young, male
PI.2	I	po	sd	healthy + renally impaired, 20 - 80 years, male + female
PI.3	I	po	md	healthy, elderly, male
PI.4	I	po	md	healthy, elderly, male + female
PI.5	IIa	po	md	mild AD patients, elderly, male + female
PI.6	IIa	po	md	mild AD patients, elderly, male + female

iv: intravenous, po: oral; sd: single dose; md: multiple dose

PI.1 contained young subjects, study PI.2 included a wide range of ages, the remaining studies recruited only elderly subjects. For studies PI.5 and PI.6 an additional inclusion criteria was a MMSE[37] score of 20 - 26 and a modified Hachinski Ischemic Scale (HIS) score[71] no greater than 4.

2.5.1.4 Treatments

Different types of formulations in different strengths were used within the studies. Table 7.2 (Appendix, Page 116) gives an overview of the dosage forms, the formulation strengths and further information about the formulations. Overall, a wide range of NS2330 doses from 0.3 mg up to 2 mg was administered with different loading and maintenance doses within all studies. Table 7.3 (Appendix, Page 116) gives an overview of the treatment patterns, the different dose groups and the routes available.

To ensure treatment compliance, the drug administration on all treatment days was supervised by the investigator or his/her deputy. The exact times of medication dosing and the number of units were recorded in the case report forms (CRF). After oral drug administration a mouth and hand inspection took place. In studies PI.5 and PI.6 a study medication reconciliation was performed to verify treatment compliance during the outpatient phase of the studies. Compliance was further confirmed by the bioanalytical assessment of NS2330 in plasma samples.

2.5.1.5 Observations

Plasma samples for the determination of NS2330 and M1 concentrations were taken at the time points listed in Table 7.4 (Appendix, Page 117). Within the studies PI.3 and PI.6 different

sampling schedules were applied, dependent on the dose group of the subjects.

2.5.1.6 Data Acquisition

NS2330 and M1 concentrations in plasma were determined by a fully validated HPLC-MS/MS method, as described in section 2.2.1.1.

2.5.1.7 Modelling Strategy

The modelling strategy for this project was developed before the modelling was started. It was planned to perform the population PK modelling in a sequential manner. First, a final base model for each compound, NS2330 and M1, was developed in parallel. For modelling of M1 the dosing information of NS2330 was used.

NONMEM control files were parameterised in terms of apparent volumes of distribution, distribution and elimination clearances and absorption rate constants. One-, two- and three-compartment models were tested for NS2330 and M1 individually. A series of pharmaco-statistical models were systematically evaluated in order to identify the model that best described the data. Initially, all IIV was modelled using an exponential random effects model, and residual variability was modelled using a combined (additive/proportional) error model separately for NS2330 and M1. Other models were tried as suggested by graphical analysis. Secondly, a combined model was built, based on the information gained from the individual analysis. Initially, the structural models obtained by the individual analysis was used, then a formation process of M1 from NS2330 was used to link the two models. Different formation processes (first-order, zero-order, saturable) were evaluated. Structural modifications were investigated as well (addition or removal of compartments). IIV and residual variability were reinvestigated on the combined model. Finally, a covariate analysis, as described in section 2.1.3.5, was performed using the final base model of NS2330 and M1.

2.5.1.8 Model Evaluation

The final combined PK model and parameter estimates obtained were evaluated using an internal and external evaluation method. Additionally, the influence of outlier concentrations removed from the dataset was evaluated.

Internal Evaluation   One thousand new datasets with the same number of patients, the same covariates, the same dosing history and sampling schedule as the original dataset were simulated, based on the fixed and random effects parameters estimated from the original dataset.

The bias and precision of the simulated plasma concentrations (DV) were computed to evaluate the predictive performance of the model. The median prediction error (MPE) and median of the absolute prediction error (MAPE) were calculated across all plasma concentrations in the 1000 simulated datasets, separately for each time point. For a specific DV of an individual at a specific time point, the prediction error (PE) is defined as (Eq. 2.17):

$$PE(DV) = \frac{DV_{ij(sim)} - DV_{ij(obs)}}{DV_{ij(obs)}} \cdot 100 \tag{2.17}$$

where $DV_{ij(sim)}$ is the simulated dependent variable of the *i*-th individual at the *j*-th time point and $DV_{ij(obs)}$ is the observed dependent variable of that individual at that time point from the original dataset. Similarly, $APE(DV)$ is defined as the absolute value of $PE(DV)$. MPE and MAPE were determined separately for NS2330 and M1 concentrations.

External Evaluation   An external evaluation was performed using the data from the proof of concept trial in Alzheimer's disease patients (study PII). Plasma concentrations of NS2330 and M1 were simulated based on the individual dosing history and the individual demographic characteristics. Simulation was performed using the final combined PK model estimates and setting the number of evaluations to zero, i.e. no iteration was performed. The population and individual predictions were estimated based on the parameter estimates obtained by the final model. The quality of the evaluation was assessed by graphical presentation of the observed concentrations vs. the population and individual predictions. In addition, the distribution of the individual estimates η of the interindividual variability was investigated graphically, to evaluate whether they were normally distributed.

Outliers   The influence of outliers was investigated on the final base and final covariate model.   A new dataset including outlier concentrations was built and used with the final models. The influence of the outliers on the parameter estimates was evaluated and assessed as described in section 2.2.2.3.

2.5.2 Project II

2.5.2.1 Project Objectives

The aim of this analysis was to develop a population pharmacokinetic model for NS2330 and its metabolite M1 based on data obtained from the proof of concept (PoC) study in Alzheimer's disease patients. The model development should include a covariate screening to identify covariates that might influence the pharmacokinetics of NS2330 and/or its metabolite M1.

2.5.2.2 Study

A double-blind, randomised, placebo controlled proof of concept study (clinical phase II) was conducted in patients with mild to moderate dementia of Alzheimer's type at 63 sites in the United States and 10 sites in Canada. Data obtained was used for the modelling of project II. The objective of this study was to determine the safety, tolerability, pharmacokinetics and efficacy of treatment with 0.25 mg, 0.5 mg, and 1 mg NS2330 over 14 weeks compared with placebo in patients with mild to moderate Dementia of Alzheimer's type. Study was performed between March 2003 and March 2005.

2.5.2.3 Project Population

A total of 288 patients (72 per group) were planned to complete the study. Assuming a dropout rate of approximately 31%, 420 patients were planned to be randomised in order to achieve 288 completed patients.

Patients were included into the study if they fulfilled the following inclusion criteria: 40 to 85 year old males or females with a mild to moderate Dementia of the Alzheimer's Type (ADAS-COG > 12 and MMSE 10-24). Co-administration of drugs approved for the treatment of AD (donepezil, galantamine, rivastagmine, tacrine) was prohibited.

2.5.2.4 Treatments

NS2330 was supplied as oral tablets (0.25, 0.5, 1 mg and placebo). All tablets were identical in appearance, so that the four treatment groups were indistinguishable (double-blind).

Patients were advised to self-administer one tablet every day in the morning for 14 weeks. At each visit the investigating staff checked the compliance by counting the tablets. Patients must have taken 80% to 120% of their prescribed study medication to be considered compliant for the entire trial.

2.5.2.5 Observations

Plasma sampling was performed at the following time points: before and 3 - 6 h after administration of the first dose, at the beginning and 3 - 6 h later at the clinic visits after 4, 9 and 14 weeks of treatment and at any time during the clinic visit throughout week 20 (6 weeks after the last dosing). Nine plasma samples were planned to be taken from each patient. Additionally, a more intensive sampling was conducted in a small group of 14 patients at week 14 (predose, 2, 4, 6, 8, 12 h). In most cases the samples taken at the beginning of the visits were

trough values, however some patients changed their typical administration time, so that for these patients the samples taken at the beginning of the visit were not trough samples.

2.5.2.6 Data Acquisition

NS2330 and M1 concentrations in plasma were determined by a fully validated HPLC-MS/MS method, as described in section 2.2.1.1.

2.5.2.7 Modelling Strategy

Development of a combined population PK model for the PoC study was planned to start when approximately 2/3 of all patients intended to be treated finished the study. The remaining 1/3 of the patients were planned to be used for model evaluation.

For the first 2/3 of the patients the population PK modelling was performed in a sequential way. First, simple structural base models for parent compound and metabolite were developed. Second, a combined population PK model for NS2330 and M1 was developed, identical to the development of the combined model for project I described in section 2.5.1.7. Finally, a covariate analysis was performed using the final base model of NS2330 and M1.

2.5.2.8 Model Evaluation

Internal Evaluation Model evaluation was performed by using the complete dataset containing all patients (3/3) treated. First, final base and final model were re-estimated using the complete dataset. Parameter estimates were compared by numerical comparison and a visual comparison of typical plasma concentration-time profiles gained by simulation. The final base model was used to re-check the individual PK parameters versus the covariates available, to check new correlations occurred by the new patients. If any new correlations occurred, they were further investigated. A backward elimination, as described in section 2.1.3.5, was performed with the final model to evaluate whether the covariates remained significant.

External Evaluation A randomised, double-blind, placebo-controlled, five parallel groups efficacy and safety exploratory study of NS2330 (placebo, 0.125, 0.25, 0.5 and 1.0 mg) administered orally once daily over 14 weeks in levodopa treated Parkinson patients with motor fluctuations was performed in 202 patients between April 2003 and February 2005. This study was used for external evaluation purpose. The placebo arm was not used for evaluation.

Plasma concentrations of NS2330 and M1 were simulated based on the individual dosing history and the individual demographic characteristics. Simulation was performed using the

final combined PK model and setting the number of evaluations to zero, i.e. no iteration was performed. The population and individual predictions were estimated based on the parameter estimates obtained by the final model. The quality of the evaluation was assessed by graphical presentation of the observed concentrations vs. the population and individual predictions. In addition, the distribution of the individual estimates η of the interindividual variability was investigated graphically, to evaluate whether they were normally distributed.

2.5.3 Project III

2.5.3.1 Project Objectives

The aim of this analysis was to develop a mechanistic population PK model that described the multiple peak phenomenon of NS2330 in plasma. This model development was based on the hypothesis of an enterohepatic circulation (EHC) and should investigate whether the observed multiple peak phenomenon might have been caused by EHC.

2.5.3.2 Study

To avoid complications which might appear during the absorption process, an intravenous administration study was selected for this analysis. Therefore, the study PI.1 was chosen for model development. This study was also part of the combined analysis of project I and described there in detail (see section 2.5.1).

2.5.3.3 Modelling Strategy

As part of the modelling process, different EHC models available in literature should be investigated in detail to assess if one or more could be applied successfully. If application failed a new or modified model should be developed based on the knowledge and background of the EHC.

2.5.3.4 Model Evaluation

The model developed should be evaluated by applying it to another drug, where an EHC was already confirmed. For this evaluation purpose a study with meloxicam as a drug undergoing EHC[72] was chosen. Additionally, the model should be evaluated by predicting the effects of an interruption of the EHC by cholestyramine and the results should be compared to the results obtained by the evaluation study.

Evaluation Study   The study was performed in the human pharmacology centre in Biberach, Germany, in 1989. A brief summary of the study used for evaluation purpose is given here. Further details of the study can be found in the literature[72]. Twelve healthy male subjects, aged between 27 and 50 years, were treated in a randomised cross-over study with 30 mg meloxicam single dose given intravenously (bolus) either alone or concomitantly with cholestyramine (4 g Quantalan$^©$ 50 suspended in 200 mL water) given three times a day for four days. Consecutive meloxicam doses were separated by a wash-out period of at least 14-days. Plasma samples were taken 0.05, 0.08, 0.16, 0.25, 0.5, 0.75, 1, 2, 3, 3.5, 4, 5, 6, 7, 8, 9.5, 10, 12, 24, 32, 48, 72 and 96 h after administration of meloxicam.

2.5.4 Project IV

2.5.4.1 Project Objectives

The aim of this analysis was to develop a mechanistic population PK model that allowed the assessment of the maximum effect of a complete CYP3A4 inhibition on the elimination of NS2330.

2.5.4.2 Study

For this investigation a drug-drug interaction study investigating the effect of CYP3A4 inhibition by itraconazole (ITZ) on the single oral dose pharmacokinetics of 2 mg NS2330 in two parallel groups of healthy male volunteers was chosen. The study was conducted by Boehringer Ingelheim at the Human Pharmacology Centre in Ingelheim, Germany, between October 2002 and December 2002.

2.5.4.3 Project Population

Overall 28 healthy male volunteers, aged between 21 to 50 years and with a BMI between 18.5 - 29.9 kg/m^2, were included in this study.

2.5.4.4 Treatments

Subjects were divided in two parallel groups of 14 subjects each. NS2330 alone (treatment 1) or NS2330 in combination with itraconazole (treatment 2) were to be tested within each group. Every subject was to be tested only within one group. NS2330 was administered orally as a 0.5 mg tablet, ITZ orally as a 100 mg capsule (Sempera$^©$ Kapseln, Janssen-Cilag GmbH, Neuss, Germany). Table 7.5 (Appendix, Page 117) summarises the dosage and treatment schedule.

2.5.4.5 Observations

Plasma sampling of NS2330 was performed at the following time points: 2, 4, 6, 8, 10, 24, 32, 48, 72, 96, 120, 144, 168, 336, 504, 672 and 840 h after administration of NS2330. Itraconazole samples were taken at the following time points: -26, -2, 46, 94 and 144 h, where the time points are relative to administration time of NS2330.

2.5.4.6 Data Acquisition

NS2330 and itraconazole concentrations in plasma were determined by a fully validated HPLC-MS/MS method, as described in section 2.2.1.1.

2.5.4.7 Modelling Strategy

For modelling purpose, first a descriptive ITZ model was developed. Due to the limited information during the absorption phase prior knowledge from literature[73] was used to stabilize the model. In parallel, a separate model for NS2330 was developed to assess the structural model. Subsequently, a model should be developed that implemented the pharmacokinetic of ITZ and its possible influence on the PK of NS2330. For this combined model the PK parameters of ITZ should first be fixed and the model should be finalised. Afterwards, PK of ITZ were not fixed, to see if the PK of both drugs could be assessed simultaneously.

2.5.4.8 Model Evaluation

Model evaluation was done by comparing findings from the population PK analysis of project II with results obtained from this project.

2.5.5 Project V

2.5.5.1 Project Objectives

The main objective of this project was to evaluate the potency of the metabolite M1 relative to the parent compound NS2330 using population PK/PD models.

A further objective was to assess whether additional first-pass metabolites were formed during the absorption phase. Finally, the PK properties of NS2330 and M1 should be explored in mice.

2.5.5.2 Study

For the investigation of this project a pharmacological study in mice was chosen. This study was conducted at Neurosearch A/S, Denmark, in October 2003.

2.5.5.3 Project Population

Female Naval Medical Research Institute (NMRI) mice (Taconic M&B, Ry, Denmark) with an average weight of 25 g were used in this study. The animals were housed in standard plastic cages under normal 12-h light/dark cycles and a temperature of 19 - 21 °C. Tap water and food (Brogaarden, Hørsholm, Denmark) were provided ad libitum. Overall, 228 (132 treated, 64 vehicle and 32 non-specific binding) mice were used within this study.

2.5.5.4 Treatments

Mice received the salt of NS2330 or the salt of M1 as solution either orally or intravenously (bolus). Doses administered were calculated based on the salt form. Bioanalytical measurements and modelling used the doses reflecting the free base. Oral doses of NS2330 and M1 were 1, 3, 10 and 20 mg/kg, and intravenous doses were 0.3, 1, 3, 5 and 10 mg/kg. Vehicle or test substance dissolved in the vehicle were administered to the NMRI mice (iv: 0.25 ml; po: 0.75 ml). The vehicle was an aqueous solution containing 5% Tween 80$^{©}$. Each mouse was weighed and dosed according to the body weight. Forty-five minutes before the respective sampling time point 2.0 μCi of $[^3H]$WIN35,428 in 0.2 ml saline were injected intravenously via the tail vein. Additional animals were used for the determination of non-specific binding where unlabelled WIN35,428 (2.5 mg/kg, ip) was injected at the time of $[^3H]$WIN35,428 injection.

2.5.5.5 Observations

Plasma samples for the determination of NS2330 and M1 concentrations and samples for the determination of the PD parameters were taken at the time points listed in Table 7.6 (Appendix). At the planned sampling time points the mice were sacrificed by cervical dislocation. Overall, 228 mice were investigated in this study. In detail, three mice per sample point were treated with the parent compound or the metabolite (n=132), four mice per time point were treated with vehicle (n=64) and two mice per time point (n=32) were investigated to determine the non-specific binding.

The samples for the determination of inhibition of the dopamine transporter by NS2330 and/or M1 were obtained as follows: Mice were decapitated at the planned sampling time

points and the brains were quickly removed and dissected on ice. Striatum, which contains the highest concentration of dopamine transporters, was isolated and tissue was weighed and dissolved in 1 mL 2% sodium-laurylsulfate for 24 - 48 h.

2.5.5.6 Data Acquisition

NS2330 and M1 concentrations in plasma were determined as described in section 2.2.1.1.

Measurement of dopamine transporter inhibition was achieved by the following procedure: To the solubilized tissue 2 mL of a scintillation cocktail were added and the amount of radioactivity per mg of tissue was determined by conventional liquid scintillation counting. Groups of vehicle mice served as controls for estimation of total binding. Percentage of inhibition of the dopamine transporter was used as parameter for the pharmacological activity (=pharmacodynamics) and was calculated as follows (Eq. 2.18):

$$\text{Inhibition [\%]} = 1 - \left(\frac{\text{Radioactivity}_{\text{treated}} - \text{Radioactivity}_{\text{non-specific binding}}}{\text{Radioactivity}_{\text{vehicle}} - \text{Radioactivity}_{\text{non-specific binding}}} \right) \cdot 100 \quad (2.18)$$

2.5.5.7 Modelling Strategy

PK/PD modelling was performed in a sequential manner. First, the PK models for NS2330 and M1 were developed. Modelling started with the intravenous data of M1, then the intravenous data of NS2330, subsequently the oral data of M1 and finally the oral data of NS2330 were added. Thus, four key PK models were available. Based on the final PK models parameter estimates were fixed and the PD data were fitted sequentially as described for PK. Ultimately, PK/PD models were estimated again without fixing the PK parameters, allowing a simultaneous estimation of PK and PD parameters. Considering the model building strategy, four different PK/PD models describing a different raw data situation were developed, optimised and finalised. The model with all data included was the final model. The other three were named intermediate key models.

Each mouse was considered as an individual. The individual pharmacokinetic and pharmacodynamic parameters θ_j were modelled assuming a log-normal distribution (Eq. 2.19):

$$\theta_j = \theta \cdot e^{\eta_j} \quad (2.19)$$

where θ is the population mean, and η_j are independent normally distributed random effects parameters with zero mean and variance ω^2. For the PK models this type of random variability was implemented on the volume of distribution and for the PD models IIV on the EC_{50} parameters. As only one PK and PD data point per mouse was available the estimated random variability represents both, IIV and residual variability.

2.5.5.8 Model Evaluation

No model evaluation was planned to be performed.

2.5.6 Project VI

2.5.6.1 Project Objectives

The aim of this analysis was to develop a population pharmacokinetic/pharmacodynamic model that described the relationship between plasma concentrations of NS2330 and M1 and the change in the ADAS-COG score as an efficacy parameter. In addition, a covariate screening should be performed to explore covariates that might influence the PD characteristics of NS2330 and M1.

2.5.6.2 Studies

To investigate the population PK/PD relation in mild Alzheimer's disease patients studies PI.5 and PI.6 were selected. These studies were part of the project I and described there in detail (see section 2.5.1). Within the following section only the relevant parts for the PK/PD modelling are mentioned.

2.5.6.3 Project Population

The studies PI.5 and PI.6 recruited elderly male and female subjects with a MMSE score of 20 - 26 and a modified HIS score no greater than 4. No co-medication was allowed influencing the mental status of the patients.

2.5.6.4 Treatments

Treatments and dosing schedules were described in detail in section 2.5.1.4. Following initial screening, all patients in each dose group had an acclimatisation period of two days before the treatment started.

All patients participated an inpatient phase, i.e. stationary, consisting of acclimatisation, loading dose and maintenance dose, prior to the outpatient maintenance dose phase. The length of the inpatient phase varied depending on the dose group and is summarised in Table 7.7 (Appendix, Page 119). Following the inpatient phase, all patients had weekly return visits on an outpatient, i.e. ambulant basis through day 28.

2.5.6.5 Observations

Details regarding the plasma samples taken for the determination of NS2330 and M1 concentrations have been described in section 2.5.1.5. For the determination of the pharmacodynamic measurements psychometric tests (ADAS-COG) were performed at the following time points: Screening, day 1, day 28 (last day on treatment) and day 42, where screening was allowed to take place up to 14 days until start of treatment.

2.5.6.6 Data Acquisition

NS2330 and M1 concentrations in plasma were determined as described in section 2.2.1.1.

Measurements of the efficacy variable ADAS-COG were conducted by adequately trained staff at approximately the same time of day, in the same test order and by the same health care professional(s) at the designated study visits, with the intention to minimise variability. The score obtained by the ADAS-COG questionnaire was used for PD modelling.

2.5.6.7 Modelling Strategy

Development of the PK/PD modelling was performed in a sequential way. As the studies used for this project were also part of project I, the PK/PD model development was based on the final PK covariate model obtained by project I. PK parameter estimates were fixed and different PD models were investigated. The PD model was linked initially to the PK model by implementing effect compartments. If data could not be described adequately other links were to be tested. Potency of the metabolite was implemented based on the findings of project V. Data obtained within the placebo arm was investigated as well to explore a possible placebo effect.

2.5.6.8 Model Evaluation

No model evaluation was planned to be performed.

3 Results

3.1 Project I – Combined Population PK Analysis

A combined population PK analysis of NS2330 and M1 was performed based on the data of four phase I and two phase IIa studies.

3.1.1 Dataset

A complete dataset was created containing the information of both analytes as described in section 2.2.2. In addition, for modelling purpose the dataset was separated into subsets for the different analytes.

3.1.1.1 Observations

Due to implausibility all M1 (n=15, 0.5% of all samples) plasma concentrations from one subjects were removed *a priori* during the data checkout process. No observations were missing. The final dataset included 119 subjects contributing 1819 NS2330 and 1333 M1 plasma concentrations above the lower limit of quantification. Table 7.8 (Appendix, Page 119) gives detailed information about the distribution of subjects and plasma concentrations across the studies. For study PI.1 only a few M1 plasma concentrations above LLOQ were available due to the low doses of NS2330 administered. Overall, the distributions across the studies can be considered as balanced. Figure 7.1 (Appendix, Page 137) shows the plasma concentrations versus time separated by studies and analytes. Overall, a dose-dependent increase in plasma concentrations was observed. Concentrations were in a wide range from 0.202 ng/mL to 32.9 ng/mL for NS2330 and from 0.020 to 7.57 ng/mL for M1.

3.1.1.2 Population Characteristics

The main characteristics of the population investigated are summarised in Tables 7.9 and 7.10 (Appendix, Page 120). Statistics were calculated from data at the start of treatment, no changes over time were observable. The study population of this project contained 37 females and 82

males. Due to the inclusion criteria no females were present in the studies PI.1 and PI.3. Distributions of the covariates are shown in Figure 7.2 (Appendix, Page 138). Overall, the histograms showed the expected distributions pattern. Age showed a bimodal distribution, mainly caused by the composition of phase I studies performed in healthy young subjects and the phase IIa studies performed in elderly mild AD patients. Correlations between continuous covariates are also shown in Figure 7.2. No unexpected correlations between covariates were observed. Creatinine clearance showed a wide range of 14 mL/min up to 148 mL/min. Overall, 42.9% of the population displayed a reduced kidney function (CLCR < 80 mL/min), but only 5% and 6.7% showed a moderate and severe renal impairment, respectively (Table 7.11, Appendix, Page 120).

3.1.2 Population Pharmacokinetic Modelling

3.1.2.1 Model Development

As described in the modelling strategy (section 2.5.1.7), the model development was performed in a sequential way. First, a model describing the plasma concentration-time profiles of NS2330 was built. In parallel, a model for the metabolite M1 was built. Finally, a combined model was developed, simultaneously describing plasma concentration-time profiles of parent compound and metabolite.

NS2330 was best described by a two-compartment model with a first-order absorption and elimination process. Interindividual variability was included in the central and peripheral volume of distribution, clearance, inter-compartmental clearance and the bioavailability. Residual variability was described by a proportional random effect model for NS2330.

All parameters obtained from the modelling of M1 contain the unknown factor of the formation of M1 out of NS2330 and were handled with care. Thus, this modelling approach was taken to explore the structural model of M1. The metabolite was best described by a two-compartment model with a first-order absorption and elimination process. Interindividual variability was included for the central volume of distribution, clearance, intercompartmental clearance and the absorption rate constant. Residual variability was described by a proportional random effect model for M1.

The fact that M1 had never been administered separately and the volume of distribution was unknown complicated the model building of the combined model. Due to this gap in knowledge the parameters of the metabolite were non-identifiable, i.e. the parameters effected the value of the data but they could not be estimated accurately. To overcome this problem different hypothesis based on *a priori* knowledge were tested and checked which assumptions

described the data best. Two main hypotheses were developed. Hypothesis A was based on the structural similarity between the parent compound and the metabolite. It was assumed that the volume of distribution of both compounds was identical for the central compartment. Hypothesis B was based on the findings of a radioactive labelled mass balance study which showed that approximately 7% of M1 were excreted unchanged in urine after administration of NS2330. Therefore, it was assumed that 7% of the overall eliminated NS2330 was transformed into M1. Consequently, the metabolisation constant was fixed to 7% of the overall elimination rate of NS2330. Hypothesis A and B were intensively investigated. Both hypotheses could successfully be applied to a combined population PK model. Different structural modifications of the model were tested. In brief, the structure of the parent and the metabolite compound was modified to test a 1+1, 1+2, 2+1 and 2+2 combined model, where the first number denotes the number of compartments of the parent, the second number for the metabolite compartments. For both hypotheses the best base model achievable was developed.

The comparison of the diagnostic and individual plots between the final models using hypotheses A and B showed no relevant differences. But parameter estimates of NS2330 using hypothesis A showed discrepancies compared to the single model of NS2330. This indicates that this hypothesis influenced the model to a great extent. Parameter estimates of NS2330 under hypothesis B were comparable to the single model of NS2330. In consequence hypothesis B was assessed to be superior over A and was used for further model development.

3.1.2.2 Base Model

Plasma concentration-time profiles were best described by a two compartment model for NS2330 as well as for M1 with first-order absorption and elimination. The formation of M1 from NS2330 was accounted for by a first-order metabolism step, where this rate constant was fixed to 7% of the overall elimination of NS2330. A schematic illustration of the PK model is shown in Figure 3.1.

Interindividual variability was included in clearance of NS2330 (ωCL_{NS2330}) and M1 (ωCL_{M1}), in the central volumes of distribution of NS2330 ($\omega V2$) and M1 ($\omega V4$) and the bioavailability ($\omega F1$). A correlation between CL_{NS2330} and CL_{M1} was implemented in the model. Residual variability was modelled with a proportional random effect model for NS2330 and M1.

Parameter estimates of the base model can be found in Table 7.12 (Appendix, Page 121). All parameters were estimated with good precision (relative standard errors ranging from 5.5 to 35.1%, Table 7.12). The goodness of fit plots of NS2330 and M1 are shown in Figure 7.3 (Appendix, Page 139). All concentrations (predicted versus observed) are spread around the line of identity, indicating that the data was well described by the model.
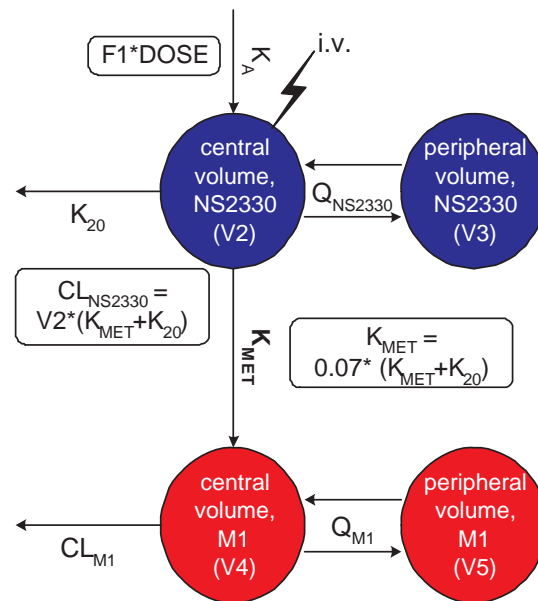
Figure 3.1 Schematic PK model of NS2330 and its major metabolite M1

3.1.2.3 Final Covariate Model

The covariates tested on the individual PK parameters of the final base model were selected as described within the method section (2.1.3.5). Covariates selected by the GAM method are listed in Table 7.13 (Appendix, Page 122). In addition, physiologically plausible covariates were also tested (Table 7.13).

The covariate analysis was performed as described in section 2.1.3.5. The analysis identified a statistically significant influence of creatinine clearance on the central volume of distribution of M1 (V4). The mathematical expression for the relation found is listed in Table 7.12. Also, a different V4 was found for the studies PI.5 and PI.6. According to the relations and the 5th and 95th percentiles of the creatinine clearance values the typical V4 will increase from 6.6 L to 34.7 L for subjects from studies PI.1 to PI.4 and from 21.9 L to 115.8 L for subjects from studies PI.5 and PI.6 as the creatinine clearance will increase from 26.7 mL/min to 135.5 mL/min. In addition an 35% increase of the bioavailability in females was found.

The parameter estimates of the final covariate model can be found in Table 7.12 (Appendix, Page 121). Large volumes of distribution were estimated for NS2330 and M1. The overall volume of distribution was 782 L for NS2330. Depending on the study the overall volume of distribution of M1 was 160 L for studies PI.1-4 and 210 L for studies PI.5-6. The low clearances of NS2330 and M1 resulted in long half-lives of 247 h for NS2330 and 275 h (Studies PI.1-4) or 361 h (Studies PI.5-6) for M1.

Estimates for the interindividual variability were moderate to high with 23.9% in CL_{NS2330}, 40.1% in CL_{M1}, 47.6% in V2, 79.9% in V4 and 19% in F1. Compared to the base model the variability was 30.7% (i.e. -35.4 percent points) reduced in V4 and 21.8% (i.e. -5.3 percent points) reduced in F1 (Table 7.14, Page 122). The proportional residual variability was determined with 14.1% and 14.3% for NS2330 and M1, respectively. All parameters were estimated with good precision (standard errors ranging from 5.5 to 37.2 %, Table 7.12). The goodness of fit plots of NS2330 and M1 are shown in Figure 7.4 (Appendix, Page 140). All concentrations (predicted versus observed) are spread around the line of identity, indicating that the data is well described by the model.

3.1.3 Evaluation

3.1.3.1 Outlier

As described in section 3.1.1.1 all M1 concentrations from one subject were removed due to implausibility. During the combined analysis new reliable measurements of the M1 plasma concentrations for this subject were available. These concentrations were not included in the dataset because the modelling process was ongoing. The influence of the new concentrations on the parameter estimates of the base and final model was retested. Parameter estimates obtained were comparable. Consequently, the exclusion of the plasma concentrations had no influence on the development of base and final model.

3.1.3.2 Internal Evaluation

For internal validation of the model the MPE and MAPE were determined to evaluate the predictive performance of the PK model as described within the method section (2.5.1.8).

The results are given in Table 3.1. The MPEs and MAPEs for all plasma concentrations were low and the 90% confidence interval of the MPE included zero, indicating a low bias and good precision of these estimates.

Table 3.1 Results Internal Validation

Parameter	MPE (%)		MAPE (%)	
	Median	5th - 95th Percentile	Median	5th - 95th Percentile
Concentrations NS2330	-2.5	-54.7 - 101.8	25.4	2.3 - 101.8
Concentrations M1	-5.1	-62.5 - 116.6	30.3	2.8 - 116.6

3.1.3.3 External Evaluation

The external simulation was performed as described in the method section (2.5.1.8). The predicted concentrations versus the observed concentrations were shown in Figure 7.5 (Appendix, Page 141). All values of the parent compound were overall well distributed around the line of identity. For the metabolite the low concentration ranges were also well distributed around the line of identity, for concentrations above 10 ng/mL the model predictions showed a tendency to underpredict higher M1 values.

The parameter distribution of the evaluation run is presented in Figure 7.6 (Appendix, Page 142) . All parameters were normally distributed with mean zero, indicating that all individual values were normally distributed without showing any bias.

3.1.4 Simulation

Simulations were performed to assess the influence of the covariates on the plasma concentration-time profile of NS2330 and M1, respectively. For the simulation a dosing regimen of 1 mg NS2330 administered once daily po for 166 days (4000 h) was assumed. Model and parameter estimates from the final covariate model were used for simulation.

3.1.4.1 Influence of Sex

A simulation was performed to assess the impact of sex on the plasma concentration-time profiles. Bioavailability values of 1.07 for males and a 35% increased value for females were used for simulation. The plasma concentration-time profiles of NS2330 are shown in Figure 7.7 (Appendix, Page 142). Females showed a 35% increased NS2330 steady-state concentration compared to males. The resulting M1 plasma concentration-time profile showed the same tendency.

3.1.4.2 Influence of Study

A simulation was performed to assess the impact of the covariate "study" on the plasma concentration-time profiles. The estimated V4 values for studies PI.1-4 (21.7 L) and PI.5-6 (72.5 L) were used for simulation. The study difference did not show a relevant influence on the NS2330 plasma concentration-time profile. The plasma concentration-time profiles of M1 are shown in Figure 7.8 (Appendix, Page 143). For study PI.5-6 a longer period of 3 - 4 weeks was necessary to reach steady-state concentration, at steady-state no difference occurred.

3.1.4.3 Influence of Creatinine Clearance

A simulation was performed to assess the impact of creatinine clearance on the plasma concentration-time profiles. The 5th and 95th percentile of the population values were used for simulation. In addition, the central volume of distribution estimated for studies PI.1-4 was used for simulation. Creatinine clearance did not show a relevant on NS2330 plasma concentration-time profiles. The plasma concentration-time profiles of M1 are shown in Figure 7.9 (Appendix, Page 143). For subjects with a higher creatinine clearance a longer period was necessary to reach steady-state concentration, at steady-state no difference occurred.

3.2 Project II – Population PK Analysis in Proof of Concept Study

As described within the method section (2.5.2.7), population pharmacokinetic modelling of NS2330 and its metabolite in AD patients was performed in a sequential manner. First, an interim analysis was performed using data from approximately 75% of all patients treated with NS2330. Finally, the remaining patients and some additional samples from already included patients were incorporated into the dataset to evaluate the final model obtained by the interim analysis.

3.2.1 Dataset

Two datasets (A and B) were built for modelling purposes. Dataset A was used for the interim analysis including a subset of 254 out of all 320 patients treated. This dataset was developed before database lock was completed using all data available. Dataset B was built after database lock was completed and used for the model evaluation of the interim analysis where all 320 patients treated were included. During this step additional plasma samples from already included patients were incorporated into the database and some already existing measurements were cleaned.

3.2.1.1 Observations

Due to implausibility 53 NS2330 and 44 M1 concentrations of dataset A (3.6% of all observations) and 36 NS2330 and 33 M1 concentrations from dataset B (1.8% of all observations) were removed *a priori*. The final dataset A included 254 patients contributing 1370 NS2330 and 1196 M1 plasma concentrations above the lower limit of quantification. The final dataset B included 320 patients contributing 1969 NS2330 and 1714 M1 plasma concentrations above the lower

limit of quantification. Compared to dataset A the number of plasma concentrations increased by 44.7% for NS23330 and 43.3% for M1. This increased number results from measurements of the new patients included but also from new measurements of the already included 2/3 of the patients obtained after database lock. All observations were well distributed over each dose group (Table 7.15, Page 122). Figure 7.10 (Appendix, Page 144) shows the plasma concentration versus time of all patients. Plots are separated by dose groups and analyte. Overall, a dose-dependent increase in plasma concentration was observable. Concentrations observed showed a wide range from 0.101 ng/mL to 105 ng/mL for NS2330 and from 0.118 ng/mL to 47.3 ng/mL for M1.

3.2.1.2 Population Characteristics

The characteristics of the population of dataset A and B are summarised in Table 7.16, Table 7.17 and 7.18 (Appendix, Pages 123 and 124). Characteristics reported reflect the measurements taken at the start of treatment (visit 2). Composition of population B showed no difference compared to population A. Over time no significant changes within the values were observable within both populations. Distributions of the continuous covariates of population B are shown in Figure 7.11 (Appendix, Page 145). Distributions of population A were comparable. Elevated liver enzyme concentrations were only observed in a few subjects and only at start of treatment. Correlations between continuous covariates of population B are shown in Figure 7.11 (Appendix, Page 145). No unexpected correlation between covariates was observed. Correlations of population A were comparable.

3.2.2 Population Pharmacokinetic Modelling

3.2.2.1 Model Development

In accordance with the modelling strategy (2.5.2.7), the population PK modelling was performed in a sequential manner. First, the interim dataset A was used to built a base and covariate model, subsequently dataset B was used after data base lock to evaluate the models developed with dataset A.

Dataset A - Interim Analysis   First, NS2330 and M1 concentrations were modelled individually to explore the best structural base model for each compound. Subsequently, a model for both compounds was to be developed where different structural modifications were tested and evaluated.

NS2330 was best described by a one compartment model with a first-order absorption and elimination process. Interindividual variability was implemented on Ka, V and CL. M1 was also best described by a one compartment model with first-order absorption and elimination and IIV on all parameters. In addition, a lag time had to be implemented for M1. For the combined model of parent compound and metabolite one compartment models were used for NS2330 and M1 as obtained within the individual analysis. Formation of M1 from NS2330 was accounted for by a first-order metabolism process. Absorption of NS2330 and elimination of both compounds was accounted for by a first-order process. As described in section 3.1.2.1 assumptions had to be made for a successful simultaneous modelling of parent compound and its metabolite. Two main hypotheses were tested. The first hypothesis A was described and used as in section 3.1.2.1 for Project I. It was assumed that 7% of the overall elimination of NS2330 were transformed into M1. Therefore, the metabolism rate constant was fixed to 7% of the overall elimination rate constant of NS2330. The second hypothesis B was based on the findings from Project V, which had been completed in the meantime. In this analysis M1 showed a 23.2% reduced volume of distribution in mice compared to the volume of distribution of NS2330. Thus, the assumption was made that this ratio might also occur within humans. Consequently, the volume of distribution of M1 was fixed to the 0.768-fold volume of NS2330. Both hypotheses were tested and compared on the basis of the objective function value and of visual inspection of the diagnostic plots. Hypothesis A could not be transferred into an adequate and stable base model. Implementation of interindividual variability on PK parameters was not possible and the objective function of the best model achievable by hypothesis A showed a significant increase compared to the best model achievable with hypothesis B. Consequently, hypothesis B was used for further development.

Dataset B - Final Dataset Base and final covariate model were re-estimated using dataset B. The estimates from the base model were used to check for further covariates that showed a relation to a model parameter. No additional relations were observed. The final covariate model underwent a backward elimination as described in section 2.1.3.5.

3.2.2.2 Base Model

Plasma concentration-time profiles of NS2330 and M1 were best described by one compartment models with first-order elimination processes for both compounds. Elimination of NS2330 from the central compartment was split into a non-metabolic clearance ($CL_{non-met}/F$) which accounted for any elimination pathways except the formation of M1 out of NS2330 and a metabolic clearance (CL_{met}/F) which accounted for this metabolic process. Absorption of

NS2330 was modelled as a first-order absorption process (KA). According to hypothesis B the typical volume of distribution of M1 (V3/F) was set to the 0.768-fold factor of the typical relative volume of distribution of NS2330 (V2/F). A schematic illustration of the PK model is shown in Figure 3.2.
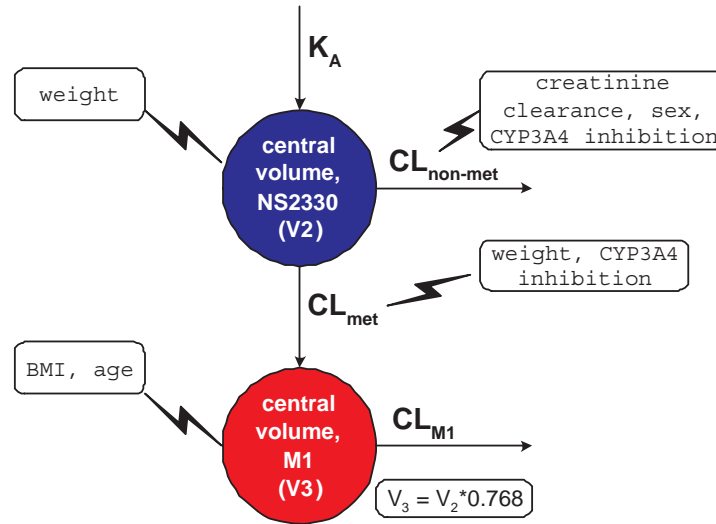

Figure 3.2 Schematic PK model of NS2330 and its major metabolite M1

Interindividual variability was included in non-metabolic clearance (ωCL$_{\mathrm{non-met}}$/F), metabolic clearance (ωCL$_{\mathrm{met}}$/F), central volume of distribution of NS2330 (ωV2/F) and M1 (ωV3/F) and the absorption rate constant (ωKA). A correlation between oral CL$_{\mathrm{non-met}}$ and V2 was implemented in the model. Residual variability was modelled with a combined random effect model for NS2330 and a proportional random effect model for M1.

Dataset A - Interim Analysis   Parameter estimates using dataset A can be found in Table 7.20 (Appendix, Page 125). All parameters were estimated with good precision (relative standard errors ranging from 3.9 to 22.6%, Table 7.20, Appendix), only the additive residual variability of NS2330 was estimated with a higher relative standard error of 69.3%.

Dataset B - Final Dataset   Dataset B could be described successfully by the base model. Parameter estimates using dataset B were comparable to the estimates obtained by the interim dataset A (Table 7.20, Page 125). All parameters were estimated with good precision (relative standard errors ranging from 2.3 to 47.1%, Table 7.20, Appendix). Overall, the precision of the parameter estimates improved compared to the estimates obtained from dataset A, indicating that the additional data supported the developed model. The goodness of fit plots

of NS2330 and M1 are shown in Figure 7.12 (Appendix, Page 146). All concentrations were spread around the line of identity, indicating that the data was well described by the model.

3.2.2.3 Final Covariate Model

The covariates tested on the individual PK parameters of the final base model are listed in Table 7.19 (Appendix, Page 124). They were selected as described within the method section (2.1.3.5).

Even though less than 10% of the plasma concentrations were taken under the influence of each of the co-medication groups (CYP3A4 inhibitors and inducers) all co-medications were tested for informative purpose. Additionally, CLCR on V3 was tested based on the findings in project I.

The covariate analysis identified weight as a statistically significant covariate on CL_{met}/F and V2/F. For patients with a creatinine clearance lower than 62.5 mL/min an influence of CLCR on $CL_{non-met}/F$ was found. In addition a sex difference was depicted for $CL_{non-met}/F$. Body mass index and age were explored to have a statistically significant influence on V3/F. The mathematical expressions for the relations found are listed in Table 7.21 (Appendix, Page 126).

The influence of co-medications was tested exploratory using the final covariate model and revealed that CYP3A4 inhibitors had a statistically significant influence on both clearances of NS2330.

Dataset A - Interim Analysis Parameter estimates of the final covariate model can be found in Table 7.21 (Appendix, Page 126). All parameters were estimated with good precision (relative standard errors ranging from 2.7 to 33.1%, Table 7.21), only the additive residual variability of NS2330 was estimated with a higher standard error of 65.0%.

As mentioned before CYP3A4 inhibitors had a statistically significant influence on the clearances of NS2330. The overall clearance of NS2330 was found to be reduced by 40% and 45% in females and males, respectively. Overall, only 4.4% of the NS2330 plasma samples (61 of 1370) were taken under CYP3A4 inhibitor treatment.

Dataset B - Final Dataset Dataset B could be described successfully by the final covariate model. Parameter estimates using dataset B were comparable to the estimates obtained by using the interim dataset A (Table 7.21, Appendix, Page 126). Backward elimination revealed that all covariates described before remained in the model as statistically significant. The mathematical relations can be found in Table 7.21. According to those relations and the 5th and

95th percentile covariate values of the dataset (Table 7.17, Page 123) the typical $CL_{non-met}/F$ for males will decrease from 1.52 L/h to 1.04 L/h and for females from 1.16 L/h to 0.795 L/h as creatinine clearance decreases from $\geq$62.5 to 35.6 mL/min. The typical CL_{met}/F will decrease from 0.42 to 0.352 L/h as weight increases from 47.7 kg to 103 kg. The typical V2/F will increase from 509 L to 890 L as weight increases from 47.7 kg to 103 kg. For a typical patient with an age of 75.5 years (median) the typical V3/F will increase from 440 to 598 L as BMI increases from 19.8 to 35.3 kg/m^2. For a typical patient with a BMI of 25.5 kg/m^2 (median) V3/F will increase from 386 to 568 L as age increases from 60 to 86 years.

The parameter estimates of the final covariate model can be found in Table 7.21 (Appendix, Page 126). Large relative volumes of distribution were estimated for NS2330 and M1. The overall relative volume of distribution was 649 L for NS2330 and 499 L for NS2330. The low relative clearances of NS2330 and M1 in combination with the large relative volumes of distribution revealed long half-lives with 234 h (males) or 289 h (females) for NS2330 and with 373 h for M1.

Estimates for interindividual variability were moderate to high with 70.2% in $CL_{non-met}/F$, 23.6% in CL_{met}/F, 30.5% in V2/F, 33.2% in V3/F and 95.6% in Ka. Compared to the base model the variability was reduced by 15.5% (i.e. -5.6 percent points) for V2/F, 8.7% (i.e. -6.7 percent points) for $CL_{non-met}/F$, 7.5% (i.e. -2.7 percent points) for V3/F and 2.9% (i.e. -0.7 percent points) for CL_{met}/F.

The proportional components of the residual variability were determined to be 19.4% and 19.9% for NS2330 and M1, respectively. The additive residual variability for NS2330 was 0.146 ng/mL. All parameters were estimated with good precision (relative standard errors ranging from 2.2 to 45.9%, Table 7.21). Overall, the precision of the parameter estimates improved compared to the estimates obtained from dataset A, indicating that the additional data supported the model developed. The goodness of fit plots of NS2330 and M1 are shown in Figure 7.13 (Appendix, Page 147). The additional data from the new patients and the cleaned or additional data of the patients already included in dataset A did not showed a trend in the goodness of fit plot. All concentrations (observed versus predicted) are spread around the line of identity, indicating that the data was well described by the model.

Also with dataset B the CYP3A4 inhibitors had a statistically significant influence on the clearances of NS2330. The overall clearance of NS2330 was found to be reduced by 20% using dataset B. Overall, only 5.8% of the NS2330 plasma samples (114 of 1969) were taken under CYP3A4 inhibitor treatment.

3.2.3 Evaluation

3.2.3.1 Internal Evaluation

The application of the additional data (dataset B) to the final model developed with dataset A was also used to evaluate the model internally. As described within the previous section the internal validation was successful. The additional data was well supported by the model.

3.2.3.2 External Evaluation

The external evaluation was performed as described in the method section (2.5.2.8). The predicted concentrations versus the observed concentrations are shown in Figure 7.14 (Appendix, Page 148). All values of the parent compound were well distributed around the line of identity, indicating that the measurements are very well predicted by the model.

The parameter distribution of the evaluation run is presented in Figure 7.15 (Appendix, Page 149). The individual estimates η of the interindividual variability were normally distributed around mean zero, indicating that the estimated population parameters revealed no bias.

3.2.4 Simulation

For all simulations performed the profiles of male subjects are shown. Female profiles always showed the same trend but were generally lower.

3.2.4.1 Interim Model vs. Final Model

Simulation was performed using the final covariate model results from interim model (dataset A) and final model (dataset B) and the median covariate values. For the simulation a dosing regimen of 1 mg NS2330 orally administered once daily for 166 days (4000 h) was assumed. Plasma concentration-time profiles of NS2330 and M1 did not showed a difference between the final models (Figure 7.16, Page 149), indicating that the new data used did not influence the parameter estimates.

3.2.4.2 Influence of Covariates

Simulations were performed to assess the impact of covariates on the plasma concentration-time profile of NS2330 and M1, respectively. For the simulations a dosing regimen of 1 mg

NS2330 orally administered once daily for 166 days (4000 h) was assumed. Model and parameter estimates from the final covariate model obtained with dataset B were used for simulation. Except for the covariate relations investigated for the remaining ones the median covariate values were considered.

Influence of Sex   A simulation was performed to assess the impact of sex on the plasma concentration-time profiles (Figure 7.17, Page 150). At steady-state females showed 23% increased trough concentrations compared to males. The resulting M1 profile showed the same trend.

Influence of Creatinine Clearance   A simulation was performed to assess the impact of creatinine clearance on the plasma concentration-time profiles (Figure 7.18, Page 150). The 5th and 95th percentiles (35.6 mL/min and 112.9 mL/min) of the population values were used for simulation. Steady-state concentrations for reduced CLCR values were significantly increased. The resulting M1 profile showed the same trend. According to the mathematical relation of the covariate influence the profile for all patients with a CLCR greater than the median value (62.5 mL/min) were identical.

Influence of Weight, BMI and Age   Simulation were performed to assess the impact of weight, BMI and age on the plasma concentration-time profiles. For Weight no significant difference between the simulated NS2330 plasma concentration-time profiles at steady-state was observable (Figure 7.19, Page 151). The resulting M1 profile showed the same trend. As BMI and age showed only an influence on parameters of M1, no difference occurred within the NS2330 profiles. At steady-state no significant difference between the simulated M1 plasma concentration-time profiles was observable for BMI and Age (Figures 7.20 and 7.21, Page 151).

Influence of Sex and Creatinine Clearance   A simulation was performed to assess the impact of the two covariates (CLCR and SEX) with the largest influence on the exposure in combination (Figure 3.3). The trough concentration at steady-state for a female subject wit CLCR of 35.6 mL/min is increased by 62% compared to the trough concentration of a male subject with CLCR = 62.5 mL/min (34 vs. 21 ng/mL).

3.2.4.3 Project I vs. Project II

A simulation was performed showing the typical profiles for NS2330 and M1 for a median male patient based on the final covariate models of project I and project II (dataset B). For the
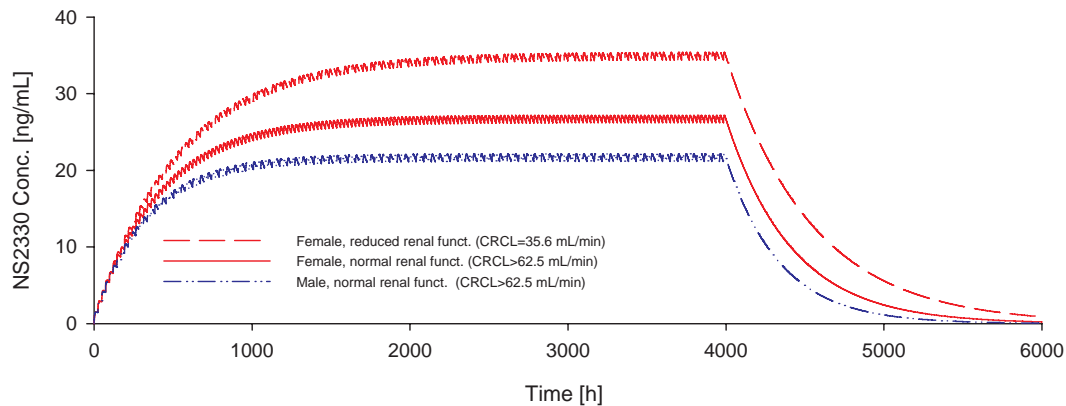
Figure 3.3 Impact of sex and CRCL on the plasma concentration-time profiles of NS2330 after oral administration of 1 mg NS2330 once daily for 166 days (4000 h). Typical profiles of a male with normal renal function, a female subject with normal renal function and a female subject with reduced renal function.

simulations a dosing regimen of 1 mg NS2330 orally administered as single dose or once daily for 166 days (multiple dose) was assumed.

Both models predicted comparable single dose profiles for NS2330 (Figure 7.22, Page 153). Logarithmic plot shows that the terminal elimination phase is slightly faster for Project I. The M1 plasma concentration-time profile using the project II model was slightly increased. The multiple dose profiles predicted by the models were comparable (Figure 7.22, Page 153) for NS2330, for M1 the steady-state predictions using the project II model were slightly increased ($\approx$9 vs. $\approx$7 ng/mL).

3.3 Project III – Enterohepatic Circulation

During graphical analysis of the NS2330 plasma concentration-time profiles multiple peaks were realised. The hypothesis was generated whether an EHC might be responsible for this phenomenon. The aim of this analysis was to develop a mechanistic population PK model that describes the multiple peak phenomenon of NS2330 in plasma.

3.3.1 Dataset

The dataset was created by extraction of the data from study PI.1 (iv, single dose escalation study) from the dataset created for project I. Only NS2330 plasma concentration-time profiles were investigated.

3.3.1.1 Observations

The dataset used for PK modelling included 409 NS2330 plasma concentrations from 21 subjects. Plots of the individuals separated by dose groups are shown in Figure 7.23 (Appendix, Page 154). The multiple peak phenomenon is well observable within the plots. Observed concentrations ranged from 0.103 ng/mL up to 1.86 ng/mL. No observations were missing.

3.3.1.2 Population Characteristics

Twenty-one healthy Caucasian males aged between 21 and 45 years were included in this study. Characteristics of the population are summarised in Table 7.22 (Appendix, Page 127). Overall, the ranges of the demographics were small and within the reference ranges.

3.3.2 Population Pharmacokinetic Modelling

3.3.2.1 Model Development

As described within the modelling strategy (section 2.5.3.3) several models found in the literature[74–76] were examined. In all cases the application failed presumably caused by the fact, that most of the models presented were limited within their number of gall bladder emptyings. As NS2330 is a drug with a long half-life, the multiple peak phenomenon in the plasma concentration-time profile was still observable over a long period. These later peaks were not covered by most models published. An improved model was presented by Wajima et al.[77] overcoming these limitation. Wajima et al. used a 2-compartment model (representing central and gall bladder) with first-order elimination. The mass transfer from gall bladder to the central compartment was controlled by a trigonometric function FX as described in the following equation (Eq. 3.1):

$$FX = sin \left(\frac{2\pi}{\Omega} \cdot (TDEL + TIME) \right) \geq 0 \tag{3.1}$$

where TIME denotes the time elapsed from the first dose administered, Ω is the period of the sine function and TDEL denotes the shift of the sine function to the origin. The function presented allows a pulsatile release of the gall bladder over the whole study period. Unfortunately, this model could not successfully be applied to the data available. When inspecting the behaviour of the model more closely the major limitation for drugs with long half-lives become apparent: In Figure 3.4 (left panel) the gall bladder emptying function (FX) versus the clock time on the first three days after administration is shown using the following function parameter: $\Omega = 6.28$ h and TDEL = 1.5 h.
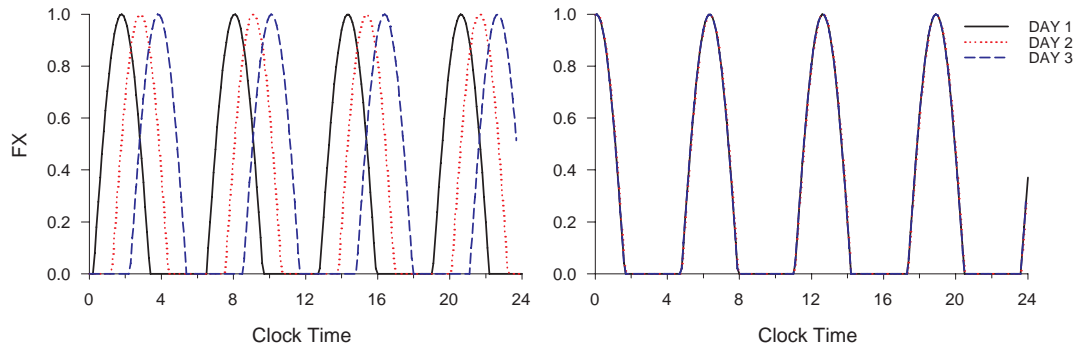
Figure 3.4 FX Curve - Project III

As can be seen, on each day the gall bladder emptying occurred at different clock times of the day. This shift will always occur, as long as the value for Ω is no integer factor of 24, e.g. 6, 8 or 12 h. This day to day variability of the gall bladder emptying suggests that the model will be instable for long half-life drugs, mainly caused by the varying gall bladder rhythm across the study days. To overcome this limitation several modifications of the model were developed. The most promising was the implementation of the clock time (CLOCK) in the model rather than the time elapsed from the first dose (Eq. 3.2).

$$FX = sin\left(\frac{2\pi}{\Omega} \cdot (TDEL + CLOCK)\right) \geq 0 \tag{3.2}$$

This modification allowed to describe a constant circadian rhythm of the gall bladder release each day. The right panel in Figure 3.4 shows this situation as an example using the same function parameters as mentioned above.

The clock time was calculated on the basis of the administration according to the following equation (Eq. 3.3):

$$CLOCK = ATIM + TIME - \left(INTEGER\left(\frac{ATIM + TIME}{24}\right) \cdot 24\right) \tag{3.3}$$

where ATIM denotes the clock time as a decimal number of the first dose administered (= start time of the study) and TIME is the time elapsed from the first dose. Implementation of the clock time drastically stabilised the model and allowed the successful application to the data available. Consequently, the modified FX function was used for further model development. In addition, a significant stabilisation of the model was achieved when a parameter FBIL was implemented and estimated instead of K12. FBIL reflects the fraction excreted into the bile within each cycling step and was defined according to the following equation (Eq. 3.4):

$$FBIL = \frac{K_{12}}{K_{12} + K_{10}} \tag{3.4}$$

where K_{12} denotes the mass transfer from the central compartment to the bile compartment and K_{10} describes the first-order elimination rate constant from the central compartment.

3.3.2.2 Base Model

Data was best described by a two compartment model (central and gall bladder) with first order elimination. The change of the amounts in the compartments was described using the following differential equations (Eq. 3.5):

$$\frac{dA}{dt}(central) = -K_{12} \cdot A(central) + K_{21} \cdot A(gall\ bladder) \cdot FX - K10 \cdot A(central)$$
$$\frac{dA}{dt}(gall\ bladder) = +K_{12} \cdot A(central) - K_{21} \cdot A(gall\ bladder) \cdot FX \tag{3.5}$$

As described within section 3.3.2.1, implementation of "clock time" rather than "time elapsed from first dose" in the gall bladder control function (FX) was found to be a prerequisite for the successful application of this EHC model. The model is schematically illustrated in Figure 3.5.
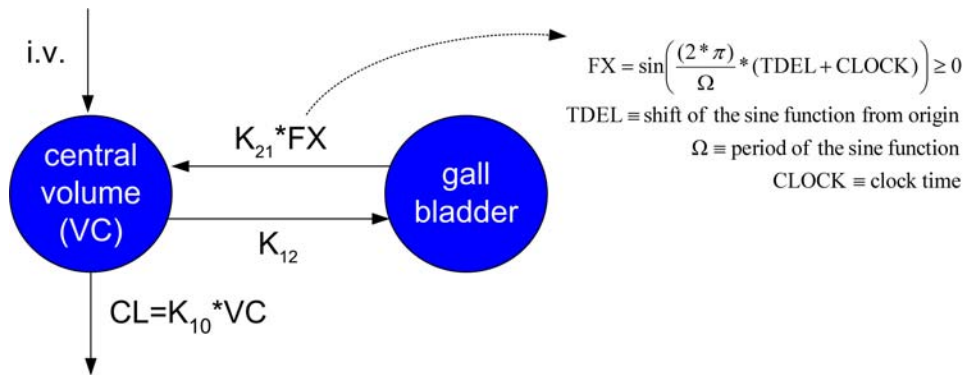
Figure 3.5 Schematic NS2330 Model - Project III

Interindividual variability was included in clearance (ωCL) and the central volume of distribution (ωVC). Residual variability was modelled with a combined random effects model for NS2330. The Laplacian estimation method was applied. Parameter estimates of the final model can be found in Table 7.23 (Appendix, Page 127).

The low clearance and large volume of distribution resulted in a long terminal half-life of 197 h. Parameter estimates for Ω and TDEL were 6.28 h and 1.5 h, respectively. Figure 3.4 (Page 58, right panel) shows the resulting gall bladder release function at each day. The curve

shows a 3.5-fold emptying every day, with full peaks at approximately 6 am, 12 am, 6 pm and a reduced peak at midnight. Standard errors for the parameter estimates were not available due to an aborted covariance step. Estimates for interindividual variability were low with 21.9% in CL and 14.5% in VC. The proportional components of the residual variability were determined to be 11.5%, the additive residual variability for NS2330 was ± 0.08 ng/mL. The goodness of fit plots are shown in Figure 7.24 (Appendix, Page 155). All concentrations were spread around the line of identity, indicating that the data was well described by the model.

3.3.3 Evaluation

Evaluation was performed as described in the methods section 2.5.3.4. In brief, the model was to be evaluated by using data of meloxicam, a drug known to undergo EHC[72]. Evaluation was to be performed by a) fitting the model developed to observed meloxicam plasma concentrations and b) by predicting the effect on the pharmacokinetics of meloxicam when the EHC is interrupted by co-administration of cholestyramine.

3.3.3.1 Dataset

Twelve healthy male subjects, aged between 27 and 50 years were included in the study and used for modelling. The dataset contained 227 and 217 plasma concentrations above LLQ from the meloxicam and the meloxicam plus cholestyramine treatment arm, respectively.

3.3.3.2 Population Pharmacokinetic Modelling

A three compartment model (central, peripheral and bile) with first-order elimination (Figure 7.25, Page 155) described the data best. Both study arms were modelled simultaneously. For the cholestyramine treatment arm an additional elimination rate constant from the gall bladder compartment (K_{20}) was implemented. Both sine functions using time (3.1) or clock time (3.2) to control the gall bladder release were explored. The clock time (Eq. 3.2) as a control variable was again found to be superior over the time function and was used for finalising the model. Implementation and estimation of FBIL instead of K_{12} stabilised the model significantly. FBIL reflected the fraction excreted into the bile within each cycling step and was defined according the following equation (3.6):

$$FBIL = \frac{K_{12}}{K_{12} + K_{13} + K_{10}} \tag{3.6}$$

where K_{12} denotes the mass transfer from the central compartment to the bile compartment, K_{13} the mass transfer from the central compartment to the peripheral compartment and K_{10}

describes the first order elimination rate constant from the central compartment.

Interindividual variability was included in clearance (ωCL) and the central volume of distribution (ωVC). Residual variability was modelled with a combined random effects model for meloxicam. The centering Laplace estimation method was applied. Parameter estimates of the final model can be found in Table 7.23 (Appendix, Page 127). All parameters were estimated with good precision (standard errors ranging from 1.04 to 43.9%, Table 7.23). Estimates for interindividual variability were low with 29.6% in CL and 9% in VC. The proportional component of the residual variability was determined to be 9.9%, the additive residual variability for meloxicam was ±0.03 mg/L. The goodness of fit plots are shown in Figure 7.26 (Appendix, Page 156). All concentrations were spread around the line of identity, indicating that the data was well described by the model. Clearance and half-life of meloxicam after intravenous administration were determined to be 0.396 L/h and 18.9 h respectively. These model-predicted values were in close agreement with the observed results from the individual compartmental analysis (Table 7.24, Page 128). Parameters Ω and TDEL revealed a three times daily release of the gall bladder at physiologically reasonable time points (Figure 7.27, Page 157).

3.3.3.3 Interruption of EHC

Prediction of the complete interruption of the EHC was mimicked by setting the rate transfer constant from bile to central compartment (K21) to zero, resulting in an increased clearance of 0.75 L/h and a shortened half-life of 10.0 h. These model-predicted values were in close agreement with the observed results from the individual compartmental analysis[72] (Table 7.24, Page 128), but the predicted values showed a slight over-prediction compared to the observed values, presumably caused by an incomplete inhibition of meloxicam reuptake by cholestyramine which was observable in the representative individual profiles (Figure 7.27, Page 157).

3.3.4 Simulation

3.3.4.1 Interruption of EHC

A simulation was performed to predict the influence of a completely interrupted EHC on the plasma concentration-time profiles (Figure 7.28, Page 158). An infusion of 1 mg NS2330 over 6 h was simulated. The interruption of the EHC was mimicked by setting K21 to zero. The interrupted profile showed an extreme decrease in plasma concentrations. The half-life was reduced from 192 h to approximately 5 h.

A simulation was performed using an intensive sampling schedule where a sample was taken every 0.1 h. Exemplarily, two individuals were selected and their individual parameters were used for simulation to illustrate the observed concentrations and the individual predicted concentration-time profiles. Figures 3.6 and 7.29 (Appendix, Page 159) show the individual plots of subjects A and B, respectively, for the first 80 h after administration. Individual predictions described the observed concentrations well and showed the multiple peak phenomenon predicted by the model. In addition, the gall bladder release curve (FX) is shown. Peaks in the NS2330 plasma concentration-time profiles occurred with an approximately 2 h delay compared to the peaks of the FX curve. Overall, 4 peaks per day were observable. The reduced emptying of the gall bladder at midnight also results in a reduced plasma peak. In summary, the EHC is a very plausible mechanism to account for multiple peak phenomenon.
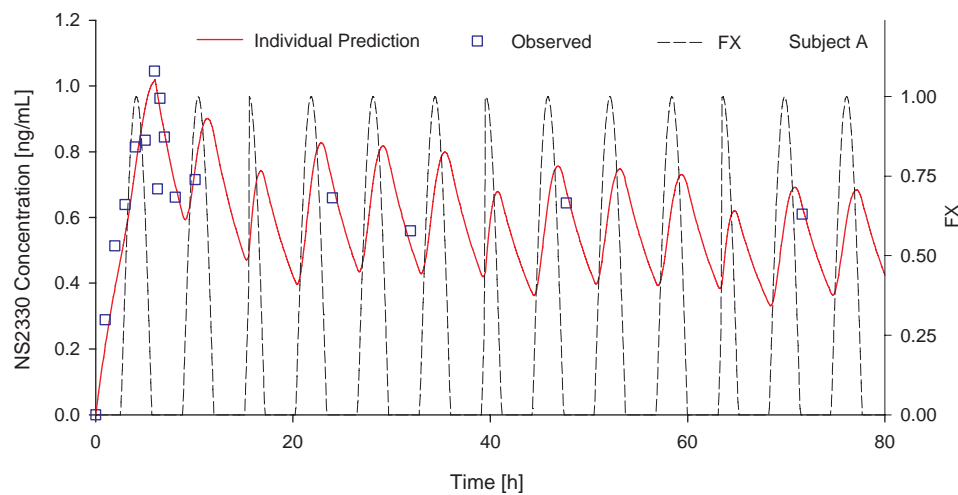

Figure 3.6 Simulated individual profiles of subject A.

3.4 Project IV – Impact of CYP3A4 Metabolism

The aim of this analysis was to develop a mechanistic population PK model that allowed the assessment of the maximum effect of a complete CYP3A4 inhibition on the elimination of NS2330.

3.4.1 Dataset

A complete dataset was created for the interaction model. For the development of the itra-conazole model a subset of this dataset (co-administration with ITZ) was used.

3.4.1.1 Observations

The dataset used for PK modelling included 455 NS2330 plasma concentrations from 28 sub-jects, 14 of them contributed 70 itraconazole plasma concentrations (Table 7.25, Page 128). Plasma concentrations of NS2330 and ITZ versus time are shown in Figure 7.30 (Appendix, Page 160). Itraconazole showed increasing trough concentrations over time, indicating that steady-state had not completely been reached at the end of treatment.

Observed NS2330 concentrations ranged from 0.109 ng/mL up to 4.2 ng/mL, itraconazole concentrations ranged from 184 ng/mL up to 912 ng/mL. NS2330 values below the lower limit of quantification occurred only within the elimination phase and were removed *a priori* from the dataset.

3.4.1.2 Population Characteristics

Twenty-eight healthy Caucasian males aged between 25 and 46 years were included in this study. Characteristics of the population are summarised in Table 7.26 (Appendix, Page 128). Both treatment arms showed comparable population characteristics. Overall, the ranges of the demographics were small and within the reference ranges.

3.4.2 Population Pharmacokinetic Modelling

3.4.2.1 Model Development

As described within the modelling strategy (section 2.5.4.7) the model development was per-formed in a sequential manner. First, a separate model for itraconazole was built. Subse-quently, an interaction model was built.

Itraconazole Model Initially, standard one and two compartment models were tried to ap-ply to the data. Goodness of fit plots of all standard models showed a significant trend of the weighted residuals over the time. An example is shown in Figure 7.31 (left panel, Page 161), where a standard one compartment model with interindividual variability on clearance is shown. This trend clearly indicates that the models tested were inappropriate for the data

situation. In depth evaluation showed that the bias observed was mainly caused by the increasing concentrations over time, presumably caused by a change of the ITZ clearance over the treatment duration. In the literature an increase in half-life after 14 days of treatment has been described[78]. This phenomenon might be caused by either a saturable elimination of ITZ or by an auto-inhibition of ITZ elimination. As ITZ is also metabolised by CYP3A4[79] this hypothesis seems reasonable. Both approaches were implemented into the models. A Michaelis-Menten (MM) elimination was implemented to investigate the saturable elimination hypothesis. This model could not be applied successfully. The goodness of fit plots still showed a trend of the weighted residuals over time. A more complicated model was applied to describe the auto-inhibition hypothesis. Therefore, a hypothetical auto-inhibition compartment was implemented in the model where the respective concentrations within the compartment ($C_{INH, ITZ}$) were responsible for the inhibition of the ITZ elimination. The auto-inhibition model could successfully be applied and the bias over time entirely disappeared (Figure 7.31, Page 161). Thus, the auto-inhibition model was used for further model development.

NS2330 Interaction Model   Initially, NS2330 data was modelled independently from the ITZ data to explore an adequate structural model describing the data. A one compartment model with first-order absorption and elimination was found to describe the data adequately. Subsequently, a combined interaction model was created where the parameter estimates for the PK of ITZ were initially fixed. An Emax model was used to describe the inhibitory effect of ITZ on the elimination of NS2330. Emax was coded as a reduction in percent (see Eq. 3.7). Different links to the ITZ concentration were tested. First, a link from the concentrations of the auto-inhibition compartment ($C_{INH, ITZ}$) was investigated. Second, a link from the concentrations in the central compartment of ITZ was examined. Finally, the ITZ concentration within an additional effect compartment was tested. It was found that a direct link to the ITZ concentration was sufficient to describe the NS2330 data. An additional effect compartment did not show any improvement. A link to the $C_{INH, ITZ}$ concentration could not be implemented successfully. The selected structural model was finalised and the PK of ITZ was unfixed to allow a simultaneous estimation of the PK of NS2330 and ITZ.

3.4.2.2 Base Model

Itraconazole   Data of itraconazole was best described by a one-compartment model. Absorption was described using a zero-order absorption. Elimination was described using a first-order elimination rate constant. The influence of the auto-inhibition was best accounted for by using a hypothetical inhibition compartment where the concentration within this com-

partment determined the extent of inhibition. This concentration was determined by a first-order rate constant (KEO). A schematic illustration of the model can be found in Figure 3.7, the mathematical expression as differential equations can be found in the following (Eq. 3.7):

$$\frac{dA}{dt}(ITZ) = -A(1) \cdot K_{EL,ITZ} \cdot \left(1 - \frac{I_{MAX,ITZ} \cdot C_{INH,\,ITZ}}{IC_{50,ITZ} + C_{INH,\,ITZ}}\right) + INPUT$$

$$\frac{dA}{dt}(INH,\,ITZ) = K_{EO} \cdot (C_{ITZ} - C_{INH,\,ITZ})$$

$$INPUT = \begin{cases} \frac{DOSE}{D1} & \text{if TIME} \leq \text{D1} \\ 0 & \text{if TIME} = 0 \end{cases}$$

(3.7)

where $K_{EL,ITZ}$ denotes the elimination rate constant of itraconazole, $I_{MAX,ITZ}$ describes the maximum effect of ITZ on its own elimination, $C_{INH,\,ITZ}$ denotes the ITZ concentration within the ITZ hypothetical inhibition compartment, $IC_{50,ITZ}$ is the ITZ concentration in the hypothetical inhibition compartment yielding 50% $I_{MAX,ITZ}$, INPUT describes the zero-order input and D1 denotes the duration of the zero-order input.

Due to the sparse data situation some parameters had to be fixed to obtain reliable values. V/F was fixed to 700 L, a value reported within the literature[73]. D1 was fixed to 0.4 h and KEO was fixed to 0.01 1/h, both values best describing the data available.

Interindividual variability was included in $IC_{50,ITZ}$ ($\omega IC_{50,ITZ}$). Residual variability was modelled with a proportional random effect model for ITZ. The FOCE INTERACTION estimation method was applied. Parameter estimates for ITZ can be found in Table 7.27 (Appendix, Page 129). No differences in estimates compared to the single ITZ model occurred. All parameters were estimated with good precision (relative standard errors ranging from 1.8 to 51%, Table 7.27). Estimates for interindividual variability were high with 55.3% in $IC_{50,ITZ}$. The proportional residual variability was determined to be 11.1%. The goodness of fit plots are shown in Figures 7.31 and 7.32. In Figure 7.32 all concentrations were spread around the line of identity, indicating that the data was well described by the model. Figure 7.31 shows that no trend over time was observable, indicating that the model well covers the change in clearance over time. Considering the administered dosing regimen for ITZ within this trial the half-life of ITZ increased from $\approx$17 h at day 1 to $\approx$44 h at day 11. These results are in close agreement with changes in half-life reported in literature[78].

NS2330 Data of NS2330 was best described by a one compartment model. Absorption and elimination of NS2330 were best described using a first-order rate constant. Influence of ITZ on the elimination of NS2330 was accounted for by using a proportional Emax model describ-
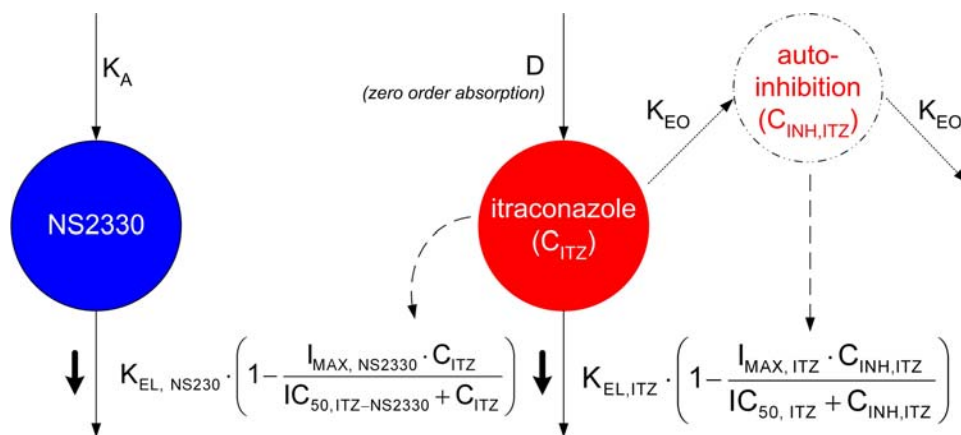
Figure 3.7 Interaction Model - Project IV

ing the maximum inhibitory effect in a percentage manner. The Emax model was linked from the ITZ concentrations within the central compartment of ITZ. A schematic illustration of the model can be found in Figure 3.7, the mathematical expression can be found in the following differential equations (Eq. 3.8):

$$
\frac{dA}{dt}(Absorpt.) = -A(Absorpt.) \cdot K_A
$$
$$
\frac{dA}{dt}(Central) = +A(Absorpt.) \cdot K_A - A(Central) \cdot K_{EL,NS2330} \cdot \left(1 - \frac{I_{MAX,NS2330} \cdot C_{ITZ}}{IC_{50,ITZ-NS2330} + C_{ITZ}}\right)
$$
$$(3.8)$$

where KA denotes the first-order absorption rate constant, $K_{EL,NS2330}$ describes the elimination constant of NS2330, $I_{MAX,NS2330}$ is the maximum inhibitory effect of ITZ on the elimination of NS2330, C_{ITZ} is the plasma concentration of ITZ and $IC_{50,ITZ-NS2330}$ is the ITZ concentration yielding 50% $I_{MAX,NS2330}$.

Interindividual variability was included in V_{NS2330}/F (ω V_{NS2330}/F), in KA (ωKA) and in $K_{EL,NS2330}$ (ω $K_{EL,NS2330}$). Residual variability was modelled with a proportional random effect model. All parameters from NS2330 and ITZ were simultaneously estimated by the FOCE INTERACTION estimation method. Parameter estimates of the final run can be found in Table 7.27 (Appendix, Page 129). The parameters estimates for KA, V and CL (=$K_{EL,NS2330}$ · V_{NS2330}/F) were comparable to the estimates revealed in projects I and II (Tables 7.12 and 7.21). The maximum inhibitory effect of ITZ was estimated to cause a 39% reduction in the relative clearance of NS2330, resulting in an increased exposure of approximately 63%. All parameters were estimated with good precision (relative standard errors ranging from 1.8 to 46.5%, Table 7.27), only $IC_{50,NS2330}$ was estimated with a lower precision of 86.1%.

Estimates for interindividual variability were mild to moderate with 15.6% in V_{NS2330}, 17.0% in $K_{EL,NS2330}$ and 53.4% in KA. The proportional residual variability was determined to be 15.8% for NS2330. The goodness of fit plots are shown in Figure 7.33 (Appendix, Page 161). All concentrations were spread around the line of identity, indicating that the data was well described by the model.

3.4.3 Simulation

3.4.3.1 Influence of Itraconazole on NS2330 Plasma Concentration

A simulation was performed to visualise the influence of ITZ co-administration on the NS2330 plasma concentration-time profile and the impact of ITZ on the relative clearance of NS2330, i.e. 100% illustrates an unaltered NS2330 clearance by ITZ (Figure 3.8). The same treatment pattern as used for this evaluated study was used for the simulation purpose, i.e. a 2 mg oral single dose of NS2330 was administered, ITZ was administered for 6 days prior to and 5 days after the NS2330 administration. The impact on the relative NS2330 clearance was a 39% reduction over the period of co-administration. The area under the curve (AUC) of NS2330 showed a 9% increase for the first 144 h (AUC_{0-144}) and 20% until infinity ($AUC_{0-\infty}$) under ITZ co-administration compared to the absence of ITZ.
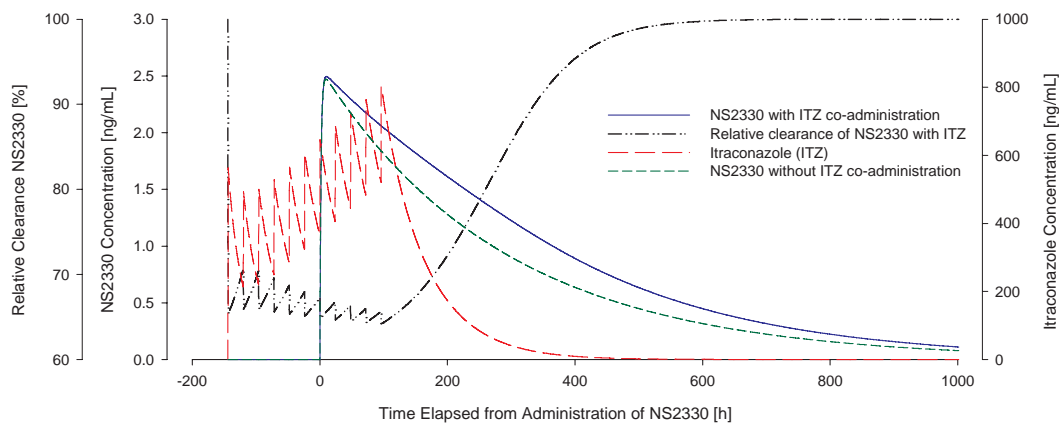

Figure 3.8 Simulated plasma concentration-time profiles of NS2330 with (solid line) and without ITZ co-administration (short dashed line) and ITZ (conc.: long dashed line). In addition the influence of ITZ on the relative clearance of NS2330 is shown (dotted line).

3.4.3.2 Long-term Co-medication with Itraconazole

A simulation was performed to assess the influence of ITZ on the NS2330 steady-state concentration assuming different long-term treatments of ITZ (Figure 3.9). For the simulation of NS2330 a dosing regimen of 1 mg NS2330 administered once daily po for 250 days (6000 h) was assumed. A complete inhibition of the CYP3A4 system after 125 days was assumed for 2 weeks and for 18 weeks, respectively. The simulations showed that after a 2 week inhibition the exposure increased by 34% if the inhibition occurred for a longer period the exposure would increase up to the maximum effect of 63%.
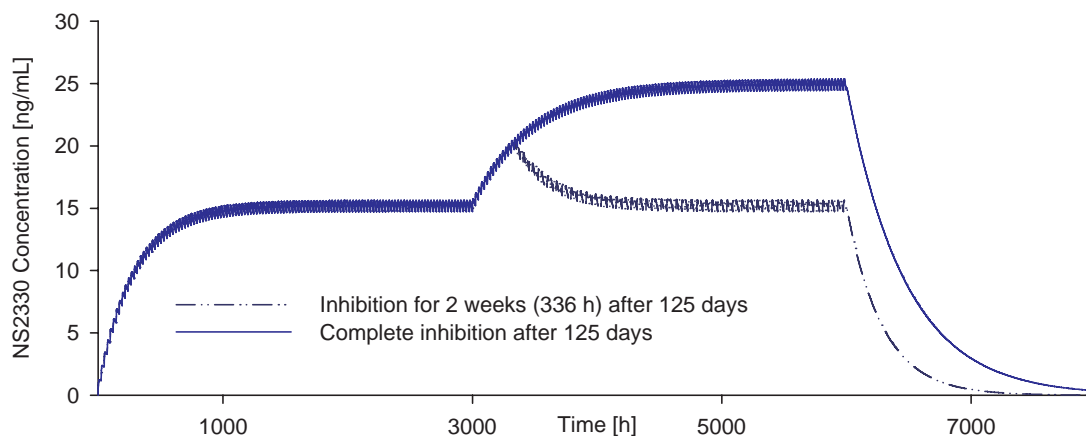
Figure 3.9 Simulated plasma concentration-time profiles of NS2330 administered with ITZ coadministration starting after 125 days (3000 h) for 2 weeks (dotted line) or a permanent inhibition (solid line).

3.5 Project V – Potency of the Metabolite

For this project the potency of the metabolite M1 relative to NS2330 it should be investigated using population PK/PD models. A further objective was to assess whether additional first-pass metabolites were formed during the absorption phase. Finally, the PK properties of NS2330 and M1 were to be explored in mice.

3.5.1 Dataset

A complete dataset was developed for the development of the PK/PD model. For the development of the intermediate key models a subset of this dataset was used. The dataset for PK modelling consisted of 197 plasma concentrations from 132 mice with 65 plasma concentration

measurements of NS2330 and 132 plasma concentration measurements of M1. One plasma concentration value of NS2330 was below the lower limit of quantification and was removed from the dataset. A detailed description of the dataset can be found in Table 7.28 (Appendix, Page 129). Plasma concentrations versus time are shown in Figure 7.34 (Appendix , Page 162) and showed a wide range from 1.26 ng/mL up to 296 ng/mL for NS2330 and from 2.67 ng/mL up to 483 ng/mL for M1. The interindividual variability of the plasma concentrations within a dose group at a particular time point was very low.

The dataset for PD modelling included 132 measurements from 132 mice. Seven PD values were lower than zero and were set to zero for modelling purposes. A detailed description of the dataset can be found in Table 7.28 (Appendix, Page 129). Observed dopamine transporter inhibition versus NS2330 and M1 plasma concentrations are shown in Figure 7.35 (Appendix, Page 163). A wide range from 0% to 94% was observable.

3.5.2 Population Pharmacokinetic Modelling

3.5.2.1 Model Development

As described within the modelling strategy (section 2.5.5.7), the model development was performed in a sequential manner, coming stepwise to the final PK model. First, a PK model for the M1 iv data was developed. A one-compartment model with a saturable MM elimination kinetic adequately described the data. The structural model found was to be identical to the one described for M1 before. In parallel, a PK model for the NS2330 iv data was developed. Subsequently, a combined model was built using data from both intravenous arms. A one-compartment model for NS2330 and M1 was applied and different types of metabolism formation kinetics were investigated. A saturable MM metabolism kinetic best described the data. The saturable elimination of NS2330 was described by different clearance values for the 5 and 10 mg/kg dose group, respectively. Based on this model, oral data from NS2330 was added. The absorption process was described by first order kinetics. In addition, the implementation of a MM first-pass metabolism step and a MM elimination of NS2330 was necessary. At last, the oral data from M1 was added to develop the final base model containing all data available. The final base model will be described in detail in the following section 3.5.2.2. All intermediate models could successfully be developed, describing the data well. Parameter estimates from all final intermediate key models were comparable (Appendix, Tables 7.29, 7.30 and 7.31).

3.5.2.2 Base Model

NS2330 and M1 plasma concentrations versus time of of all data available were described by one compartment models with saturable MM elimination kinetics for both compounds. Absorption of NS2330 after oral administration was described by a first-order process combined with a MM process accounting for a first-pass metabolism. Absorption of M1 was modelled using a first-order absorption process. Metabolic formation of M1 from NS2330 was accounted for by a MM metabolism step. A schematic representation of the model can be found in Figure 3.10, the model was described by the following differential equations that expressed the mass (amount) balance for each of the four compartments (Eq. 3.9):

$$
\begin{aligned}
\frac{dA_{A,NS2330}}{dt} =& D_{NS2330,po} \cdot F_{NS2330} - KA_{NS2330} \cdot A_{A,NS2330} - \frac{A_{A,NS2330} \cdot VM_{FP}}{A_{A,NS2330} + KM_{FP}} \\
\frac{dA_{A,M1}}{dt} =& D_{M1,po} \cdot F_{M1} - KA_{M1} \cdot A_{A,M1} \\
\frac{dA_{C,NS2330}}{dt} =& D_{NS2330,iv} + KA_{NS2330} \cdot A_{A,NS2330} - \frac{A_{C,NS2330} \cdot VM_{MET}}{A_{C,NS2330} + KM_{MET}} \\
& - \frac{A_{C,NS2330} \cdot VM_{EL,NS2330}}{A_{C,NS2330} + KM_{EL,NS2330}} \\
\frac{dA_{C,M1}}{dt} =& D_{M1,iv} + KA_{M1} \cdot A_{A,M1} + \frac{A_{C,NS2330} \cdot VM_{MET}}{A_{C,NS2330} + KM_{MET}} \\
& + \frac{A_{A,NS2330} \cdot VM_{FP}}{A_{A,NS2330} + KM_{FP}} - \frac{A_{C,M1} \cdot VM_{EL,M1}}{A_{C,M1} + KM_{EL,M1}}
\end{aligned}
\tag{3.9}
$$

where $A_{A,NS2330}$ and $A_{A,M1}$ were the amounts of NS2330 and M1 in the absorption compartments and $A_{C,NS2330}$ and $A_{C,M1}$ were the respective amounts in the central compartments, respectively. $D_{NS2330,po}$, $D_{NS2330,iv}$, $D_{M1,po}$ and $D_{M1,iv}$ were the doses of NS2330 or M1 administered orally or intravenously, F_{NS2330} and F_{M1} were the fractions of dose available for absorption and first-pass metabolism after oral administration of NS2330 and M1, respectively. KA_{NS2330} and KA_{M1} were the first-order absorption rate constants of the two compounds. VM_{FP} was the maximum first-pass metabolism rate for NS2330 after oral administration and KM_{FP} the amount yielding 50% VM_{FP}. VM_{MET} was the maximum metabolism rate for the formation of M1 from NS2330 and KM_{MET} the amount yielding 50% VM_{MET}. $VM_{EL,NS2330}$ and $VM_{EL,M1}$ were the maximum elimination rates of NS2330 and M1 from the central compartments and $KM_{EL,NS2330}$ and $KM_{EL,M1}$ the amounts yielding 50% $VM_{EL,NS2330}$ and $VM_{EL,M1}$, respectively.

Amounts calculated in the central compartments were related to the measured plasma concentrations using a scaling factor, where the amounts were divided by the central volumes of distribution of NS2330 (V_{NS2330}) or M1 (V_{M1}), respectively.

Parameter estimates of the final PK model using all data available are shown in Table 7.32 (Appendix, Page 131). Volumes of distribution were found to be large with 17.7 L/kg (NS2330) and 13.6 L/kg (M1), respectively. Due to the limited data in the absorption phase, absorption rate constants (KA) were fixed to constant values of 10 h^{-1} and 5 h^{-1} for NS2330 and M1, respectively. By varying the fixed KA values by a factor of 10 it was shown that fixing had no significant impact on the parameter estimates. As expected only VM_{FP} changed in the same direction all other parameters remained similar. The data did not allow to estimate significantly different MM constants (KM) for the four nonlinear MM processes of the model. Thus, all KM values were assumed to be equal and estimated to be 3.59 mg/kg. Setting this value in relation to the corresponding volumes in the central compartments (i.e. KM/V) revealed KM_{MET} and $KM_{EL,NS2330}$ of 203 ng/mL and a $KM_{EL,M1}$ of 264 ng/mL.

Within the linear range (plasma concentration « KM/V) of NS2330 and M1 the PK parameters clearance (CL) and terminal half-life ($t_{1/2}$) could be derived from the MM parameters estimated by the final model according the following equations (Eq. 3.10 and Eq. 3.11):

$$CL = \begin{cases} \frac{VM_{EL,NS2330} \cdot V_{NS2330}}{KM_{EL,NS2330}} & \text{NS2330} \\ \frac{VM_{EL,M1} \cdot V_{M1}}{KM_{EL,M1}} & \text{M1} \end{cases} \tag{3.10}$$

$$t_{1/2} = \begin{cases} \frac{ln2 \cdot KM_{EL,NS2330}}{VM_{EL,M1}} & \text{NS2330} \\ \frac{ln2 \cdot KM_{EL,M1}}{VM_{EL,M1}} & \text{M1} \end{cases} \tag{3.11}$$

Clearance of NS2330 was found to be high with 5.3 L/h/kg and moderate for M1 with 1.9 L/h/kg. The resulting half-lives in mice were 2.3 h and 4.9 h for NS2330 and M1, respectively.

All parameters were estimated with high precision (RSE < 39.7%, Table 7.32) applying the FO estimation method. Random variability (including IIV and residual variability) was moderate with 35.7% and 36.4% for the PK of NS2330 and M1, respectively. The goodness of fit plot showing the observed versus the predicted concentrations of both compounds is presented in Figure 7.36, left panel (Appendix, Page 164). In general, all concentrations were randomly spread around the line of identity, indicating that the data was well described by the model.

3.5.3 Population Pharmacokinetic/Pharmacodynamic Modelling

3.5.3.1 Model Development

As described within the modelling strategy (section 2.5.5.7) different intermediate models were developed where different types of pharmacodynamic models were necessary to investigate the effect of NS2330 and M1 on the inhibition of the dopamine transporter. The effect of

M1 given alone was described by an Emax model (Eq. 3.12)

$$E(C_{M1}) = \frac{E_{max} \cdot C_{M1}^{N_{M1}}}{EC_{50,M1}^{N_{M1}} + C_{M1}^{N_{M1}}} \tag{3.12}$$

where Emax was the maximum effect attributable to M1 and $EC_{50,M1}$ was the concentration producing 50% of the maximum effect, N_{M1} was the Hill factor affecting the shape of the curve and C_{M1} reflected the concentration of M1 in the central or hypothetical effect compartment, depending on the link chosen between PK and PD.

If parent compound and metabolite were present a competitive interaction between NS2330 and M1 at the binding site of the dopamine transporter occurred. Considering this pharmacological situation, a model reflecting this interaction situation[80] was applied (Eq. 3.13),

$$E(C_{NS2330}, C_{M1}) = \frac{E_{max,NS2330} \cdot \left(\frac{C_{NS2330}}{EC_{50,NS2330}}\right)^{N_{NS2330}} + E_{max,M1} \cdot \left(\frac{C_{M1}}{EC_{50,M1}}\right)^{N_{M1}}}{1 + \left(\frac{C_{NS2330}}{EC_{50,NS2330}}\right)^{N_{NS2330}} + E_{max,M1} \cdot \left(\frac{C_{M1}}{EC_{50,M1}}\right)^{N_{M1}}} \tag{3.13}$$

where two different E_{max} values and Hill factors were present for each compound. For further model development it was assumed that both compounds achieved a complete inhibition of the dopamine transporter. Consequently, the potency parameter E_{max} for both compounds was set to 1. This assumption was further substantiated as the E_{max} was 0.95 when estimated, and this model did not show a statistically significant drop in the objective function and other parameter estimates were not significantly influenced. Under the assumption that the two pharmacodynamic parameters were equal for both compounds Equation 3.13 could be simplified to Equation 3.14:

$$E(C_{NS2330}, C_{M1}) = \frac{E_{max} \cdot \left(\frac{C_{NS2330}}{EC_{50,NS2330}}\right)^{N} + \left(\frac{C_{M1}}{EC_{50,M1}}\right)^{N}}{1 + \left(\frac{C_{NS2330}}{EC_{50,NS2330}} + \frac{C_{M1}}{EC_{50,M1}}\right)^{N}} \tag{3.14}$$

where C_{NS2330} and C_{M1} reflected the concentration of NS2330 and M1, respectively, in the central or hypothetical effect compartment, depending on the link chosen between PK and PD. Implementation of a Hill factor was examined on all intermediate key models and found to be redundant, as a Hill factor of ≈0.98 was estimated which did not have any significant influence on the objective function.

The link between pharmacokinetics and pharmacodynamics chosen for the respective intermediate key models is listed in Table 7.34 (Appendix, Page 132). For all available data the linkage was achieved using hypothetical effect compartments. For the intermediate key models using only iv data effect compartments could also be applied but did not show any

statistical improvement. Parameter estimates were unchanged with and without effect compartments. Consequently and according to the principle of parsimony, they were not implemented in the final model. Mathematically, the concentration-time profiles in the hypothetical effect compartments were described by the following differential equations (3.15):

$$
\begin{aligned}
\frac{dE_{NS2330}}{dt} &= K_{EO,NS2330} \cdot \left(\frac{A_{C,NS2330}}{Vd_{NS2330}} - E_{NS2330} \right) \\
\frac{dE_{M1}}{dt} &= K_{EO,M1} \cdot \left(\frac{A_{C,M1}}{Vd_{M1}} - E_{M1} \right)
\end{aligned}
\tag{3.15}
$$

where $K_{EO,NS2330}$ and $K_{EO,M1}$ reflected the rate constants of NS2330 and M1, $\frac{A_{C,NS2330}}{Vd_{NS2330}}$ and $\frac{A_{C,M1}}{Vd_{M1}}$ were the plasma concentrations in the central compartments and E_{NS2330} and E_{M1} the concentrations in the hypothetical effect compartments, respectively.
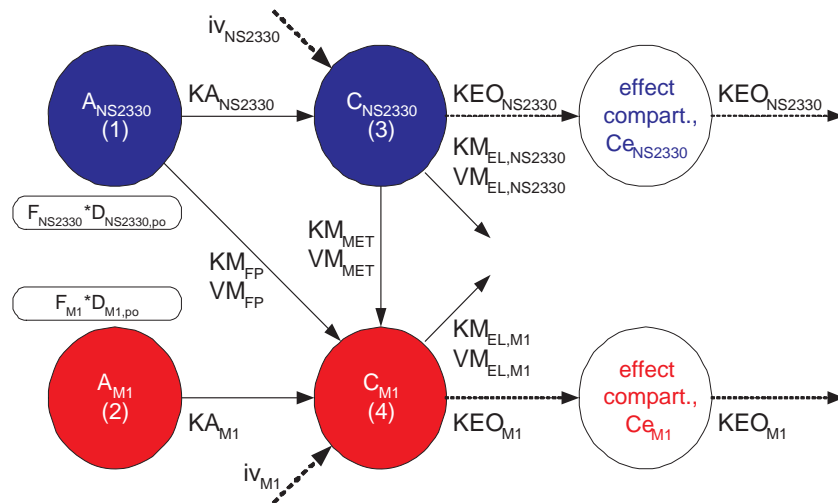
Figure 3.10 Schematic PK/PD model of NS2330 and its metabolite

3.5.3.2 Base Model

The pharmacodynamic effect of all data available was best described by an extended E_{max} model (Eq. 3.14) which accounted for the competitive interaction between NS2330 and M1 on the binding site of the dopamine re-uptake transporter (Figure 3.10).

PD parameter estimates of the final PK/PD model including all data available are shown in Table 7.33 (Appendix, Page 132). EC_{50} values were 23.7 ng/mL for NS2330 and 114 ng/mL for the metabolite M1. Recalculating these values on a molar level revealed EC_{50} values of 72.3 nM for NS2330 and 363.1 nM for M1. PD parameter estimates obtained by intermediate

key models are listed in Table 7.34 (Appendix, Page 132). Comparison of parameter estimates for EC_{50} showed a 4.1- to 5-fold increased EC_{50} value of M1 in comparison to the EC_{50} values of NS2330. Comparing EC_{50} values regarding different administration routes no significant changes in EC_{50} parameter estimates were found between iv administration and a combination of iv and po administration.

All reported PK and PD parameters were estimated simultaneously using the FO estimation method. All PD parameters were estimated with high precision (RSE < 29%, Table 7.33). Random variability (including interindividual and residual variability) was found to be high with 77.5 % and 89.3 % for the PD of NS2330 and M1, respectively. The goodness of fit plot showing the observed versus the predicted inhibition measurements of both compounds is presented in Figure 7.36, right (Appendix, Page 164). All measurements were randomly spread around the line of identity, indicating that the data was well described by the model.

3.5.4 Simulation

The final PK model was used to simulate mean concentration-time profiles after different dosage regimens (1, 3, 5, 10, 20 mg/kg) of intravenous administration of NS2330 or M1. Simulation results are shown in Figure 3.11 (Appendix, Page 74). At concentrations >200 ng/mL for NS2330 and >100 ng/mL for M1 non-linearity was observed for the plasma concentration-time profiles.
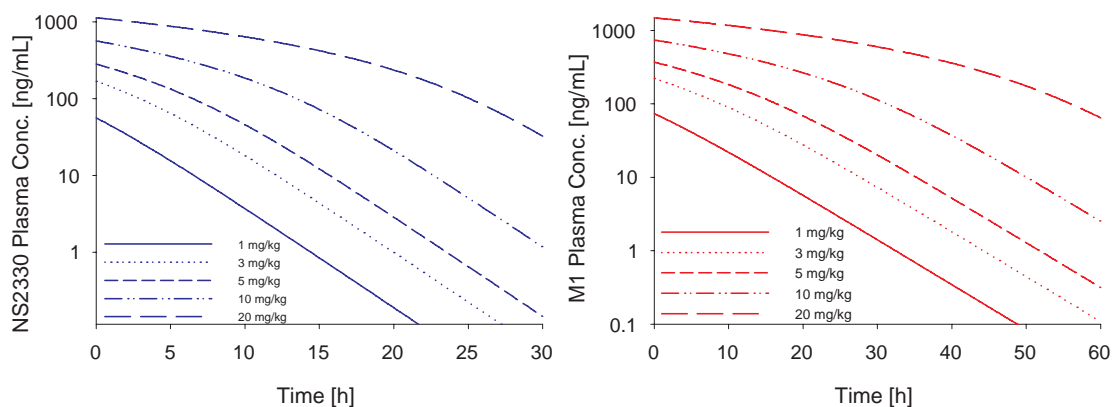

Figure 3.11 Project V - Simulated plasma concentration-time profiles after bolus infusion of different doses of NS2330 (left panel) and M1 (right panel) are shown.

3.6 Project VI – Population PK/PD in Alzheimer's Disease

A population PK/PD analysis was performed based on the data of two phase IIa studies performed in mild Alzheimer's disease patients. Studies investigated were part of the combined analysis presented in section 3.1.

3.6.1 Dataset

The dataset was created as described in section 2.2.2. For analysis of the treatment and the placebo response the dataset was split into the two treatment groups (NS2330 and placebo).

3.6.1.1 Observations

As the PK observations of the dataset have already been described in section 3.1, only the PD observations will be described in the following.

Overall, 62 patients were included in this study, 18 received placebo treatment, the remaining 44 patients were treated with verum. Four ADAS-COG measurements were taken per patients, resulting in 176 verum and 72 placebo measurements (Table 7.35, Page 132). Figure 7.37 (Appendix, Page 165) shows the ADAS-COG measurements versus time separated by treatment group. In addition, verum and placebo treatment were separated by responder status. Thirty-two responders (72.7% of all patients) under NS2330 treatment achieved a reduction of the ADAS-COG value at the end of treatment (648 h) compared to the baseline value. Twelve non-responders (27.3% of all patients) under NS2330 demonstrated a slight increase in the ADAS-COG value at the end of treatment (648 h). The placebo group could also be separated into a non-responder and responder group, but no clear reduction or increase was observable. ADAS-COG measurements showed a range from 1.3 to 22 points for NS2330 treated patients and from 1 to 23.7 points for placebo treated patients.

3.6.1.2 Population Characteristics

The main characteristics of the investigated population are summarised in Tables 7.36 and 7.37 for NS2330 and in Tables 7.38 and 7.39 for the placebo treatment.

Population characteristics of the placebo and verum group were comparable. Correlations between continuous covariates of all patients are shown in Figure 7.38 (Appendix, Page 166). No unexpected distributions were observed. Overall, the investigated population showed the typical composition for mild Alzheimer's Disease patients. Forty-one percent of the NS2330 treated patients were females, the remaining 59% were males. For the placebo population no

information about the serum creatinine, the creatinine clearance and the smoking status was available. Nearly all patients treated with placebo or verum were Caucasian, only 2 of the overall 62 patients were African descent. Thus, no influence of the ethnic origin on the PD could be investigated.

Within each treatment arm (placebo and NS2330) a separated statistic was calculated for the responder groups. The median values of the responder and the non-responder subgroups were almost comparable across both treatment arms, only age and ADAS-COG baseline values showed small differences. The non-responder group treated with NS2330 showed a 25% lower ADAS-COG baseline (i.e. better cognitive function) compared to the responder group (9.0 vs. 6.7) and in median they were 2.5 years older than the responder subgroup (72.5 vs. 70 years).

3.6.2 Population Pharmacokinetic/Pharmacodynamic Modelling

3.6.2.1 Model Development

As described in the modelling strategy (section 2.5.6.7), the model development was performed in a sequential manner. First, NS2330 treated patients were analysed. Secondly, the disease progression was tried to be implemented. Finally, the data of the placebo patients was explored.

NS2330 Treatment Initially, a dataset containing all NS2330 patients (responder and non-responder) was used for modelling purposes. As the non-responder patients influenced the model development, they were removed from the dataset and their influence was tested on the final base model for evaluation purposes.

For the development of a PK/PD model the PK model obtained by combined analysis (section 3.1) was used and the parameter estimates were fixed. Different types of pharmacodynamic models were investigated to assess the effect of NS2330 and M1 on the ADAS-COG score. Initially the extended E_{max} model obtained in the PK/PD analysis in mice (Equation 3.14) was used to describe the competitive interaction of the parent compound and the metabolite. The effect of parent compound on the metabolite was described according to the following equation (Eq. 3.16):

$$\text{Effect} = \text{Baseline} \cdot \left(1 - \frac{E_{max} \cdot \left(\frac{Ce_{NS2330}}{EC_{50,NS2330}} + \frac{Ce_{M1}}{EC_{50,M1}} \right)}{1 + \left(\frac{Ce_{NS2330}}{EC_{50,NS2330}} + \frac{Ce_{M1}}{EC_{50,M1}} \right)} \right) \tag{3.16}$$

where E_{max} was the maximum effect attributable to NS2330 and M1 expressed in percent

change from baseline, $EC_{50,NS2330}$ was the concentration producing 50% of the maximum effect of NS2330, for M1 the $EC_{50,M1}$ was assumed to be five-fold higher than the $EC_{50,NS2330}$ value, based on the findings revealed in section 3.5. Ce_{NS2330} and Ce_{M1} reflect the concentrations of NS2330 and M1 in the hypothetical effect compartments. Baseline reflects the ADAS-COG baseline value of each individual at the start of treatment.

Equation (3.16) was modified to equation (3.17) where E_{max} describes an absolute effect on the baseline to test whether an absolute effect describes the data better.

$$\text{Effect} = \text{Baseline} - \frac{E_{max} \cdot \left(\frac{Ce_{NS2330}}{EC_{50,NS2330}} + \frac{Ce_{M1}}{EC_{50,M1}} \right)}{1 + \left(\frac{Ce_{NS2330}}{EC_{50,NS2330}} + \frac{Ce_{M1}}{EC_{50,M1}} \right)} \tag{3.17}$$

Investigations revealed that the percentage model (Eq. 3.16) was superior over the absolute E_{max} model (3.17). For the link between pharmacokinetics and pharmacodynamics the implementation of hypothetical effect compartments was necessary to describe the time delay between concentration and effect. Mathematically, the concentration-time profiles in the hypothetical effect compartments were described by the following differential equations (3.18):

$$\begin{aligned} \frac{dCe_{NS2330}}{dt} &= K_{EO,NS2330} \cdot \left(\frac{A_{C,NS2330}}{Vd_{NS2330}} - Ce_{NS2330} \right) \\ \frac{dCe_{M1}}{dt} &= K_{EO,M1} \cdot \left(\frac{A_{C,M1}}{Vd_{M1}} - Ce_{M1} \right) \end{aligned} \tag{3.18}$$

where K_{EO} reflect the rate constant of NS2330 and M1, $\frac{A_{C,NS2330}}{Vd_{NS2330}}$ and $\frac{A_{C,M1}}{Vd_{M1}}$ were the plasma concentrations in the central compartments and E_{NS2330} and E_{M1} the concentrations in the hypothetical effect compartments, respectively.

Disease Progression As Alzheimer's disease is a neurodegenerative disease with a resulting deterioration of the baseline over time a disease progression was explored to be incorporated into the model. A deterioration in cognition over the study period could not be detected. Thus, the deterioration reported in literature with an increase of the ADAS-COG value between 3 and 6 points per year[81] was investigated be to implemented into the model using a linear slope model where the disease progression was added to the overall effect.

Overall, the implementation of disease progression depicted no improvement in the objective function value and was omitted during further model development.

Placebo Treatment The patients under placebo treatment were modelled in total, i.e. they were not split into responder and non-responder subgroups, as no indicator for their responder behaviour was obvious.

All values taken at the follow up visit (day 42) were removed from the dataset since no more placebo effect during follow up might be expected. Initially, it was assumed that no statistically significant placebo effect occurred. Thus, all ADAS-COG values were described as a baseline where no change over the time occurred (Eq. 3.19).

$$ADAS - COG = Baseline \tag{3.19}$$

Implementation of a placebo effect over time was accounted for by the implementation of a slope model, where the ADAS-COG value could be described by the following equation (3.20):

$$ADAS - COG = Baseline + SLOPE \cdot TIME \tag{3.20}$$

where SLOPE describes the linear decrease or increase over the time. As with two observations only limited data were available other models than a linear and a base model were not applied.

3.6.2.2 Base Model

NS2330 Treatment The pharmacodynamic effect of NS2330 and M1 on the ADAS-COG value was best described by an extended E_{max} model accounting for the competitive interaction of NS2330 and M1 and where the maximum effect was coded as a percentage change from baseline (Eq. 3.16).

Interindividual variability was included in E_{max}. Residual variability was modelled with an additive random effect model for the ADAS-COG score. A schematic representation of the PK/PD model is given in Figure 3.12. PK parameters can be found in Table 7.12 (Appendix, Page 121). The PD parameter estimates of the base model are shown in Table 7.40 (Appendix, Page 136).

Due to the limited data situation KEO had to be fixed to 0.0001 1/h. By varying the fixed KEO by different factors it was shown that fixing had no significant impact on the parameter estimates. As expected only EC_{50} changed in the same direction. E_{max} remained similar. The estimates for interindividual variability was moderate with 43.2% in E_{max}. The additive residual variability was moderate with ± 1.8 points on ADAS-COG score.

All parameters were estimated with good precision (relative standard errors ranging from 12.6 to 34.9 %, Table 7.40), only the EC_{50} value was estimated with a higher standard error of 84%. The goodness of fit plots are shown in Figure 7.39 (Appendix, Page 167). All measurements were uniformly spread around the line of identity and no trend over time was
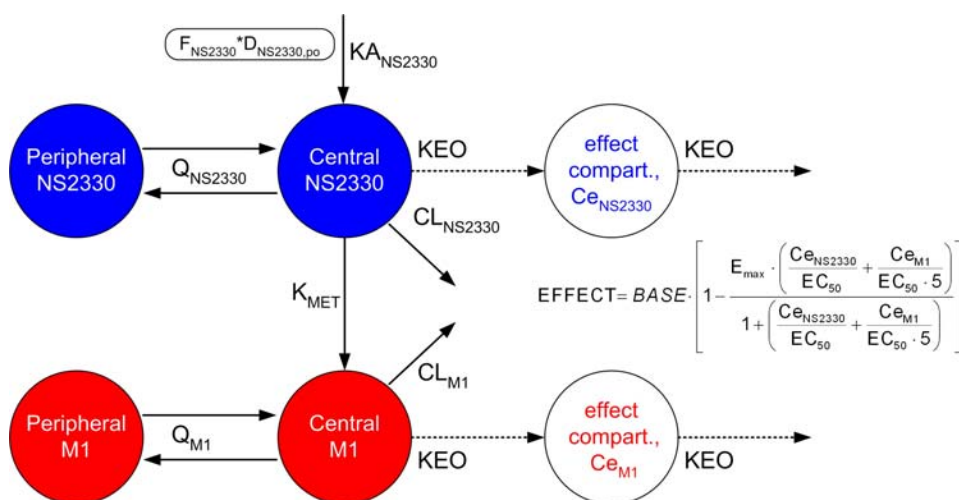
$$\text{EFFECT} = BASE \cdot \left[1 - \frac{E_{max} \cdot \left(\dfrac{Ce_{NS2330}}{EC_{50}} + \dfrac{Ce_{M1}}{EC_{50} \cdot 5} \right)}{1 + \left(\dfrac{Ce_{NS2330}}{EC_{50}} + \dfrac{Ce_{M1}}{EC_{50} \cdot 5} \right)} \right]$$

Figure 3.12 Schematic PK/PD model of NS2330 and its metabolite

observable, indicating that the data was well described by the model.

Placebo Treatment   The placebo arm was best described by a simple base model (Eq. 3.19). Implementation of a slope did not showed a significant influence on the objective function value and was removed from the model. The slope model did not showed a trend over time and was found to be sufficient to describe the observations under placebo treatment.

3.6.2.3 Final Covariate Model

NS2330 treatment   The covariates tested on the individual PD parameters of the final base model were selected as described within the method section (2.1.3.5). Only AGE was identified as a significant covariate by the GAM procedure. In addition, baseline was tested on the PD parameters.

The ADAS-COG baseline revealed influence on the objective function value. Only AGE showed a significant influence on E_{max}, where the E_{max} was reduced with an increasing age of the patients. The mathematical expression for the relationship found and the parameter estimates are listed in Table 7.40 (Appendix, Page 136). According to this relationship E_{max} will decrease from 60.4% to 14.6% as age increases from 60 to 80 years.

Parameter estimates for the model parameter E_{max} and EC_{50} and the residual variability estimates were comparable to the final base model. The interindividual variability in E_{max} could significantly be reduced by 37% (43.2% vs. 27.4%) by the implementation of the covariate effect.

All parameter were estimated with good precision (relative standard errors ranging from 10.7 to 42.3%, Table 7.40), only the EC_{50} value was estimated with a higher standard error of 95.7%. The goodness of fit plots are shown in Figure 7.40 (Appendix, Page 168). All measurements were uniformly spread around the line of identity and no trend over time was observable, indicating that the data was well described by the model. Figure 3.13 selectively shows the goodness of fit plots for day 28 (last day on NS2330 treatment). All observations were well described by the model, indicating a good predictability for this time point.
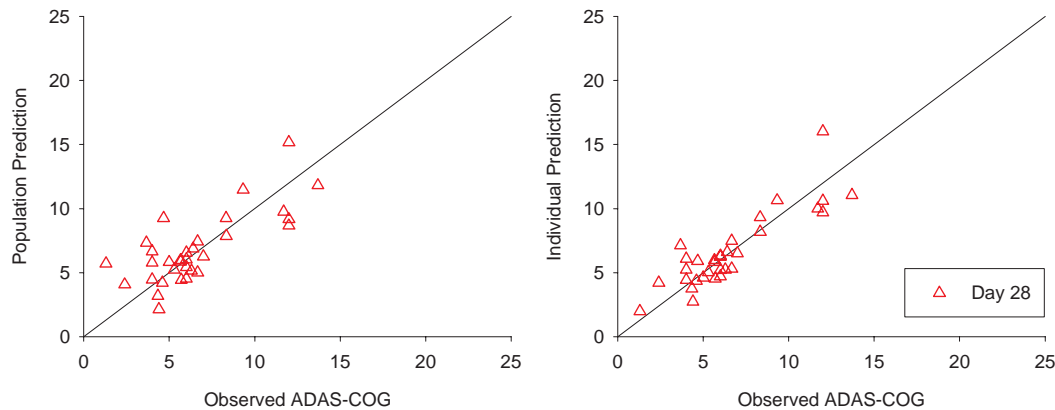

Figure 3.13 Population and individual predictions (Fig. b) versus observed ADAS-COG values on day 28.

Figure 7.41 (Appendix, Page 169) shows eight representative individual ADAS-COG vs. time profiles including the population and the individual predictions. The 24 h values could not be described appropriately, but no systematic over- or under-prediction can be observed. The follow up observation (964 h) could in some cases be well described (Subjects A-H), for the subjects G and H a large ADAS-COG increase appeared which was under-predicted by the model.

Placebo Treatment   As no placebo effect could be observed no influence of any covariates could be investigated.

3.6.3 Evaluation

As described within section 3.6.2.1 non-responders were removed form the dataset for the development of the base model. To assess the influence of the non-responders on the parameter estimates, the final base model was re-estimated with all patients. Parameter estimates can be

found in Table 7.41 (Appendix, Page 136). E_{max} was reduced approximately 20% compared to the responder subgroup. Interindividual variability on E_{max} was increased by approximately 45% compared to the responder subgroup. The additional residual variability showed an 28% increase.

3.6.4 Simulation

Different simulations were performed to show the influence of age, the individual baseline value and the dose on the maximum effect achievable. The ADAS-COG value on the Y-axis is shown in a normalised way, i.e. baseline reflects 100%.

The influence of age on E_{max} is depicted in Figure 3.14. Patients with an increased age showed a reduced E_{max}. The ADAS-COG scale was reduced e.g. 15% and 59% for a 80 and 60 year old patient, repectively.
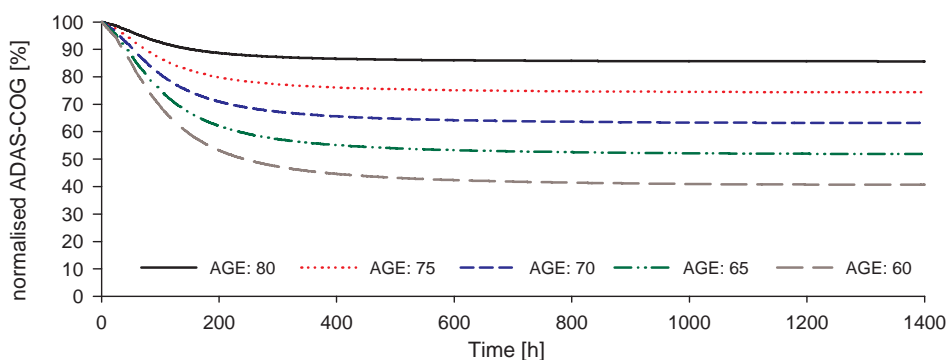

Figure 3.14 Impact of age on the effect-time profile: Typical profiles of patients aged between 60 and 80 years.

A simulation was performed showing the influence of different baseline values on E_{max} (Figure 7.42, Page 170). As expected from the mathematical expression the absolute drug effect decreased with decreasing baseline, i.e. patients with high baseline values showed a higher absolute drug effect.

The influence of different dosing regimen on the reduction of the ADAS-COG value is depicted in Figure 7.43 (Appendix, Page 170). Four different doses (0.125, 0.25, 0.5, 1 mg) were simulated, where NS2330 was administered orally for 4000 h once daily. During the first phase of treatment ($\leq$1000 h) a significant difference between the maximum effect achievable by the doses occurred, after 4000 h the maximum effect of all doses was comparable.

4 Discussion

The investigations and data analyses presented provide new information about the pharmacokinetics and pharmacodynamics of NS2330 and the major metabolite M1. The results obtained will be discussed in the following.

4.1 Population Pharmacokinetic Analyses

The population pharmacokinetic properties of NS2330 and its metabolite M1 were extensively investigated within projects I and II. Overall, 439 subjects were investigated to characterise the population pharmacokinetic parameters of NS2330 and M1, to quantify the variability of the pharmacokinetic parameters and to explore covariates influencing the pharmacokinetic properties of both compounds.

Population Pharmacokinetic Parameters

Volume of Distribution The volumes of distribution of NS2330 and M1 were found to be large within both projects. They were exceeding the total volume of body water, suggesting an extensive distribution of both compounds into tissues. Projects I and II revealed comparable parameter estimates for the overall volume of distribution of NS2330 assuming F to be close to 1. Normalised to body weight, the volumes of distributions for NS2330 were estimated as 9.8 L/kg for project I and 8.6 L/kg for project II. These findings were consistent with those found in animals, e.g. the volumes of distribution of NS2330 in rats, minipigs and cynomolgus monkeys were 18 L/kg, 8 - 14 L/kg and 9.2 L/kg, respectively[5].

Clearance Projects I and II also revealed comparable parameter estimates for the NS2330 clearance assuming F to be close to 1. In females the clearance was 1.56 L/h and 1.48 L/h in projects I and II, respectively, and the clearance for males was 2.07 L/h and 1.86 L/h in projects I and II, respectively. When referenced to bodyweight the NS2330 clearance in humans was very low at $\approx$0.03 L/h/kg. All other species showed a significantly higher clearance. For example in cynomolgus monkey and minipig a moderate clearance of NS2330 of 1.8 L/h/kg and

1.5 to 2.6 L/h/kg, respectively, was found[5]. The difference is presumably caused by the very low affinity of the drug to the human CYP3A4 system[5] in comparison to other species investigated. Besides, other reason might cause and/or contribute to the difference, e.g. different elimination pathways (e.g. biliary excretion), enterohepatic circulation (see project III).

Metabolite Kinetics The metabolite M1 has so far not been administered to humans, so the true volume of distribution and the clearance of the metabolite are unknown. Therefore, different assumptions had to be made for the model building process of the combined model. Because the parameter estimates of the metabolite are mainly influenced by the formation step chosen and as within projects I and II different approaches were used to describe its formation (7% transformation to M1 in project I and assumed ratio of distribution volume in project II), a direct comparison of the parameter estimates of M1 obtained in the different projects is difficult.

To obtain at least animal data, within project V M1 was pharmacokinetically characterised in mice. It could be shown that the volume of distribution of M1 was still large in mice, but reduced by 23% compared to the volume of distribution of NS2330. This reduction was presumably caused by the increased hydrophilic properties of the metabolite resulting in a less extensive distribution into tissue. For the PK analysis of project II this acquired knowledge was implemented in the model building process, assuming the same ratio of the volume of distribution of the metabolite in humans as in mice. It could be shown that this hypothesis was superior to other hypothesis tested. It can be concluded that the metabolite in relation to the parent drug also shows the same reduction of volume of distribution in humans as in mice. The M1 clearance was found to be 64% reduced in mice compared to the NS2330 clearance (see project V). As the clearance of NS2330 and M1 in humans seems to be different compared to the animals investigated the draw of conclusions from mice to men with respect to the M1 clearance should be handled with care.

Structural Model Comparison Population PK model development of NS2330 and its metabolite revealed two different structural models for projects I and II. Data of project I required two compartment models for each compound, whereas the data for project II was sufficiently described using a less complex model with a one compartment model for each compound.

As outlined above, the numerical comparison of parameter estimates of the clearance and the overall volume of distribution of NS2330 obtained by both projects revealed high similarities. Simulations of the plasma concentration-time profiles of both models were performed. Project II showed after a single dose administration of NS2330 a mildly and moderately in-

creased exposure for NS2330 and M1, respectively (Figure 7.22). Profiles of the single dose administration depicted identical shapes for the NS2330 and M1 plasma concentration-time plots. Consequently, the question for the necessity of the more complex model in project I arises. This additional complexity was presumably attributable to the frequent sampling schedules of project I. The additional compartment in combination with more variability parameters allowed the adaptation to situations observable during the frequent sampling period. In particular, it should be considered that the more complex model in project I allowed adaptation to the first peak of the multiple peak phenomenon.

However, simulations of the steady-state scenario showed the comparability of both models, the structural differences did not affect the steady-state profiles, except that the M1 steady-state concentrations predicted by the model of project I were approximately 25% lower compared to project II. Within project I concentrations of the metabolite were mainly available after single dose administration of NS2330. The few multiple dose studies included in project I were performed over a short treatment period, resulting in low M1 concentrations far removed from the steady-state. Within project II concentrations of the metabolite close to steady-state were available allowing a more precise estimation of the metabolism parameters.

Covariate Analysis

The covariate analysis in projects I and II identified sex, creatinine clearance, weight, body mass index, study and co-medication of CYP3A4 inhibiting drugs as statistically significant covariates. The influences will be discussed in the following.

Sex In both projects sex was found to have a significant influence on the pharmacokinetic properties of NS2330. In project I females were found to have a 35% increased bioavailability compared to males. In project II the non-metabolic clearance of NS2330 was found to be reduced in females resulting in a 18.7% reduction of the total clearance of NS2330 (=CLmet + CLnon-met). Simulations showed that the sex effect resulted in a 35% and a 23.2% increased steady-state exposure of NS2330 for projects I and II, respectively (Figures 7.7 and 7.17). Overall, the influences of sex predicted by both models were comparable. Two additional phase I studies conducted in males and females also showed increased exposures in females [5]. As only a limited number of subjects was investigated (n=18) this finding was not statistically significant. However, as a sex difference was also observed in projects I and II with more than 400 subjects (healthy volunteers and patients) this finding cannot be dismissed and its cause should be further investigated. In the following it will be discussed whether the difference observed might be caused by an increased bioavailability or by a reduced clearance in

females.

Project I revealed a 35% increased bioavailability in females. In depth evaluation of this finding shows several drawbacks with respect to the sexual composition of the study population. Only 38% of the population investigated were females and the sexual distribution across the studies was unbalanced. Especially within study PI.1, where NS2330 was administered intravenously, no females were included. However, during the evaluation of the final covariate model it was additionally investigated whether a sex difference on clearance revealed a higher significance, but the influence on bioavailability was stronger. In the literature several examples are given (e.g. [82;83]) where a higher bioavailability in females was observed, but no physiological explanation was given. As the cross comparison of iv and po studies revealed a bioavailability of >90% of NS2330 in males, a 35% increased bioavailability in females would result in a value of more than 100% which is physiologically implausible and disproves the bioavailability hypothesis. It might be speculated that the increased bioavailability in females in project I is a masked difference in clearance which could not be clearly distinguished due to the limited data situation available, i.e. no females with iv data. However, due to the missing information about the pharmacokinetics in females after intravenous administration it could not be clearly distinguished between these two hypotheses within project I.

In project II a decreased non-metabolic clearance of NS2330 was observed. In the literature several examples of sex dependent differences in clearance have been reported where reduced as well as increased clearances in females were observed [84–89].

As the influence in project II was found on the non-metabolic clearance of NS2330, which comprised any elimination pathway of NS2330 except the formation into M1, different hypotheses can be generated. First, the metabolism into an additional metabolite (except M1) could be decreased in females. This hypothesis could not be investigated, as no data about sex differences in the formation of further metabolites was available. Second, the renal elimination could be reduced in females. It is known that NS2330 is partly eliminated via the kidney [5] and that the renal function is slightly lower in females [70]. However, as the creatinine clearance was found to have an influence on this non-metabolic clearance as well, the sex effect seems to represent an additional effect. Third, a reduced biliary excretion of NS2330 in females might explain the difference in the non-metabolic clearance. There are several lines of evidence supporting this hypothesis. In animals it was shown that the biliary excretion of NS2330 is significant [5]. In addition, the enterohepatic circulation of NS2330 in humans (project III) suggests a biliary excretion in humans as well. Mass balance studies with ^{14}C radioactive labelled NS2330 were performed in rats, minipigs and humans. These studies showed that the amount of ^{14}C excreted via the faeces was reduced by 22% and 11% in female rats

and minipigs, respectively, after iv administration and by 26%, 23% and 40% in female rats, minipigs and humans after oral administration. The results show that there are sex differences across the species within the biliary excretion of the overall radioactivity. Unfortunately, this detection method only allows for the quantification of the overall elimination of radioactive compounds, therefore it can not be directly attributed to the NS2330 elimination. Another drawback in these studies was the small number of subjects included, per treatment arm 3 to 4 males or females were investigated. Despite these limitations in the mass balance studies this third hypothesis is excellently supported by these findings.

Based on this hypothesis, the question about mechanisms of the biliary excretion of NS2330 arises. Generally, most drugs are excreted into bile via active transport processes, but also passive excretion was reported[90]. Currently, it is unknown which transporters or mechanisms might be responsible for the biliary excretion of NS2330. In the literature sex differences in expression pattern of membrane transporters[91] involved in biliary excretion are reported. The most well known transporter protein responsible for biliary excretion of drugs is P-glycoprotein (P-gp). In healthy livers, males had approximately 2.4-fold higher P-gp levels, compared to females[92], indicating a higher biliary clearance of P-gp substrates in males. For the remaining transporters involved in biliary excretion no information about sex specific expression has been reported. Nevertheless, the presented hypothesis of a sex difference of the biliary clearance of NS2330 seems reasonable and can be supported by several findings. Further investigations are necessary to reveal the mechanisms responsible for the biliary excretion of NS2330.

Creatinine Clearance   Within project I a correlation between the creatinine clearance and the central volume of distribution of M1 was found. This finding was only present in project I and no physiologically plausible explanation can be given. Simulations were performed to assess the impact on the plasma concentration-time profiles. They showed that the steady-state concentration was unaltered but that the time until steady-state had been reached was influenced (Figure 7.9). Consequently, this covariate influence can be regarded as statistically significant but not clinically relevant.

In project II creatinine clearance was found to have a significant influence on the non-metabolic clearance of NS2330 for patients with a creatinine clearance value of less than 62 mL/min. It was found, that the total clearance of NS2330 (=CLmet+CLnon-met) was reduced up to 25% in moderately to severely renally impaired AD patients compared to renally healthy AD patients. This finding is in close agreement with a mass balance study performed[5], where it was revealed that the contribution of the renal clearance to the overall clearance of NS2330

was about 15 - 20%. Simulations showed that the steady-state concentrations of NS2330 and M1 increased significantly (+33%) as a result of the impaired renal function (Figure 7.18).

The influence of creatinine clearance on the clearance of NS2330 could not be detected within project I. This was probably due to the limited number of patients with low CLCR values in project I. Only 14 subjects (11.7%) had a CLCR value lower than 50 mL/min in project I. In project II the median CLCR value at baseline was 62.5 mL/min, indicating that 160 subjects (50%) of the population were at least mildly renally impaired, which provided the opportunity to detect the influence of this covariate in a larger population.

Weight and Body Mass Index Project II revealed influences of the body weight and the body mass index on the pharmacokinetics of NS2330 and M1. The volume of distribution of NS2330 was found to be influenced by the body weight ($\approx$1% change per 1 kg change) and the volume of distribution of M1 was influenced by the BMI ($\approx$2% change per 1 kg/m^2 change). During model development these two highly correlated covariates were exchanged, but the findings remained. Explanations why different but highly correlated covariates were found for the volumes of distribution are speculative. Presumably this outcome is arbitrary and only based on statistical significance. However, it is a well known phenomenon that the volumes of distribution of lipophilic drugs are correlated with body weight[93]. As for NS2330 and M1 high distribution into tissues was observed[5], this finding is in agreement with the findings in the literature. Simulations showed that the influences of body weight and BMI on the steady-state profiles of NS2330 and M1 were negligible and without clinical relevance (Figures 7.19 and 7.20). The time necessary to reach steady-state in obese patients was prolonged. To achieve the steady-state earlier in patients with a higher body weight a loading dose might be appropriate. Within the model development of project I an influence of weight on the volume of distribution of NS2330 was found as well, during the backward elimination this covariate relation was deleted from the model. This might be caused by the different and smaller population investigated in project I. Within the model development of project I an influence of weight on the volume of distribution of NS2330 was found as well, during the backward elimination this covariate relation was deleted from the model. This might be caused by the different and smaller population investigated in project I.

Within project II weight was also found to have an influence on the metabolic clearance of NS2330. The influence with respect to the total clearance of NS2330 was low. A 102 kg patient showed a $\approx$4% reduced total clearance compared to an 37 kg patient. Usually the size of the liver increases proportionally with the body weight and consequently the metabolic clearance is expected to increase[94]. However, there are also several drugs reported in the literature

where the volume of distribution is increased and the clearance is slightly reduced in obese patients[95], but explanations are not given. One suggestion might be that due to the increased distribution into other tissues with increased body weight, the availability of NS2330 within the liver would be reduced. This would result in a lower metabolic clearance, despite the higher liver weight and increased metabolic function. Further investigations would be necessary to confirm this hypothesis. However, simulations showed that the influence of body weight on the steady-state profile was negligible and clinically not relevant (Figure 7.19).

Age   An influence of age on the volume of distribution of M1 was found in project II. As age and weight were not correlated within this population (Figure 7.11), a displaced weight effect can be excluded. This finding is in agreement with the literature[96], as with increasing age a progressive reduction in total body water occurs resulting in a relative increase in body fat[97]. Thus, in elderly patients lipophilic drugs would generally show larger volumes of distribution[96]. However, simulations showed that the influence of age on the steady-state profile of M1 was negligible and clinically not relevant (Figure 7.21).

Study Effect   Patients of the studies PI.5 and PI.6 showed an increased central volume of distribution of M1 in project I. This might be a displaced age effect, as those patients were slightly older compared to the remaining subjects. This effect could also be explained by the reduced number of sampling points available from these studies. An effect of their mild Alzheimer's disease can be excluded, as comparisons between projects I and II revealed no disease-related differences. However, simulations showed that the influence of these studies on the steady-state profile of M1 was negligible and clinically not relevant (Figure 7.8).

Co-medication   The influence of co-medications was exploratively investigated in project II. It was found that CYP3A4 inhibitors had a statistically significant influence on the clearance of NS2330. The overall clearance of NS2330 was reduced by 20% - 45%, depending on the dataset investigated. Unfortunately there were only a few NS2330 samples ($\approx$5%) taken under CYP3A4 inhibitor treatment, so this finding needed further investigation which was performed in project IV and will be discussed there in detail (Page 92).

Short summary, application and outlook   The pharmacokinetic models developed within projects I and II described the data very well. In addition, the external evaluation processes showed a very good predictability of the models. The model obtained by project I predicted the plasma concentrations of project II data very well. Higher metabolite concentrations were

slightly under-predicted by the model. However, as the model was developed within a concentration range of M1 only up to 8 ng/mL while the evaluation dataset contained M1 concentrations up to 40 ng/mL the mild under-prediction of the higher concentrations seems reasonable. The external validation of project II showed good results. The model very well predicted the plasma concentrations of 204 Parkinson's disease patients treated with NS2330.

The covariate analysis in projects I and II revealed physiologically plausible covariate effects. Within project I less covariate effects were found due to the limited number of patients, the shorter duration of treatment and the smaller ranges of covariates available. In both projects the covariate analysis partly explained the variability observed in the pharmacokinetic parameters. In project II a high interindividual variability on the non-metabolic clearance of NS2330 still remained even after the incorporation of the covariates sex and CLCR. This indicates that there still might be as yet undiscovered covariates additionally influencing the non-metabolic elimination of NS2330.

Nevertheless, several covariates have been identified as having an influence on the pharmacokinetics of NS2330 or M1. Simulations showed that only creatinine clearance and sex had a significant impact on the steady-state plasma concentration-time profiles, considering an intended long term-treatment of NS2330 in Alzheimer's disease patients. As both covariates might occur within one patient the question of a combined influence of sex and CLCR occurs. Simulations showed that the exposure in a renally impaired female was increased by 62% compared to a male with a normal renal function (Figure 3.3). Assuming the incidence of additional covariates influencing the plasma concentration-time profiles at steady-state, e.g. presumably CYP3A4 inhibiting drugs, a larger increase in exposure might to be expected.

4.2 Enterohepatic Circulation

The multiple peak phenomenon in the pharmacokinetics of NS2330 was investigated within project III to assess whether NS2330 undergoes enterohepatic circulation. In the following, the model developed and the physiological background of the estimated parameters will be discussed. In addition, the evaluation of the model and the clinical implications of an EHC will be discussed in detail.

Mechanistic Model The most challenging issues during the model development were the following: the model was aimed to describe an unrestricted number of gall bladder releases which should be controlled by a physiologically plausible mechanism. Both issues could be solved by a mechanistic PK model successfully describing the multiple peak phenomenon

of NS2330 after intravenous administration. The gall bladder release was controlled by a trigonometric sine function, considering the clock time as a control element. This allowed a pulsatile release of the gall bladder mimicking a circadian rhythm. Especially for drugs with a long half-life the implementation of the clock time in the model allowed a release of the gall bladder at the same clock time each day for an unlimited number of days and releases (Figure 3.4).

For the NS2330 data analysed in project III (only iv data was chosen), a rhythm allowing the gall bladder to empty four times a day was predicted. The emptying occurred three times during the day with maxima at 6 am, 12 am and 6 pm, at midnight a reduced emptying was predicted. This predicted gall bladder release rhythm is in accordance with physiology. The gall bladder normally stores bile during fasting and releases it into the duodenum short after ingestion of a meal [98]. As meal intake very often occurs three times during the day, the model predicted gall bladder release is in full agreement. In humans the gall bladder slowly empties up to 75% of its contents [99]. This slow release is covered by the model using the periodic sine function imitating this physiological behaviour. Furthermore, the gall bladder is not static during fasting [98]. In the absence of food a periodical emptying of up to 35% of its content occurs as part of the migratory motor complex. This is mimicked by the model by an incomplete sine wave predicted around midnight.

Model Evaluation and Predictability The parameter estimates of clearance and volume of distribution of NS2330 obtained by this mechanistic model were comparable to the values obtained within projects I and II. Intensive simulations of individual plasma concentration-time profiles showed that the multiple peak phenomenon was very well described (Figure 7.29).

For evaluation purpose the model was applied to meloxicam, a drug where the presence of an EHC has been confirmed [72]. The model could easily be applied to data of intravenously administered meloxicam, only some drug specific structural modifications had to be done. The final model successfully described the multiple peak phenomenon of meloxicam (Figure 7.27, Page 157).

The meloxicam data used for evaluation purposes offered the opportunity to assess the predictability of the model in predicting the influence of interrupting the EHC with cholestyramine on the PK parameters of meloxicam. The model impressively showed its predictive performance. Clearance and half-life after interruption of the EHC could successfully be described. The model predicted slightly higher clearance values than observed by Busch et al. [72]. This deviations were presumably caused by an incomplete absorption of meloxicam within

the duodenum due to cholestyramine presence.

Overall, the application to a drug that undergoes EHC allows the conclusion that the model developed covered the principle behaviour of an EHC and was also capable to quantify the impact of an EHC on the pharmacokinetics. For NS2330 it can be concluded that the multiple peaks are a most propably result of an enterohepatic circulation.

Clinical Implications   Assuming an EHC of NS2330 several questions about the clinical implications arose. First, the effect of an interruption of the EHC needed to be clarified. A simulation was performed to assess the influence of a complete interruption of the EHC of NS2330. Simulation showed a dramatic decrease in plasma concentrations. Half-life of NS2330 was reduced by more than 90% from 200 h to less than 10 h (Figure 7.28). From this an extensive biliary excretion of NS2330 and an extensive reabsorption in the intestine could be derived.

Leflunomide is an example where a comparable impact on the PK properties due to the interruption of EHC occurred[100]. Orally administered leflunomide was almost completely converted into its active metabolite A77 1726. The plasma half-life of A77 1726 was approximately 2 weeks in patients and could be decreased to 1 to 2 days after administration of cholestyramine or activated charcoal due to an interruption of the EHC. This behaviour is in close agreement with the predicted behaviour of NS2330.

This large effect of enterohepatic circulation on the pharmacokinetics of NS2330 would offer a simple and effective manner for a detoxification strategy after overdosing with NS2330 and would allow concentration-dependent side effects to be antagonised occurring during therapy.

Enterohepatic circulation offers also potential drug interactions within clinical application of NS2330. The co-administration of drugs inhibiting the enterohepatic circulation, like activated charcoal, might result in reduced, sub-therapeutic plasma concentrations in the patients and should be considered during therapeutic use of NS2330.

As the biliary excretion of drugs is mostly driven by active transporters[90] an interaction between co-administration of drugs inhibiting these transporters might be possible. This would result in a reduced biliary clearance and increased plasma concentrations. As long as the mechanisms of the biliary clearance of NS2330 remains unconfirmed, possible interactions are difficult to be considered during therapeutic use. Consequently, in-depth investigations regarding the biliary excretion of NS2330 are highly recommended.

Also, considering an enterohepatic circulation of NS2330, different diseases might influence the plasma concentrations of patients. Diarrhoea, Morbus Crohn and colitis ulcerosa might effect the reabsorption of NS2330 from the duodenum and consequently the plasma

concentrations might be reduced in patients with these diseases. Converse results are to be expected in patients with liver disease where increased plasma concentrations might occur due to reduced biliary clearance properties of hepatically impaired patients[101;102].

The impact of the EHC on the PK of NS2330 needs to be further investigated in humans as the biliary excretion is poorly predictable via allometric scaling[103;104]. In summary, the hypothesis of an enterohepatic circulation of NS2330 could further be supported by the development of the mechanistic PK model.

4.3 Impact of CYP3A4 Metabolism

The maximum impact of a CYP3A4 inhibition on the elimination of NS2330 was investigated in project IV and explored within the covariate analysis of project II. In the following, the results and implications from project IV will be discussed and compared to the results from project II.

Project IV investigated a standard drug-drug interaction study between NS2330 and itraconazole. A mechanistic model could successfully be developed, simultaneously describing the pharmacokinetics of itraconazole, NS2330 and the influence of itraconazole on the elimination of both compounds. The mechanistic modelling approach predicted a 39% reduced clearance of NS2330 resulting in 63% increase in exposure under maximum inhibition of CYP3A4. Also a non-compartmental analysis (NCA) of this study was performed. The AUC was calculated as a recommended exposure measurement endpoint for drug-drug interaction studies[51]. This NCA revealed an 8% increased exposure for the time frame of the co-administration with itraconazole (AUC_{0-144})[5]. The exposure extrapolated to infinite time ($AUC_{0-\infty}$) was increased by 20%[5]. This extent of increase would normally not be regarded as clinically relevant[51].

However, deviations between the NCA and the mechanistic modelling approach (project IV) were substantial and cannot be ignored. Consequently, the question arises whether the NCA under-predicted or the mechanistic modelling approach over-predicted the impact of the CYP3A4 inhibition.

A simulation was performed using the model obtained in project IV with the study design of the study PIV (Figure 3.8). Mean plasma concentration-time profiles with and without itraconazole were simulated and the parameters AUC_{0-144} and $AUC_{0-\infty}$ were calculated using an NCA approach. The analysis showed that the AUCs of the simulated curves increased in the same range (+8.9% and +19.8%) as the observed data. This indicated that the data description by the mechanistic modelling approach is identical to the NCA approach, only the interpretations of the results were different. This means that the NCA approach highly under-

estimated the impact of the CYP3A4 inhibition. This simulation also showed, that the AUC is an inadequate parameter to detect those kinds of changes in the clearance.

The conclusions from the NCA results were mainly attributable to the limited duration of the itraconazole co-administration. Within the study PIV itraconazole was co-administered 6 days before the NS2330 administration and 5 days after. In summary, the CYP3A4 enzymes were only completely inhibited over 144 hours in the presence of NS2330 in plasma, which was less than one half-life of NS2330. Consequently, NS2330 concentrations were present for another 3 to 4 half-lives ($\approx$600 - 800 h) in plasma during which no or only a reduced inhibition occurred. To overcome these limitations and to assess the whole impact of a CYP3A4 inhibition by an NCA approach, itraconazole would need to be administered over a longer period, at best over the whole exposure period of NS2330 (up to 1000 h). However, due to ethical considerations itraconazole can only be administered to healthy volunteers for a maximum of 14 days. This limits the classical NCA approach for the analysis of drug-drug interaction studies in long half-life drugs.

Another recommended tool for the detection of possible drug-drug interactions is the population pharmacokinetic analysis in studies conducted at later phases of drug development[51]. Within project II this approach was applied and revealed a reduction of the NS2330 clearance between 20 and 45% under co-administration of CYP3A4 inhibiting compounds. Usually, this finding should be interpreted with caution, as only a limited number of samples ($\approx$5%) were taken under co-administration of CY3A4 inhibiting drugs. However, as project IV revealed a comparable impact for the CYP3A4 inhibition those results can be seen as mutual evaluations for the results obtained by projects II and IV.

The impact of a CYP3A4 inhibition on the exposure of NS2330 lies within the same range observed for different other drugs[105]. Simulations were performed to assess the clinical impact of short- and long-term co-medications with CYP3A4 inhibiting drugs on the steady-state plasma concentration-time profiles of NS2330. The two week inhibition initiated during steady-state of NS2330 resulted in a $\approx$34% increased exposure, after 6 weeks of co-administration the exposure was increased up to the maximum effect of 63%.

The investigations of projects II and IV showed that CYP3A4 is mainly involved in the elimination of NS2330 and that the inhibition of CYP3A4 results in increased plasma concentrations. In a next step it should be considered that the opposed reaction might occur as well, i.e. co-administration of drugs inducing the CYP3A4 enzymes might increase the clearance of NS2330. In the literature several examples of drugs have been reported, showing a reduced clearance under inhibition and an increased clearance under induction of CYP3A4[106]. For NS2330 the impact of CYP3A4 inducing drugs could not be investigated so far, but the

hypothesis should be proved within upcoming trials.

For the evaluation of drug-drug interaction potentials of long half-life drugs the projects II and IV impressively showed the necessity to use the mechanistic modelling approach or the population modelling approach to gain knowledge about the impact of a CYP3A4 inhibition. In consequence, the prolongation of the co-administration duration of the inhibiting drug, like itraconazole, is ethically not justifiable and not necessary.

The knowledge of the impact of CYP3A4 inhibition on the pharmacokinetics of NS2330 is of major importance especially as Alzheimer's disease patients are usually multi-morbid and receive different kinds of co-medications. This polypharmacy dramatically increases the risk of drug-drug interactions [107] and should be considered during the long term treatment of NS2330.

4.4 Potency of the Metabolite

During project V the potency of the active metabolite M1 relative to NS2330 was investigated. Additionally, the pharmacokinetic properties of NS2330 and M1 in mice which have not been available so far could be characterised.

Pharmacokinetics

Volumes of distribution were found to be large for NS2330 and M1, exceeding the total volume of body water, suggesting that both compounds were extensively distributed into the tissues. These findings were consistent with results from other animals treated with NS2330, e.g. the volumes of distribution of NS2330 in rats and minipigs were 18 L/kg and 14 L/kg, respectively [5]. As M1 had never been administered to any species before, comparisons are not possible. Compared to the V of NS2330 the V of M1 in mice was 23% lower which might be caused by the increased hydrophilic properties of the metabolite.

During this investigation, pharmacokinetics of NS2330 and M1 showed non-linearity in mice which had never been noticed before in any species treated. The non-linearity was described by saturable elimination of both compounds and saturable metabolism steps of NS2330. To assess the influence of the non-linearity on the plasma concentration-time profiles in mice simulations were performed with different doses of NS2330 and M1 given intravenously as bolus. Results of the simulation studies showed that non-linearity occurred only at high concentrations of NS2330 and M1 which were caused by the high doses administered in this pharmacological study. As the aim of this pharmacological study design was to achieve a wide range of the pharmacodynamic effect, high doses of up to 20 mg/kg were

administered to the mice. Considering the fact that the highest non-lethal dose of NS2330 in mice is $\approx$7 mg/kg[5], the detection of saturated pharmacokinetic/metabolic processes seems reasonable. As in humans a much lower therapeutic dose of $\approx$0.00625 mg/kg (0.25 - 1 mg absolute dose) was administered in long-term treatments (Project II) non-linearity in human PK has not been observed so far and is not expected to occur within the therapeutic plasma concentration range.

Within the linear PK range of NS2330 and M1, the PK parameters clearance and half-life could be derived from the estimated Michaelis-Menten parameters. Clearance of NS2330 in mice was found to be high at 5.3 L/h/kg within the linear PK range and in rats a comparable clearance at 6 L/h/kg was found[5]. In cynomolgus monkey and minipig a moderate clearance of NS2330 of 1.8 L/h/kg and 1.5 to 2.6 L/h/kg was found, respectively[5]. Clearance of M1 in mice was found to be moderate at 1.9 L/h/kg and approximately 64% lower than the clearance of NS2330.

Pharmacodynamics

Both compounds were able to achieve the maximum inhibition of 100%. Comparison of EC_{50} values of intermediate key models revealed a 4.1- to 5-fold higher *in vivo* potency of NS2330 in mice in comparison to M1 with respect to the inhibition of the dopamine re-uptake transporter in mice. Previously, studies had been performed to assess the *in vitro* activity of NS2330 and its metabolites[5]. The effect of NS2330, M1 and other metabolites on the uptake of [^{3}H]-DA, [^{3}H]-5-HT and [^{3}H]-NA in synaptosomes prepared from rat brain were explored. Investigations of the [^{3}H]-DA uptake resulted in IC_{50} values of 6.5 nM and 3.0 nM for NS2330 and M1, respectively. These *in vitro* results are contrary to the results of the present *in vivo* analysis. One explanation for the differences might be a poorer blood-brain barrier penetration of the more hydrophilic M1 compared to NS2330. *In vivo* investigations in mice, however, showed a very good blood-brain barrier permeability in mice of both compounds[4]. No differences in the permeability of both compounds could be revealed. This finding might reject this hypothesis. The difference might also be explained by a significant discrepancy in the *in vivo* plasma protein binding between NS2330 and M1 . Investigations revealed that the *in vivo* plasma protein binding between NS2330 (94.7%) and M1 (94.9%) in mice was comparable, rejecting this hypothesis as well. Another explanation might be the differences in the assays that were used to determine *in vitro* and *in vivo* activity. It should be noticed that the assessment of the *in vitro* activity of NS2330 and the metabolites were performed time shifted using different batches, which might cause also differences. In general, discrepancies between *in vivo* and *in vitro* investigations are well known in the literature[108–110]. Moreover, it has to be realized that

in vitro methods are in general static systems whereas *in vivo* methods reflect a more complex time- and concentration-dependent dynamic system. However, as *in vivo* investigations are closer to the biological reality and system behaviour, results from *in vivo* investigations should be favoured[111] when evaluating the contribution of metabolites to the pharmacological effect.

NS2330 and M1 showed multiple modes of action in inhibiting the transporters of the neurotransmitters NA, HT and DA. The *in vivo* activity of both compounds with respect to the dopamine transporter was successfully investigated in this study, but the *in vivo* activity of both compounds with regard to the noradrenalin and the serotonin transporters is still unknown. *In vitro* investigations[5] of the investigational compounds at the remaining transporters resulted in IC_{50} values for NS2330 of 11 nM and 1.7 nM for the $[^3H]$-5-HT and $[^3H]$-5-NA uptake, respectively. IC_{50} values for M1 were 2.0 nM and 0.6 nM for the $[^3H]$-5-HT and $[^3H]$-5-NA uptake, respectively. Thus, both compounds showed comparable ratios of the in vitro potency at the HT and NA transporter when compared to the dopamine transporter. Therefore, it might be speculated that results from the dopamine transporter investigation could be transferable to the other transporters. However, further *in vivo* investigation are warranted to confirm this hypothesis.

Due to the complexity of an administration of metabolites to humans (e.g. toxicology investigations, availability of a metabolite formulation), the investigation was performed in mice with the resulting question of predictability to humans. Allometric scaling is a widely used tool in pharmacokinetics to extrapolate data from the animal to the human situation[112]. Unfortunately, there are currently only a few examples available where this technique was applied to pharmacodynamic data[113]. Additionally, allometric scaling requires data from more than one species for a reliable extrapolation to humans. Wu and Gu performed *in vitro* studies[114] where the drug inhibition profiles of four different dopamine transporter inhibiting drugs were investigated with regard to the dopamine transporter of mouse (mDAT) and human (hDAT). DAT from both species showed the same affinity (Kd: 0.75 μM) to bupropione and amphetamine, hDAT showed a higher affinity than the mDAT against cocaine (Kd: 0.14 μM and 0.29 μM, respectively) and ritalin (Kd: 0.038 μM and 0.12 μM, respectively). Wu and Gu also investigated the amino acid homology of the dopamine transporter from both species and found that the mDAT is 93.5% identical to the hDAT[114]. On the whole the high structural amino acid homology and the comparable affinity of the hDAT and the mDAT might suggest that the results could possibly be transferred to the human situation.

Data analysis showed that the pharmacodynamic effect lagged behind the plasma concentration-time profile which was accounted for by introducing an effect compartment model to link the PD with the PK. The rate constants KEO which determined the concentrations

in the effect compartments indicated that at a constant steady-state concentration the plasma concentrations would equal the site of action concentrations after 6.2 and 3.9 hours for NS2330 and M1, respectively. This slight time delay might be caused by distribution processes of the molecules between the plasma and the CNS where several permeation barriers (e.g. blood-brain-barrier) have to be overcome[115]. However, considering the planned indications of Alzheimer's disease and Parkinson's disease where a continuous treatment of the patients with NS2330 is intended and required, this time delay is most probably not of importance.

As both compounds were separately administered by different routes the question could be investigated whether additional active first-pass metabolites were formed during the absorption phase that would have resulted in reduced EC_{50} values after oral administration in comparison to iv administration. No significant changes in EC_{50} parameter estimates were found between iv administration and a combination of iv and po administration indicating that no further and/or currently unknown active metabolites were built in mice during the first-pass process of NS2330.

Combining the finding of this project of a five-fold lower potency of M1 with approximately 60% lower steady-state plasma concentrations of M1 in humans suggests that the contribution of the active metabolite M1 to the overall efficacy is low in humans.

4.5 Efficacy in Alzheimer's Disease Patients

Project VI investigated the relationship between the pharmacokinetic behaviour and the pharmacodynamic response of NS2330 and M1. The ADAS-COG value was investigated as a pharmacodynamic surrogate parameter. A PopPK/PD model could successfully be developed describing the relationship between plasma concentrations and the response in patients. The developed model included prior knowledge gained within projects I and V. The population PK model developed in project I was used to describe the PK. Details of the PK model have been described and discussed there in detail.

The PD effect was described by a competitive interaction model where the potency of M1 was based on the findings of project V, i.e. a 5-fold lower potency of M1 was assumed. The maximum effect achievable was a 37.5% reduction of the ADAS-COG baseline values in the patients. As for other drugs approved for AD the efficacy is expressed in absolute values, a recalculation considering the median ADAS-COG baseline value (8.7) of the population investigated revealed a median reduction of 3.3 points in the population investigated. Particularly, it should be considered that the absolute reduction of 3.26 points reflects only a snapshot and is dependent on the median of the population (Figure 7.42). Hence, a comparison to other

competitor drugs cannot be done easily. Nevertheless, even for a population with this mild disease status (baseline value: 8.7), NS2330 is at least effective if not even better than other Alzheimer's disease[116] drugs. For a better comparison of drug effects in Alzheimer's disease it should be recommended to express the efficacy additionally in percent of reduction as this method allows a cross-comparison independent from the baseline values of the patient population investigated.

The covariate analysis revealed a significant influence of age on the maximum effect of NS2330. The influence of age showed that an increasing age resulted in a reduced efficacy in patients. The age effect on Emax predicted by the model was substantial (Figure 3.14). Due to the limited number of patients investigated during this project the absolute impact of age predicted should be handled with care and it should be further investigated in a larger number of patients. Nevertheless, the incorporation of this covariate into the model explained a large extent of the variability in this parameter and age can be seen as an important covariate. Considering the mode of action of NS2330 this covariate effect also seems physiologically plausible. The effect might presumably be caused by age-related alterations in neurotransmitter functions in the human brain[117], resulting in less efficacy of drugs[96].

Data analysis showed that the pharmacodynamic effect lagged behind the plasma concentration-time profile which was accounted for by introducing an effect compartment model. This time delay might be caused by distribution processes between the plasma and the CNS[115] and additionally by different adaptation processes of the human neurotransmitter systems. Especially the increase of the acetylcholine release caused by NS2330 is controlled by a feedback mechanism responding to the increased dopamine concentrations[2,3]. Unfortunately, feedback durations in humans have not been reported. However, the delayed pharmacodynamic onset of CNS active drugs is well known (e.g.[118-121]) and is for NS2330 of no clinical importance considering the continuous treatment of the Alzheimer's disease patients. Simulations showed that due to different doses administered, the maximum effect might be earlier achievable (Figure 7.43).

The percentage of the non-responders within project VI was low at 27% compared to other drugs approved for AD, where non-responder rates up to 75% were reported[122]. In depth analysis of the non-responder population of NS2330 showed that their median baseline values were decreased by 25% (9.0 vs. 6.7) compared to the responder group (Table 7.37). The median age of the non-responders was 2.5 years older than the responder group (72.5 vs. 70 years). Considering the results obtained from the covariate analysis, the age and baseline differences in combination might have synergistically influenced the subjects' response status to the drug.

For several drugs, the existence of a placebo effect is well known[123]. In project VI the anal-

ysis of the placebo group revealed no clear improvement or deterioration in the ADAS-COG values. Nevertheless, to identify a clear placebo effect, larger numbers of patients treated with verum and placebo will be necessary to distinguish between placebo and verum effect.

For Alzheimer's disease progression is well known, showing an increase of the ADAS-COG value of 3 to 6 points per year[81]. As the studies of project VI were performed over only 4 weeks, a disease progression could not be determined by the model. However, for the evaluation of further trials conducted over a longer period the disease progression needs to be considered during model building.

Overall, the analysis revealed a promising efficacy of NS2330 for the treatment of Alzheimer's disease. As only a small number of patients were investigated in project VI all findings need to be confirmed in a larger number of patients treated over a longer period of time. Results from covariate analysis might help to understand the responder status of the patients and will allow identification of possible non-responder subgroups within the population. The model developed will be able to serve as a tool to optimise the dosing regimens with the aim of achieving the maximum effect while avoiding plasma concentrations evoking adverse events.

5 Conclusions

The overall objective of this thesis was to contribute to the PK/PD characterisation of the promising new compound NS2330 and its major metabolite M1 in healthy volunteers and in the Alzheimer's target population. The following conclusions regarding the PK and PD based on six modelling projects can be drawn.

Pharmacokinetics

- NS2330 and M1 plasma concentrations were successfully modelled for both compounds simultaneously with first-order eliminations and a first-order absorption of NS2330 in humans. Formation of M1 from NS2330 was accounted for by a first-order metabolism process (Projects I and II).

- The pharmacokinetics of AD patients and healthy subjects were comparable (Projects I and II).

- The covariate analysis identified weight, BMI, age, sex, creatinine clearance and CYP3A4 inhibitors as covariates influencing the clearances and volumes of distribution. Simulations showed that only CYP3A4 inhibitors, sex and creatinine clearance influenced the steady-state plasma concentration-time profiles of NS2330 and M1 significantly (Project II).

- The overall clearance of NS2330 was reduced by 20.5% in females compared to males (1.48 L/h vs. 1.86 L/h) resulting in 25.8% increased NS2330 steady-state concentrations in females compared to males (Project II).

- The typical non-metabolic clearance (which accounted for any elimination pathways except the formation of M1 out of NS2330) for AD patients with a creatinine clearance lower than 62.5 mL/min, was reduced by 1.2% per 1 mL/min reduction in creatinine clearance. In a renally impaired patient (CLCR: 35.6 mL/min) the overall clearance was 25% reduced, resulting in 33% increased steady-state concentrations (Project II).

- Enterohepatic circulation might have been the most reasonable explanation for the multiple peak phenomenon of NS2330. In combination with the low metabolic clearance, the enterohepatic circulation might have contributed to the long half-life of NS2330. Additionally, the interruption of the EHC suggested a fast and efficient detoxification of NS2330 (Project III).

- The maximum inhibitory effect of CYP3A4 inhibiting drugs caused a 39% reduction in the overall clearance of NS2330, resulting in an exposure increase of 63% (Project IV).
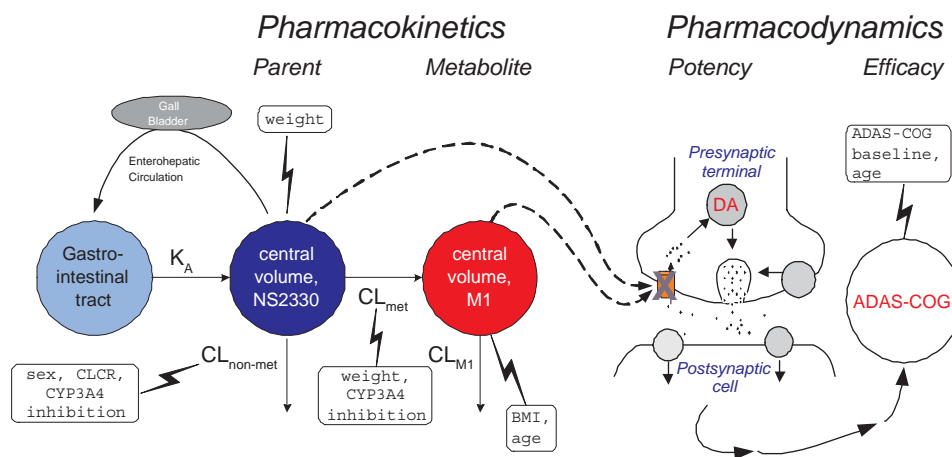

Figure 5.1 Schematic PK/PD model summarising results from thesis.

Pharmacodynamics

- NS2330 revealed a 4.1 - 5.0 fold higher *in vivo* potency in mice in comparison to M1 with respect to the inhibition of the dopamine re-uptake transporter. A five-fold lower potency of M1 and approximately 60% lower steady-state plasma concentrations of M1 in humans compared to NS2330 suggest that the contribution of the active metabolite M1 to the overall efficacy was probably low (Project V).

- NS2330 achieved good efficacy in mild AD patients after a four week short term treatment with NS2330 with a maximum reduction of 39% from the ADAS-COG baseline. ADAS-COG baseline values and age influenced the efficacy in mild AD patients. A higher baseline value increased the absolute efficacy of NS2330. With increasing age the maximum effect achievable (Emax) was reduced in the population investigated (Project VI).

6 Bibliography

[1] U. Thatte. NS-2330 NeuroSearch. *Current Opinion in Investigational Drugs*, 2(11):1592–1594, 2001.

[2] R. Bertorelli, M. Zambelli, G. Di Chiara, and S. Consolo. Dopamine depletion preferentially impairs D1- over D2-receptor regulation of striatal in vivo acetylcholine release. *Journal of Neurochemistry*, 59(1):353–357, 1992.

[3] Y. Ikarashi, A. Takahashi, H. Ishimaru, T. Arai, and Y. Maruyama. Regulation of dopamine D1 and D2 receptors on striatal acetylcholine release in rats. *Brain Research Bulletin*, 43(1):107–115, 1997.

[4] K.D. Bornemann, H. Rosenbrock, and F. Sams-Dodd. Amyloid β-lowering activity of the neurotransmitter reuptake inhibitor NS 2330 in vitro and in an APP transgenic mouse model. submitted, 2006.

[5] Investigator's Brochure NS2330. Boehringer Ingelheim, 2004.

[6] J.L. Cummings and G. Cole. Alzheimer disease. *Journal of the American Medical Association*, 287(18):2335–2338, 2002.

[7] E. Von Strauss, M. Viitanen, D. De Ronchi, B. Winblad, and L. Fratiglioni. Aging and the occurrence of dementia: Findings from a population-based cohort with a large sample of nonagenarians. *Archives of Neurology*, 56(5):587–592, 1999.

[8] H. Bickel. Dementia and Alzheimer's disease: An estimate of prevalent and incident cases in Germany [Demenzsyndrom und Alzheimer Krankheit: Eine Schätzung des Krankenbestandes und der jährlichen Neuerkrankungen in Deutschland]. *Gesundheitswesen*, 62(4):211–218, 2000.

[9] R. Brookmeyer, S. Gray, and C. Kawas. Projections of Alzheimer's disease in the United States and the public health impact of delaying disease onset. *American Journal of Public Health*, 88(9):1337–1342, 1998.

[10] J.D.W. Greene, J.R. Hodges, and A.D. Baddeley. Analysis of the episodic memory deficit in early Alzheimer's disease: Evidence from the doors and people test. *Neuropsychologia*, 34(6):537–551, 1996.

[11] B. Pillon, B. Deweer, Y. Agid, and B. Dubois. Explicit memory in Alzheimer's, Huntington's, and Parkinson's diseases. *Archives of Neurology*, 50(4):374–379, 1993.

[12] B.H. Price, H. Gurvit, S. Weintraub, C. Geula, E. Leimkuhler, and M. Mesulam. Neuropsychological patterns and language deficits in 20 consecutive cases of autopsy-confirmed Alzheimer's disease. *Archives of Neurology*, 50(9):931–937, 1993.

[13] C. Esteban-Santillan, H. Ueda, D.S. Geldmacher, and R. Praditsuwan. Clock drawing test in very mild Alzheimer's disease. *Journal of the American Geriatrics Society*, 46(10): 1266–1269, 1998.

[14] A. Kirk and A. Kertesz. On drawing impairment in Alzheimer's disease. *Archives of Neurology*, 48(1):73–77, 1991.

[15] G. McKhann, D. Drachman, and M. Folstein. Clinical diagnosis of Alzheimer's disease: Report of the NINCDS-ADRDA work group under the auspices of Department of Health and Human Services Task Force on Alzheimer's disease. *Neurology*, 34(7): 939–944, 1984.

[16] D. Galasko, C. Ernesto, R. Thomas, M. Grundman, D. Bennett, M. Sano, and S. Ferris. An inventory to assess activities of daily living for clinical trials in Alzheimer's disease. *Alzheimer Disease and Associated Disorders*, 11(Suppl. 2):33–39, 1997.

[17] M.S. Mega, J.L. Cummings, T. Fiorello, and J. Gornbein. The spectrum of behavioral changes in Alzheimer's disease. *Neurology*, 46(1):130–135, 1996.

[18] L. Bracco, R. Gallato, F. Grigoletto, A. Lippi, V. Lepore, G. Bino, M.P. Lazzaro, F. Carella, T. Piccolo, C. Pozzilli, B. Giometto, and L. Amaducci. Factors affecting course and survival in Alzheimer's disease: A 9-year longitudinal study. *Archives of Neurology*, 51(12): 1213–1219, 1994.

[19] E. Kokmen, C.M. Beard, G.E. Smith, T. Petterson, P.C. O'Brien, and C. Sigler. Cause of death in Alzheimer's disease. *Annals of Epidemiology*, 6(3):195–200, 1996.

[20] M. Ball, H. Braak, P. Coleman, D. Dickson, C. Duyckaerts, P. Gambetti, L. Hansen, B. Hyman, K. Jellinger, W. Markesbery, D. Perl, J. Powers, J. Price, J.Q. Trojanowski,

H. Wisniewski, C. Phelps, and Z. Khachaturian. Consensus recommendations for the postmortem diagnosis of Alzheimer's disease. *Neurobiology of Aging*, 18(4 Suppl.):S1–S2, 1997.

[21] G.M. Cole, Z.S. Khachaturian, J.L. Cummings, and H.V. Vinters. Alzheimer's disease: Etiologies, pathophysiology, cognitive reserve, and treatment opportunities. *Neurology*, 51(1 Suppl.):S2–S17, 1998.

[22] P. Lantos and N. Cairns. *Dementia*. Arnold, 2000.

[23] J. Hardy and D.J. Selkoe. The amyloid hypothesis of Alzheimer's disease: Progress and problems on the road to therapeutics. *Science*, 297:353–356, 2002.

[24] J.L. Cummings. Alzheimer's disease. *New England Journal of Medicine*, 351(1):56–67, 2004.

[25] A. Goate, M.C. Chartier-Harlin, M. Mullan, J. Brown, F. Crawford, L. Fidani, L. Giuffra, A. Haynes, N. Irving, L. James, R. Mant, P. Newton, K. Rooke, P. Roques, C. Talbot, M. Pericak-Vance, A. Roses, R. Williamson, and J. Hardy. Segregation of a missense mutation in the amyloid precursor protein gene with familial Alzheimer's disease. *Nature*, 349(6311):704–706, 1991.

[26] M. Mullan, F. Crawford, K. Axelman, H. Houlden, L. Lilius, B. Winblad, and L. Lannfelt. A pathogenic mutation for probable Alzheimer's disease in the APP gene at the N-terminus of beta-amyloid. *Nature Genetics*, 1(5):345–347, 1992.

[27] J. Hardy. Framing beta-amyloid. *Nature Genetics*, 1(4):233–234, 1992.

[28] L. Hendriks, C.M. van Duijn, P. Cras, M. Cruts, W. Van Hul, F. van Harskamp, A. Warren, M.G. McInnis, S.E. Antonarakis, and J.J. Martin. Presenile dementia and cerebral haemorrhage linked to a mutation at codon 692 of the beta-amyloid precursor protein gene. *Nature Genetics*, 1(3):218–221, 1992.

[29] J. Kang, H.G. Lemaire, and A. Unterbeck. The precursor of Alzheimer's disease amyloid A4 protein resembles a cell-surface receptor. *Nature*, 325(6106):733–736, 1987.

[30] D. Goldgaber, M.I. Lerman, and O.W. McBride. Characterization and chromosomal localization of a cDNA encoding brain amyloid of Alzheimer's disease. *Science*, 235 (4791):877–880, 1987.

[31] R.E. Tanzi, J.F. Gusella, and P.C. Watkins. Amyloid β protein gene: cDNA, mRNA distribution, and genetic linkage near the Alzheimer locus. *Science*, 235(4791):880–884, 1987.

[32] N.K. Robakis, N. Ramakrishna, G. Wolfe, and H.M. Wisniewski. Molecular cloning and characterization of a cDNA encoding the cerebrovascular and the neuritic plaque amyloid peptides. *Proceedings of the National Academy of Sciences of the United States of America*, 84(12):4190–4194, 1987.

[33] M.I. Olson and C.M. Shaw. Presenile dementia and Alzheimer's disease in mongolism. *Brain*, 92(1):147–156, 1969.

[34] K.R. Bales, T. Verina, R.C. Dodel, Y. Du, L. Altstiel, M. Bender, P. Hyslop, E.M. Johnstone, S.P. Little, D.J. Cummins, P. Piccardo, B. Ghetti, and S.M. Paul. Lack of apolipoprotein E dramatically reduces amyloid beta-peptide deposition. *Nature Genetics*, 17(3):263–264, 1997.

[35] D.S. Knopman, B.F. Boeve, and R.C. Petersen. Essentials of the proper diagnoses of mild cognitive impairment, dementia, and major subtypes of dementia. *Mayo Clinic Proceedings*, 78(10):1290–1308, 2003.

[36] A.K. Desai and G.T. Grossberg. Diagnosis and treatment of Alzheimer's disease. *Neurology*, 64(12 Suppl. 3):S34–S39, 2005.

[37] M.F. Folstein, S.E. Folstein, and P.R. McHugh. 'Mini mental state'. A practical method for grading the cognitive state of patients for the clinician. *Journal of Psychiatric Research*, 12(3):189–198, 1975.

[38] T.N. Tombaugh and N.J. McIntyre. The Mini-Mental State Examination: A comprehensive review. *Journal of the American Geriatrics Society*, 40(9):922–935, 1992.

[39] D. Galasko, M.R. Klauber, C.R. Hofstetter, D.P. Salmon, B. Lasker, and L.J. Thal. The mini-mental state examination in the early diagnosis of Alzheimer's disease. *Archives of Neurology*, 47(1):49–52, 1990.

[40] *EMEA Note for guidance on medical products in the treatment of Alzheimer's disease*, 1997.

[41] W.G. Rosen, R.C. Mohs, and K.L. Davis. A new rating scale for Alzheimer's disease. *American Journal of Psychiatry*, 141(11):1356–1364, 1984.

[42] P. Johannsen. Long-term cholinesterase inhibitor treatment of Alzheimer's disease. *CNS Drugs*, 18(12):757–768, 2004.

[43] A. Benson. Alzheimer's disease: A tangled issue. *Drug Discovery Today*, 10(11):749–751, 2005.

[44] J.T. Coyle, D.L. Price, and M.R. DeLong. Alzheimer's disease: A disorder of cortical cholinergic innervation. *Science*, 219(4589):1184–1190, 1983.

[45] J. Grutzendler and J.C. Morris. Cholinesterase inhibitors for Alzheimer's disease. *Drugs*, 61(1):41–52, 2001.

[46] J.L. Cummings. Cholinesterase inhibitors: A new class of psychotropic compounds. *American Journal of Psychiatry*, 157(1):4–15, 2000.

[47] J.T. Greenamyre, W.F. Maragos, R.L. Albin, J.B. Penney, and A.B. Young. Glutamate transmission and toxicity in Alzheimer's disease. *Progress in Neuro-Psychopharmacology and Biological Psychiatry*, 12(4):421–430, 1988.

[48] B. Reisberg, S. Ferris, R. Doody, A. Stöffler, H.J. Möbius, and F. Schmitt. Memantine in moderate-to-severe Alzheimer's disease. *New England Journal of Medicine*, 348(14): 1333–1341, 2003.

[49] L. Aarons. Population pharmacokinetics: Theory and practice. *British Journal of Clinical Pharmacology*, 32(6):669–670, 1991.

[50] L.B. Sheiner, B. Rosenberg, and V.V. Marathe. Estimation of population characteristics of pharmacokinetic parameters from routine clinical data. *Journal of Pharmacokinetics and Biopharmaceutics*, 5(5):445–479, 1977.

[51] *FDA Guidance for industry: Population Pharmacokinetics*, 1999.

[52] J.W. Mandema. *Pharmacokinetics: Regulatory, Industrial, Academic Perspectives.* Marcel Dekker, 1995.

[53] L.B. Sheiner and S.L. Beal. Evaluation of methods for estimating population pharmacokinetic parameters II. Biexponential model and experimental pharmacokinetic data. *Journal of Pharmacokinetics and Biopharmaceutics*, 9(5):635–651, 1981.

[54] C. Minto and T. Schnider. Expanding clinical applications of population pharmacodynamic modelling. *British Journal of Clinical Pharmacology*, 46(4):321–333, 1998.

[55] S. Jonsson and M.O. Karlsson. A rational approach for selection of optimal covariate-based dosing strategies. *Clinical Pharmacology and Therapeutics*, 73(1):7–19, 2003.

[56] L. Aarons. Software for population pharmacokinetics and pharmacodynamics. *Clinical Pharmacokinetics*, 36(4):255–264, 1999.

[57] S.L. Beal and L.B. Sheiner. *NONMEM Users Guides.* Universtity of California, 1998.

[58] F. Mentre. History and new developments in estimation methods in nonlinear mixed-effects models. *PAGE*, 14, 2005.

[59] L.B. Sheiner. Analysis of pharmacokinetic data using parametric models. I: Regression models. *Journal of Pharmacokinetics and Biopharmaceutics*, 12(1):93–117, 1984.

[60] M.O. Karlsson and L.B. Sheiner. The importance of modeling interoccasion variability in population pharmacokinetic analyses. *Journal of Pharmacokinetics and Biopharmaceutics*, 21(6):735–750, 1993.

[61] J.W. Mandema, D. Verotta, and L.B. Sheiner. Building population pharmacokinetic-pharmacodynamic models. I. Models for covariate effects. *Journal of Pharmacokinetics and Biopharmaceutics*, 20(5):511–528, 1992.

[62] H. Akaike. A new look at the statistical model identification. *IEEE Transactions on Automatic Control*, 19(6):716–723, 1974.

[63] P.O. Maitre, M. Buhrer, D. Thomson, and D.R. Stanski. A three-step approach combining bayesian regression and NONMEM population analysis: Application to midazolam. *Journal of Pharmacokinetics and Biopharmaceutics*, 19(4):377–384, 1991.

[64] E.N. Jonsson and M.O. Karlsson. Automated covariate model building within NON-MEM. *Pharmaceutical Research*, 15(9):1463–1468, 1998.

[65] L. Aarons, P. Balant l., F. Mentre, P.L. Morselli, M. Rowland, J.L. Steimer, and S. Vozeh. Population approaches in drug development. Report on an expert meeting to discuss population pharmacokinetic/pharmacodynamic software. *European Journal of Clinical Pharmacology*, 46(5):389–391, 1994.

[66] S.L. Beal. Population pharmacokinetic data and parameter estimation based on their first two statistical moments. *Drug Metabolism Reviews*, 15(1-2):173–193, 1984.

[67] S.L. Beal and L.B. Sheiner. *NONMEM Users Guide. Conditional Estimation Methods.* Universtity of California, 1998.

[68] E.N. Jonsson and M.O. Karlsson. Xpose - An S-PLUS based population pharmacokinetic/pharmacodynamic model building aid for NONMEM. *Computer Methods and Programs in Biomedicine*, 58(1):51–64, 1999.

[69] D. Du Bois and E.F. Du Bois. A formula to estimate the approximate surface area if height and weight are known. *Archives Internal Medicine*, 17:863–871, 1916.

[70] D.W. Cockcroft and M.H. Gault. Prediction of creatinine clearance from serum creatinine. *Nephron*, 16(1):31–41, 1976.

[71] W.G. Rosen, R.D. Terry, and P.A. Fuld. Pathological verification of ischemic score in differentiation of dementias. *Annals of Neurology*, 7(5):486–488, 1980.

[72] U. Busch, G. Heinzel, and H. Narjes. The effect of cholestyramine on the pharmacokinetics of meloxicam, a new nonsteroidal anti-inflammatory drug (NSAID), in man. *European Journal of Clinical Pharmacology*, 48(3-4):269–272, 1995.

[73] C.H.W. Koks, A.D.R. Huitema, J.H. Beijnen, E.D.M.B. Kroon, T. Chuenyam, J.M.A. Lange, and R.W. Sparidans. Population pharmacokinetics of itraconazole in Thai HIV-1-infected persons. *Therapeutic Drug Monitoring*, 25(2):229–233, 2003.

[74] F. Ezzet, G. Krishna, D.B. Wexler, P. Statkevich, T. Kosoglou, and V.K. Batra. A population pharmacokinetic model that describes multiple peaks due to enterohepatic recirculation of ezetimibe. *Clinical Therapeutics*, 23(6):871–885, 2001.

[75] J.L. Steimer, Y. Plusquellec, A. Guillaume, and J.F. Boisvieux. A time-lag model for pharmacokinetics of drugs subject to enterohepatic circulation. *Journal of Pharmaceutical Sciences*, 71(3):297–302, 1982.

[76] T. Funaki. Enterohepatic circulation model for population pharmacokinetic analysis. *Journal of Pharmacy and Pharmacology*, 51(10):1143–1148, 1999.

[77] T. Wajima, Y. Yano, and T. Oguma. A pharmacokinetic model for analysis of drug disposition profiles undergoing enterohepatic circulation. *Journal of Pharmacy and Pharmacology*, 54(7):929–934, 2002.

[78] T.C. Hardin, J.R. Graybill, R. Fetchick, R. Woestenborghs, M.G. Rinaldi, and J.G. Kuhn. Pharmacokinetics of itraconazole following oral administration to normal volunteers. *Antimicrobial Agents and Chemotherapy*, 32(9):1310–1313, 1988.

[79] N. Isoherranen, K.E. Thummel, K.L. Kunze, K.E. Allen, and W.L. Nelson. Role of itraconazole metabolites in CYP3A4 inhibition. *Drug Metabolism and Disposition*, 32(10): 1121–1131, 2004.

[80] N.H. Holford and L.B. Sheiner. Kinetics of pharmacologic response. *Pharmacology & Therapeutics*, 16(2):143–166, 1982.

[81] P.L.S. Chan and N.H.G. Holford. Drug treatment effects on disease progression. *Annual Review of Pharmacology and Toxicology*, 41:625–659, 2001.

[82] M.W. Jann, T.L. ZumBrunnen, S.N. Tenjarla, Jr Ward, and D.J. Weidler. Relative bioavailability of ondansetron 8-mg oral tablets versus two extemporaneous 16-mg suppositories: Formulation and gender differences. *Pharmacotherapy*, 18(2 I):288–294, 1998.

[83] E. Seaber, N. On, R.M. Dixon, M. Gibbens, W.J. Leavens, J. Liptrot, G. Chittick, J. Posner, P.E. Rolan, and R.W. Peck. The absolute bioavailability and metabolic disposition of the novel antimigraine compound zolmitriptan (311C90). *British Journal of Clinical Pharmacology*, 43(6):579–587, 1997.

[84] I. Beierle, B. Meibohm, and H. Derendorf. Gender differences in pharmacokinetics and pharmacodynamics. *International Journal of Clinical Pharmacology and Therapeutics*, 37 (11):529–547, 1999.

[85] M. Gandhi, R.M. Greenblatt, F. Aweeka, and T.F. Blaschke. Sex Differences in Pharmacokinetics and Pharmacodynamics. *Annual Review of Pharmacology and Toxicology*, 44: 499–523, 2004.

[86] R.Z. Harris, L.Z. Benet, and J.B. Schwartz. Gender effects in pharmacokinetics and pharmacodynamics. *Drugs*, 50(2):222–239, 1995.

[87] B. Meibohm, I. Beierle, and H. Derendorf. How important are gender differences in pharmacokinetics? *Clinical Pharmacokinetics*, 41(5):329–342, 2002.

[88] J.B. Schwartz. The influence of sex on pharmacokinetics. *Clinical Pharmacokinetics*, 42(2): 107–121, 2003.

[89] E. Tanaka. Gender-related differences in pharmacokinetics and their clinical significance. *Journal of Clinical Pharmacy and Therapeutics*, 24(5):339–346, 1999.

[90] M.S. Roberts, B.M. Magnusson, F.J. Burczynski, and M. Weiss. Enterohepatic circulation: Physiological, pharmacokinetic and clinical implications. *Clinical Pharmacokinetics*, 41 (10):751–790, 2002.

[91] M.E. Morris, H.J. Lee, and L.M. Predko. Gender differences in the membrane transport of endogenous and exogenous compounds. *Pharmacological Reviews*, 55(2):229–240, 2003.

[92] E.G. Schuetz, K.N. Furuya, and J.D. Schuetz. Interindividual variation in expression of P-glycoprotein in normal human liver and secondary hepatic neoplasms. *Journal of Pharmacology and Experimental Therapeutics*, 275(2):1011–1018, 1995.

[93] H. Boxenbaum. Interspecies scaling, allometry, physiological time, and the ground plan of pharmacokinetics. *Journal of Pharmacokinetics and Biopharmaceutics*, 10(2):201–227, 1982.

[94] H. Boxenbaum. Interspecies variation in liver weight, hepatic blood flow, and antipyrine intrinsic clearance: Extrapolation of data to benzodiazepines and phenytoin. *Journal of Pharmacokinetics and Biopharmaceutics*, 8(2):165–176, 1980.

[95] G. Cheymol. Effects of obesity on pharmacokinetics: Implications for drug therapy. *Clinical Pharmacokinetics*, 39(3):215–231, 2000.

[96] A.A. Mangoni and S.H.D. Jackson. Age-related changes in pharmacokinetics and pharmacodynamics: Basic principles and practical applications. *British Journal of Clinical Pharmacology*, 57(1):6–14, 2004.

[97] Jr Fulop, I. Worum, and J. Csongor. Body composition in elderly people. I. Determination of body composition by multiisotope method and the elimination kinetics of these isotopes in healthy elderly subjects. *Gerontology*, 31(1):6–14, 1985.

[98] E.A. Shaffer. Control of gall-bladder motor function. *Alimentary Pharmacology and Therapeutics, Supplement*, 14(2):2–8, 2000.

[99] R.S. Fisher, F. Stelzer, E. Rock, and L.S. Malmud. Abnormal gallbladder emptying in patients with gallstones. *Digestive Diseases and Sciences*, 27(11):1019–1024, 1982.

[100] B. Rozman. Clinical pharmacokinetics of leflunomide. *Clinical Pharmacokinetics*, 41(6): 421–430, 2002.

[101] A.J. McLean and D.J. Morgan. Clinical pharmacokinetics in patients with liver disease. *Clinical Pharmacokinetics*, 21(1):42–69, 1991.

[102] D.E. Rollins and C.D. Klaassen. Biliary excretion of drugs in man. *Clinical Pharmacokinetics*, 4(5):368–379, 1979.

[103] I. Mahmood and C. Sahajwalla. Interspecies scaling of biliary excreted drugs. *Journal of Pharmaceutical Sciences*, 91(8):1908–1914, 2002.

[104] I. Mahmood. Interspecies scaling of biliary excreted drugs: A comparison of several methods. *Journal of Pharmaceutical Sciences*, 94(4):883–892, 2005.

[105] S. Zhou, S.Y. Chan, E. Chan, B.C. Goh, W. Duan, M. Huang, and H.L. McLeod. Mechanism-based inhibition of cytochrome P450 3A4 by therapeutic drugs. *Clinical Pharmacokinetics*, 44(3):279–304, 2005.

[106] K.E. Thummel and G.R. Wilkinson. In vitro and in vivo drug interactions involving human CYP3A. *Annual Review of Pharmacology and Toxicology*, 38:389–430, 1998.

[107] I.K. Björkman, J. Fastbom, I.K. Schmidt, C.B. Bernsten, I.K. Björkman, M. Caramona, G. Crealey, B. Frøkjær, E. Grünberger, T. Gustafsson, M. Henman, H. Herborg, C. Hughes, J.C. McElnay, M. Magner, F. Van Mil, M. Schaeffer, S. Silva, B. Søndergaard, I. Sturgess, D. Tromp, L. Vivero, and A. Winterstein. Drug-drug interactions in the elderly. *Annals of Pharmacotherapy*, 36(11):1675–1681, 2002.

[108] R. Barnard and K.G. Gurevich. In vitro bioassay as a predictor of in vivo response. *Theoretical Biology and Medical Modelling*, 2, 2005.

[109] J. Heykants, M. Michiels, R. Woestenborghs, F. Awouters, J.E. Leysen, J. Schuurkes, and J.M. Van Nueten. Pharmacokinetic evaluation of the in vitro and in vivo pharmacological profile of the major metabolites of ketanserin in the rat. *Arzneimittel-Forschung/Drug Research*, 38(6):785–788, 1988.

[110] J.H. Lin, I.W. Chen, and T.H. Lin. Blood-brain barrier permeability and in vivo activity of partial agonists of benzodiazepine receptor: A study of L-663,581 and its metabolites in rats. *Journal of Pharmacology and Experimental Therapeutics*, 271(3):1197–1202, 1994.

[111] *FDA Guidance for industry: Drug metabolism/drug interaction studies in the drug development process, studies in vitro*, 1997.

[112] R.M.J. Ings. Interspecies scaling and comparisons in drug development and toxicokinetics. *Xenobiotica*, 20(11):1201–1231, 1990.

[113] E.I. Lepist and W.J. Jusko. Modeling and allometric scaling of s(+)-ketoprofen pharmacokinetics and pharmacodynamics: a retrospective analysis. *Journal of Veterinary Pharmacology & Therapeutics*, 27(4):211–218, August 2004.

[114] X. Wu and H.H. Gu. Molecular cloning of the mouse dopamine transporter and pharmacological comparison with the human homologue. *Gene*, 233(1-2):163–170, 1999.

[115] W.M. Pardridge. CNS drug design based on principles of blood-brain barrier transport. *Journal of Neurochemistry*, 70(5):1781–1792, 1998.

[116] M.W. Jann, K.L. Shirley, and G.W. Small. Clinical pharmacokinetics and pharmacodynamics of cholinesterase inhibitors. *Clinical Pharmacokinetics*, 41(10):719–739, 2002.

[117] D.G. Morgan, P.C. May, and C.E. Finch. Dopamine and serotonin systems in human and rodent brain: Effects of age and neurodegenerative disease. *Journal of the American Geriatrics Society*, 35(4):334–345, 1987.

[118] M.J. Kuhar and A.R. Joyce. Slow onset of CNS drugs: Can changes in protein concentration account for the delay? *Trends in Pharmacological Sciences*, 22(9):450–456, 2001.

[119] H.H. Stassen, J. Angst, and A. Delini-Stula. Delayed onset of action of antidepressant drugs? Survey of results of Zurich meta-analyses. *Pharmacopsychiatry*, 29(3):87–96, 1996.

[120] H.H. Stassen, J. Angst, and A. Delini-Stula. Delayed onset of action of antidepressant drugs. Survey of recent results. *European Psychiatry*, 12(4):166–176, 1997.

[121] H.H. Stassen and J. Angst. Delayed onset of action of antidepressants: Fact or fiction? *CNS Drugs*, 9(3):177–184, 1998.

[122] K.L. Lanctôt, N. Herrmann, L.R. Khan, B.A. Liu, K.K. Yau, M.M. LouLou, and T.R. Einarson. Efficacy and safety of cholinesterase inhibitors in Alzheimer's disease: A meta-analysis. *Canadian Medical Association Journal*, 169(6):557–564, 2003.

[123] F.M. Quitkin. Placebos, drug effects, and study design: A clinician's guide. *American Journal of Psychiatry*, 156(6):829–836, 1999.

7 Appendix

7.1 Tables

Table 7.1 Methods - Overview of bioanalytical measurements

Project	Study	Analytical Method	Validated Range [ng/mL]	LLOQ$^\alpha$ [ng/mL]	Measurement Site
I	PI.1	HPLC-MS/MS	0.1-50.0	0.1	Quintiles AB$^\beta$
I	PI.2	HPLC-MS/MS	0.02-50.0	0.02	Quintiles AB$^\beta$
I	PI.3	HPLC-MS/MS	0.1-50.0	0.1	Quintiles AB$^\beta$
I	PI.4	HPLC-MS/MS	0.1-50.0	0.1	Quintiles AB$^\beta$
I	PI.5	HPLC-MS/MS	0.1-50.0	0.1	Quintiles AB$^\beta$
I	PI.6	HPLC-MS/MS	0.1-50.0	0.1	Quintiles AB$^\beta$
II	PII	HPLC-MS/MS	0.1-50.0	0.1	Boehringer Ingelheim$^\gamma$
IV	PIV	HPLC-MS/MS	0.1-50.0	0.1	Boehringer Ingelheim$^\gamma$
V	PV	HPLC-MS/MS	1.0-50.0	1.0	Boehringer Ingelheim$^\gamma$

$^\alpha$ LLOQ: lower limit of quantification, $^\beta$ Uppsala, Sweden, $^\gamma$ Biberach, Germany

Table 7.2 Methods - Overview of treatments administered in project I

Study	Dosage form	Treatment [days]	Batch Nr.	Manufacturer
PI.1	solution for iv infusion	1	B021204	BI Pharma GmbH&Co. KG
PI.2	tablet (1 mg)	1	0001E017	Siegfried CMS, Switzerland
PI.3	tablet (0.25 mg)	14	9809E008	Siegfried CMS, Switzerland
	tablet (1 mg)	14	9809E009	Siegfried CMS, Switzerland
PI.4	tablet (0.25 mg)	28	0111B033	Siegfried CMS, Switzerland
	tablet (0.5 mg)	28	0111B035	Siegfried CMS, Switzerland
PI.5	tablet (0.125 mg)	28	n.a.	Quintiles Clinical
PI.6	tablet (0.125 mg)	28	n.a.	Quintiles Clinical
	tablet (0.25 mg)	28	n.a.	Quintiles Clinical
	tablet (1.0 mg)	28	n.a.	Quintiles Clinical

n.a. not available

Table 7.3 Methods - Overview of treatment patterns administered in project I

Study	Dose Group	Dose Route	Loading Dose [mg]	Maintenance Dose [mg]	Dose Regimen
PI.1	1	iv	0.3	-	once
	2	iv	0.6	-	once
	3	iv	0.9	-	once
	4	iv	1.2	-	once
PI.2	1	po	1.0	-	once
PI.3	1	po	1.0 (day 1), 2.0 (day 2)	0.5 (day 3-14)	once daily
	2	po	2.0 (day 1-3)	0.5 (day 4-14)	once daily
PI.4	1	po	1.5 (day 1-6)	0.75 (day 7-28)	once daily
PI.5	1	po	0.5 (day 1-3)	0.125 (day 4-28)	once daily
	2	po	1.0 (day 1-3)	0.125 (day 4-28)	once daily
	3	po	1.5 (day 1-3)	0.25 (day 4-28)	once daily
	4	po	2.0 (day 1-3)	0.25 (day 4-28)	once daily
PI.6	1	po	2.0 (day 1-3)	0.5 (day 4-28)	once daily
	2	po	2.0 (day 1-3)	1.0 (day 4-28)	once daily

Table 7.4 Methods - Overview of observations taken in project I

Study	Dose Group	Blood Sampling [h]
PI.1	1	0, 1, 2, 3, 4, 5, 6, 6.25, 6.5, 7, 8, 10, 24, 32, 48, 72, 120, 168, 336, 504, 672, 840, 1008, 1176, 1344, 1512, 1680
PI.2	1	0, 2, 4, 6, 8, 10, 12, 24, 48, 120, 240, 360, 528, 696, 864, 1032, 1200, 1368, 1536
PI.3	1	0, 24, 26, 28, 30, 32, 34, 36, 48, 72, 96, 144, 192, 240, 288, 312, 314, 316, 318, 320, 322, 324, 336, 384, 480, 648, 984, 1320
	2	0, 24, 48, 50, 52, 54, 56, 58, 60, 72, 96, 144, 192, 240, 288, 312, 314, 316, 318, 320, 322, 324, 336, 384, 480, 648, 984, 1320
PI.4	1	0, 6, 24, 168, 312, 480, 486, 648, 649, 650, 652, 654, 656, 658, 660, 672, 696, 720, 816, 984, 1320
PI.5	1, 2, 3, 4	0, 96, 168, 312, 648, 984, 1320
PI.6	1	0, 96, 168, 174, 312, 648, 654, 984, 1320
	2	0, 6, 69, 102, 168, 174, 312, 480, 486, 648, 650, 652, 654, 655, 656, 658, 660, 672, 984, 1320

Table 7.5 Methods - Dosage and treatment pattern in project IV

Medication	Day -5 (ambulatory)	Day -4 to -1 (ambulatory)	Day 1 (in-house)	Day 2 (in-house)	Day 3 to 6 (ambulatory)
Treatment 1 (Itraconazole qd, NS2330 sd)	400 mg ITZ evening	200 mg ITZ morning	200 mg ITZ morning +2 mg NS2330 morning	200 mg ITZ morning	200 mg ITZ morning
Treatment 2 (NS2330 sd)	-	-	2 mg NS2330 morning	-	-

ITZ: itraconazole

Table 7.6 Methods - Overview of doses administered and sampling time points in project V

Treatment	Dose [mg/kg]$^\alpha$	PK$^\beta$ and PD$^\gamma$ Sample Time Points [h]
NS2330 iv	0.3	0.75, 1.5, 3
	1	0.75, 1.5, 3
	3	0.75, 1.5, 3
	5	17.5
	10	17.5
M1 iv	0.3	0.75, 1.5, 3
	1	0.75, 1.5, 3
	3	0.75, 1.5, 3
	5	17.5
	10	17.5
NS2330 po	1	0.75, 1.5, 3
	3	0.75, 1.5, 3
	10	0.75, 1.5, 3, 16
	20	16
M1 po	1	0.75, 1.5, 3
	3	0.75, 1.5, 3
	10	0.75, 1.5, 3, 16
	20	16

$^\alpha$ dosed according to the salt form

$^\beta$ PK: NS2330 and/or M1 plasma measurements

$^\gamma$ PD: inhibition of *in vivo* $\left[^3\text{H}\right]$WIN 35,428 binding

Table 7.7 Methods - Overview of inpatient phases in project VI

Study	Dose Group	Inpatient Phase (Days)			
		total	*acclimatisation*	*loading dosing*	*maintenance dosing*
PI.5	1	7	2	3	2
	2	7	2	3	2
	3	7	2	3	2
	4	11	2	3	6
PI.6	1	11	2	3	6
	2	14	2	3	9

Table 7.8 Project I - Distribution of observations by study

Study	Subjects		Number of Samples*		Average Samples per Subject*	
	n	%	NS2330	M1	NS2330	M1
PI.1	21	18	409	21	19	1
PI.2	30	25	498	454	17	15
PI.3	12	10	315	297	26	25
PI.4	12	10	240	220	20	18
PI.5	24	20	115	106	5	4
PI.6	20	17	242	235	12	12
SUM	119	100	1819	1333	15	11

* above lower limit of quantification

Table 7.9 Project I - Distribution of categorical covariates

Covariate		Number of Subjects	%
Sex	*female*	36	30
	male	83	70
Smoking status	*non-smoker*	85	71
	former smoker	16	13
	current smoker	18	15
Ethnic origin	*Caucasian*	115	97
	African escent	2	2
	Asian or Pacific Islander	2	2

Table 7.10 Project I - Distribution of continuous covariates

Covariate		Median	Mean	Range	5th - 95th Percentile
Age	[y]	62.0	55.4	21.0 - 80.0	27.0 - 77.1
Weight	[kg]	80.0	80.7	54.0 - 120.0	60.0 - 102.5
Height	[cm]	174.0	173.7	147.0 - 190.0	157.5 - 187.0
Body mass index	[kg/m^2]	25.9	26.7	20.4 - 39.4	21.9 - 35.0
Serum creatinine	[μmol/L]	88.4	112.8	53.0 - 607.9	61.9 - 265.0
Creatinine clearance	[mL/min]	86.6	86.1	14.0 - 148.2	26.7 - 135.5

Table 7.11 Project I - Renal status

Renal Impairment	CLCR [mL/min]	Number of Subjects	% of Population
none	> 80	68	57
mild	50 - 80	37	31
moderate	30 - 50	6	5
severe	< 30	8	7

Table 7.12 Project I - Parameter estimates base and final model

Parameter		Base Model		Final Model	
Fixed Effects		Estimate	RSE%	Estimate	RSE%
KA	[1/h]	0.320	9.9	0.323	9.8
V2	[L]	213	23.6	218	23.9
Q_{NS2330}	[L/h]	201	16.8	203	16.9
V3	[L]	564	5.5	564	5.5
CL_{NS2330}	[L/h]	2.19	6.4	2.22	6.4
$V4_{PI.\ 1,2,3,4}$	[L]	24.1	19.5	21.7	18.6
$V4_{PI.\ 5,6}$	[L]	24.1	19.5	72.5	16.3
Q_{M1}	[L/h]	6.77	11.6	6.75	11.0
V5	[L]	141	10.1	138	9.6
CL_{M1}	[L/h]	0.420	7.4	0.426	7.3
$F1_{Male}$	[%]	117	7.4	107	7.3
$F1_{Female}$	[%]	117	7.4	142	7.5
Covariate Influence					
θ_{V4_CLCR} [1]	[%]	n.a.	n.a.	0.0119	11.6
[1] $V4 = \theta V4 \cdot [1 + \theta_{V4\_CLCR} \cdot (CLCR - 85.3)] \cdot EXP(\omega^2 V4)$					
Random Effects					
ωCL_{NS2330}	[CV%]	25.0	13.0*	23.9	13.0*
ωCL_{M1}	[CV%]	41.4	13.7*	40.1	14.0*
$\omega V2$	[CV%]	43.9	35.1*	47.6	37.2*
$\omega V4$	[CV%]	115.3	19.3*	79.9	21.1*
$\omega F1$	[CV%]	24.3	20.2*	19.0	21.5*
$Corr\_CL_{NS2330}/_{M1}$		0.801	14.5§	0.787	15.0§
prop. error $_{NS2330}$	[%]	14.1	7.0*	14.0	7.0*
prop. error $_{M1}$	[%]	14.3	9.0*	14.3	9.0*

* RSE is given on the variance scale

§ RSE of the covariance estimate

n.a. not applicable

Table 7.13 Project I - Covariates to be implemented in the model

Parameter	GAM	Additional Covariates Tested
CL_{NS2330}	BMI, AGE	CLCR, WT, SEX
CL_{M1}	BMI, AGE	CLCR
V2	BMI, SCR	WT
V4	BMI, SEX, CLCR, STUDY	WT, SCR
F1	WT, SEX, AGE, SCR	CLCR

BMI: Body Mass Index; WT: Weight; CLCR: Creatinine Clearance, SCR: Serum Creatinine

Table 7.14 Project I - Reduction in interindividual variability

Interindividual Variability		Base Model	Final Model	Δ Final - Base (in percent points)	Δ Change (in percent)
ωCL_{NS2330}	[CV%]	25.0	23.9	-1.1	- 4.4 %
ωCL_{M1}	[CV%]	41.4	40.1	-1.3	-2.4 %
$\omega V2$	[CV%]	43.9	47.6	+3.7	+8.4 %
$\omega V4$	[CV%]	115.3	79.9	-35.4	-30.7 %
$\omega F1$	[CV%]	24.3	19.0	-5.3	-21.8 %

Table 7.15 Project II - Distribution of observations per dose group and dataset

	DATASET A - INTERIM				DATASET B - FINAL			
	NS2330		M1		NS2330		M1	
	Obs.*[n]	Perc.$	Obs.*[n]	Perc.$	Obs.*[n]	Perc.$	Obs.*[n]	Perc.$
Dose 0.25	511	37.3%	457	38.2%	724	36.8%	646	36.8
Dose 0.5	453	33.1%	387	32.4%	646	32.8%	556	32.8
Dose 1.0	406	29.6%	352	29.4%	599	30.4%	512	30.4
Total	1370	100%	1196	100%	1969	100.0%	1714	100.0

*Observations, $Percentage of total number

Table 7.16 Project II - Distribution of continuous covariates dataset A

Covariate		Median	Mean	Range	5th - 95th Percentile
Age	[y]	75.5	74.7	52.0-91.0	60.0-86.0
Weight	[kg]	68.0	70.9	37.0-117.0	47.7-103.0
Height	[cm]	163	164	137-200	147-183
BMI	[kg/m^2]	25.6	26.2	14.5-44.5	19.8-35.3
SCR	[mg/dL]	0.9	0.91	0.5-1.7	0.6-1.34
CLCR	[mL/min]	62.6	67.1	26.1-140.0	35.6-113.0
ALT	[U/L]	17	19	4-106	9-34
AST	[U/L]	20	22	10-135	13-30
AP	[U/L]	79	82	24-219	49-124
Bilirubin	[mg/dL]	0.4	0.4	0.1-1.6	0.2-0.8

BMI: Body Mass Index; SCR: Serum Creatinine; CLCR: Creatinine Clearance

ALT: Alanine Transferase; AST: Aspartate Transaminase; AP: Alkaline Phosphatase

Table 7.17 Project II - Distribution of continuous covariates dataset B

Covariate		Median	Mean	Range	5th - 95th Percentile
Age	[y]	76.0	74.7	45.0-91.0	59.0-86.0
Weight	[kg]	68.7	71.1	37.2-136.1	47.6-102.5
Height	[cm]	162	164	132-200	147-183
BMI	[kg/m^2]	25.6	26.4	14.5-51.3	19.8-36.3
SCR	[mg/dL]	0.9	0.9	0.2-1.8	0.6-1.3
CLCR	[mL/min]	62.6	67.1	26.1-140.0	35.6-113.0
ALT	[U/L]	16	18	4-106	9-32
AST	[U/L]	20	21	10-135	13-30
AP	[U/L]	79	82	24-219	49-124
Bilirubin	[mg/dL]	0.4	0.4	0.1-1.8	0.2-0.8

BMI: Body Mass Index; SCR: Serum Creatinine; CLCR: Creatinine Clearance

ALT: Alanine Transferase; AST: Aspartate Transaminase; AP: Alkaline Phosphatase

Table 7.18 Project II - Distribution of categorical covariates

Covariate		Dataset A - Interim		Dataset B - Final	
		n	%	n	%
Sex	*male*	97	38	119	37
	female	157	62	201	63
Ethnic origin	*Caucasian*	238	94	299	93
	African	13	5	17	5
	Asian	3	1	4	1
Smoking status	*never smoker*	136	53	170	53
	ex-smoker	97	38	118	37
	current smoker	21	8	32	10
Alcohol history	*no alcohol*	143	56	181	57
	average consumption	111	44	139	43
	excessive consumption	0	0	0	0

Table 7.19 Project II - Covariates to be implemented in the model

	GAM	Additional Covariates Tested
KA	SCR	
$CL_{non-met}$	SEX, BMI, CLCR, AP	CYP3A4 inhibitors, CYP3A4 inducers
CL_{met}	WT, ASTA	CLCR, SEX, CYP3A4 inhibitors, CYP3A4 inducers
V2	SEX, WT, CLCR, AP, BIL	BMI, BSA
V3	SEX, BMI, AGE, ASTA	WT, BSA, CLCR

BMI: Body Mass Index; BSA: Body Surface Area; CLCR: Creatinine Clearance

SCR: Serum Creatinine; WT: Weight; BIL: Bilirubin

ASTA: Alcohol Status; AP: Alkaline Phosphatase

Table 7.20 Project II - Parameter estimates base model

Parameter		Dataset A		Dataset B	
Fixed effects		Estimate	RSE%	Estimate	RSE%
KA	[1/h]	0.398	9.7	0.377	8.8
V2/F	[L]	654	19.4	653	2.3
$CL_{non-met}/F$	[L/h]	1.07	3.9	1.14	3.5
CL_{met}/F	[L/h]	0.396	4.5	0.396	3.6
V3/F	[L]	502.5	—	501.7	—
CL_{M1}/F	[L/h]	0.946	4.7	0.936	3.7
Random effects					
$\omega CL_{non-met}/F$	[CV%]	78.2	19.8*	76.9	14.5*
$\omega CL_{met}/F$	[CV%]	23.4	22.6*	24.3	12.4*
$\omega V2/F$	[CV%]	39.2	17.9*	36.1	15.2*
$\omega V3/F$	[CV%]	34.8	14.5*	35.9	11.2*
ωKA	[CV%]	97.4	19.3*	96.6	17.9*
Corr_$CL_{non-met}$_V2		0.662	22.6[$]	0.66	17.8[$]
prop. error$_{NS2330}$	[%]	19.3	14.5*	19.4	11.6*
prop. error$_{M1}$	[%]	20.8	14.6*	20.0	11.5*
add. error$_{NS2330}$	[ng/mL]	±0.09	69.3*	±0.142	47.1*

* RSE is given on the variance scale; [$] SE of the covariance estimate; n.a. not applicable

Table 7.21 Project II - Parameter estimates final model

Parameter		Dataset A		Dataset B	
Fixed effects		Estimate	RSE%	Estimate	RSE%
KA	[1/h]	0.410	9.8	0.385	8.8
V2/F	[L]	655	2.7	649	2.2
$CL_{non-met-male}$/F	[L/h]	1.46	5.8	1.52	5.0
$CL_{non-met-female}$/F	[L/h]	1.08	6.5	1.16	5.8
CL_{met}/F	[L/h]	0.400	4.5	0.395	3.6
V3/F	[L]	503.2	—	498.6	—
CL_{M1}/F	[L/h]	0.944	4.4	0.925	3.6
Covariate Influence					
θV2_WT[1]	[%]	1.08	16.1	1.06	14.9
$\theta CL_{non-met}$_*CLCR*[2]	[%]	1.21	24.8	1.17	20.9
θCL_{met}_WT[3]	[%]	0.480	20.9	0.310	30.6
θV3_BMI[4]	[%]	2.23	33.1	2.05	33.2
θV3_AGE[4]	[%]	1.22	23.2	1.41	18.7

[1] $V2/F = \theta V2 \cdot [1+ \theta_{V2\_WT} \cdot (WT\text{-}68.04)] \cdot EXP(\omega^2 V2)$

[2] *if CLCR < 62.5 mL/min :*

$CL_{non-met}/F = \theta CL_{non-met-male/female} \cdot [1+ \theta CL_{non-met}\_CLCR \cdot (CLCR\text{-}62.5)] \cdot EXP(\omega^2 CL_{non-met})$

if CLCR $\geq$ 62.5 mL/min :

$CL_{non-met}/F = \theta CL_{non-met-male/female} \cdot EXP(\omega^2 CL_{non-met})$

[3] $CL_{met}/F = \theta CL_{met} \cdot [1- \theta CL_{met}\_WT \cdot (WT\text{-}68.04)] \cdot EXP(\omega^2 CL_{met})$

[4] $V3/F = \theta V3 \cdot [1+ \theta V3\_BMI \cdot (BMI\text{-}25.5)] \cdot [1+ \theta V3\_AGE \cdot (AGE\text{-}76)] \cdot EXP(\omega^2 V2)$

Random effects					
$\omega CL_{non-met}$/F	[CV%]	71.0	21.7*	70.2	16.1*
ωCL_{met}/F	[CV%]	21.4	15.2*	23.6	13.9*
ωV2/F	[CV%]	32.7	16.7*	30.5	13.8*
ωV3/F	[CV%]	31.9	16.4*	33.2	12.7*
ωKA	[CV%]	97.8	19.6*	95.6	18.0*
Corr_$CL_{non-met}$_V2		0.606*	26.0$^\$$	0.585	20.6$^\$$
prop. error$_{NS2330}$	[%]	19.4	14.5*	19.4	11.6*
prop. error$_{M1}$	[%]	20.7	14.7*	19.9	11.6*
add. error$_{NS2330}$	[ng/mL]	±0.09	65.0*	±0.146	45.9*

* RSE is given on the variance scale; $^\$$ SE of the covariance estimate; n.a. not applicable

Table 7.22 Project III - Distribution of continuous covariates

		Median	Mean	Range	5th - 95th Percentile
Age	[y]	32	32	21 - 45	25 - 39
Weight	[kg]	84	83	70 - 94	72 - 90
Height	[cm]	182	180	168 - 188	168 - 187
Body mass index	[kg/m^2]	25.7	25.6	22.6 - 29.7	23.1 - 28.3
Serum creatinine	[μmol/L]	88.4	89.2	70.7 - 106.1	79.6 - 97.2
Creatinine clearance	[mL/min]	125.8	125.0	95.6 - 148.2	100.5 - 143.6

Table 7.23 Project III - Parameter estimates NS2330 and meloxicam

Parameter		NS2330		Meloxicam	
Fixed effects		Estimate	RSE%	Estimate	RSE%
VC	[L]	453	n.d.	5.04	1.04
CL	[L/h]	2.76	n.d.	0.396	1.1
FBIL	[%]	95.8	n.d.	8.42	9.4
K_{21}	[1/h]	0.605	n.d.	3.85	28.8
K_{13}	[1/h]	n.a.	—	0.683	4.7
K_{31}	[1/h]	n.a.	—	0.664	3.9
K_{20}	[1/h]	n.a.	—	1.63	51.2
TDEL	[h]	1.5	n.d.	-0.285	44.9
Ω	[h]	6.3	n.d.	7.46	1.4
Interindividual variability					
ωCL	[CV%]	21.9	n.d.	29.6	29.7*
ωVC	[CV%]	14.5	n.d.	9.00	24.4*
Residual variability					
proportional	[CV%]	11.5	n.d.	9.9	14.9*
additive	[ng/mL]	0.08	n.d.	0.03	43.9*

* SE is given on the variance scale; n.a. not applicable; n.d. not determined

Table 7.24 Project III - Comparison of half-life and clearance of meloxicam

Parameter		Meloxicam		Meloxicam + Cholestyramine	
		reported by Busch et al.*	estimated by PK model	reported by Busch et al.*	predicted by PK model[§]
$t_{1/2}$	[h]	19.5	18.9	12.7	10.0
Clearance	[L/h]	0.426	0.396	0.636	0.75

* Busch et al. [72] by individual compartmental analysis

[§] mimicked by setting K21 of EHC population PK model to zero

Table 7.25 Project IV - Observations

Treatment Arm	Subjects	Number of NS2330 Samples*	Number of ITZ Samples*
NS2330	14	231	0
NS2330 + Itraconazole	14	224	70

* = above lower limit of quantification

Table 7.26 Project IV - Continuous covariates

		NS2330			NS2330 + Itraconazole		
		Median	Mean	Range	Median	Mean	Range
Age	[y]	34	33	25 - 46	35	35	25 - 45
Weight	[kg]	81	79	66 - 93	85	82	72 - 94
Height	[cm]	180	180.4	173 - 188	180	180.1	168 - 193
BMI	[kg/m^2]	25.7	24.5	20.4 - 27.1	25.5	25.4	21.4 - 27.8
SCR	[μmol/L]	79.6	84.0	70.7 - 106.8	79.6	81.5	70.7 - 88.4

BMI: Body Mass Index; SCR: Serum Creatinine

Table 7.27 Project IV - Parameter estimates

Parameter		NS2330		Itraconazole	
		Estimate	RSE %	Estimate	RSE %
KA	[1/h]	0.535	12.1	n.a.	n.a.
D	[h]	n.a.	n.a.	0.4 FIX	-
V/F	[L]	783	3.1	700 FIX	-
K_{EL}	[1/h]	0.035	4.0	0.0477	12.5
IMAX	[%]	38.9	16.6	83.0	1.8
IC_{50}	[ng/mL]	69.5	88.1	24.5	46.5
K_{EO}	[1/h]	n.a.	n.a.	0.01 FIX	-
Interindividual variability					
ωKA	[CV%]	53.4	46.0*	n.a.	n.a.
ωV/F	[CV%]	15.6	23.0*	n.a.	n.a.
ωK_{EL}	[CV%]	17.0	23.4*	n.a.	n.a.
ωIC_{50}	[CV%]	n.a.	n.a.	55.3	51.0*
Residual variability					
proportional	[CV%]	15.8	10.1*	11.1	17.4*

* given on the variance scale; RSE: Relative Standard Error; n.a.: not applicable

Table 7.28 Project V - Observations

Treatment Arm	Number of Animals		Number of Samples		
	treated	control	NS2330	M1	PD
NS2330 iv	33	16	32*	33	33
M1 iv	33	16	/	33	33$
NS2330 po	33	16	33	33	33
M1 po	33	16	/	33	33§
Total	132	64	65	132	132

* one value below lower limit of quantification removed from dataset

$ four PD values set to zero

§ three PD values set to zero

Table 7.29 Project V - Pharmacokinetic parameter estimates of the intermediate key model using M1 iv data

Parameter		M1	
		Estimate	RSE%
V	[L/kg]	16.2	4.0
VM_{EL}	[mg/h/kg]	0.214	14.6
KM_{EL}	[mg/kg]	1.28	14.6
Random Variability [§]			
M1	[%]	17.0	19.4*

* given on the variance scale

[§] including interindividual and residual variability

Table 7.30 Project V - Pharmacokinetic parameter estimates of the intermediate key model using NS2330 iv + M1 iv data

Parameter		NS2330		M1	
		Estimate	RSE%	Estimate	RSE%
V	[L/kg]	9.8	7.9	12.0	8.1
VM_{MET}	[mg/h/kg]	0.776	15.5	n.a.	/
VM_{EL}	[mg/h/kg]	n.a.	/	0.254	11.7
KM_{MET}	[mg/kg]	2.43	21.9	n.a.	/
KM_{EL}	[mg/kg]	n.a.	/	0.813	26.3
$CL_{0.3, 1, 3\,mg/kg}$	[L/h/kg]	2.58	16.6	n.a.	/
$CL_{5\,mg/kg}$	[L/h/kg]	0.381	28.4	n.a.	/
$CL_{10\,mg/kg}$	[L/h/kg]	0.149	30.1	n.a.	/
Random Variability [§]					
NS2330/M1	[%]	67.8	50.2*	31.9	19.1*

* given on the variance scale; [§] including interindividual and residual variability

Table 7.31 Project V - Pharmacokinetic parameter estimates of the intermediate key model using NS2330 iv and po + M1 iv data

Parameter		NS2330		M1	
		Estimate	RSE%	Estimate	RSE%
KA	[1/h]	10 FIX	/	n.a.	/
V	[L/kg]	15.0	6.1	11.0	9.0
VM_{FP}	[mg/h/kg]	9.93	17.0	n.a.	/
VM_{MET}	[mg/h/kg]	0.711	13.9	n.a.	/
VM_{EL}	[mg/h/kg]	0.151	34.6	0.247	9.0
KM_{FP}	[mg/kg]	2.76	17.2	n.a.	/
KM_{MET}	[mg/kg]	2.76	17.2	n.a.	/
KM_{EL}	[mg/kg]	2.76	17.2	0.603	23.4
F	[%]	75.7	4.4	n.a.	/
Random Variability [§]					
NS2330/M1	[%]	36.2	17.1*	30.5	13.8*

* given on the variance scale; [§] including interindividual and residual variability

Table 7.32 Project V - Pharmacokinetic parameter estimates of the final model

Parameter		NS2330		M1	
		Estimate	RSE%	Estimate	RSE%
KA	[1/h]	10 FIX	/	5 FIX	/
V	[L/kg]	17.7	6.1	13.6	9.1
VM_{FP}	[mg/h/kg]	11.9	19.9	n.a.	/
VM_{MET}	[mg/h/kg]	0.823	21.5	n.a.	/
VM_{EL}	[mg/h/kg]	0.250	39.7	0.506	14.4
KM_{FP}	[mg/kg]	3.59	21.0	n.a.	/
KM_{MET}	[mg/kg]	3.59	21.0	n.a.	/
KM_{EL}	[mg/kg]	3.59	21.0	3.59	21.0
F	[%]	87.2	5.1	109	9.3
Random Variability [§]					
NS2330/M1	[%]	35.7	17.1*	36.3	11.4*

* given on the variance scale; [§] including interindividual and residual variability

Table 7.33 Project V - Pharmacodynamic parameter estimates of the final model

Parameter		NS2330		M1	
		Estimate	RSE%	Estimate	RSE%
E_{MAX}	[%]	100 FIX	/	100 FIX	/
EC_{50}	[ng/mL]	23.7	15.1	114.0	11.9
K_{EO}	[1/h]	0.555	29.0	0.878	24.3
Residual variability [§]					
NS2330/M1	[%]	77.5	14.9*	89.3	15.3*

* given on the variance scale; [§] including interindividual and residual variability

Table 7.34 Project V - EC_{50} values of intermediate key models

Raw Data	$EC_{50,NS2330}$ [nM]	$EC_{50,M1}$ [nM]	$\frac{EC_{50,M1}}{EC_{50,NS2330}}$
M1 iv*	n.a.	318.4	n.a.
M1 iv + NS2330 iv*	76.2	309.2	4.1
M1 iv + NS2330 iv and po	81.4	340.8	4.2
M1 iv and po + NS2330 iv and po	72.3	363.1	5.0

*no effect compartment necessary; n.a.: not applicable

Table 7.35 Project VI - ADAS-COG observations

Treatment Arm		Subjects		ADAS-COG Samples	
		n	%	Total	Per Patient
NS2330	All Patients	44	100	176	4
	Responder	32	72.7	128	4
	Non-Responders	12	27.3	48	4
Placebo	All Patients	18	100	72	4
	Responder	10	55.6	40	4
	Non-Responders	8	44.4	32	4

Table 7.36 Project VI - Categorical covariates of patients with NS2330 treatment

Covariate	All Patients		Responder		Non-Responders	
	number	%	number	%[§]	number	%[$]
Sex						
female	18	41	12	38	6	50
male	26	59	20	63	6	50
Smoking status						
non-smoker	35	80	27	84	8	67
former smoker	4	9	3	9	1	8
current smoker	5	11	2	6	3	25
Ethnic origin						
Caucasian	43	98	31	97	12	100
African	1	2	1	3	0	0
Asian or Pacific Islander	0	0	0	0	0	0

[§] of responder population (n=32)

[$] of non-responders population (n=12)

Table 7.37 Project VI - Continuous covariates of patients with NS2330 treatment

			n	Median	Mean	Range	5th - 95th Percentile
Age	[y]	All Patients	44	70.5	70.3	60.0 - 80.0	61.3 - 78.7
		Responder	32	70.0	70.0	60.0 - 80.0	60.7 - 79.3
		Non-Responders	12	72.5	71.3	64.0 - 78.0	64.0 - 78.0
Weight	[kg]	All Patients	44	79.5	81.3	54.0 - 111.0	58.6 - 110.7
		Responder	32	82.6	82.6	54.0 - 111.0	57.8 - 110.8
		Non-Responders	12	77.4	77.8	58.1 - 110.7	58.1 - 110.7
Height	[cm]	All Patients	44	173.0	170.4	147.0 - 185.4	153.0 - 183.0
		Responder	32	173.0	170.1	147.0 - 183.0	152.1 - 182.9
		Non-Responders	12	173.5	171.3	152.4 - 185.4	152.4 - 185.4
BMI	[kg/m^2]	All Patients	44	27.0	27.9	20.4 - 39.4	21.3 - 36.8
		Responder	32	27.8	28.5	20.4 - 37.0	21.7 - 36.6
		Non-Responders	12	25.3	26.3	21.0 - 39.4	21.0 - 39.4
SCR	[μmol/L]	All Patients	44	79.6	83.2	53.0 - 132.6	53 - 121.5
		Responder	32	84.0	86.2	53.0 - 132.6	53.0 - 126.9
		Non-Responders	12	79.6	75.4	53.0 - 97.2	53.0 - 97.2
CLCR	[mL/min]	All Patients	44	78.6	81.0	40.6 - 126.1	49.0 - 121.3
		Responder	32	77.6	79.8	48.0 - 112.6	52.9 - 109.7
		Non-Responders	12	81.6	84.3	40.6 - 126.1	40.6 - 126.1
ADAS-COG at Baseline		All Patients	44	8.7	9.6	3.6 - 22.0	4.2 - 18.7
		Responder	32	9.0	10.4	5.0 - 22.0	5.9 - 20.4
		Non-Responders	12	6.7	7.4	3.6 - 14.0	3.6 - 14.0

BMI: Body Mass Index; SCR: Serum Creatinine; CLCR: Creatinine Clearance

Table 7.38 Project VI - Categorical covariates of patients with placebo treatment

Covariate	All Patients		Responder		Non-Responders	
	number	%	number	%[§]	number	%[$]
Sex						
female	9	50	5	50	4	50
male	9	50	5	50	4	50
Ethnic origin						
Caucasian	17	94	10	100	7	88
African	1	6	0	0	1	13
Asian or Pacific Islander	0	0	0	0	0	0

[§] of responder population (n=10)

[$] of non-responders population (n=8)

Table 7.39 Project VI - Continuous covariates of patients with placebo treatment

			n	Median	Mean	Range	5th - 95th Percentile
Age	[y]	All Patients	18	69.5	69.9	60.0 - 78.0	60.0 - 78.0
		Responder	10	69.5	69.4	60.0 - 78.0	60.0 - 78.0
		Non-Responders	8	70.0	70.6	63.0 - 78.0	63.0 - 78.0
Weight	[kg]	All Patients	18	80.0	84.5	55.3 - 129.0	55.3 - 129.0
		Responder	10	75.4	77.4	55.3 - 117.0	55.3 - 117.0
		Non-Responders	8	88.4	93.3	68.9 - 129.0	68.9 - 129.0
Height	[cm]	All Patients	18	170.2	169.6	152.0 -188.0	152.0 - 188.0
		Responder	10	169.1	166.6	152.0 -182.9	152.0 - 182.9
		Non-Responders	8	176.5	173.4	160.0 - 188.0	160.0 - 188.0
BMI	[kg/m^2]	All Patients	18	26.8	29.3	22.5 - 45.1	22.5 - 45.1
		Responder	10	25.5	27.7	22.6 - 39.4	22.6 - 39.4
		Non-Responders	8	29.7	31.2	22.5 - 45.1	22.5 - 45.1
ADAS-COG at Baseline		All Patients	18	7.8	9.2	3.3 - 23.7	3.3 - 23.7
		Responder	10	8.7	10.4	3.3 - 23.7	3.3 - 23.7
		Non-Responders	8	7.1	7.7	4.7 - 14.0	4.7 - 14.0

BMI: Body Mass Index; SCR: Serum Creatinine; CLCR: Creatinine Clearance

Table 7.40 Project VI - Parameter estimates base and final model

Parameter		Base Model		Final Model	
Fixed effects		Estimate	RSE%	Estimate	RSE%
KEO	[1/h]	0.0001 FIX	—	0.0001 FIX	—
E_{max}	[%]	35.5	12.6	37.5	10.7
EC_{50}	[ng/mL]	0.0287	84.0	0.0304	95.7
Covariate Influence					
θE_{max}_AGE [1]	[%]	n.a.	n.a.	0.0119	11.6
[1] $E_{max,ind} = E_{max} \cdot [1 - \theta E_{max}\_AGE \cdot (AGE - 70)] \cdot EXP(\omega^2 E_{max})$					
Random effects					
ωE_{max}	[CV%]	43.2	34.9*	27.4	42.3*
add. err$_{ADAS-COG}$		1.8	22.8*	1.8	22.6*

* RSE is given on the variance scale; [§] RSE of the covariance estimate; n.a. not applicable

Table 7.41 Project VI - Parameter estimates base models all patients and responder

Parameter		Responder		All Patients	
Fixed effects		Estimate	RSE%	Estimate	RSE%
KEO	[1/h]	0.0001 FIX	—	0.0001 FIX	—
E_{max}	[%]	35.5	12.6	25.5	19.8
EC_{50}	[ng/mL]	0.0287	84.0	0.0338	109.8
Random effects					
ωE_{max}	[CV%]	43.2	34.9*	62.7	38.8*
add. err$_{ADAS-COG}$		1.8	22.8*	2.3	19.3*

* RSE is given on the variance scale; [§] RSE of the covariance estimate; n.a. not applicable

7.2 Figures
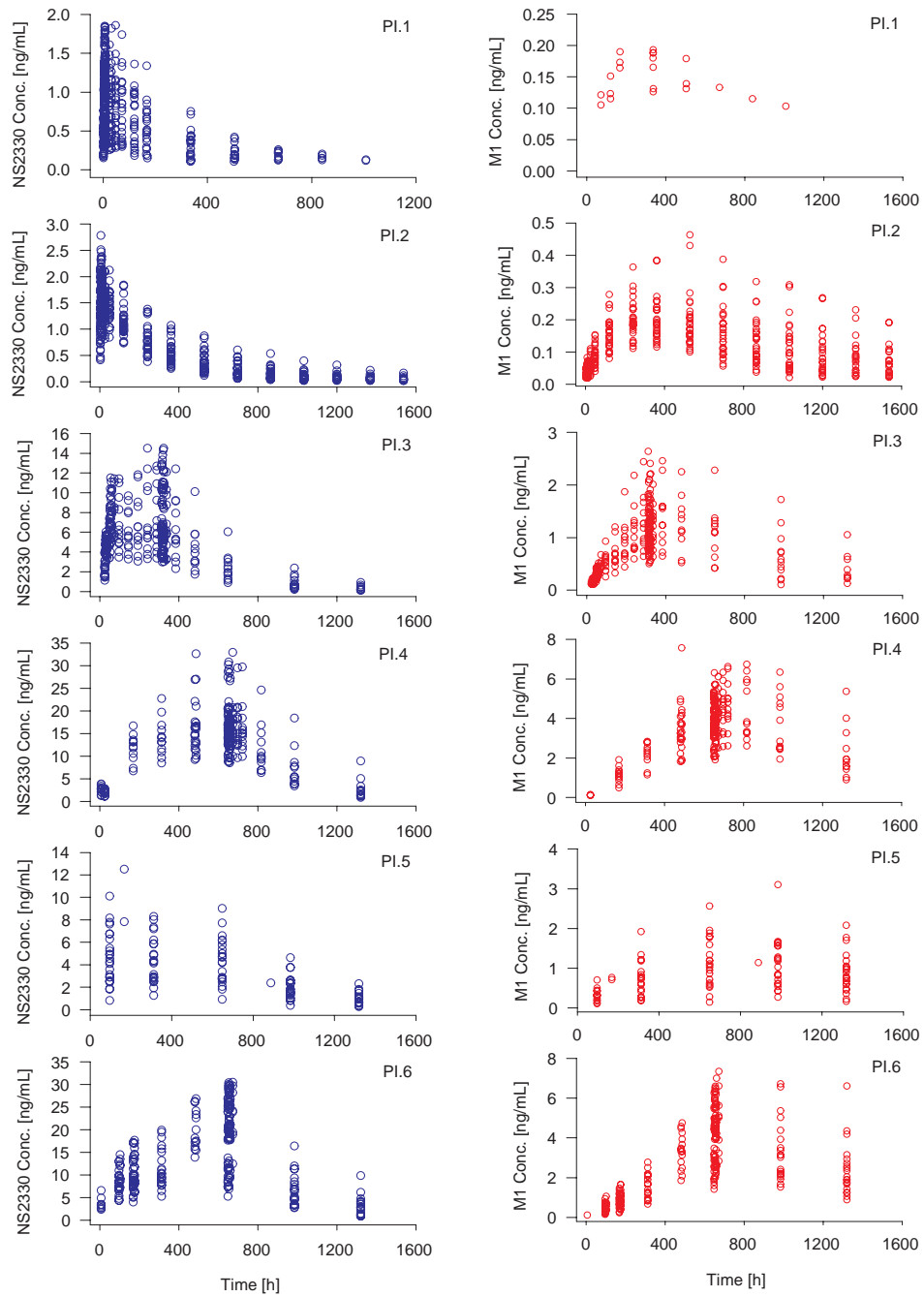
Figure 7.1 Project I - Plasma concentrations versus time of NS2330 (left) and M1 (right) separated by studies. The total number of patients was 119 with a total number of 1819 NS2330 and 1333 M1 observations above the lower limit of quantification.
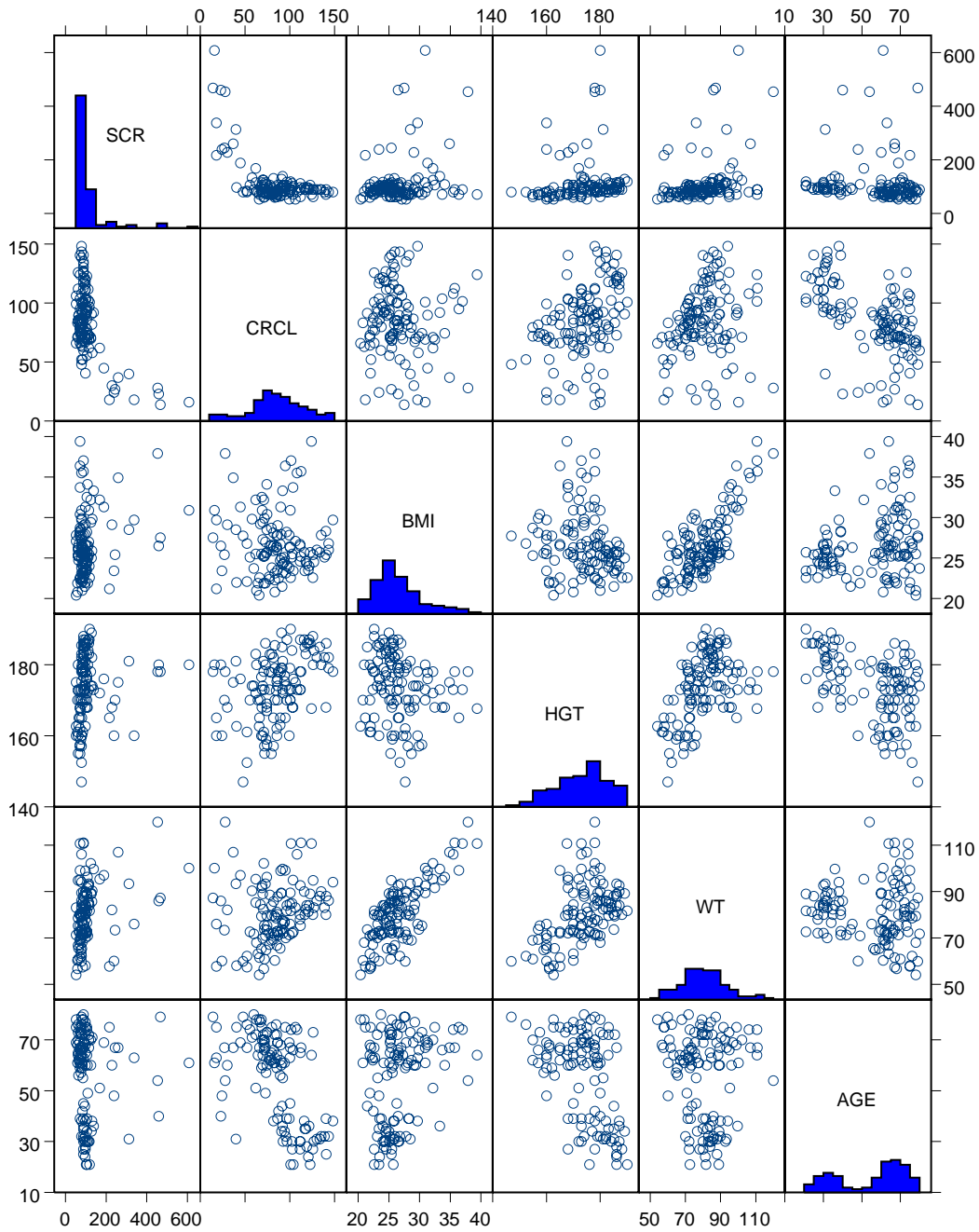
Figure 7.2 Project I - Scatter plot and distributions of the continuous covariates serum creatinine (SCR) in μmol/L, creatinine clearance (CRCL) in mL/min, body mass index (BMI) in kg/m^2, height (HGT) in cm, weight (WT) in kg and age (AGE) in years.
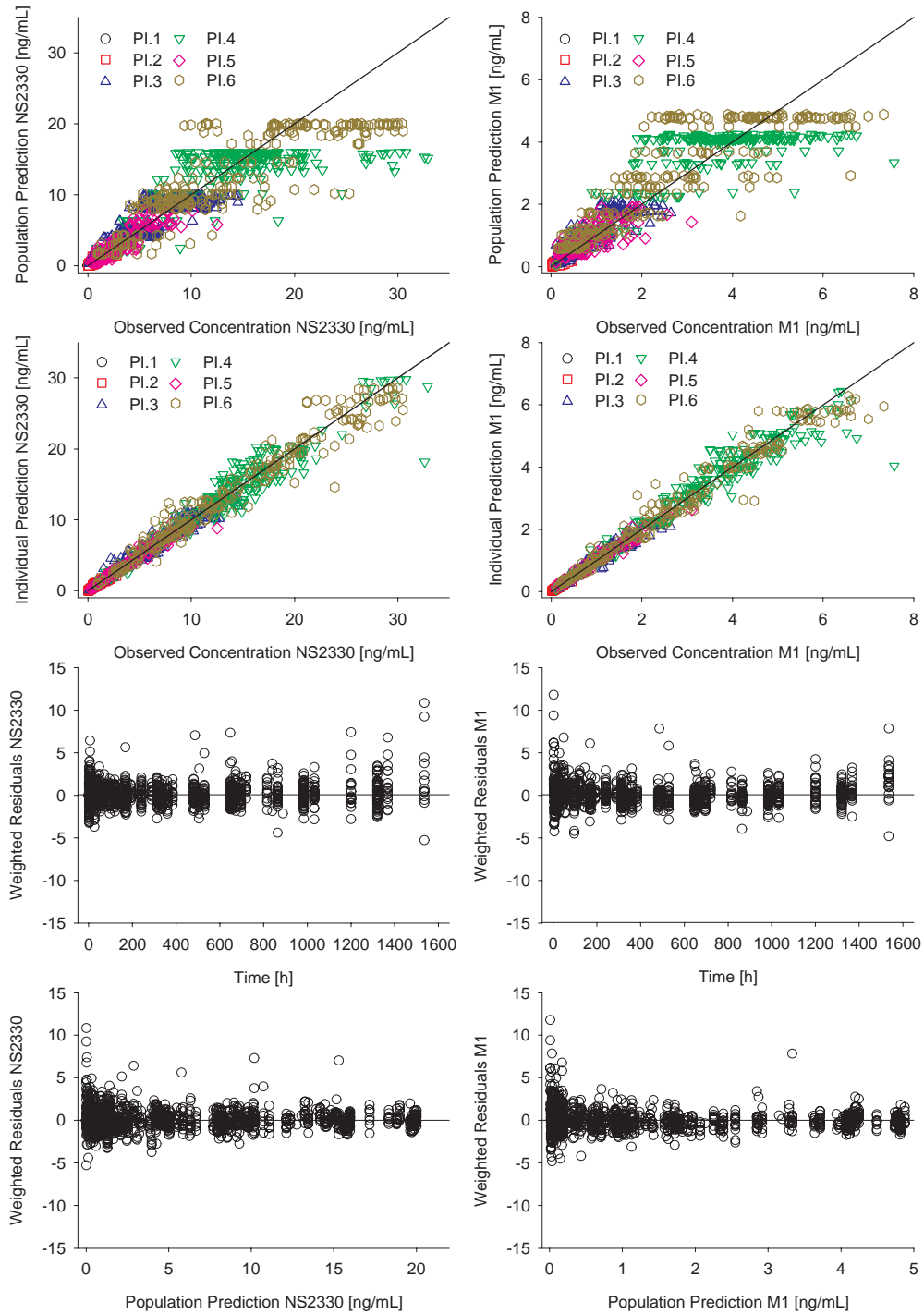
Figure 7.3 Project I - Goodness of Fit Plots - **Base Model**. Population predictions (first row) and individual predictions (second row) versus observed NS2330 (left) and M1 (right) plasma concentrations. Weighted residuals of NS2330 (left) and M1 (right) versus time (third row) and population predictions (last row).
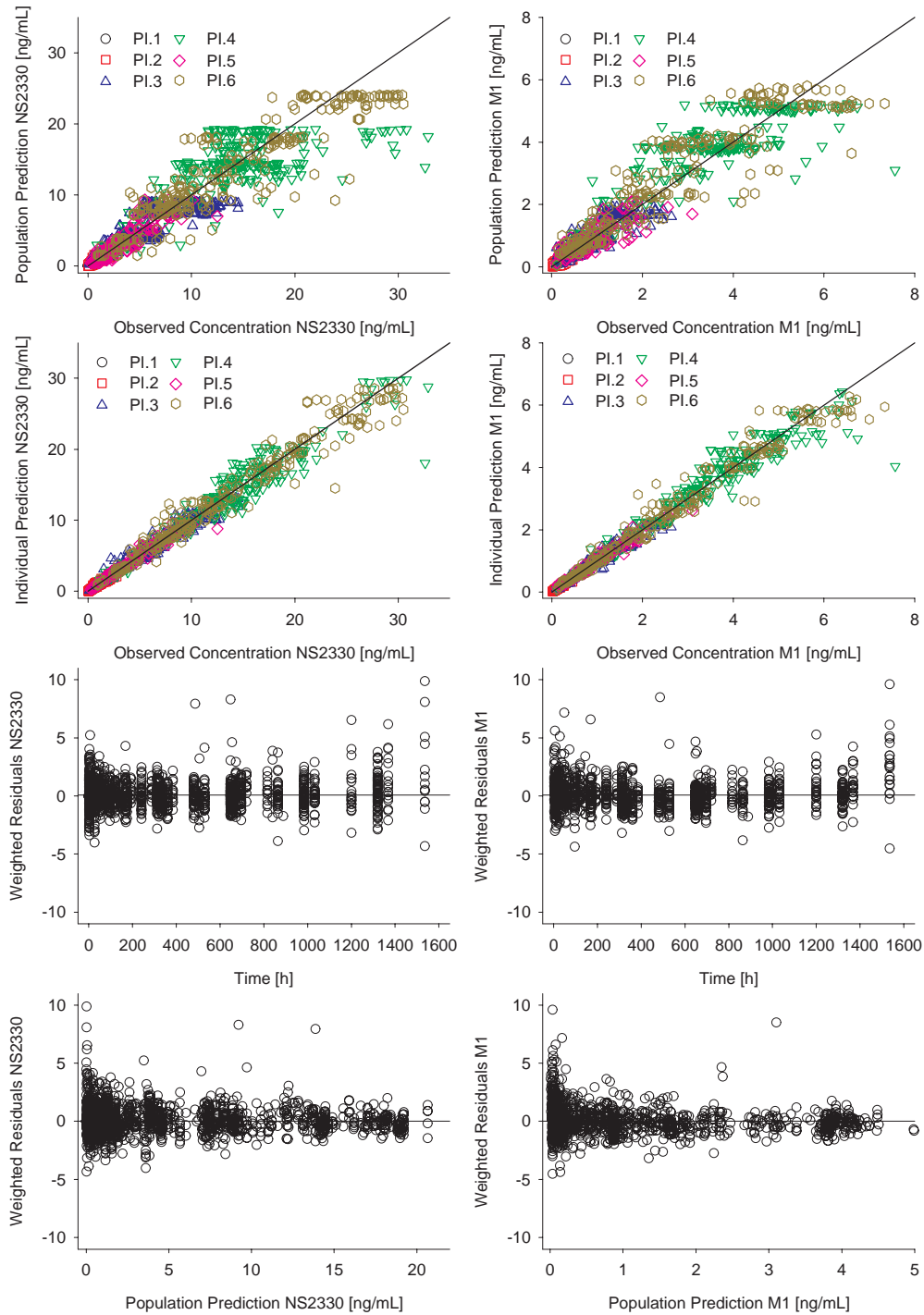
Figure 7.4 Project I - Goodness of Fit Plots - **Final Model**. Population predictions (first row) and individual predictions (second row) versus observed NS2330 (left) and M1 (right) plasma concentrations. Weighted residuals of NS2330 (left) and M1 (right) versus time (third row) and population predictions (last row).
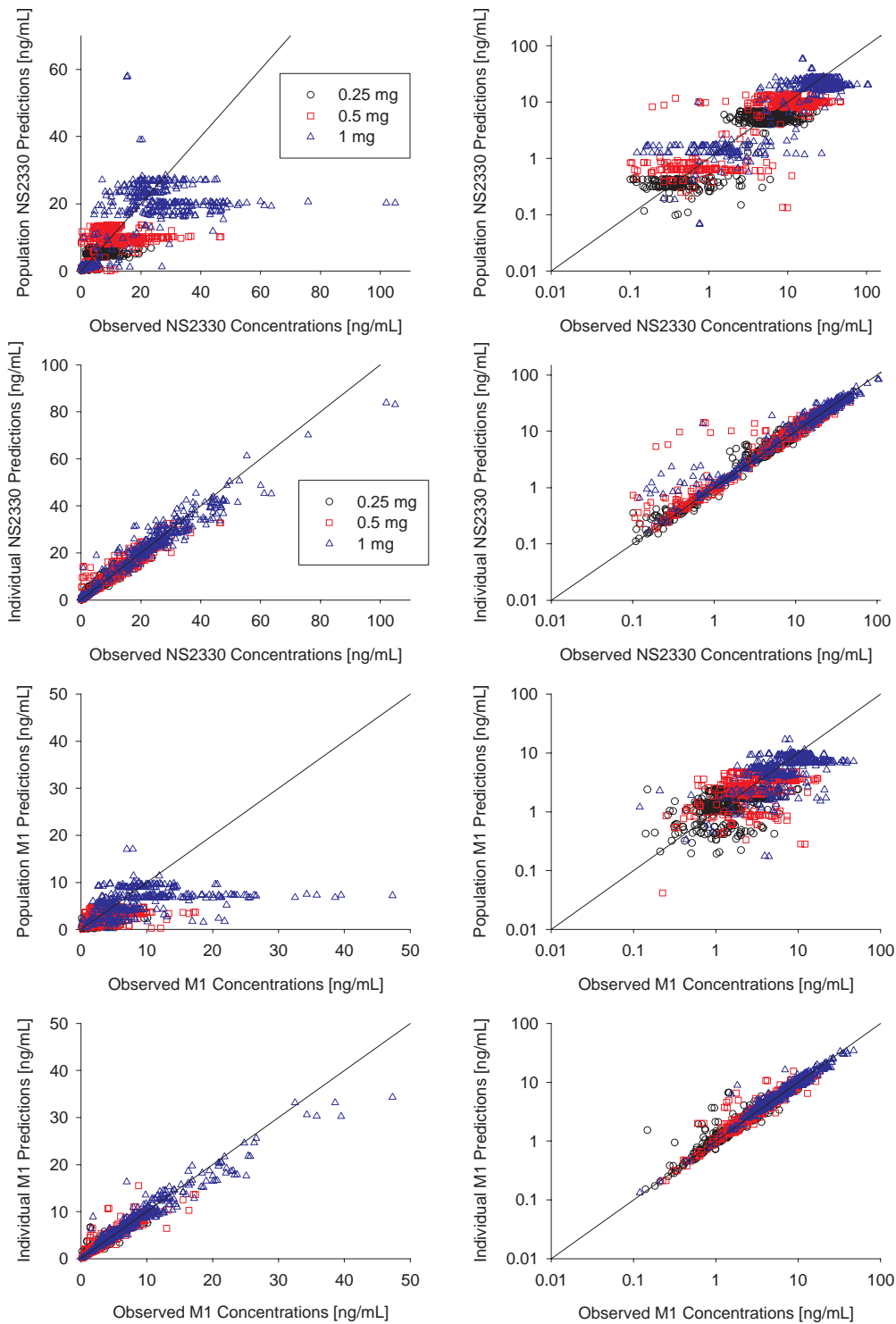
Figure 7.5 Project I - Goodness of Fit Plots - **External Validation**. Population predictions (1st and 3rd row) and individual predictions (2nd and 4th row) versus observed NS2330 (first two panels) and M1 (last two panels) plasma concentrations on linear (left) and logarithmic (right) scale of both axes.
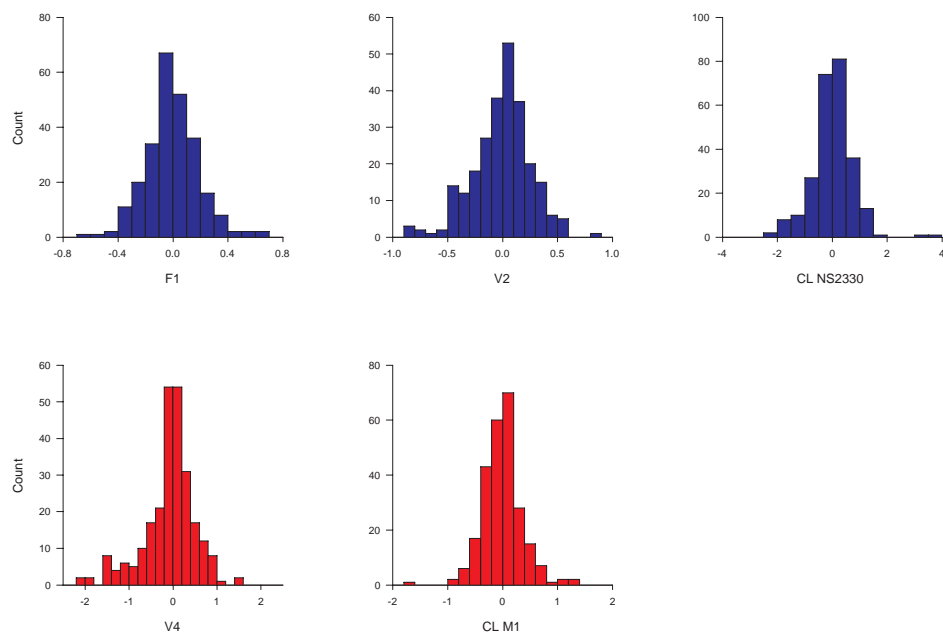
Figure 7.6 Project I - Distribution of the individual η-values - External validation.
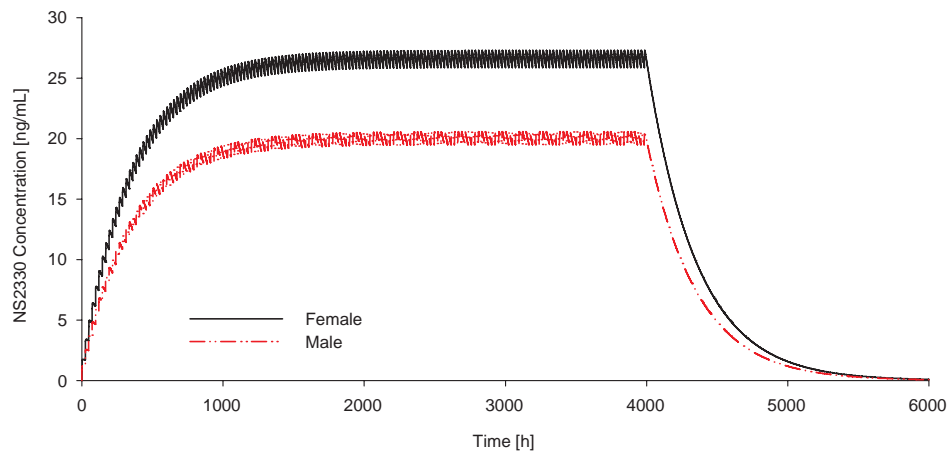
Figure 7.7 Project I - Impact of sex on the plasma concentration-time profile of NS2330 after oral administration of 1 mg NS2330 once daily for 166 days (4000 h): Typical profiles of a male and female subject.
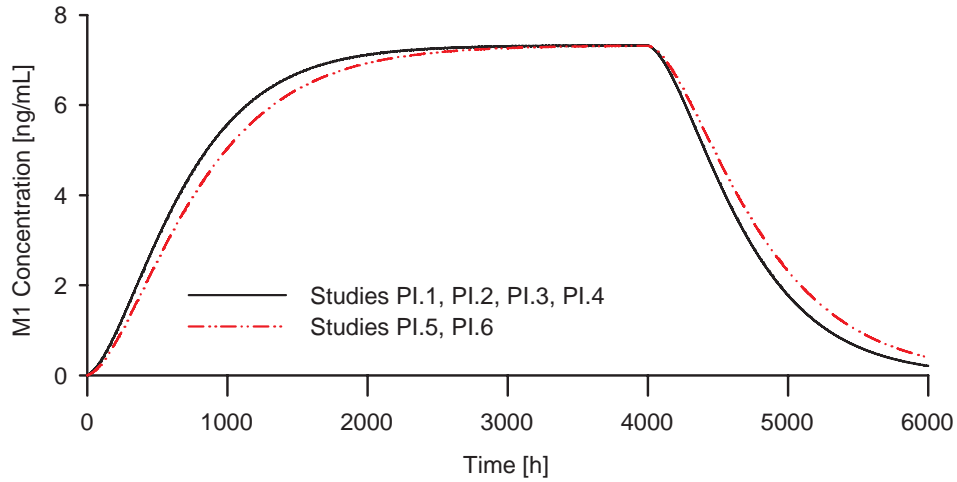
Figure 7.8 Project I - The impact of the study effect on the plasma concentration-time profiles of M1 after oral administration of 1 mg NS2330 once daily for 166 days (4000 h): Typical profiles of a male subject.
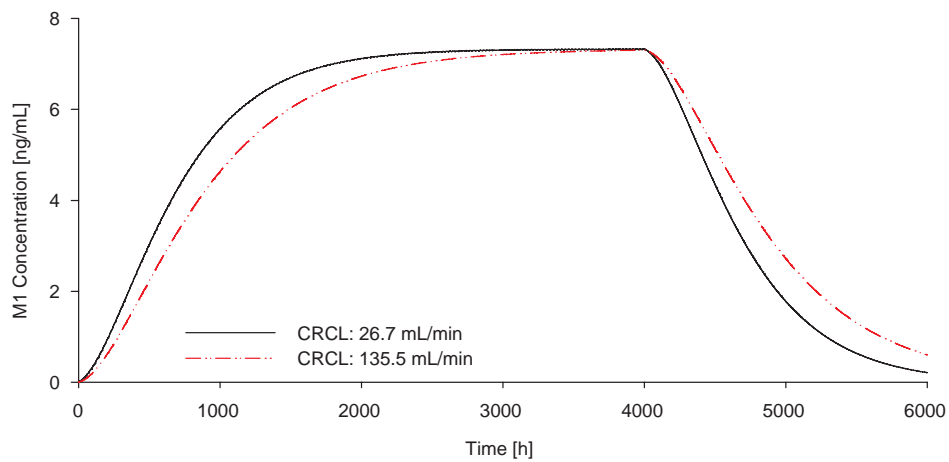
Figure 7.9 Project I - The impact of creatinine clearance (CLCR) on the plasma concentration-time profiles of M1 after oral administration of 1 mg NS2330 once daily for 166 days (4000 h): Typical profiles of a male subject with a creatinine clearance of 26.7 mL/min and 135.5 mL/min.

143
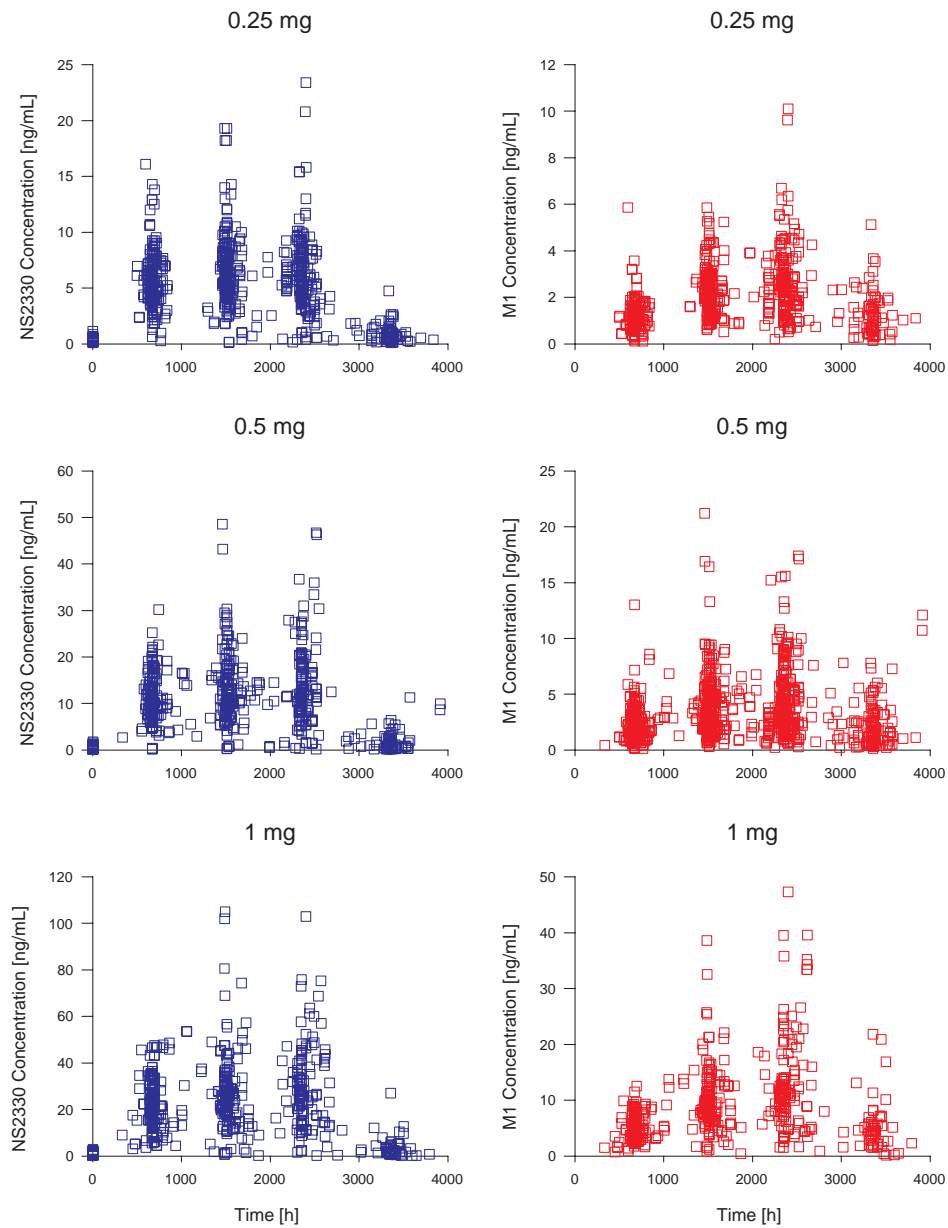
Figure 7.10 Project II - Plasma concentrations versus time of NS2330 (left) and M1 (right) separated by dose groups. The total number of patients was 320 with a total number of 1969 NS2330 and 1714 M1 observations above the lower limit of quantification (Dataset B).
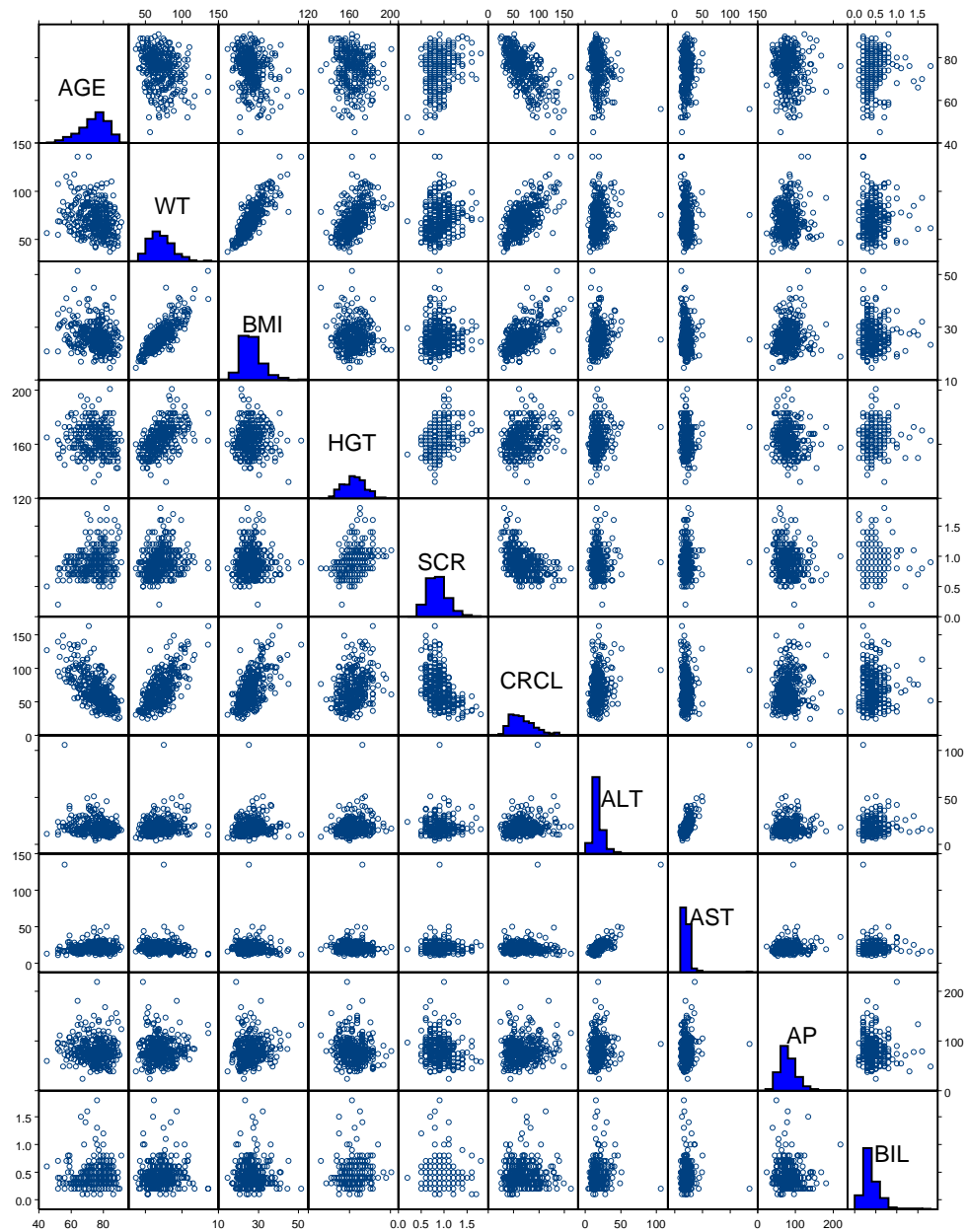
Figure 7.11 Project II - Scatter plot and distributions of the continuous covariates age (AGE) in years, weight (WT) in kg, body mass index (BMI) in kg/m^2, height (HGT) in cm, serum creatinine (SCR) in μmol/L, creatinine clearance (CRCL) in mL/min, alanine transferase (ALT) in U/L, aspartate transferase (AST) in U/L, alkaline phosphatase (AP) in U/L, bilirubin (BIL) in mg/dL.

145
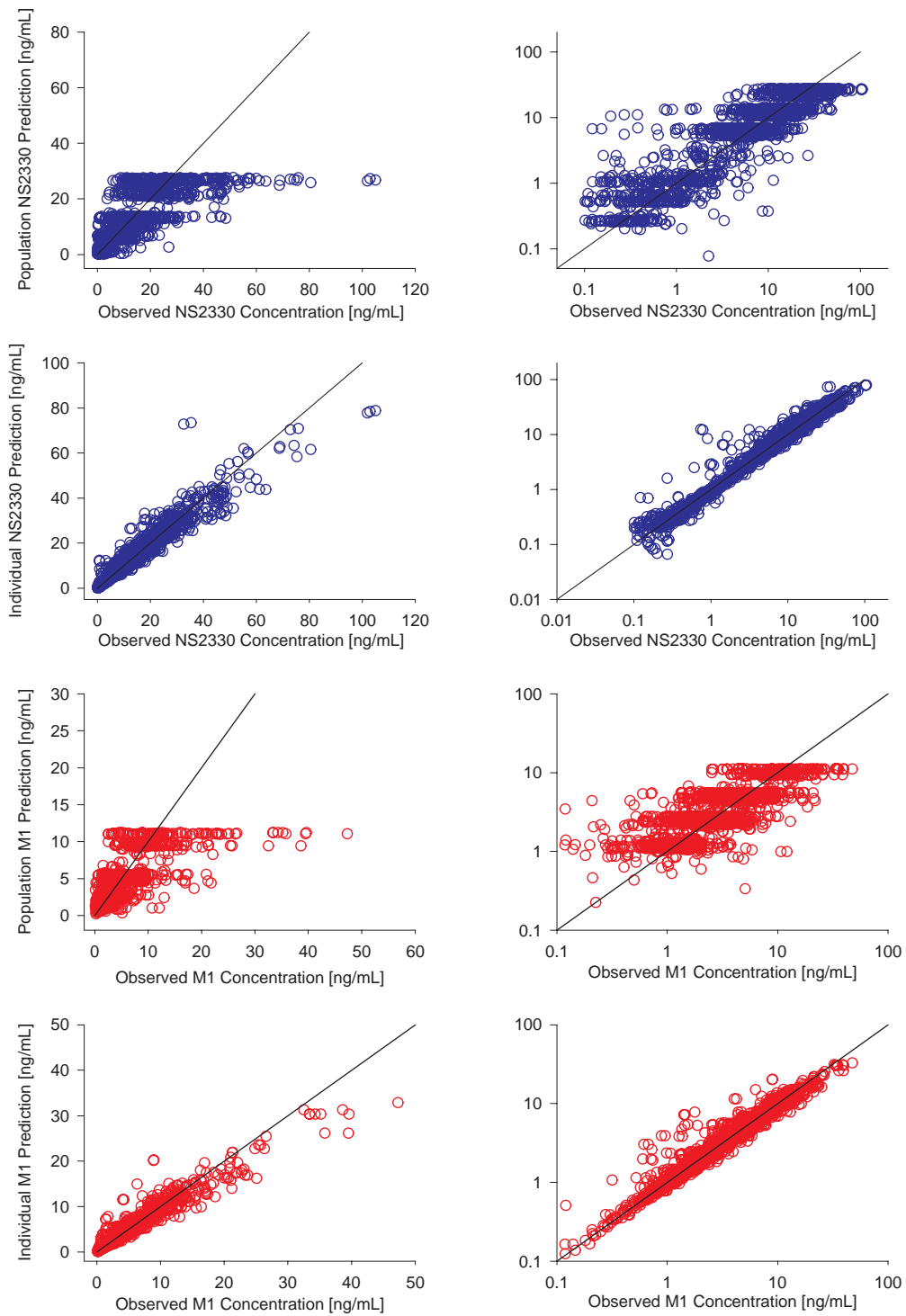
Figure 7.12 Project II - Goodness of Fit Plots - **Base Model**. Population predictions (1st and 3rd row) and individual predictions (2nd and 4th row) versus observed NS2330 (first two panels) and M1 (last two panels) plasma concentrations on linear (left) and logarithmic (right) scale of both axes.
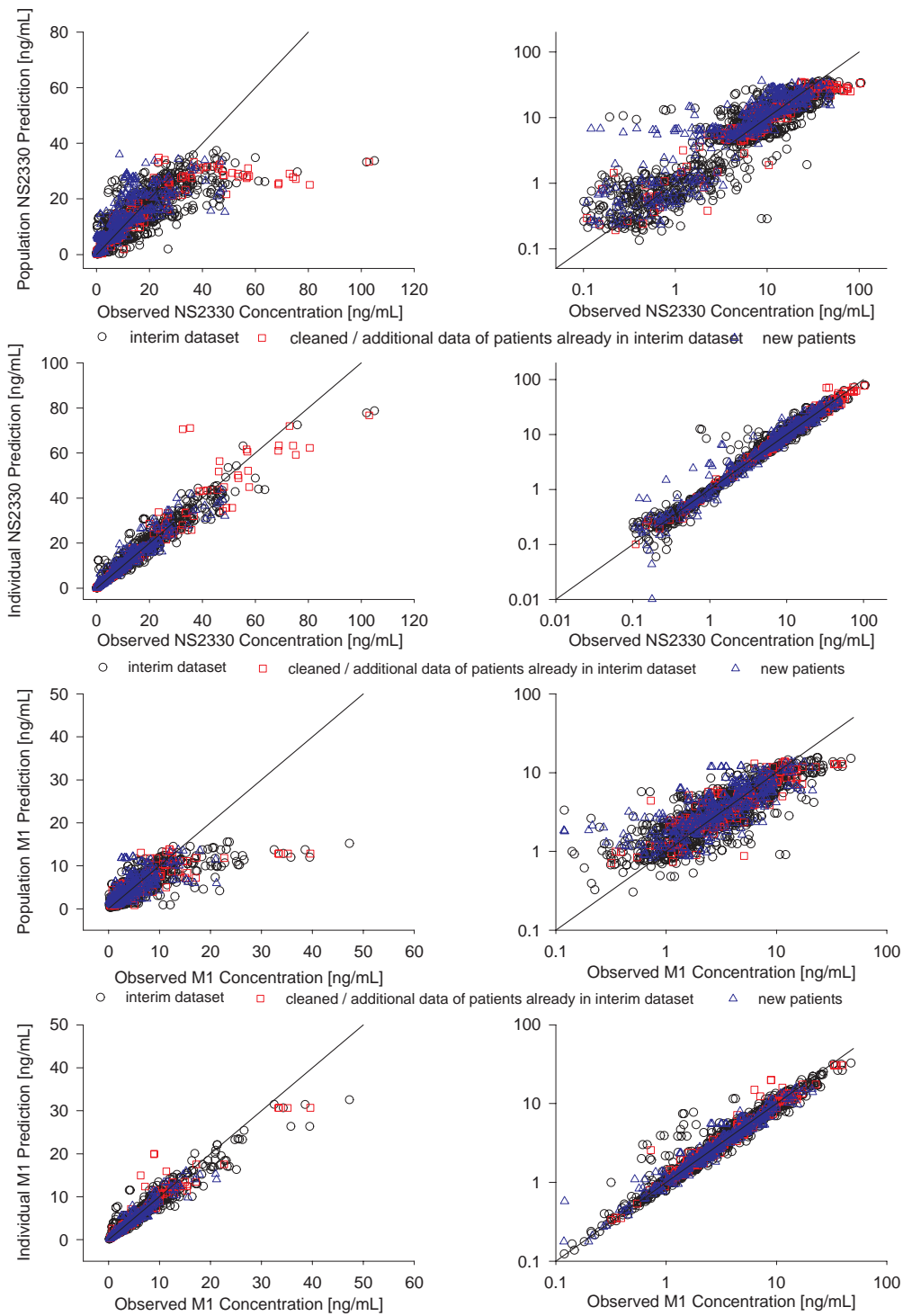
Figure 7.13 Project II - Goodness of Fit Plots - **Final Model**. Population predictions (1st and 3rd row) and individual predictions (2nd and 4th row) versus observed NS2330 (first two panels) and M1 (last two panels) plasma concentrations on linear (left) and logarithmic (right) scale of both axes.
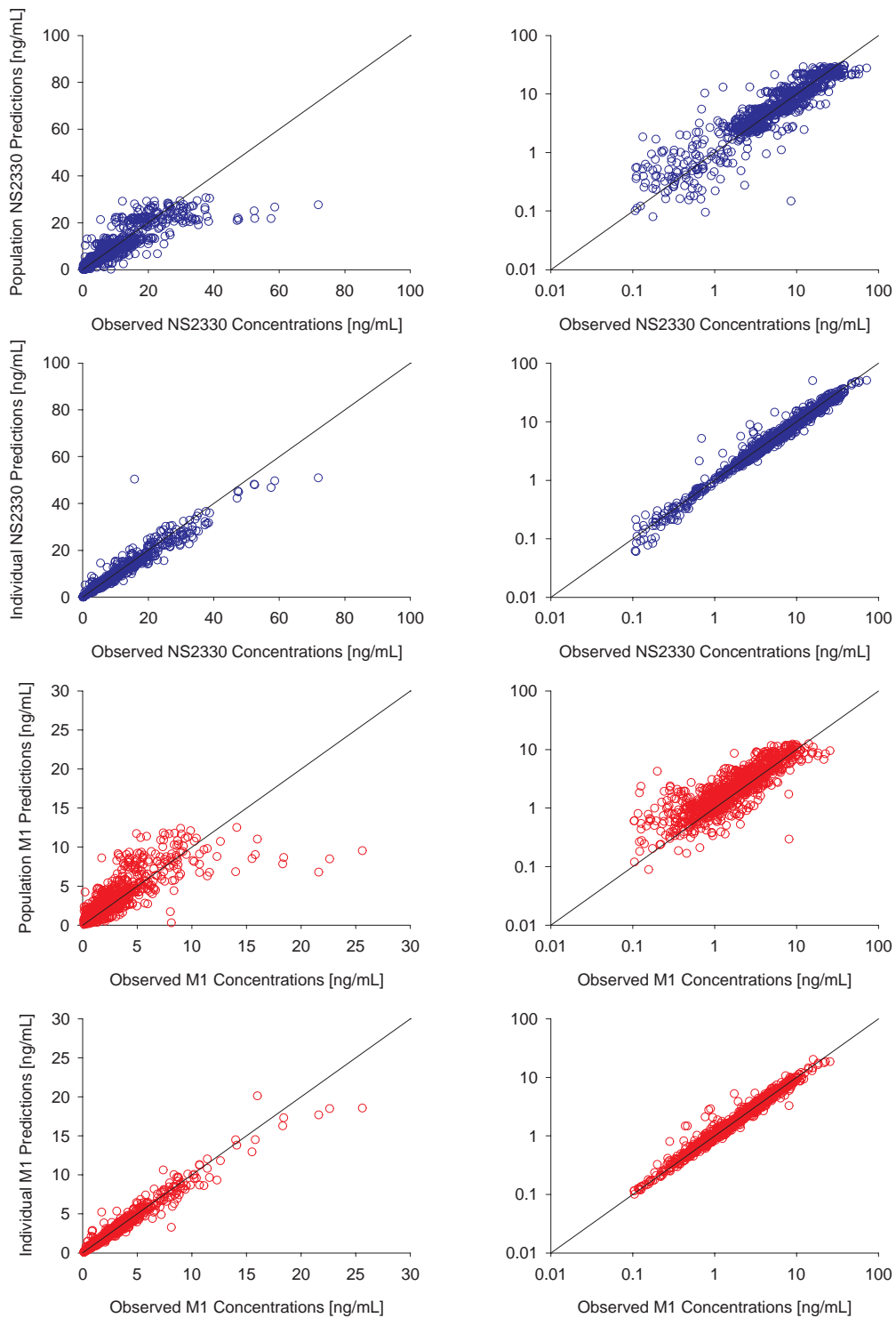
Figure 7.14 Project II - Goodness of Fit Plots - **External Validation**. Population predictions
(1st and 3rd row) and individual predictions (2nd and 4th row) versus observed NS2330
(first two panels) and M1 (last two panels) plasma concentrations on linear (left) and
logarithmic (right) scale of both axes.
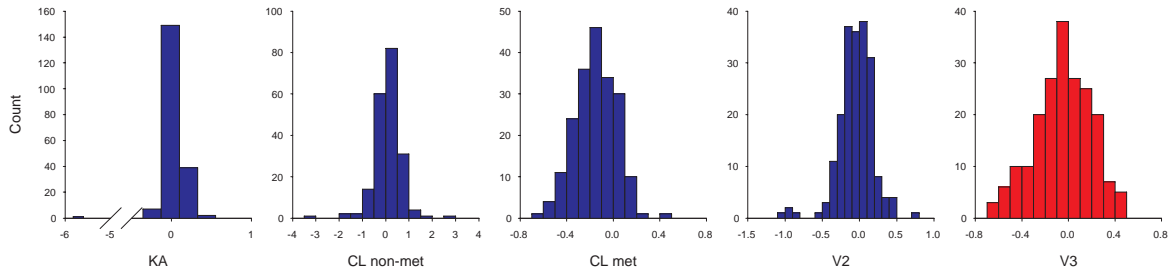
Figure 7.15 Project II - Distribution of the individual η-values - External validation.
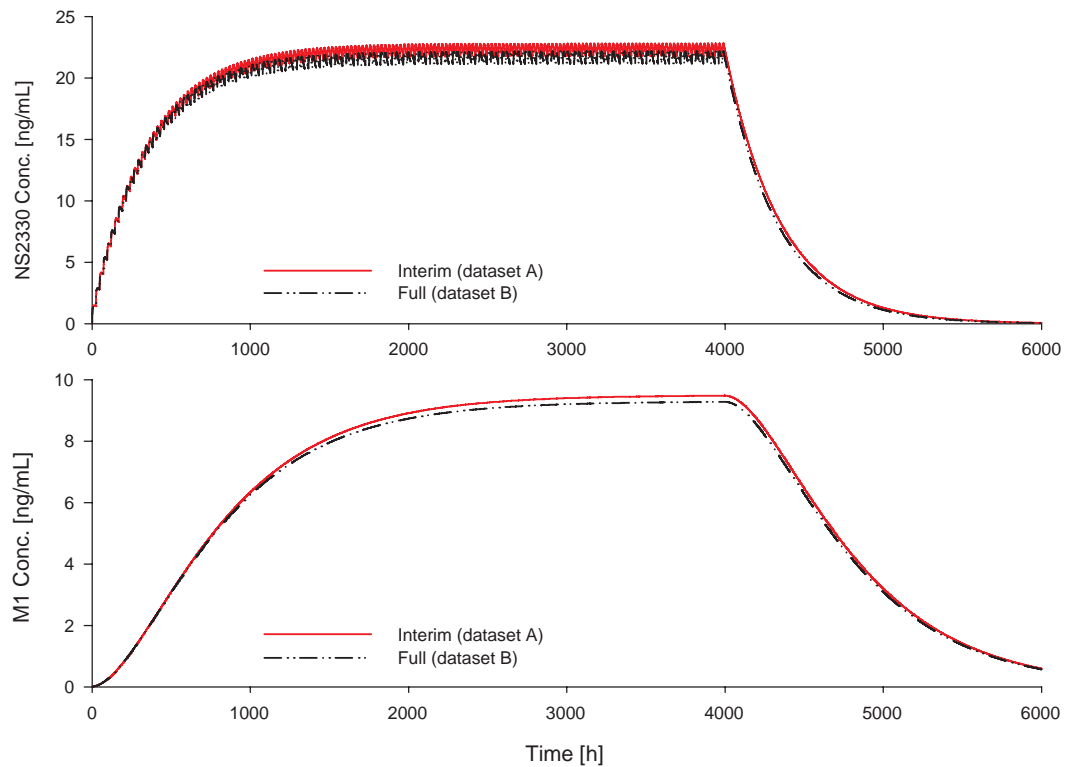
Figure 7.16 Project II - Simulation of plasma concentration-time profile of NS2330 (upper panel) and M1 (lower panel) based on the final PK parameter estimates using the interim (dataset A) and full (dataset B) analysis dataset. Typical profiles of a male subject with median covariates after oral administration of 1 mg NS2330 once daily for 166 days (4000 h).
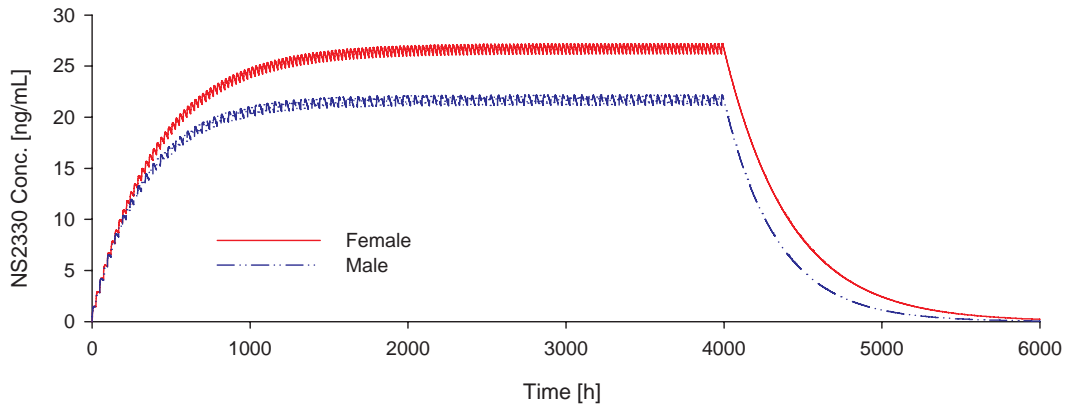
Figure 7.17 Project II - Impact of sex on the plasma-concentration time profile of NS2330 after oral administration of 1 mg NS2330 once daily for 166 days (4000 h). Typical profiles of a male and a female subject with median covariates.
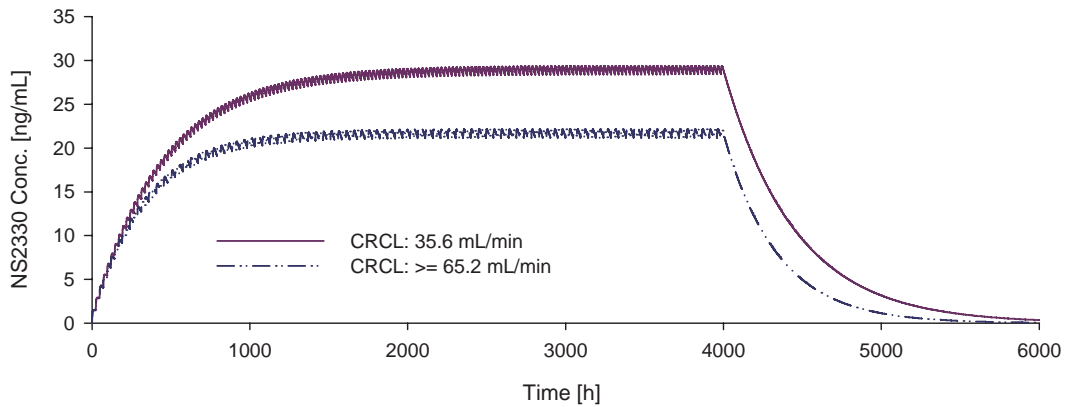
Figure 7.18 Project II - Impact of creatinine clearance (CLCR) on the plasma concentration-time profiles of NS2330 after oral administration of 1 mg NS2330 once daily for 166 days (4000 h). The typical profiles of a male subject with a creatinine clearance of 35.6 mL/min and $\geq$62.5 mL/min.
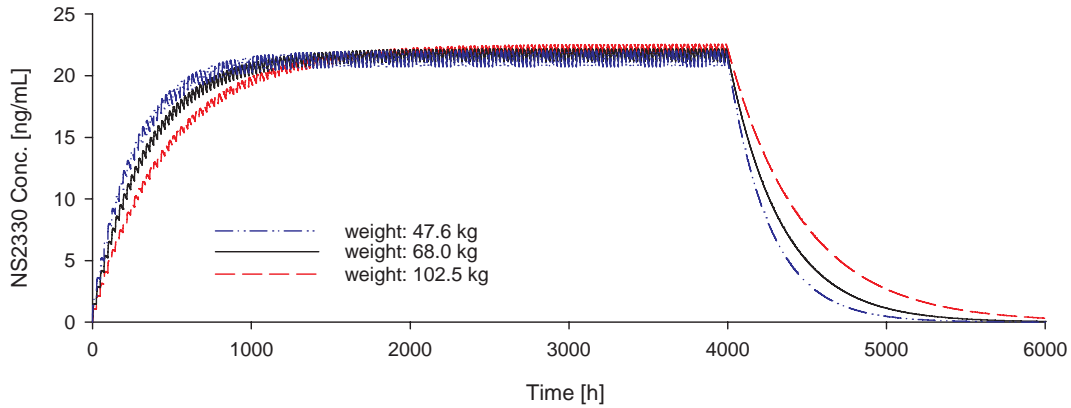
Figure 7.19 Project II - Impact of weight on the plasma concentration-time profiles of NS2330 after oral administration of 1 mg NS2330 once daily for 166 days (4000 h). Typical profiles of a male subject with median weight as well as the profiles of subjects with a weight according the 5 and 95 percentile of the weight distribution of the study population.
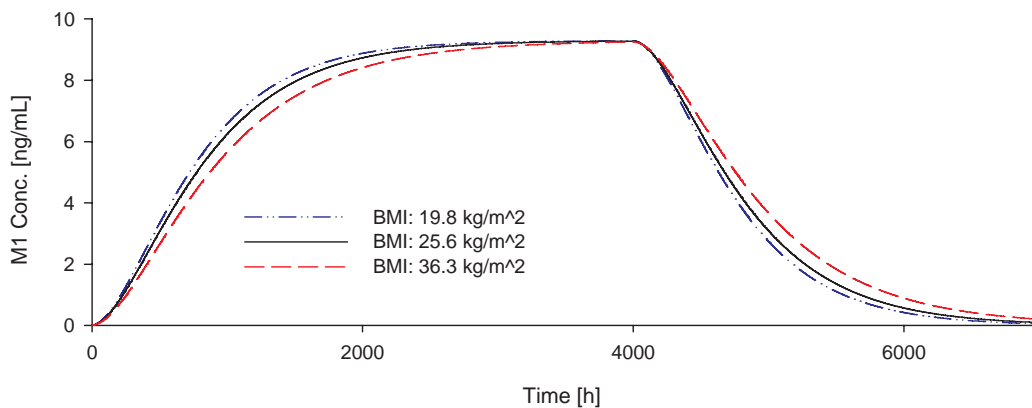
Figure 7.20 Project II - Impact of the covariate body mass index (BMI) on the plasma concentration-time profiles of M1 after oral administration of 1 mg NS2330 once daily for 166 days (4000 h). Typical profiles of a male subject with median BMI as well as the profiles of subjects with BMI according the 5 and 95 percentile of the BMI distribution of the study population. Age was assumed to be the median of the study population (75.5 years).
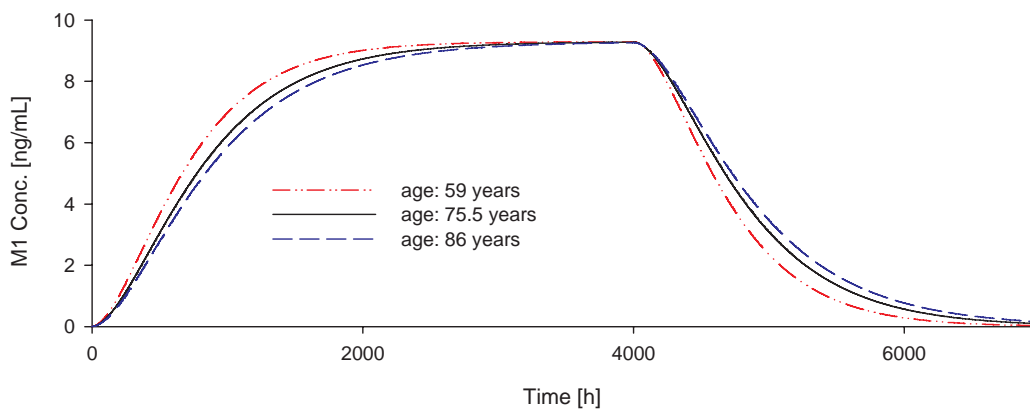
Figure 7.21 Project II - Impact of age on the plasma concentration-time profiles of M1 after oral administration of 1 mg NS2330 once daily for 166 days (4000 h). Typical profiles of a male subject with median age as well as the profiles of subjects with an age according the 5 and 95 percentile of the age distribution of the study population. Body mass index was assumed to be the median of the study population (25.6 kg/m^2).
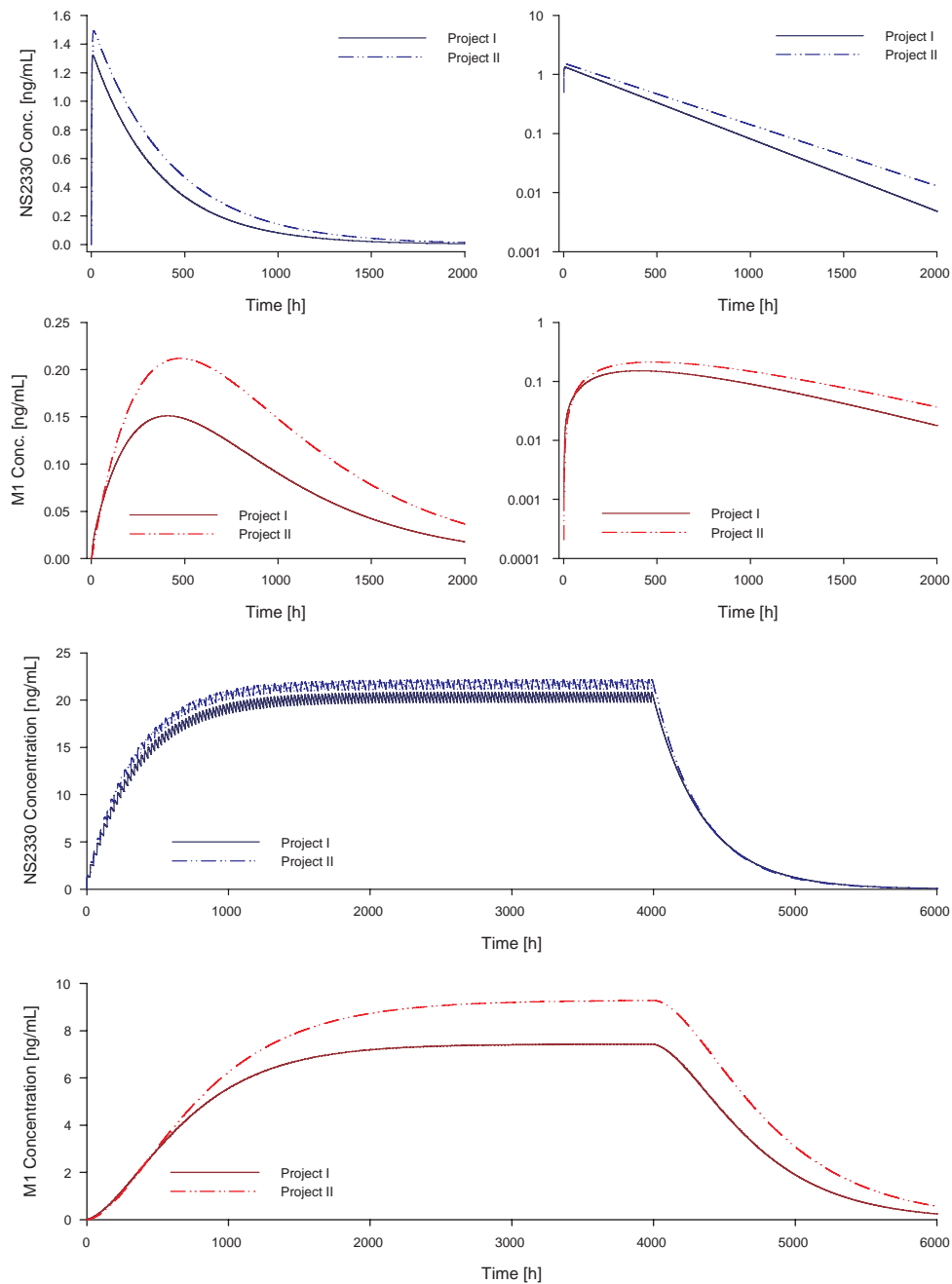
Figure 7.22 Project II - Simulations of plasma concentration-time profiles of NS2330 (upper panel) and M1 (lower panel) based on final PK models from project I (solid line) and project II (dotted line). The typical profiles of a male subject with median covariates after oral administration of 1 mg NS2330 once daily (upper panels) and once daily for 166 days (lower panels).
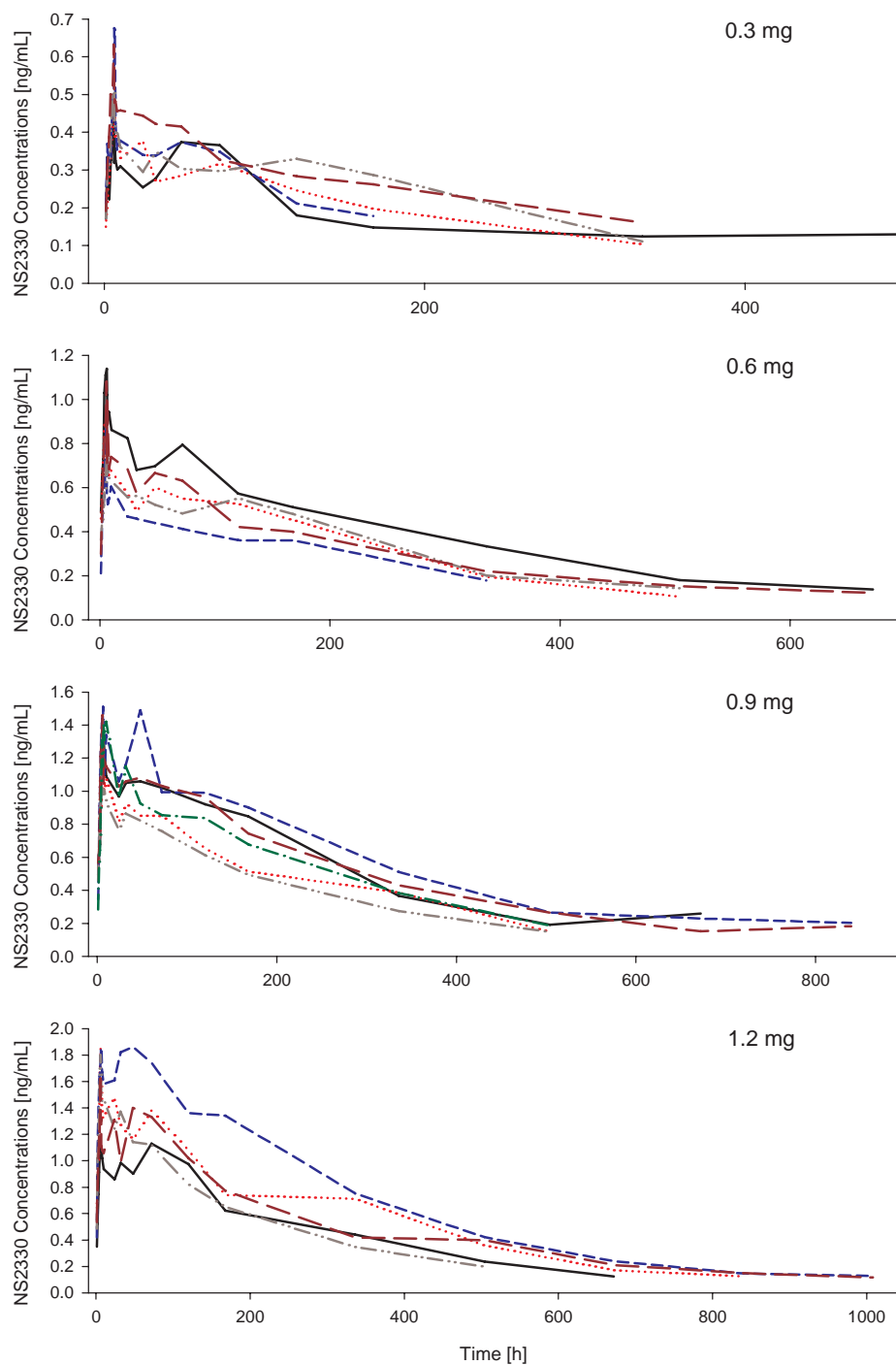
Figure 7.23 Project III - Plasma concentration-time profiles of NS2330 separated by dose groups. The total number of patients was 21 with a total number of 409 NS2330 observations above the lower limit of quantification.
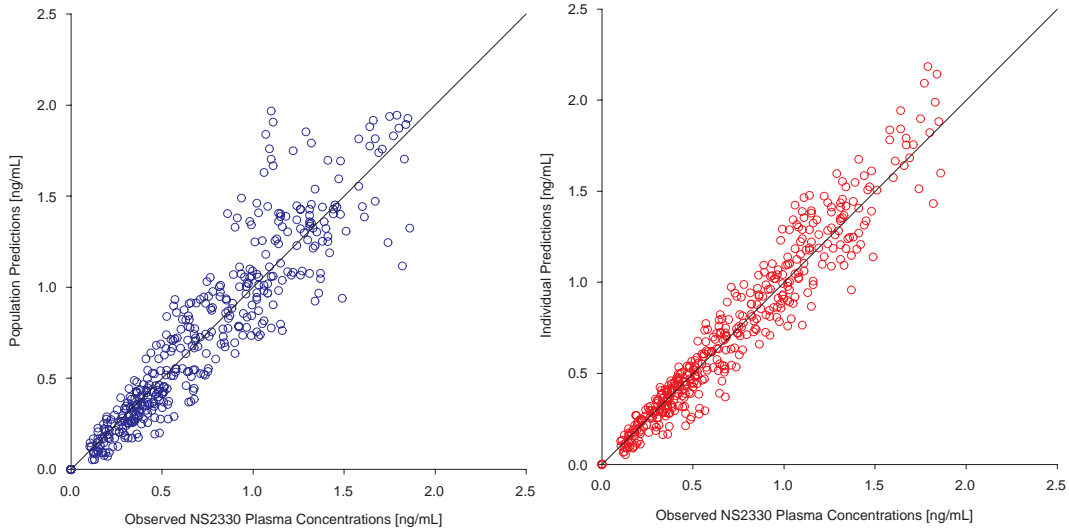
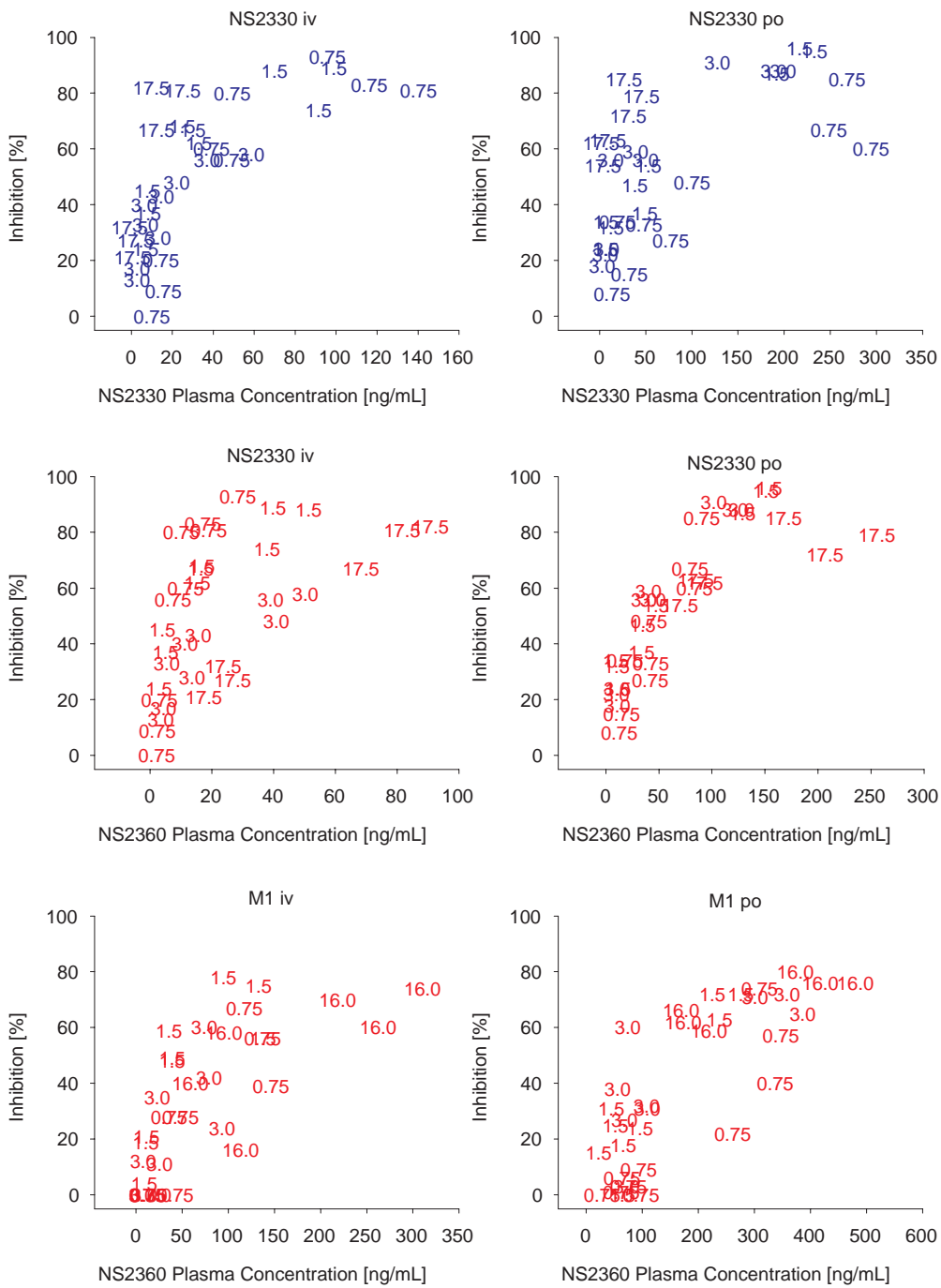**Figure 7.24** Project III - Goodness of Fit Plot - **NS2330**. Population predictions (left panel) and individual predictions (right panel) versus observed NS2330 plasma concentrations.
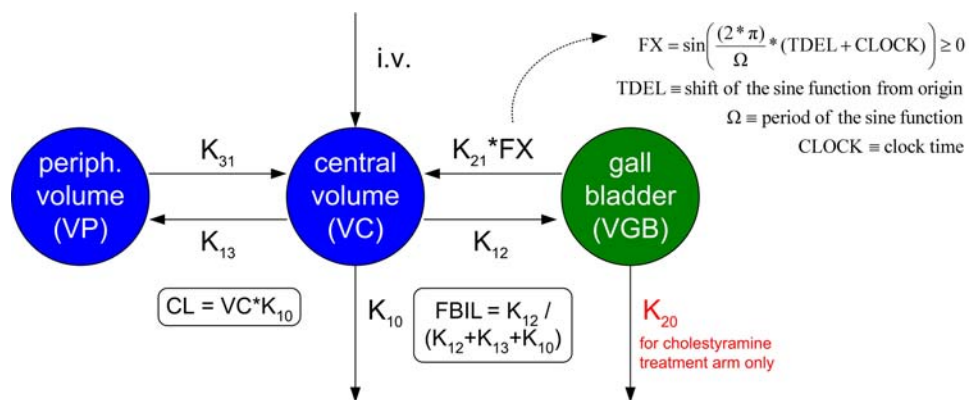
Figure 7.25 Project III - Schematic pharmacokinetic meloxicam model
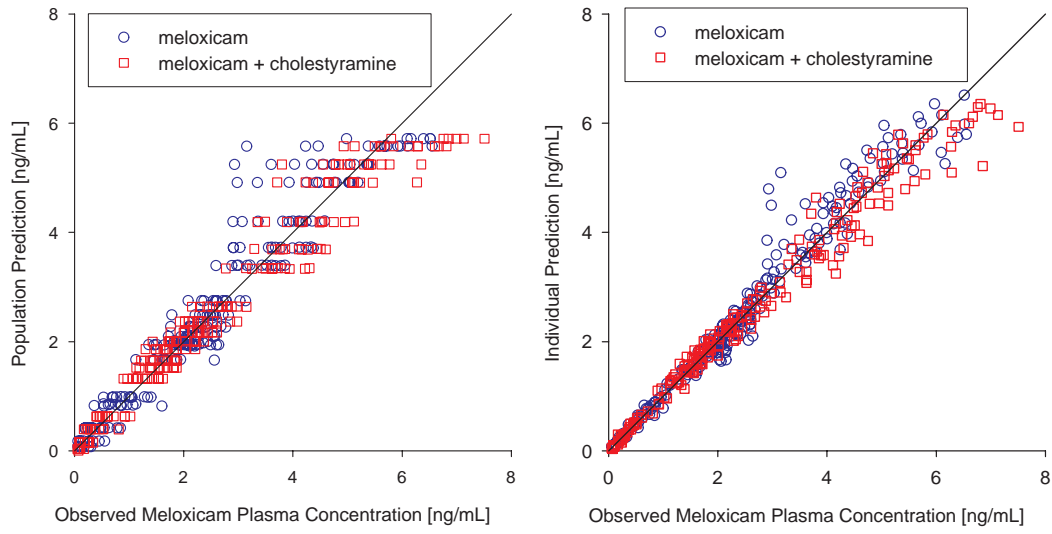
Figure 7.26 Project III - Goodness of Fit Plot - **Meloxicam**. Population predictions (left panel) and individual predictions (right panel) versus observed meloxicam plasma concentrations separated by treatment group.
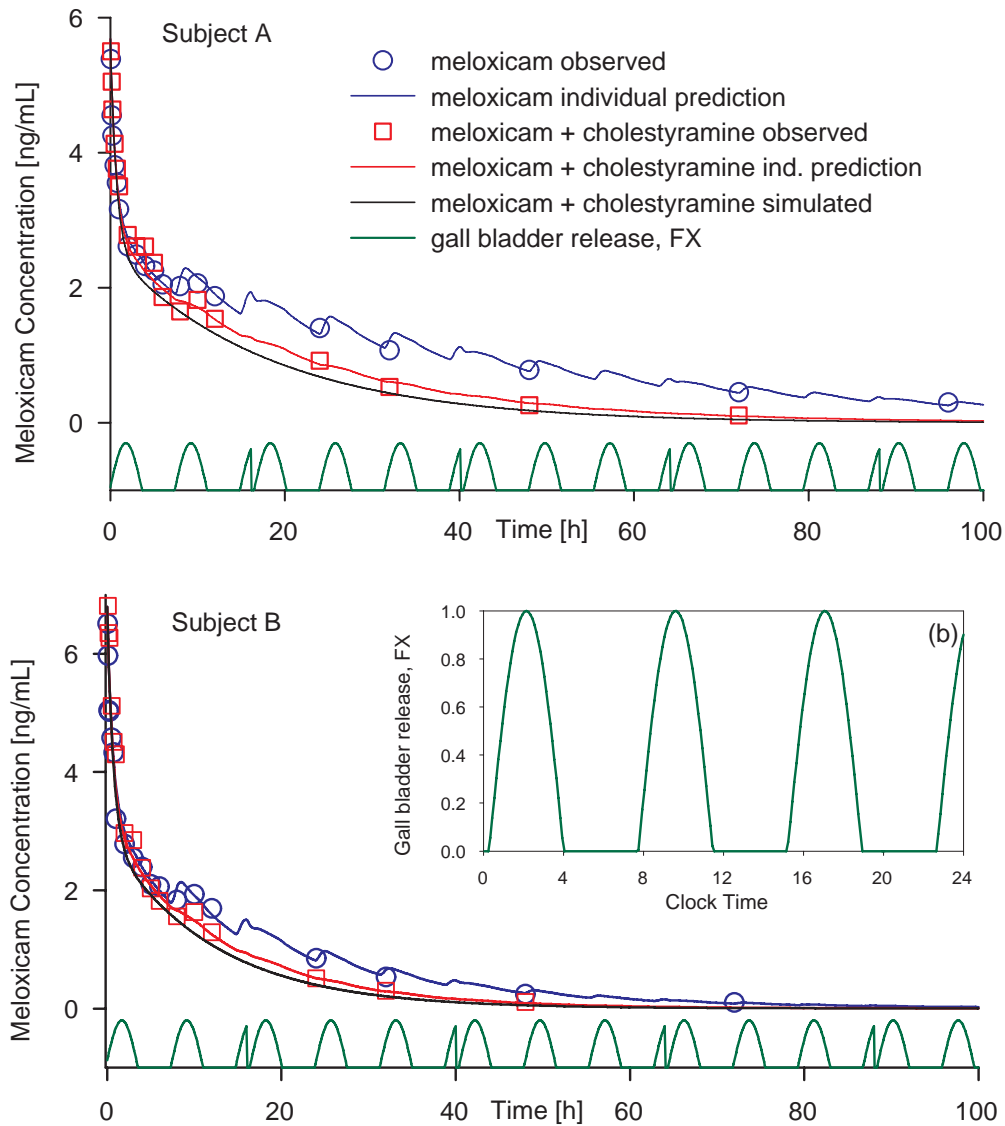
Figure 7.27 Project III - Simulated individual plasma concentration-time profiles (solid line) of an iv bolus administration of meloxicam of subjects A and B separated by treatment groups are shown. Observed plasma concentrations (bullets) of subjects A and B and the gall bladder release function (FX).
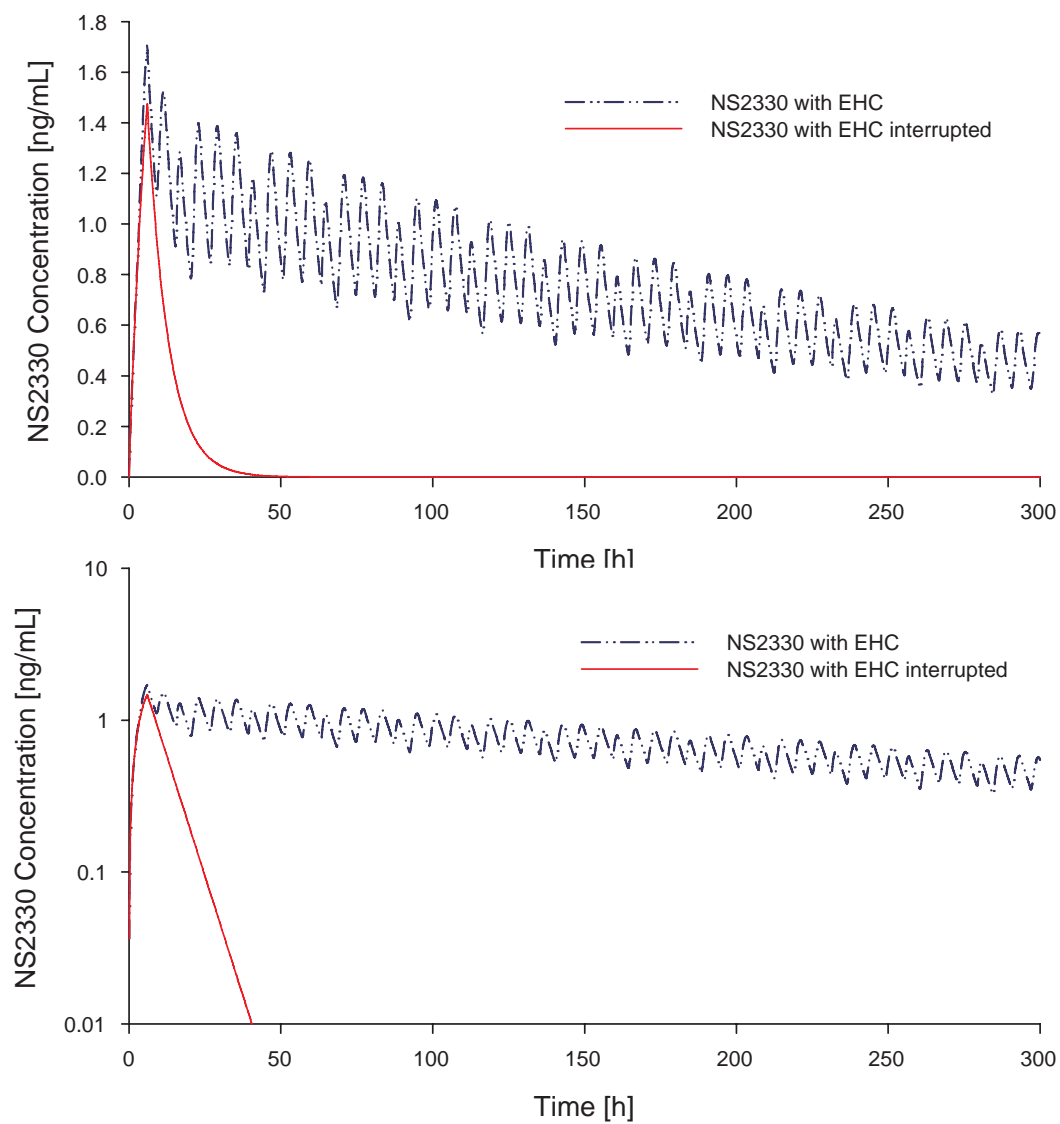
Figure 7.28 Project III - Simulated plasma concentration-time profiles of a 6 h single dose in-
fusion of 1.2 mg NS2330 with a completely interrupted enterohepatic circulation (EHC)
(dashed-dotted line) and with an unimpaired enterohepatic circulation (solid line). Up-
per panel shows the NS2330 concentrations in a linear scale, the lower panel in a loga-
rithmic scale.
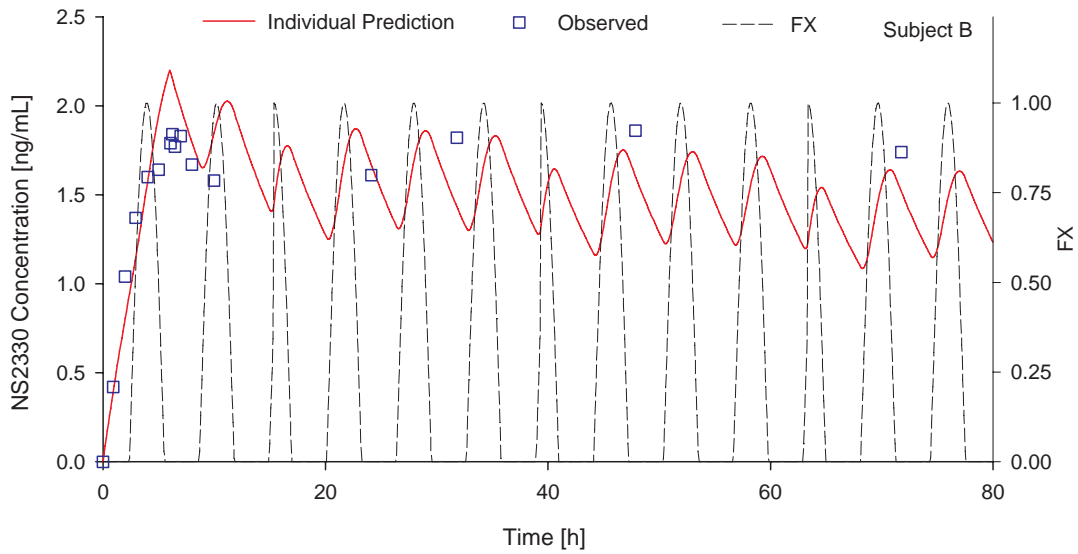
Figure 7.29 Project III - Simulated individual plasma concentration-time profiles (solid line) of a 6 h single dose infusion of NS2330 of subject B. In addition, the observed plasma concentrations (squares) of subject B and the gall bladder release function (FX; dashed line).
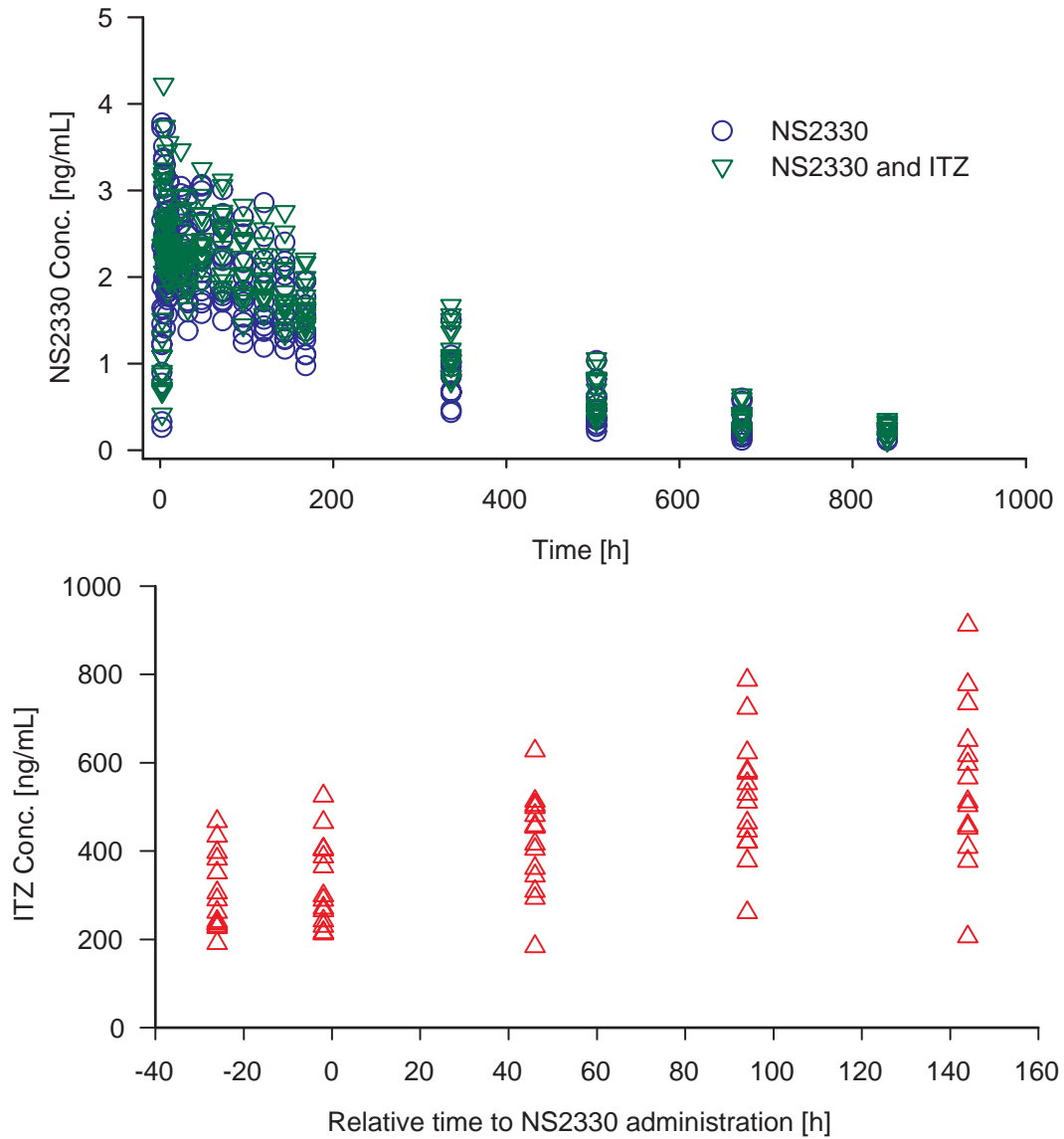
Figure 7.30 Project IV - Plasma concentrations versus time of NS2330 (upper panel) and itraconazole (ITZ) (lower panel) separated by treatment groups. The total number of patients was 28 with a total number of 455 NS2330 and 70 ITZ observations above the lower limit of quantification.
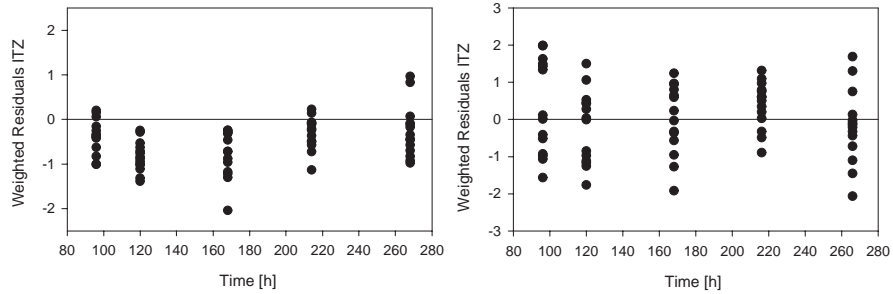
Figure 7.31 Project IV - Weighted Residuals versus time - **Itraconazole**. Left panel shows the weighted residuals over time of a standard 1 compartment model with a first-order elimination, right panel shows the weighted residuals over time of the final itraconazole (ITZ) model, considering a change of the elimination subject to the ITZ concentration.
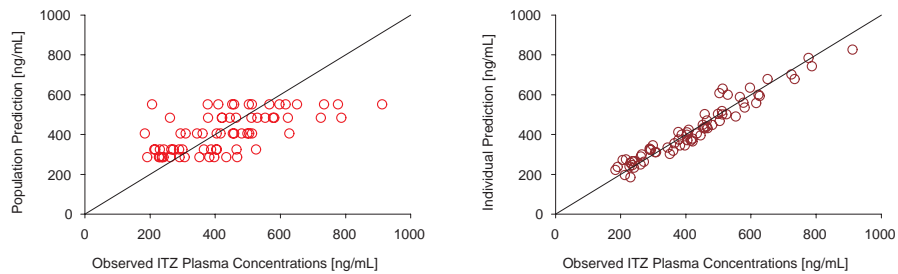
Figure 7.32 Project IV - Goodness of Fit Plots - **Itraconazole**. Population predictions (left panel) and individual predictions (right panel) versus observed itraconazole (ITZ) plasma concentrations.
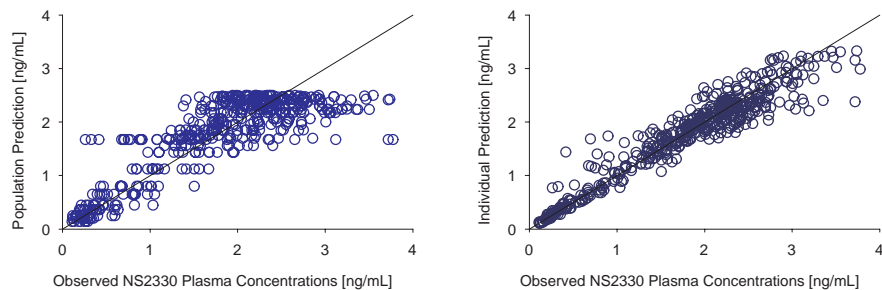
Figure 7.33 Project IV - Goodness of Fit Plots - **NS2330**. Population predictions (left panel) and individual predictions (right panel) versus observed NS2330 plasma concentrations.
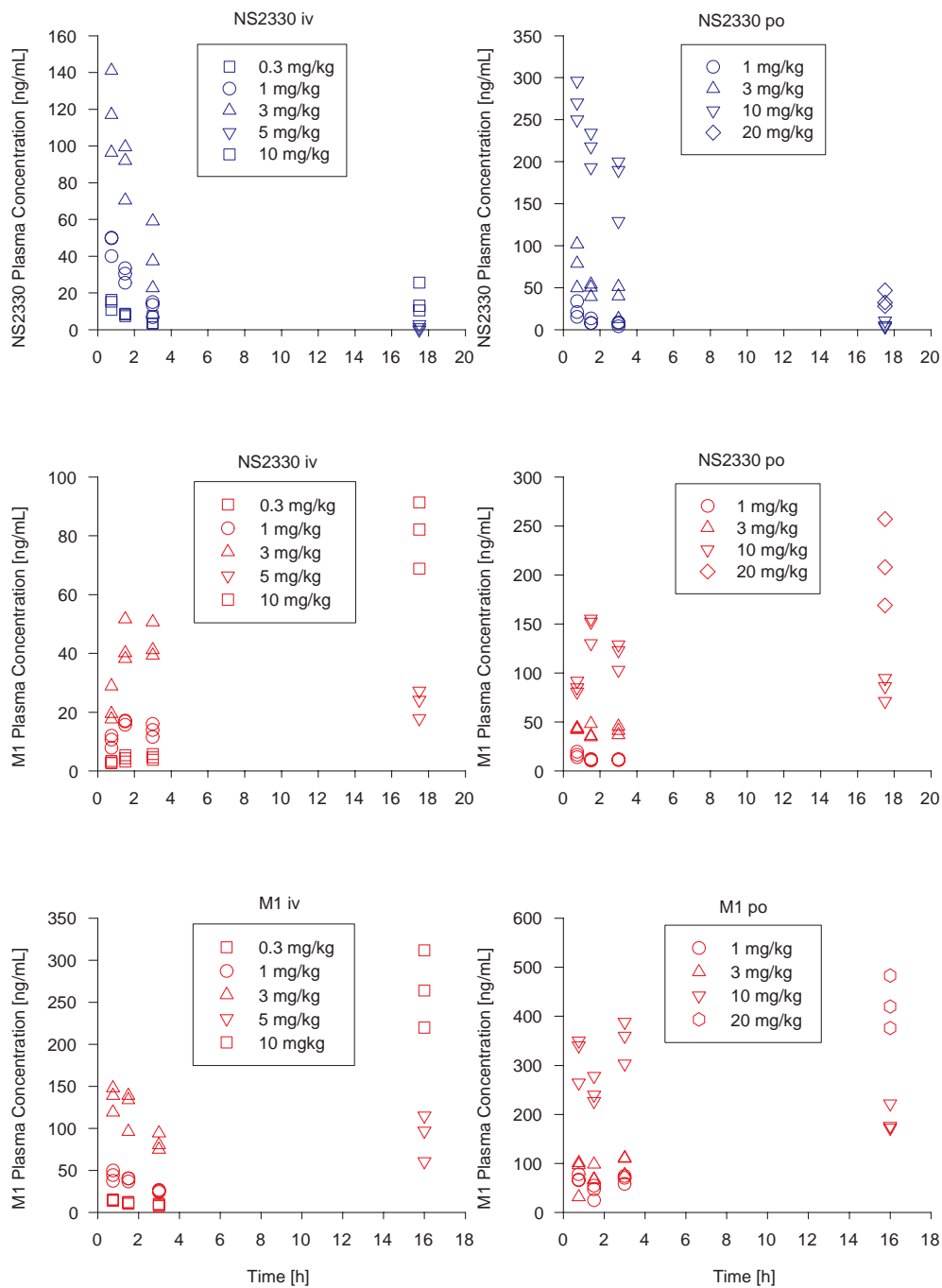
Figure 7.34 Project V - Plasma concentrations versus time of NS2330 (first row) and M1 (last two rows) separated by route and dose group. The total number of mice was 132 with a total number of 65 NS2330 and 132 M1 observations above the lower limit of quantification.

Figure 7.35 Project V - NS2330 (first row) and M1 (last two rows) plasma concentrations versus inhibition. Numbers denote time of measurement in hours.
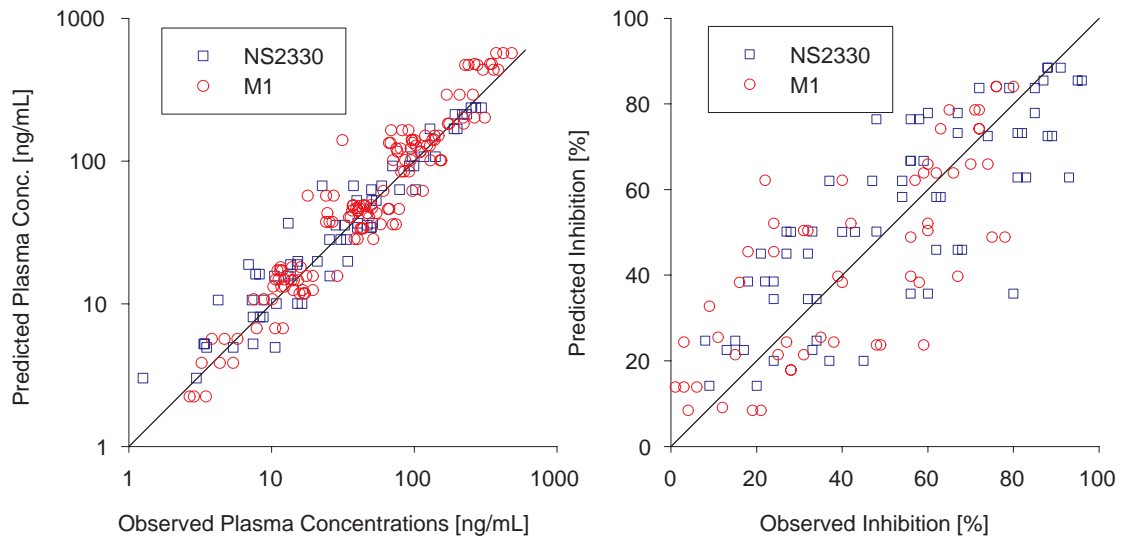
Figure 7.36 Project V - Goodness of Fit Plot. Observed versus predicted measurements separated by pharmacokinetic (left panel) and pharmacodynamic (right panel) are shown.
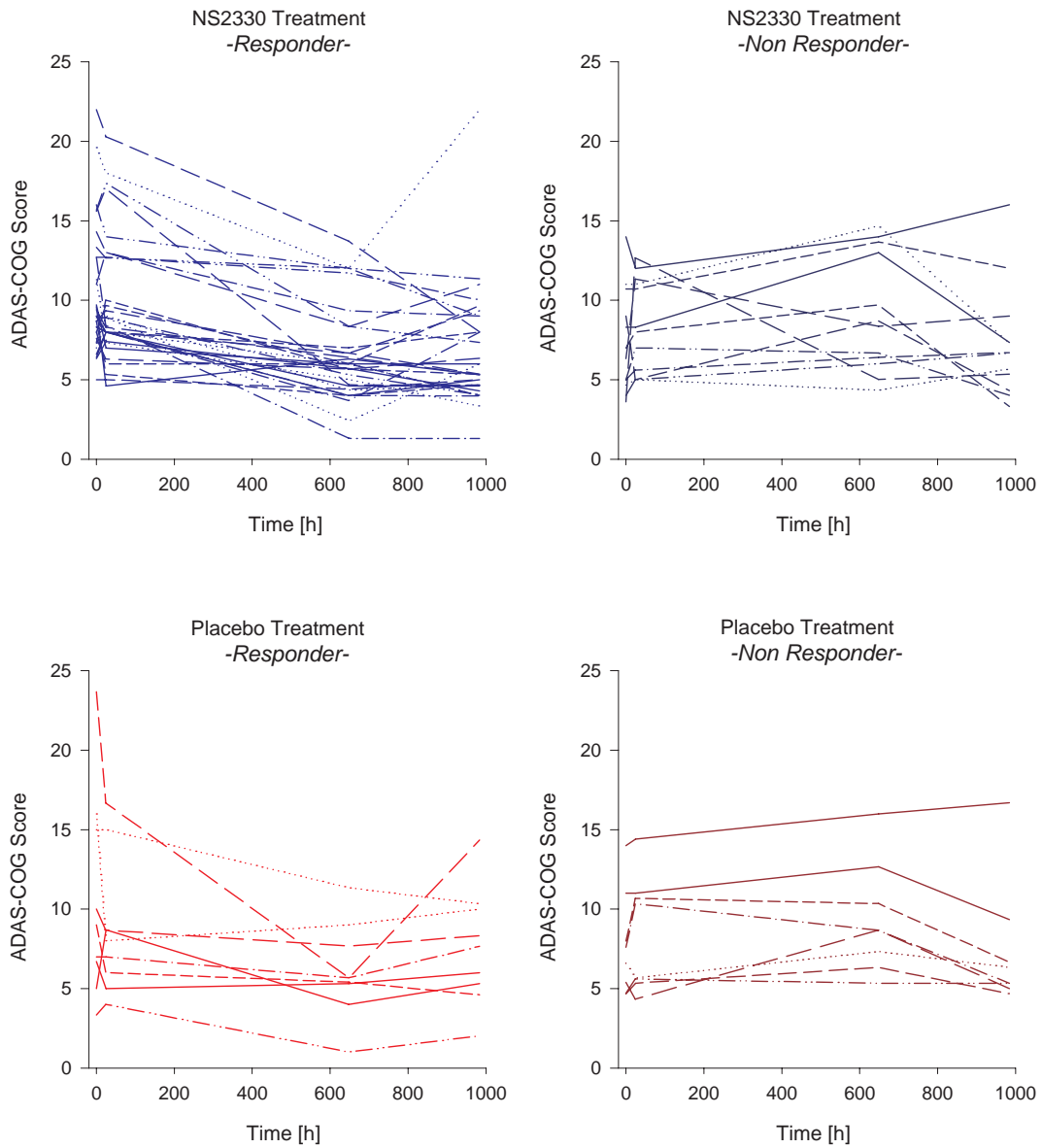
Figure 7.37 Project VI - ADAS-COG measurements versus time of the NS2330 (upper panel) and the placebo arm (lower panel) are shown. Left panels show the responder patients, right panel the non-responders. The total number of patients was 62, 18 received placbo, the remaining 44 were treated with NS2330.
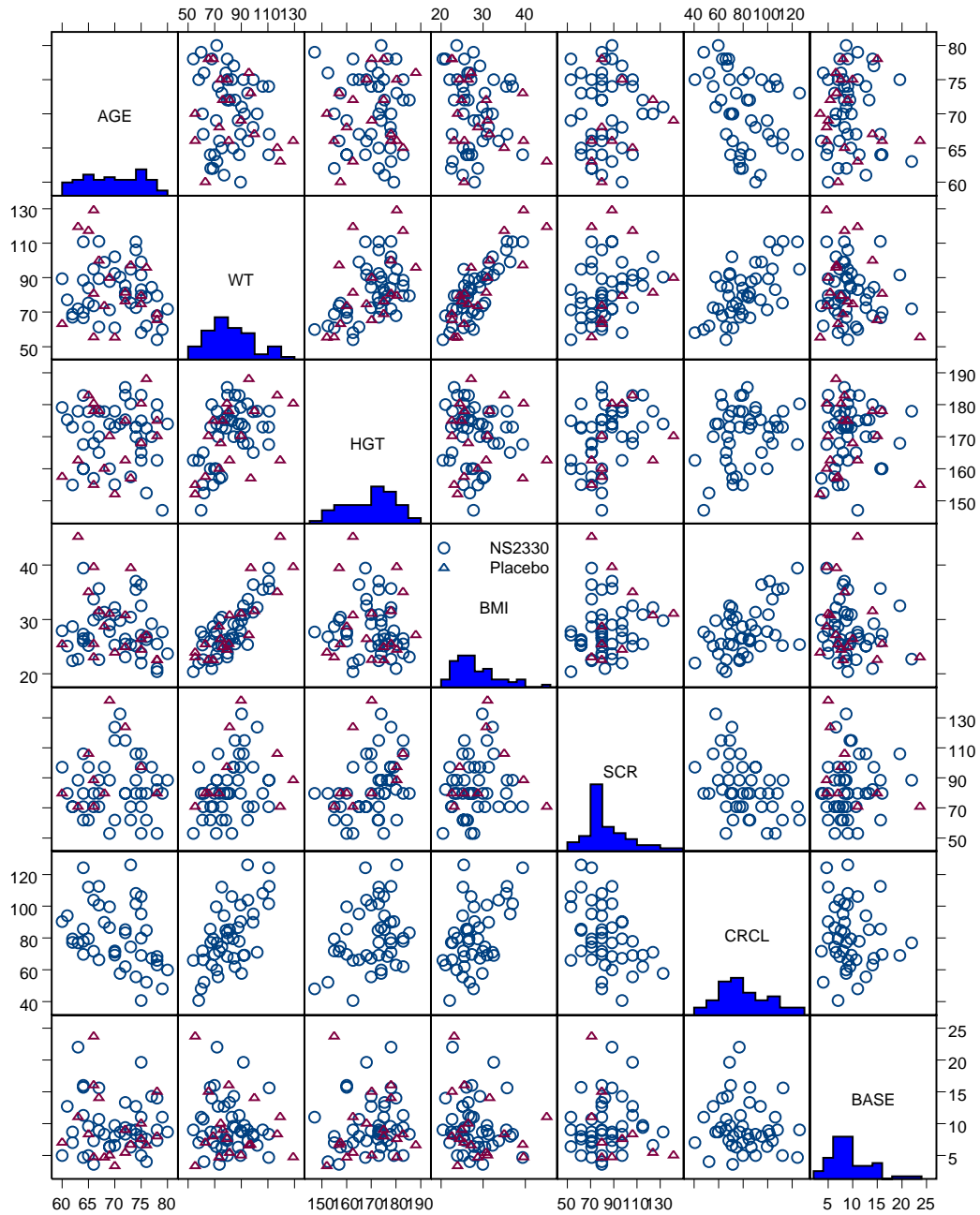
Figure 7.38 Project VI - Scatter plot and distributions of the continuous covariates age (AGE) in years, weight (WT) in kg, height (HGT) in cm, body mass index (BMI) in kg/m^2, serum creatinine (SCR) in μmol/L, creatinine clearance (CRCL) in mL/min and the ADAS-COG baseline value (BASE). O = NS2330; Δ = Placebo
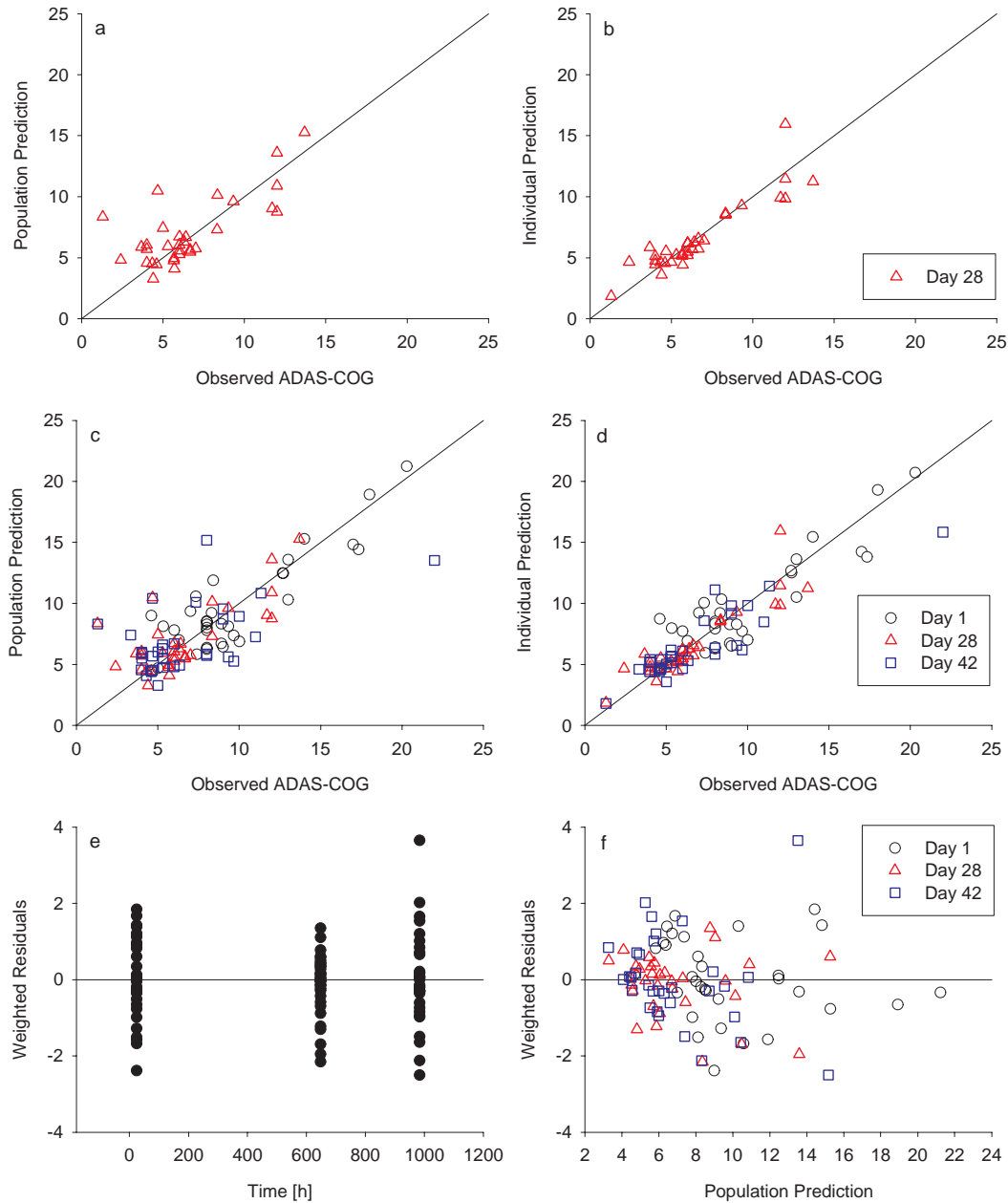
Figure 7.39 Project VI - Goodness of Fit Plots - **Base Model**. Population predictions (Fig. a and c) and individual predictions (Fig. b and d) versus observed ADAS-COG values. Figures a and c show day 28 (last day on treatment) separated. Additionally, the weighted residuals versus time (Fig. e) and population predictions (Fig. f) are shown.
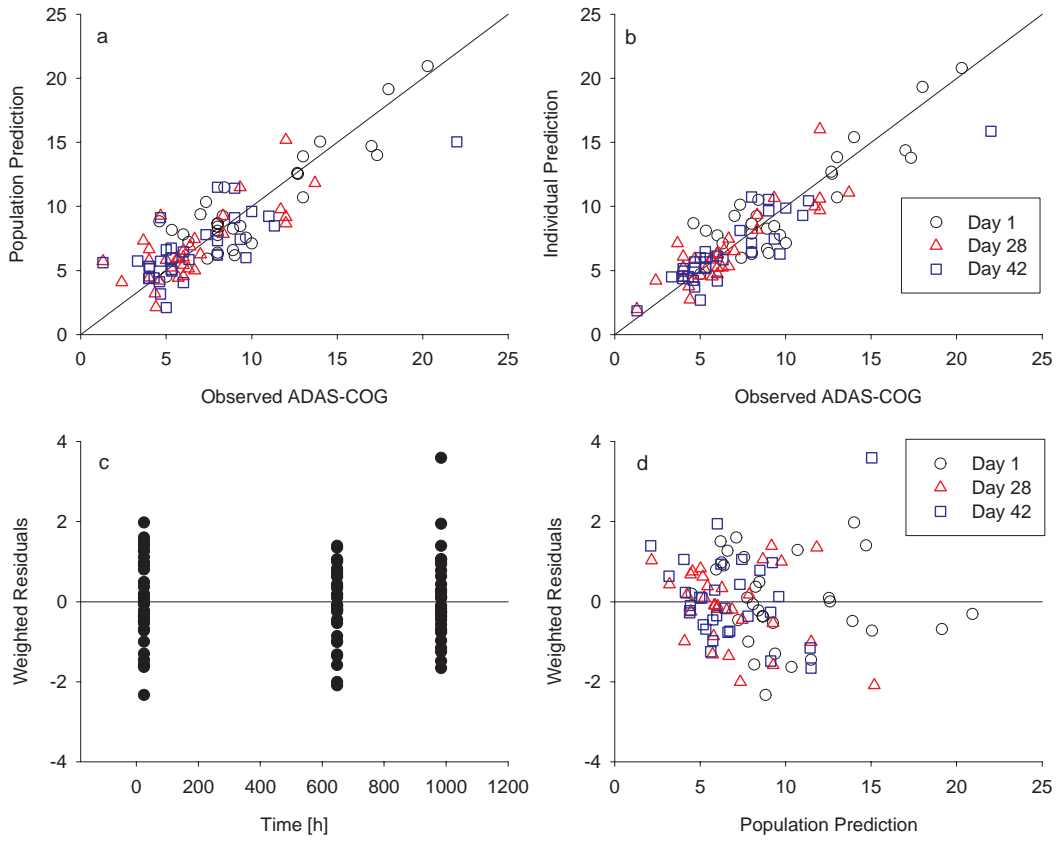
Figure 7.40 Project VI - Goodness of Fit Plots - **Final Model**. Population predictions (Fig. a) and individual predictions (Fig. b) versus observed ADAS-COG values.Additionally, the weighted residuals versus time (Fig. c) and population predictions (Fig. d) are shown.
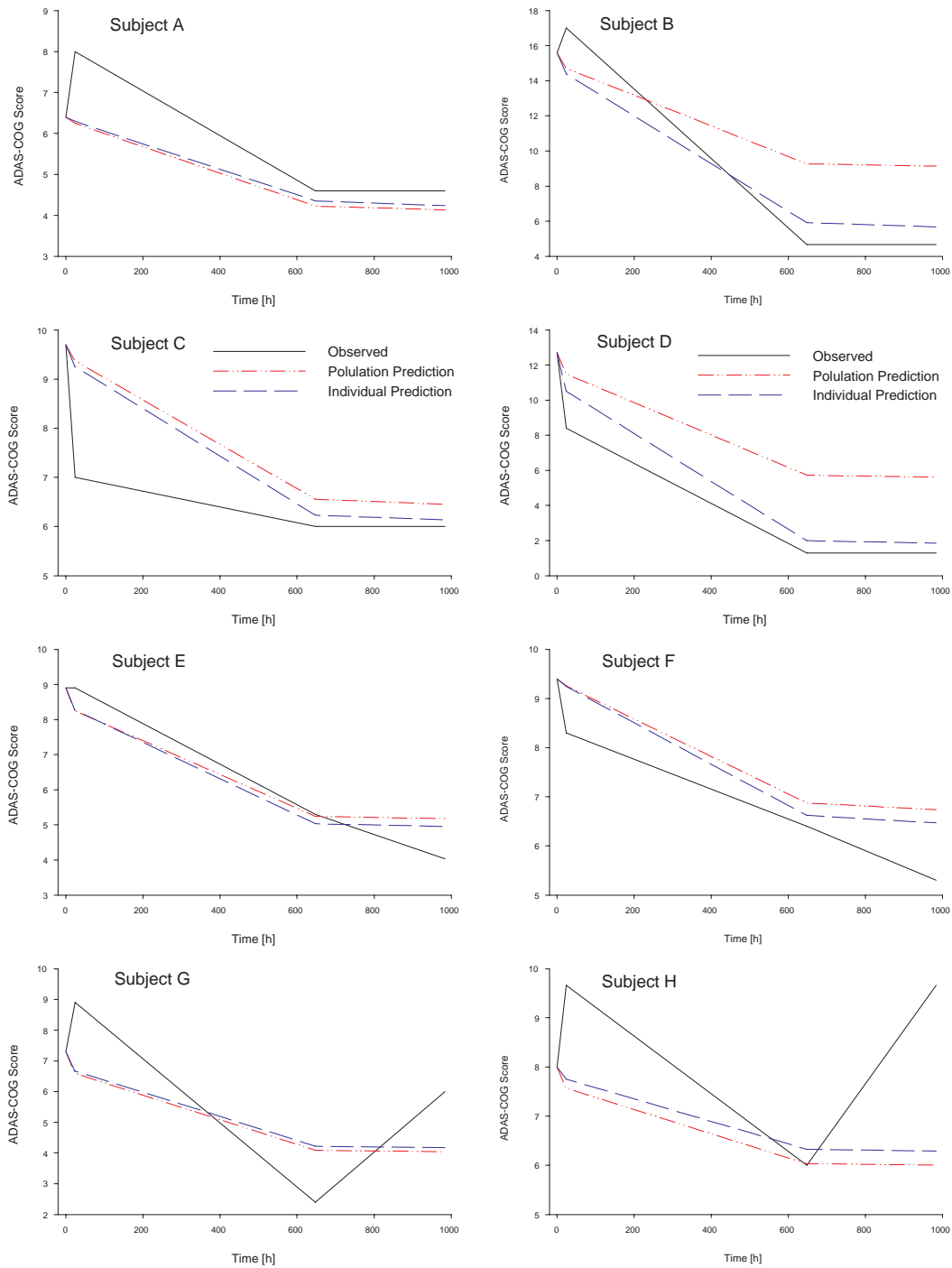
Figure 7.41 Project VI - Individual predictions, population predictions and observed ADAS-COG values versus time of eight patients (Subjects A-H).
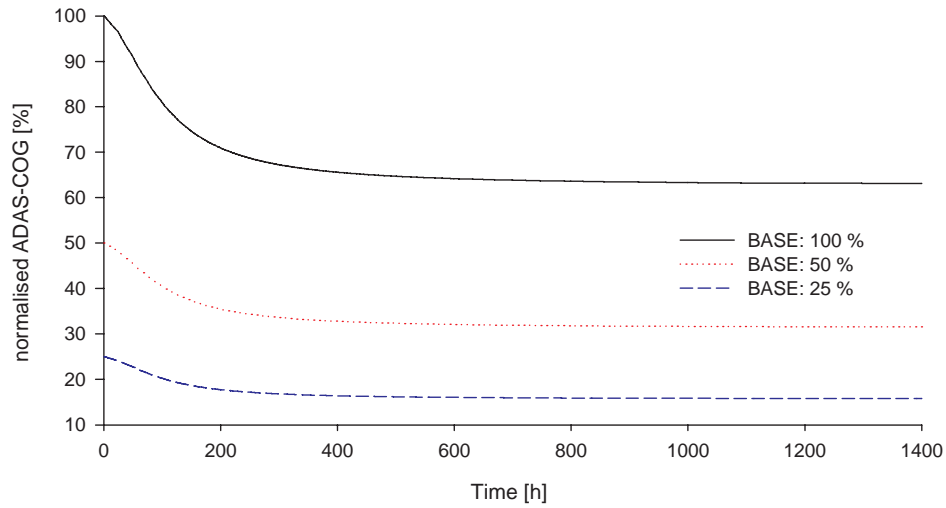
Figure 7.42 Project VI - Impact of the ADAS-COG baseline value on the effect-time profile after oral administration of 1 mg NS2330 once daily for 166 days (4000 h): Typical profiles of patients with relative baseline values of 25, 50 and 100%.
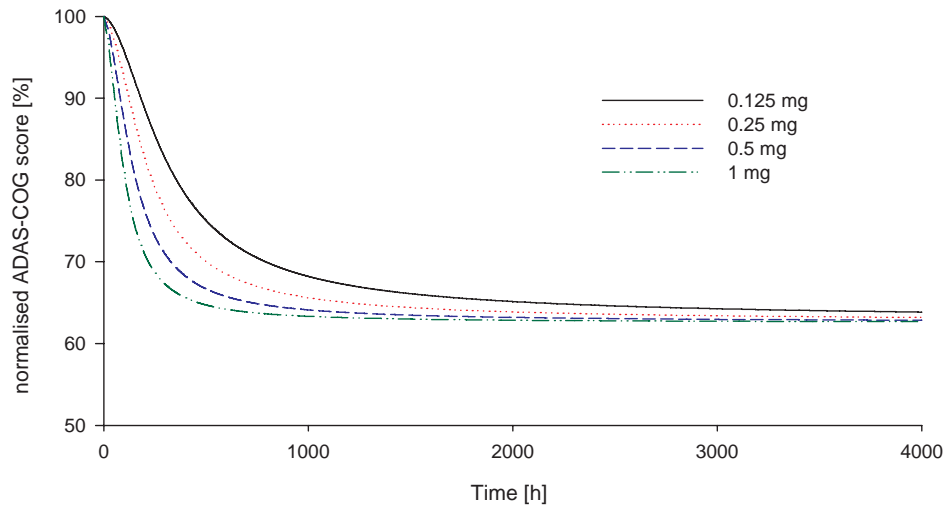
Figure 7.43 Project VI - Impact of different NS2330 doses on the effect-time profile: Typical profiles after oral administration of 0.125, 0.25, 0.5 and 1 mg NS2330 once daily for 166 days (4000 h).

Curriculum Vitae

Name	Thorsten Lehr
Date of birth	05. February 1977
Place of birth	Hanau, Germany
Nationality	German

Education and Qualifications

Since 01/2003	Doctoral thesis under the supervision of Prof. Charlotte Kloft Department Clinical Pharmacy, Freie Universität Berlin and Martin-Luther-Universität Halle-Wittenberg
12/2002	Registration as a pharmacist in Germany
10/1997 - 10/2001	Degree in Pharmacy (2. Staatsexamen) Johann Wolfgang Goethe- University, Frankfurt am Main, Germany
07/1987 - 06/1996	High school degree (Allgemeine Hochschulreife) Karl-Rehbein-Gymnasium, Hanau, Germany

Professional Experience

Since 01/2006	**Pharmacometrician** Boehringer Ingelheim Pharma GmbH& Co KG, Biberach/Riss, Germany
11/2001 - 10/2002	**Pre-registration pharmacist** Boehringer Ingelheim Pharma KG Department Drug Metabolism and Pharmacokinetics Biberach/Riss, Germany Apotheke im Hauptbahnhof Frankfurt/Main, Germany
12/1999 - 04/2002	**Graduate assistant** SocraTec R&D GmbH, Prof. Dr. H. Blume, Oberursel, Germany

Awards

06/2004	Travel award Population Approach Group Europe

Publications

Original Papers

T. Lehr, A. Staab, C. Tillmann, D. Trommeshauser, A. Raschig, H.G. Schaefer, C. Kloft.
Population pharmacokinetic modelling of NS2330 and its major Metabolite in Alzheimer's disease patients.
British Journal of Clinical Pharmacology, submitted (2006)

T. Lehr, A. Staab, E. Ø. Nielsen, C. Tillmann, D. Trommeshauser, H.G. Schaefer, C. Kloft.
The population PK/PD modelling approach for the assessment of the potency of active metabolites in vivo: Application to the novel CNS active drug NS2330.
Biochemical Pharmacology, submitted (2006)

T. Lehr, A. Staab, D. Trommeshauser, H.G. Schaefer, C. Kloft.
How long is enough? - Mechanistic population pharmacokinetic modelling to overcome limitations in drug-drug interaction studies of long half-life drugs.
in preparation

T. Lehr, A. Staab, C. Tillmann, D. Trommeshauser, H.G. Schaefer, C. Kloft.
A novel quantitative enterohepatic circulation model.
in preparation

T. Lehr, A. Staab, C. Tillmann, D. Trommeshauser, A. Raschig, H.G. Schaefer, C. Kloft.
Efficacy modelling of NS2330 and its major metabolite in Alzheimer's disease patients.
in preparation

Presentations

T. Lehr, C. Kloft.
Assessment of the potency of NS2360 relative to NS2330 using a PK/PD model for the inhibition of the dopamine re-uptake transporter in mice.
XIII. Clinical-pharmacological colloquium of Boehringer Ingelheim, March 2005, Biberach, Germany

T. Lehr, Krug-Schmid R, C. Tillmann, A. Staab, D. Trommeshauser, H.G. Schaefer, C. Kloft.
Population pharmacokinetic model of a CNS active drug and its metabolite.
Jahrestagung der Deutschen Pharmazeutischen Gesellschaft (DPhG) 2004, Regensburg, 06.-09.10.2004.
Proceedings, 138 (2004).

T. Lehr, C. Tillmann, A. Staab, D. Trommeshauser, H.G. Schaefer, C. Kloft.
Enterohepatic circulation - Influence on drug exposure and half-life.
"Der wissenschaftliche Nachwuchs stellt sich vor" Deutsche Pharmazeutische Gesellschaft (DPhG), Berlin, 05.07.2004. Proceedings, 1 (2004).

Conference Abstracts

T. Lehr, A. Staab, C. Tillmann, D. Trommeshauser, A. Raschig, H.G. Schaefer, C. Kloft.
Population pharmacokinetics of NS2330 and its major metabolite in Alzheimer's disease patients.
15th Population Approach Group Europe (PAGE), Brugge, Belgium, 14.-16.06.2006. (2006)
[www.page-meeting.org/?abstract=986]. accepted

T. Lehr, A. Staab, C. Tillmann, D. Trommeshauser, A. Raschig, H.G. Schaefer, C. Kloft.
Efficacy modelling of NS2330 in mild Alzheimer's disease patients.
15th Population Approach Group Europe (PAGE), Brugge, Belgium, 14.-16.06.2006. (2006)
[www.page-meeting.org/?abstract=985]. accepted

D. Zeumer, A. Staab, T. Lehr, C. Tillmann, K.H. Liesenfeld, H.G. Schaefer.
PROPHET - A convenient and efficient environment for the use of NONMEM in a global pharmaceutical company.
15th Population Approach Group Europe (PAGE), Brugge, Belgium, 14.-16.06.2006. (2006)
[www.page-meeting.org/?abstract=990]. accepted

T. Lehr, C. Tillmann, A. Staab, D. Trommeshauser, H.G. Schaefer, C. Kloft.
Estimating the maximum impact of CYP3A4 inhibition on the pharmacokinetics of long half-life drugs: a mechanistic modelling approach.
Annual meeting of the American Association of Pharmaceutical Scientists (AAPS), Nashville, 06.-10.11.2005. Proceedings AAPS Journal 7 (S2) 2005 Abstract M1306.

T. Lehr, C. Tillmann, A. Staab, D. Trommeshauser, H.G. Schaefer, C. Kloft.
Mechanistic PK modelling to overcome limitations in drug-drug interaction studies of long half-life drugs.
Jahrestagung der Deutschen Pharmazeutischen Gesellschaft (DPhG) 2005, Mainz, 05.-08.10.2005.
Proceedings, 94 (2005).

T. Lehr, C. Tillmann, Binder R, D. Trommeshauser, A. Staab, H.G. Schaefer, C. Kloft.
Assessment of the potency of a metabolite relative to the parent compound using a population PK/PD model for the inhibition of a neurotransmitter re-uptake transporter in mice.
14th Population Approach Group Europe (PAGE), Pamplona, Spain, 16.-17.06.2005. Proceedings 142 (2005) [www.page-meeting.org/?abstract=730].

T. Lehr, C. Tillmann, Krug-Schmid R, D. Trommeshauser, A. Staab, H.G. Schaefer, C. Kloft.
A new CNS active drug and its metabolite: A population pharmacokinetic analysis.
14th Population Approach Group Europe (PAGE), Pamplona, Spain, 16.-17.06.2005. Proceedings 59 (2005) [www.page-meeting.org/?abstract=729].

T. Lehr, C. Tillmann, A. Staab, H.G. Schaefer, C. Kloft.
Evaluation of an enterohepatic circulation model: Predicting the influence of cholestyramine on the pharmacokinetics of meloxicam.
14th Population Approach Group Europe (PAGE), Pamplona, Spain, 16.-17.06.2005. Proceedings 87 (2005) [www.page-meeting.org/?abstract=766].

C. Tillmann, H.G. Schaefer, T. Lehr, A. Staab.
Meloxicam for juvenile rheumatoid arthritis patients: Is dosing on a mg/kg body weight basis justified?.
14th Population Approach Group Europe (PAGE), Pamplona, Spain, 16.-17.06.2005. Proceedings 89 (2005) [www.page-meeting.org/?abstract=772].

T. Lehr, C. Tillmann, A. Staab, D. Trommeshauser, H.G. Schaefer, C. Kloft.
Clock time as a control variable for the gall bladder emptying in an enterohepatic circulation model.
13th Population Approach Group Europe (PAGE), Uppsala, Sweden, 17.-18.06.2004. Proceedings 703 (2004) [www.page-meeting.org/?abstract=469].

Acknowledgements

Erklärung

Hiermit erkläre ich, dass ich mich mit der vorliegenden Dissertation erstmals um die Erlangung eines Doktorgrades bewerbe.

Ferner erkläre ich, dass ich die vorliegende Arbeit selbständig und ohne fremde Hilfe angefertigt, andere als die von mir angegebenen Quellen und Hilfsmittel nicht benutzt und die den verwendeten Werken wörtlich oder inhaltlich entnommenen Stellen als solche kenntlich gemacht habe.

Halle (Saale), 19. Juli 2006